Dissertations, Master's Theses and Master's Reports

2016

SENSING AND MAPPING OF SURFACE HYDROPHOBICITY OF PROTEINS BY FLUORESCENT PROBES

Nethaniah Dorh
Michigan Technological University, ndorh@mtu.edu

Recommended Citation

SENSING AND MAPPING OF SURFACE HYDROPHOBICITY OF PROTEINS BY FLUORESCENT PROBES

By

Nethaniah Dorh

A DISSERTATION

Submitted in partial fulfillment of the requirements for the degree of

DOCTOR OF PHILOSOPHY

In Chemistry

MICHIGAN TECHNOLOGICAL UNIVERSITY

2016

This dissertation has been approved in partial fulfillment of the requirements for the Degree of DOCTOR OF PHILOSOPHY in Chemistry.

Department of Chemistry

Dissertation Advisor: *Dr. Ashutosh Tiwari*

Committee Member: *Dr. Haiying Liu*

Committee Member: *Dr. Martin Thompson*

Committee Member: *Dr. Caryn Heldt*

Department Chair: *Dr. Cary F. Chabalowski*

Dedication

This work is dedicated to my savior Jesus Christ who provided me with a loving family, caring friends, dedicated mentor, and a supportive church to get me through the PhD program.

"The fear of the Lord is the start of knowledge: but the foolish have no use for wisdom and teaching." - Proverbs 1: 7

Table Of Contents

Preface

The subject of this dissertation is the design and use of fluorescent probes to act as sensors and to eventually help map the hydrophobic surface of proteins. Fluorescence is a non-invasive and sensitive tool for investigating biological systems *in vitro* and *in vivo*. As a result, fluorescence has great potential as an effective tool for evaluating the surface hydrophobicity of proteins. In this dissertation, several novel probes for doing just that have been developed. These probes provide the opportunity for significant development in food chemistry (agricultural industry), neurodegeneration and associated fields where such information is vital. Furthermore, information garnered from using these probes can go a long way to improving future therapeutic approaches against neurodegenerative diseases.

The aim of this work is to provide sufficient background information on these novel fluorescent probes as well as methods for developing future probes that target specifically the surface hydrophobicity of proteins.

The completion of this dissertation was made possible through many individuals who provided invaluable contributions to the chapters found within this dissertation. I would like to give special thanks to my advisor Dr. Ashutosh Tiwari for all of his constructive feedback and for editing each chapter in this

Acknowledgments

I would like to acknowledge my advisor Dr. Ashutosh Tiwari for his sedulous efforts and support in the completion of these projects. His efforts helped to mold my dissertation into what it is today. I hope that this work provides a glimpse of the patience and dedication exhibited by Dr. Tiwari towards myself in the completion of this final work.

I would also like to thank the members of my committee, Dr. Haiying Liu, Dr. Martin Thompson, and Dr. Caryn Heldt for their invaluable critique of procedures, drafts, project in general and for their time. Of honorable mention is Dr. Liu and his lab for the constant collaborations that allowed the bulk of this work to be done.

Finally, I would also like to acknowledge my wife Jeanette and my daughters Kaelan and Nealah. The constant support and approval of my long hours at work allowed me to make significant progress and complete the projects described therein. It goes without saying that my mother (Marietta), father (Beniah), sister (Nellista), brothers (Sebastien, Timotheus, Kedhma and Neciah), mother-in-law (Renee) and father-in-law (Larry) are also worthy of mention. While all of these individuals here have been mentioned last, they are

by no means least as I would not have gotten to this point had it not been for all

of their efforts. I am at this point today because of all of you.

Abstract

Surface hydrophobic interactions in proteins play a critical role in molecular recognition, influence biological functions, and play a central role in many protein misfolding diseases. As significance of surface hydrophobic interactions in age-related proteinopathies is becoming clear; it has led to an increased demand for better probes and tools to sense and characterize protein surface hydrophobicity. Current commercially available fluorescent probes such as 8-anilino-1-naphthalene sulfonic acid (ANS), 4,4′ -dianilino-1,1′-binaphthyl-5,5′-disulfonic acid (Bis-ANS), 6-propionyl-2-(N,N-dimethylamino)naphthalene (PRODAN), tetraphenylethene derivative, and Nile Red can sense proteins average hydrophobicity. However, probe limitations prevents their application for measuring the protein surface hydrophobicity. Some of the major deficiencies of these fluorescent probes are: poor solubility in water, overestimation of fluorescence signal due to contribution from hydrophobic as well as electrostatic interactions, and weak signal when bound to solvent exposed hydrophobic surface of proteins due to quenching. As a consequence of these limitations the above fluorescent dyes do not provide accurate measure of proteins surface hydrophobicity. Therefore, in this study we focused on designing and testing novel fluorescent probes for selectively reporting the surface hydrophobicity of proteins. For the first project, we chose 4,4-difluoro-4-bora-3a,4a-diaza-s-indacene   (BODIPY)   based   fluorescent

probes as these are highly fluorescent in both non-polar as well polar media. To increase water solubility we substituted 2-methoxyethylamine group at 3,5-position of the BODIPY core. For increasing hydrophobic sensing we focused our efforts on substitutions at *meso* position on BODIPY dye. These BODIPY-based surface hydrophobic sensors (HPsensors) showed a much stronger signal compared to ANS, a commonly used hydrophobic probe. The probes showed a 10- to 60-fold increase in signal strength compared to ANS for the BSA protein. For the second project, we modified the commercially available ANS dye with a succinimide-functionalized ethynyl derivative that offers facile reaction with amine residues of proteins at physiological pH. This modification of ANS with a reactive NHS ester favors crosslinking of the dye on proteins surface with lysine or arginine residue present near surface hydrophobic regions. SDS-PAGE results show that the dye is covalently linked to the proteins. To map the hydrophobic surface on proteins, covalently modified proteins will be digested and analyzed using mass spectrometry. Following that, the proteins hydrophobic surface will be visualized using crystallographic structure database for *in-silico* screening of small molecule libraries. These small molecules will be tailored to fit the exposed hydrophobic surface by rational drug design approach and explored for novel therapeutic avenues.

Chapter 1: Introduction

1.1. **Hydrophobicity in a biological system**

Hydrophobicity plays a critical role in many fields and applications such as food chemistry,[1,2] biological systems[3-5] and corrosion resistance.[6-8] Hydrophobicity refers to the absence/exclusion of polar molecules (e.g. water) by nonpolar, uncharged molecules. These nonpolar molecules are unable to undergo dipole-dipole, hydrogen bonding or electrostatic interactions,[9] resulting in a non-polar (hydrophobic) region surrounded by a clathrate structure formed by the surrounding water molecules. Due to the lack of polarity, these molecules are soluble in solvents like alcohol, ether and organic solvents, but are only sparingly soluble in water.[4] Specifically, in the cellular environment, hydrophobicity has a very important role in health but unfortunately, it is implicated in disease as well.

Biological interactions require an aqueous environment,[4] and are dependent on proteins for many functions such as signaling and transport. Some of this diversity in function is facilitated through the use of hydrophobicity.[10] The use of hydrophobicity is crucial to membrane proteins and the variety of functions they perform such as transportation of ions, reception of external messages and

enzymatic function (Figure 1.1). In addition, membrane proteins are shown to account for 27% of the human proteome.[11]
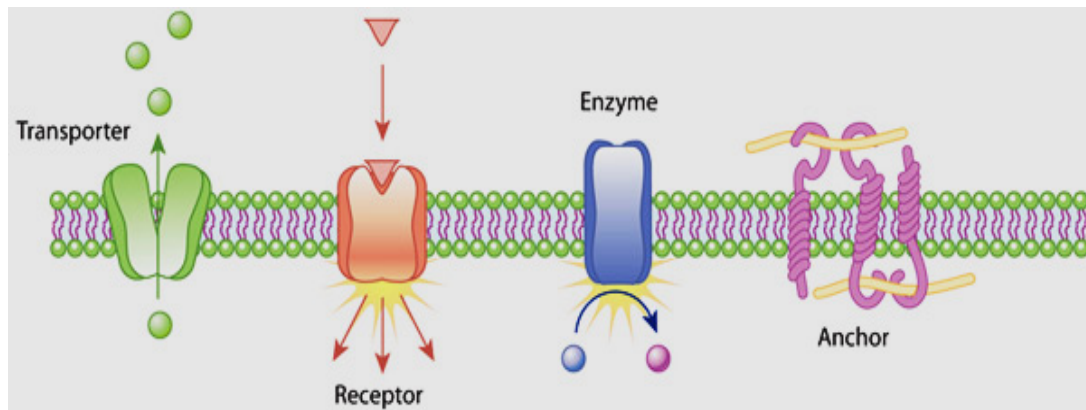
Figure 1.1. Different classes of membrane proteins.[12] These membrane proteins help the cell interact with its environment through ion shuttling reporter-receptor signal transduction, etc.

Another example of the importance of hydrophobicity in membrane proteins is found in clustering and organization of these proteins within the membrane (Figure 1.2). This is seen with SNARE (soluble N-ethylmaleimide-sensitive-factor attachment protein receptor) superfamily proteins.[13] These proteins are small, abundant and anchored in the membrane through hydrophobic C-terminal transmembrane anchors/tails.[13] Using SNARE proteins as a model system, Milovanovic et al.,(2015) showed that organization of these membrane proteins was controlled by the hydrophobic thickening of the membrane.[14] As a result, hydrophobic mismatch of individual proteins was found to contribute to the structural organization of proteins within membranes.[14] This finding was important in understanding the role of SNARE cluster formation in vesicle docking and fusion. Specifically, this study showed the importance of protein

hydrophobicity and membrane hydrophobicity and thickening in the entire mechanism of protein cluster formation.[14] It is therefore essential to recognize the presence and importance of hydrophobicity in a cellular environment.
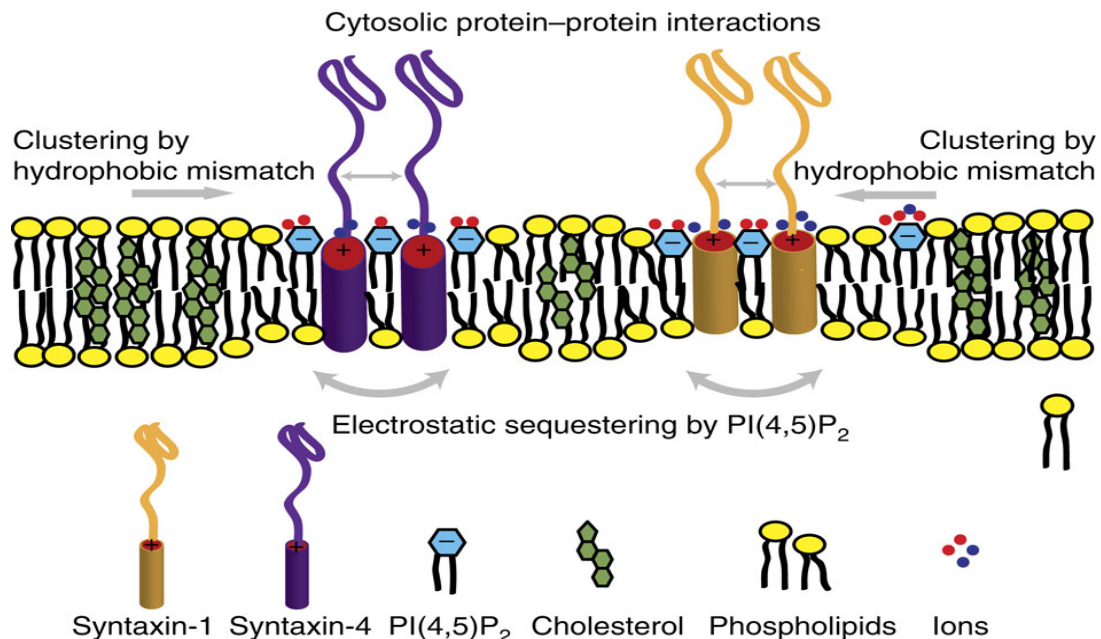
Figure 1.2. Fluid mosaic model of cell membrane.[14] Several players are involved in the cell signaling pathway across the lipid bilayer. The lipid bilayer has a polar (charged) head group at the interface and a hydrophobic interior. Hydrophobic interactions are found to be key to maintaining functions of integral/transmembrane proteins, transport proteins.

Some cells are also able to transform their membrane fluidity by controlling the degree of hydrophobicity by using different lipid tails.[10] This ability helps with resilience of cells to temperature changes and promotes cell survival.[10] Other roles of hydrophobicity within the cellular environment include: signal transduction, molecular recognition and protein-ligand interactions, as well as protein-protein interactions.
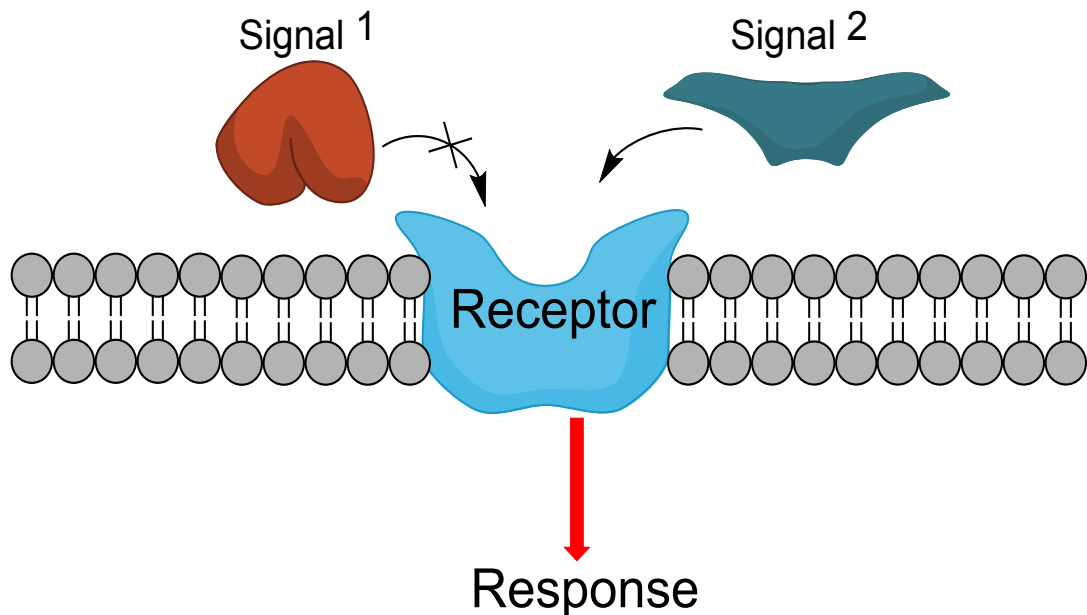
Figure 1.3. Signal transduction and signal specificity through signal-receptor complementarity.[15] The signal-receptor interaction works like a "lock and key" whereby only the correct signal (fit) with corresponding appropriate intermolecular interactions can stimulate a response. Adapted by permission from Macmillan Publishers Ltd: [Nature] (Rosenbaum, D. M., Rasmussen, S. G. F. & Kobilka, B. K. The structure and function of G-protein-coupled receptors. Nature 459, 356-363 (2009)), copyright (2009)

External signals are required for maintaining cellular health and function and are mediated through proteins called signal transducers. These can include membrane proteins that provide information about things like medium pH, osmotic strength, light, chemical agents, food availability, etc.[10] Studies have shown that each signal is specific so that cellular resources are efficiently utilized.[10] The concept of specificity is achieved through the complementarity of the transducer and signal as in hormone type signaling (Figure 1.3).[10] Hydrophobic interactions are utilized to allow reversible interactions between

the signal and receptor and facilitate transport in the case of intracellular receptors. A similar thing is seen in molecular recognition interactions.
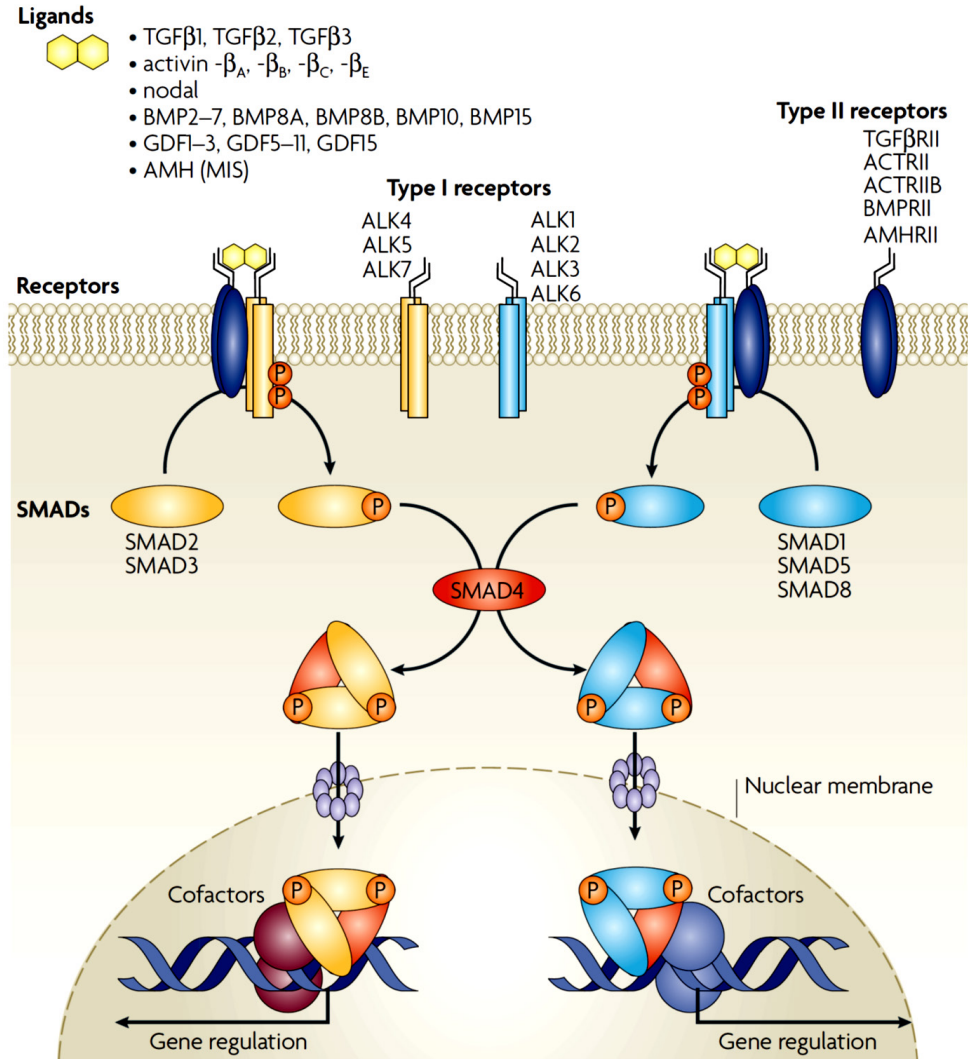
Figure 1.4. Modulation of SMAD signal transduction. Clustering of type I and II receptors allows the signals to activate the SMAD complex and regulate gene expression. Reprinted by permission from Macmillan Publishers Ltd: [Nat Rev Mol Cell Biol] Schmierer, B. & Hill, C. S. TGF[beta]-SMAD signal transduction: molecular specificity and functional flexibility. Nat Rev Mol Cell Biol 8, 970-982 (2007), copyright (2007).[16]

Molecular recognition refers to the noncovalent interaction between two or more molecules.[17] This kind of interaction is facilitated by van der Waals forces, hydrogen bonding, hydrophobic interactions or electrostatic interactions.[17] Examples of this include reactions such as the strong interaction between avidin and biotin[18] which is due to the cooperativity of hydrophobic and hydrophilic (electrostatic) interactions.[19] As such, the concept of hydrophobicity and protein hydrophobicity are important in many aspects of biological homeostasis, however, protein hydrophobicity also has a negative influence as well.

Proteins within the cell have several functions such as in immunity, catalysis, structural integrity, transport and storage, and signal relay.[20] Specifically, protein hydrophobicity is an important consideration for a protein fold, susceptibility of a protein to lysis, polymerization/aggregation of a protein, binding of a protein to lipids or micelles and protein-protein interactions.[21] As a result, a combination of hydrophobic and hydrophilic surfaces also allows for unique properties of proteins such as improved protein-protein interactions, molecular recognition and molecular signaling. Currently, hydrophobicity is shown to contribute significantly to molecular recognition, yet, the mechanisms by which these interactions are facilitated are still poorly understood.[22-24] As a result, many target regions are ignored in drug design due to a lack of understanding of surface properties of target proteins.[23,25]

While *in silico* studies have tried to model and predict the role of hydrophobicity in protein interactions,[22] prediction algorithms still require more detail from experimental data for model refinement.[23,25] This discrepancy is shown between predictions of interaction strength for biotin and streptavidin in theoretical models compared to experimental data.[23] An understanding of the role of these noncovalent interactions at a quantitative level is still lacking.[24] Similarly, in protein-protein interactions, the impact of the hydrophobic effect is well accepted,[26] but again, on a quantitative level, not much is understood.

Protein-protein interactions are responsible for many of the associated functions of proteins within the cell. Formation of protein complexes via protein-protein interactions mediate processes such as protein folding, transport and RNA interference and silencing.[27,28] The RISC complex formation and reformation after disbanding is dependent on weak intermolecular forces such as hydrophobic interactions (Figure 1.5). While electrostatic interactions and dipole-dipole interactions are also present, the predominant force for structural integrity as well as protein target identification is hydrophobic in nature.[28]
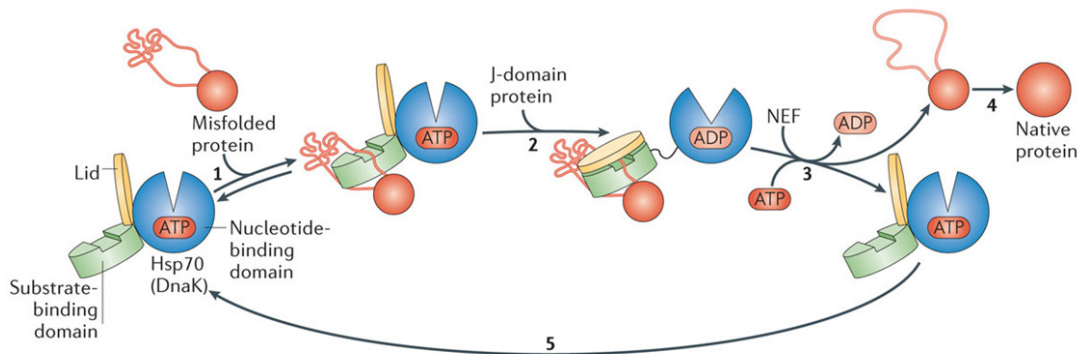
Figure 1.5. Molecular chaperone complex formation showing the interaction of the substrate binding complex with intermediate proteins to facilitate protein folding.[29] Adapted by permission from Macmillan Publishers Ltd: [Nature Reviews Molecular Cell Biology] (Doyle, S. M., Genest, O. & Wickner, S. Protein rescue from aggregates by powerful molecular chaperone machines. Nat Rev Mol Cell Biol 14, 617-629, doi:10.1038/nrm3660 (2013)), copyright (2013).

In the case of molecular chaperones, these protein-protein complexes utilize exposed hydrophobic patches to identify misfolded proteins.[28] These hydrophobic patches are due to the aberrant exposure of hydrophobic amino acids (Figure 1.6) normally found buried in the core of a properly folded protein. Heat shock proteins such as DnaK are known to interact with mostly hydrophobic side chains of amino acids in response to misfolding.[30] Other chaperones such as Hsp70s can bind to many hydrophobic sequences and exhibit allostery in detection.[31] As such, the binding pockets of these proteins have been a target for drug design in diseases.[31] This brief review of the use of hydrophobicity within the cellular environment has highlighted many areas where hydrophobicity is beneficial and necessary for normal cell function.

Although hydrophobicity is very useful, hydrophobicity, and specifically surface hydrophobicity also has a role in disease.
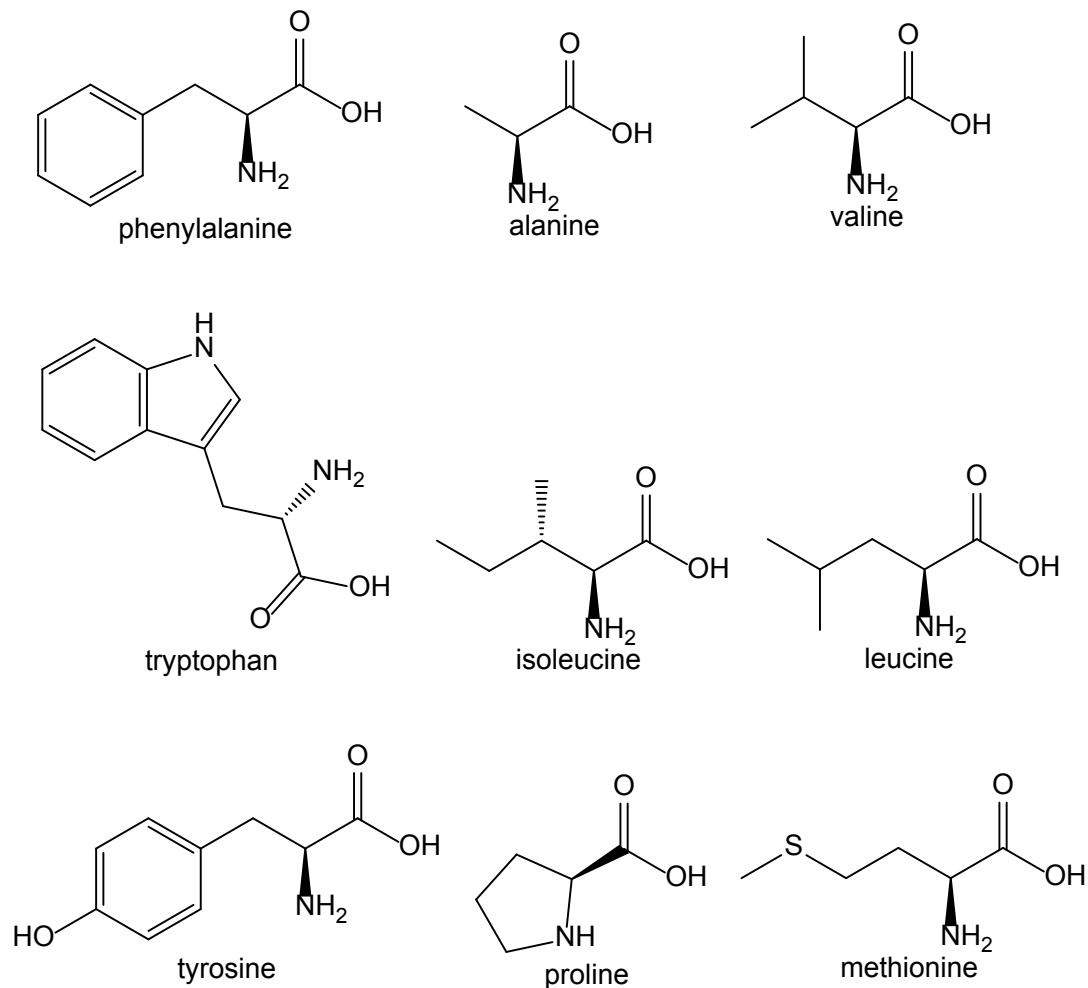
Figure 1.6. Hydrophobic amino acids. These amino acids are nonpolar and are found buried in the interior compartment of a natively folded protein.

Protein surface hydrophobicity refers to the exposed hydrophobic regions (aberrant or normal) that are present in the 3-dimensional model of a protein. It plays a role in aggregate formation due to the hydrophobic exposure of proteins common in neurodegenerative diseases such as amyotrophic lateral sclerosis

(ALS), Alzheimer's (AD), and Huntington's diseases (HD). In addition, a recent discovery of aggregation not related to neurodegeneration was found in amyloid formation at injection sites of diabetic patients.[32,33] This finding along with the role of disulfide scrambling suggests that the mechanism of aggregation is due to structure and not the protein sequence.

The degree to which aggregates are involved in neurotoxicity is still very uncertain and studies have now focused efforts on identifying the toxic species. Studies have concluded that an intermediate species between the native protein and the aggregated are responsible for the observed toxicity.[34]

Mutated proteins or proteins damaged through oxidative stress can lose their function or gain toxic ones due to misfolding and exposure of hydrophobic domains (Figure 1.7). If proteins are not refolded or sent to degradative pathways, these exposed hydrophobic domains can stabilize and facilitate the formation of oligomers and cause toxicity.[35] Studies have also shown that some aggregates may be less toxic or even protective, complicating the issue of which structure should be the target of drug design.[34]
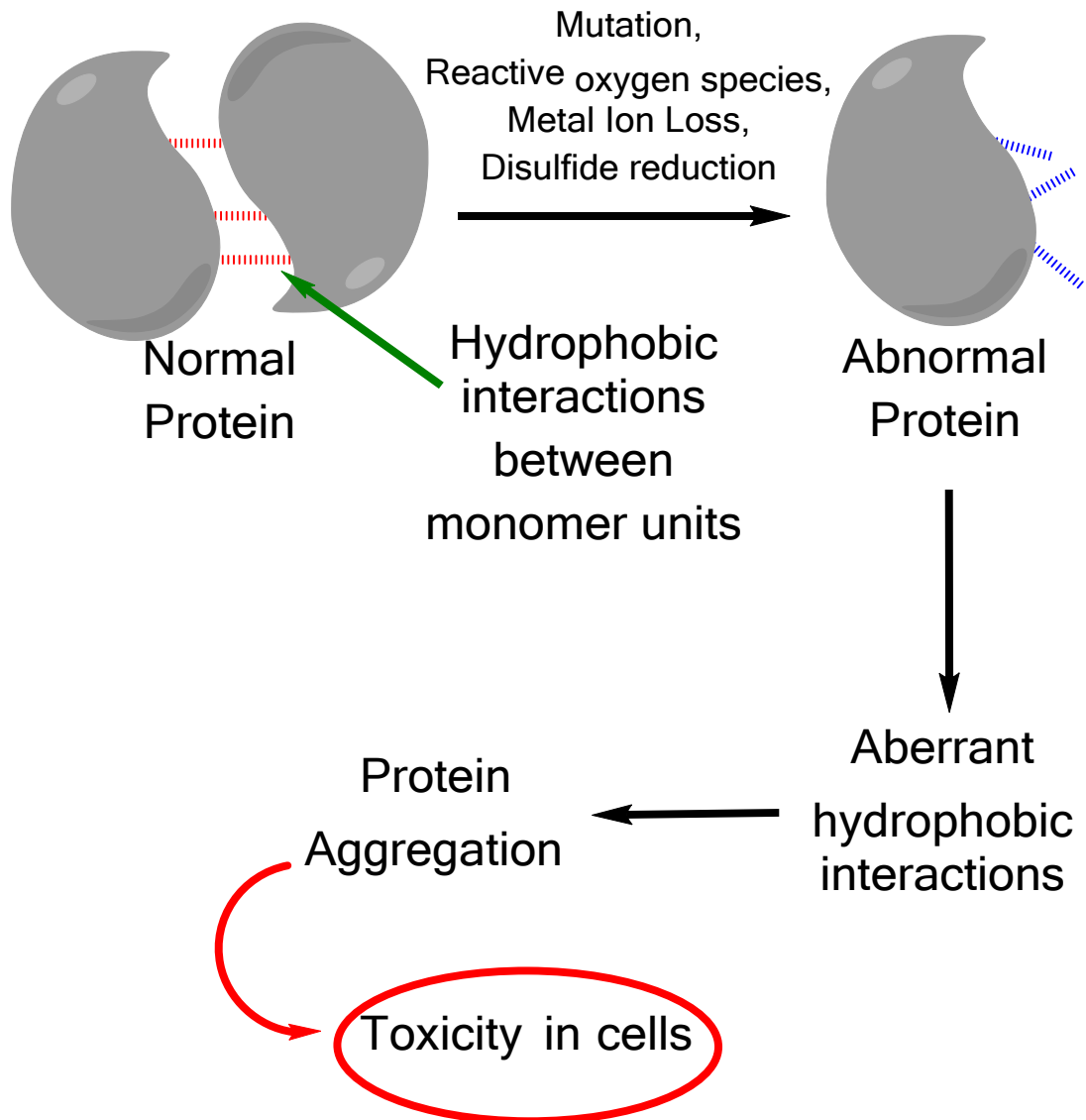
Figure 1.7. Effect of exposed surface hydrophobicity. Figure adapted from Tiwari et al., 2005.[36]

Aberrant surface hydrophobicity of proteins such as superoxide dismutase 1 (SOD1), fused in sarcoma protein or the translocated in liposarcoma protein (FUS/TLS) and tar-DNA protein 43 (TDP-43) are linked to disease progression in amyotrophic lateral sclerosis (ALS online database).[37-39] In addition,

environmental triggers have also been correlated to disease prevalence, but the mechanism of action remains unclear.[40] Military veterans of the United States of America have also been shown to be twice as likely to develop ALS when compared to the general population.[41,42] The only common thing irrespective of the initial trigger (mutation, oxidative stress or environment) is the exposed surface hydrophobicity and the resulting protein instability and aggregation.[36,43-45] Therefore, it is important to address on a quantitative level, the relationship between hydrophobicity and the regulation of toxicity in these diseases.

1.2.   **How is surface hydrophobicity evaluated?**

Current techniques for evaluating the surface hydrophobicity of a protein include ultraviolet-visible (UV-VIS) spectroscopy, fluorescence spectroscopy, molecular modeling, X-ray crystallography and nuclear magnetic resonance (NMR) spectroscopy. However, in consideration of surface hydrophobicity measurements, current tools which directly measure this property suffer from aqueous solubility and sensitivity.

UV-VIS spectroscopy is capable of indirectly evaluating changes in surface hydrophobicity due to aggregate formation by utilizing the absorption profile of dyes such as Thioflavin-T (ThT) and derivatives such as Pittsburgh compound B (PIB).[46] Aggregates are the result of hydrophobic-hydrophobic interactions

between protein molecules that form the protein polymers. This allows an indirect observation of the loss of surface hydrophobicity as a result of the formation of aggregates. While this information is useful for evaluating the aggregation profile of a protein, it does not provide information about the location or the extent of surface hydrophobicity of a particular protein. Alternatively, advancements have been made using extrinsic fluorescent probes as hydrophobicity sensors.

Extrinsic fluorescent probes for hydrophobicity measurements include dyes such as 8-Anilinonaphthalene-1-sulfonic acid (ANS), PRODAN, cis-parinaric acid (CPA), Thioflavin-T (ThT), Fluorescein, Nile Red, Diphenylhexatriene (DPH) and their derivatives (Figure 1.8). The structure of these probes reveal that they are of two major classes: ionic probes or neutral (nonpolar) probes.[47] Interestingly, these probes show very similar responses to changes in the polarity of the environment.[48,49] These extrinsic fluorescent probes can directly assay the local environment of a protein and can be further tuned or modified to function as sensors for hydrophobicity.
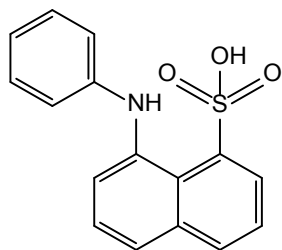
8-Anilino-1-naphthalenesulfonic acid
(ANS)
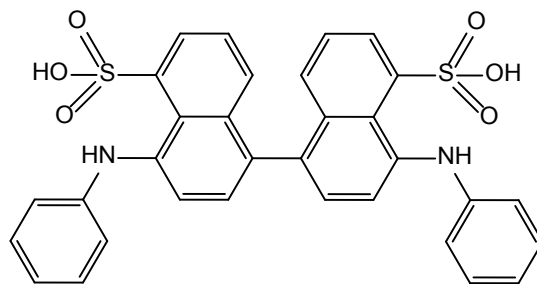
4,4'-Dianilino-1,1'-binaphthyl-5,5'-disulfonic acid
(BIS-ANS)
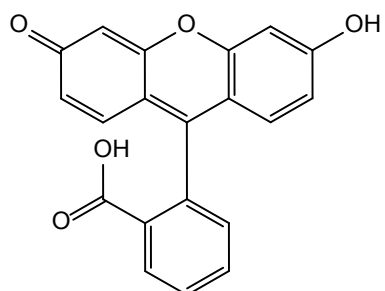
Fluorescein
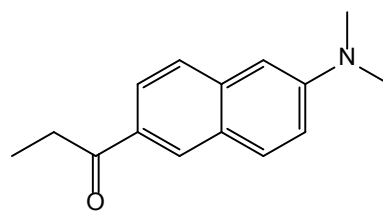
6-Propionyl-2-Dimethylamino-naphthalene
(PRODAN)
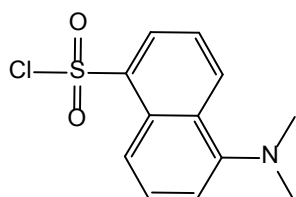
Dansyl-chloride
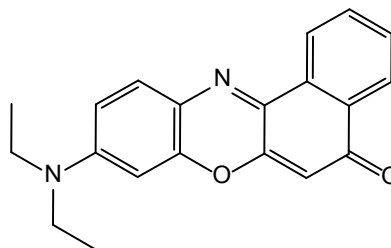
Nile Red
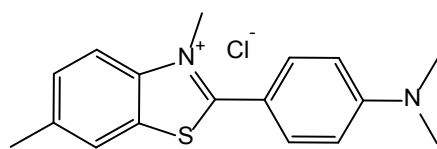
Thioflavin-T (ThT)
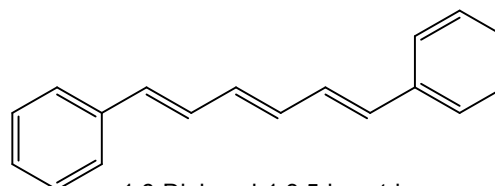
1,6-Diphenyl-1,3,5-hexatriene
(DPH)
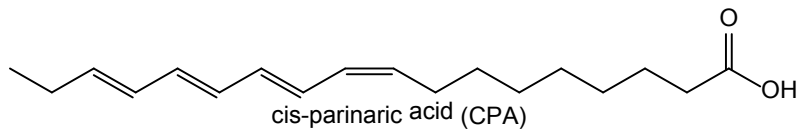
cis-parinaric acid (CPA)

Figure 1.8. Common extrinsic fluorophores for hydrophobicity measurements.

Other techniques for evaluating hydrophobicity include *in silico* techniques such a molecular modeling and docking. *In silico* modeling refers to the computational modeling of the structure of a protein. Structure prediction and protein fold are important for determining and evaluating protein function. As such, the ability to model the protein surface would provide opportunities to predict protein-ligand and protein-protein interactions. One useful application of molecular modeling is molecular docking. In docking studies, a protein and ligand are evaluated for plausible interactions based on the thermodynamics of binding for all their predicted interaction sites.[50] This provides information on binding pockets and the type of interactions at the binding site. Additional techniques that provide even greater details include NMR spectroscopy and X-ray crystallography.

In comparison to spectroscopic techniques, techniques such as X-ray crystallography and NMR spectroscopy provide a wealth of information about the protein structure. These techniques also provide significant insight into binding modes, binding location and dominant forces at play between protein-protein or protein-ligand interactions. The resultant structures have provided useful information on otherwise inaccessible interaction sites and the conditions of those sites. One major limitation to this approach is the large amount of proteins required along with the difficulty of purifying the required amounts of protein.

The current issue, however, is that a discrepancy exists between hydrophobicity measurements (based solely on the average or total hydrophobicity – H_0) as compared to surface hydrophobicity (S_0). Total hydrophobicity measurements have been the preferred hydrophobicity measurement for decades and many hydrophobicity scales have been developed based on this concept.[51,52] Essentially, the proteins are given a score based on the average hydrophobicity when all hydrophobic amino acids have been accounted relative to the entire protein sequence.[53] This sort of hydrophobicity measurement has been especially useful in predicting the level of interaction between hydrophobic resins and proteins.[54,55] Unfortunately, experimental data has shown that the hydrophobicity that these scales correspond to represent the average hydrophobicity of a protein and not the surface exposed hydrophobicity.[2,56] This distinction is quite important and is essential for considerations in providing useful information that can be used to further refine *in silico* techniques.

In pioneer work conducted by Nakai and others, it was found that the surface hydrophobicity, which can be correlated to the excess in fluorescence of a hydrophobic probe bound to a protein, gave a more complete picture of surface interactions.[2,56] On the other hand, average hydrophobicity accurately predicts protein retention in hydrophobic interaction chromatography (HIC) columns as well as high pressure liquid chromatography (HPLC). In organic solvents, the protein is unable to maintain native fold resulting in an increase in exposed

hydrophobicity which can be accounted for by the average hydrophobicity of that protein. The surface hydrophobicity, however, is measured in consideration of the 3D fold of the protein.

1.3. **Why do we need novel probes?**

When considering techniques such as NMR and X-ray crystallography, the major drawback is that these are both very time consuming and require a significant amount of protein for experiments. Purification of large amounts of a test protein are difficult and can be very expensive if commercially available protein samples are used. In addition, NMR, requires the use of radioactively labeled proteins, imposing an additional safety risk.

In silico techniques are dependent on experimental data to efficiently build models. In turn, the experimental data requires sensitive tools in order to help provide the quantitative data needed. This data can then be used to further refine the algorithms used for model prediction. As such, the current modeling capabilities are hindered by the lack of quantitative data.

In contrast, spectroscopic techniques require much less protein, are quick, and quite simple to replicate. As a result, spectroscopic tools are most commonly used. The tools are much cheaper in comparison to crystallography and are

definitely much safer compared to NMR spectroscopy. Unfortunately, even the current tools available for spectroscopic studies of proteins have limitations such as low sensitivity. Extrinsic probes like ANS, PRODAN, DPH all show reduced fluorescence signal in a polar environment, but the signal increases dramatically in a hydrophobic environment. Furthermore, poor solubility of these probes make them difficult to use in aqueous environments. To complicate things further, the electrostatic interactions of the ionic probes are also known to influence the fluorescence intensity as well. As a result, while spectroscopy is definitely the way forward, there are many areas that require significant advances in order to effectively utilize such tools.

The ability to measure surface hydrophobicity can impact rational drug development as well as its associated fields. The availability of structural information at a quantitative level can also impact the way we visualize and evaluate proteins and can be done through hydrophobic labeling and mapping.

1.4. **What is surface hydrophobicity mapping?**

The fold of a protein is essential to its function and as a result, much work has been done on understanding protein folding mechanisms. Within the cell, there are thousands of other proteins, cell components and small molecules, all within

an aqueous environment. This crowded space makes for a challenge to properly fold any protein. Currently, there are several mechanisms by which proteins are correctly folded, and these include, chaperones, the hydrophobic collapse mechanism as well as other perfectly designed mechanisms aimed to reduce error in protein folding. However, this can fail due to errors in the genetic code (mutations), cellular stress, generating misfolded protein forms leading to disease.

These misfolded proteins may lack the ability to bind to metal cofactors or maintain the rigid "lock and key" fold which in turn inhibits protein functionality. These misfolded proteins have been noted to possess or exhibit greater surface hydrophobicity which can promote aberrant interactions. An ability to measure, map and identify the locations of aberrant hydrophobic interactions is the goal of surface hydrophobic mapping.

Specifically, protein surface hydrophobicity mapping utilizes a fluorescent probe which identifies hydrophobic regions on the protein surface and allows for quantitative determination of the size of the hydrophobic site. This can be done by exploiting the hydrophobic sensing ability of these probes, and then using the covalent linker to fix the probe to the protein surface. As a result, the covalent linkage of the fluorescent probe to the protein of interest is directed by: 1) the availability of an exposed hydrophobic region on the surface of the

protein; and 2) an available linker on the protein which is near the hydrophobic site. Current linkages are routinely done via the use of an N-hydroxysuccinimide (NHS) ester linkage.

Coupled with ESI mass spectrometry and other proteomic techniques, it is then possible to identify the exact location of the fluorescent probe. Using this information along with available crystallographic data, it is then possible to evaluate the extent (quantitatively) of the hydrophobic exposure.

1.5. **Research Objective and outline**

Understanding the surface hydrophobicity of a protein allows for greater insight into protein interactions with membranes, other proteins, and the cell in general. This then allows us to understand the protein function at greater detail not conferred previously. The availability of this kind of information is also useful in helping to evaluate and determine aggregation mechanisms. Applications would also include allowing us to target specific regions of a protein or structure based solely on the exposed hydrophobic surface. This alone has the potential to exponentially improve rational drug design and help ease patient symptoms in neurodegeneration as well as other proteinopathies. A targeted approach using "designer" drugs would go a long way to improving the health of an aging population.

As emphasized previously, detection techniques employing extrinsic fluorescence probes in biological systems are currently limited due to existing probes poor solubility, low sensitivity, or a combination of both in aqueous environment. The development of these new tools is intended to provide greater structural detail on the surface properties of these proteins. The findings discussed can also be applied to fields as diverse as food chemistry (where surface interactions are a good measure of food texture and other palatable attributes) as well as to traumatic brain injury (where profiles of protein aggregation similar to as seen in neurodegeneration are found).

The aim of the research described in this work is two-fold. First, the ability to successfully and efficiently detect surface hydrophobicity of proteins by designing novel sensors with improved solubility and higher sensitivity. Second, in order to accurately characterize surface hydrophobic interactions, it is important to visualize and map the hydrophobic surface of a protein in a quantitative manner. This will be accomplished by making probes that can label the surface exposed hydrophobic regions, which ultimately can be identified using proteomics approach. For addressing both the above concerns i.e. hydrophobic sensing and mapping fluorescence probes will be employed. This will aid in quick screening of the surface hydrophobic regions on the protein.

The overall workflow of the research is shown in figure 1.9 outlining the design of hydrophobicity sensors as well as probes for surface hydrophobicity labeling and mapping. Successful and efficient probes were then utilized to evaluate systems *in vitro*. In greater detail, this research utilized functionalization on the BODIPY core to first address the water solubility issue and improve sensitivity. Further modifications by way of introducing electron donating groups were then used to evaluate the impact on efficient detection of surface hydrophobicity.
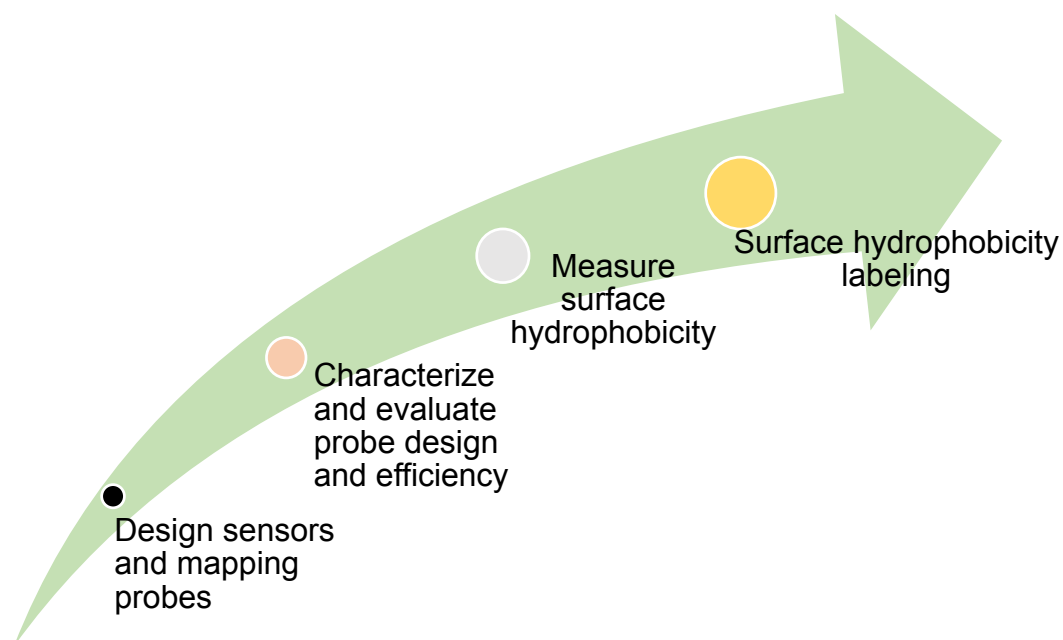
Figure 1.9. **Outline of research**. Fluorescent probes will be designed for both sensing and mapping of surface hydrophobicity. After characterization of all probes, efficient probes will be used to sense and map surface hydrophobicity.

In chapter 2, a brief description of the current design of fluorescent probes for surface hydrophobicity measurements and improvements made using the BODIPY group of hydrophobicity sensors (HPsensors) was introduced. The

concept of probe design and the rationale for using the BODIDPY system for hydrophobicity sensors was also discussed along with considerations of the substituent groups and their impact on fluorescence.

In chapter 3, all methods used were described. A brief description of every technique used as well as greater detail on some of the techniques employed in hydrophobicity measurements was addressed. This chapter served as an overview of techniques such as NMR spectroscopy, X-ray crystallography, Molecular modeling and other spectroscopic techniques. This provided the background and necessary details for experimental conditions.

Chapter 4 focused on the production and application of HPsensors for hydrophobic sensing. BODIPY-based hydrophobic sensors were made. The hydrophobic sensing property was achieved by modulation of the HOMO LUMO gap by aryl substitution at meso position and its solubility was improved by adding a methoxyethyl amine tail. The "on-off" sensing mechanism was mediated through rotational quenching and as such allowed these probes to increase sensitivity to the nonpolar/hydrophobic environment. These novel probes were tested using three well characterized proteins.

Similarly, in chapter 5, the concept of hydrophobic labeling was investigated using a modified ANS probe. Building on the capabilities of the fluorescent probe

ANS, the hydrophobic sensing ability was further exploited by covalently linking the probe to proteins. This linkage facilitated by lysine and arginine groups was dependent on two parameters: 1) the presence of a surface exposed hydrophobic region; and 2) the presence of a lysine or arginine group near the hydrophobic region.

Finally, in chapter 6, the future work using the concept of hydrophobic labeling to facilitate hydrophobic mapping along with improvements of HPsensors is discussed. In future, the attached probes can be used as markers in identifying quantitative details on the surface exposed hydrophobicity of proteins. This final application of hydrophobicity sensors would provide the necessary information required for rational drug design, allow for improvements in modeling confidence and as such provide a greater depth of understanding of the protein aggregation problem. It would then be possible to answer the age-old question about the identity and topography of the toxic species. In addition to this, improvements to functionality (sensitivity, *in vivo* application, etc.) of surface hydrophobicity sensors and hydrophobicity mapping probes via *in silico* techniques will be discussed.

In summary, this work showcases a novel suite of BODIPY probes along with a method of evaluating surface hydrophobicity with high sensitivity. In addition, labeling of surface hydrophobic regions on protein was also achieved using a

modified version of the well characterized probe ANS. These findings have applications for future studies where a greater understanding of the role of surface hydrophobicity in the test system is required. Therefore, this work makes a significant contribution to this specific field and the understanding of exposed surface hydrophobicity.

1.6. **References**

1   Wagner, J. R., Sorgentini, D. A. & Añón, M. C. Relation between solubility and surface hydrophobicity as an indicator of modifications during preparation processes of commercial and laboratory-prepared soy protein isolates. *J. Agric. Food Chem.* **48**, 3159-3165 (2000).

2   Kato, A. & Nakai, S. Hydrophobicity determined by a fluorescence probe method and its correlation with surface properties of proteins. *Biochim. Biophys. Acta* **624**, 13-20 (1980).

3   Chandler, D. Hydrophobicity: Two faces of water. *Nature* **417**, 491-491 (2002).

4   Tanford, C. *The hydrophobic effect: formation of micelles and biological membranes.* (Wiley, 1980).

5   Koga, T. *et al.* Surface hydrophobicity, adherence, and aggregation of cell surface protein antigen mutants of Streptococcus mutans serotype c. *Infection and immunity* **58**, 289-296 (1990).

6   Ahmad, Z., Khan, A. U., Farooq, R., Mastoi, N. R. & Saif, T. Hydrophobicity — A Green Technique for Enhancing Corrosion Resistance of Alloys. doi:10.5772/60815 (2015).

7   Liu, T., Yin, Y., Chen, S., Chang, X. & Cheng, S. Super-hydrophobic surfaces improve corrosion resistance of copper in seawater. *Electrochimica Acta* **52**, 3709-3713 (2007).

8   Shen, G. X., Chen, Y. C., Lin, L., Lin, C. J. & Scantlebury, D. Study on a hydrophobic nano-TiO 2 coating and its properties for corrosion protection of metals. *Electrochimica Acta* **50**, 5083-5089 (2005).

9   Mozes, N. & Rouxhet, P. G. Methods for measuring hydrophobicity of microorganisms. *J. Microbiol. Meth.* **6** 99-112 (1987).

10   Nelson, D. L., Lehninger, A. L. & Cox, M. M. *Lehninger principles of biochemistry*. (Macmillan, 2008).

11   Uhlen, M. *et al.* Proteomics. Tissue-based map of the human proteome. *Science* **347**, 1260419, doi:10.1126/science.1260419 (2015).

12   O'Connor, C. M. & Adams, J. U. in *Essentials of Cell Biology Specialized Membranes Organize the Eukaryotic Cell Cytoplasm into Compartments* (ed Clare O'Connor) (NPG Education, Cambridge, MA, 2010).

13   Ungar, D. & Hughson, F. M. SNARE Protein Structure and Function. *Annual Review of Cell and Developmental Biology* **19**, 493-517, doi:10.1146/annurev.cellbio.19.110701.155609 (2003).

14   Milovanovic, D. *et al.* Hydrophobic mismatch sorts SNARE proteins into distinct membrane domains. *Nat Commun* **6**, doi:10.1038/ncomms6984 (2015).

15   Rosenbaum, D. M., Rasmussen, S. G. F. & Kobilka, B. K. The structure and function of G-protein-coupled receptors. *Nature* **459**, 356-363 (2009).

16   Schmierer, B. & Hill, C. S. TGF[beta]-SMAD signal transduction: molecular specificity and functional flexibility. *Nat Rev Mol Cell Biol* **8**, 970-982 (2007).

17   Cleaves, H. J. in *Encyclopedia of Astrobiology*   (eds Muriel Gargaud *et al.*) 1079-1080 (Springer Berlin Heidelberg, 2011).

18   Wilchek, M. & Bayer, E. A. in *Methods in Enzymology* Vol. Volume 184 (eds Wilchek Meir & A. Bayer Edward) 5-13 (Academic Press, 1990).

19   Livnah, O., Bayer, E. A., Wilchek, M. & Sussman, J. L. Three-dimensional structures of avidin and the avidin-biotin complex. *Proceedings of the National Academy of Sciences* **90**, 5076-5080 (1993).

20   National Library of Medicine & (US). *What are proteins and what do they do?*, <https://ghr.nlm.nih.gov/handbook/howgeneswork/protein> (2016).

21   Chelh, I., Gatellier, P. & Sante-Lhoutellier, V. Technical note: A simplified procedure for myofibril hydrophobicity determination. *Meat Sci* **74**, 681-683, doi:10.1016/j.meatsci.2006.05.019 (2006).

22   Vakser, I. A. & Aflalo, C. Hydrophobic docking: a proposed enhancement to molecular recognition techniques. *Proteins* **20**, 320-329, doi:10.1002/prot.340200405 (1994).

23   Young, T., Abel, R., Kim, B., Berne, B. J. & Friesner, R. A. Motifs for molecular recognition exploiting hydrophobic enclosure in protein-ligand binding. *Proceedings of the National Academy of Sciences of the United States of America* **104**, 808-813, doi:10.1073/pnas.0610202104 (2007).

24   Chandler, D. Interfaces and the driving force of hydrophobic assembly. *Nature* **437**, 640-647 (2005).

25 Persch, E., Dumele, O. & Diederich, F. Molecular Recognition in Chemical and Biological Systems. *Angewandte Chemie International Edition* **54**, 3290-3327, doi:10.1002/anie.201408487 (2015).

26 Ma, B., Elkayam, T., Wolfson, H. & Nussinov, R. Protein-protein interactions: structurally conserved residues distinguish between binding sites and exposed protein surfaces. *Proceedings of the National Academy of Sciences of the United States of America* **100**, 5772-5777, doi:10.1073/pnas.1030237100 (2003).

27 Schwarz, D. S. *et al.* Asymmetry in the Assembly of the RNAi Enzyme Complex. *Cell* **115**, 199-208, doi:http://dx.doi.org/10.1016/S0092-8674(03)00759-1 (2003).

28 Richter, K., Haslbeck, M. & Buchner, J. The heat shock response: life on the verge of death. *Mol Cell* **40**, 253-266, doi:10.1016/j.molcel.2010.10.006 (2010).

29 Doyle, S. M., Genest, O. & Wickner, S. Protein rescue from aggregates by powerful molecular chaperone machines. *Nat Rev Mol Cell Biol* **14**, 617-629, doi:10.1038/nrm3660 (2013).

30 Zhu, X. *et al.* Structural Analysis of Substrate Binding by the Molecular Chaperone DnaK. *Science* **272**, 1606-1614 (1996).

31 Zuiderweg, E. R. *et al.* Allostery in the Hsp70 chaperone proteins. *Top Curr Chem* **328**, 99-153, doi:10.1007/128_2012_323 (2013).

32 Shikama, Y. *et al.* Localized Amyloidosis at the Site of Repeated Insulin Injection in a Diabetic Patient. *Internal Medicine* **49**, 397-401, doi:10.2169/internalmedicine.49.2633 (2010).

33 Yumlu, S., Barany, R., Eriksson, M. & Röcken, C. Localized insulin-derived amyloidosis in patients with diabetes mellitus: a case report. *Human pathology* **40**, 1655-1660 (2009).

34 Campioni, S. *et al.* A causative link between the structure of aberrant protein oligomers and their toxicity. *Nat Chem Biol* **6**, 140-147, doi:10.1038/nchembio.283 (2010).

35 Krebs, M. R. H., Morozova-Roche, L. A., Daniel, K., Robinson, C. V. & Dobson, C. M. Observation of sequence specificity in the seeding of protein amyloid fibrils. *Protein Science* **13**, 1933-1938 (2004).

36 Tiwari, A., Xu, Z. & Hayward, L. J. Aberrantly Increased Hydrophobicity Shared by Mutants of Cu,Zn-Superoxide Dismutase in Familial Amyotrophic Lateral Sclerosis. *J. Biol. Chem.* **280**, 29771-29779, doi:10.1074/jbc.M504039200 (2005).

37 Abel, O. *et al.* Development of a Smartphone App for a Genetics Website: The Amyotrophic Lateral Sclerosis Online Genetics Database (ALSoD). *JMIR Mhealth Uhealth* **1**, e18, doi:10.2196/mhealth.2706 (2013).

38 Radunovic, A. & Leigh, P. N. ALSODatabase: database of SOD1 (and other) gene mutations in ALS on the Internet. European FALS Group and ALSOD Consortium. *Amyotrophic lateral sclerosis and other motor neuron disorders*

: official publication of the World Federation of Neurology, Research Group on Motor Neuron Diseases **1**, 45-49 (1999).

39 Abel, O. *ALSoD (ALS online database)*, <http://alsod.iop.kcl.ac.uk/> (2016).

40 Wicklund, M. P. Amyotrophic Lateral Sclerosis: Possible Role of Environmental Influences. *Neurologic Clinics* **23**, 461-484, doi:10.1016/j.ncl.2004.12.016 (2005).

41 Coffman, C. J., Horner, R. D., Grambow, S. C. & Lindquist, J. Estimating the Occurrence of Amyotrophic Lateral Sclerosis among Gulf War (1990–1991) Veterans Using Capture-Recapture Methods. *Neuroepidemiology* **24**, 141-150 (2005).

42 Yu, Y. *et al.* Environmental risk factors and amyotrophic lateral sclerosis (ALS): a case-control study of ALS in Michigan. *PLoS One* **9**, e101186, doi:10.1371/journal.pone.0101186 (2014).

43 Zerze, G. H., Mullen, R. G., Levine, Z. A., Shea, J. E. & Mittal, J. To What Extent Does Surface Hydrophobicity Dictate Peptide Folding and Stability near Surfaces? *Langmuir* **31**, 12223-12230, doi:10.1021/acs.langmuir.5b03814 (2015).

44 Tanford, C. The Hydrophobic Effect and the Organization of Living Matter. *Science* **200**, 1012-1018 (1978).

45 Tiwari, A. *et al.* Metal deficiency increases aberrant hydrophobicity of mutant superoxide dismutases that cause amyotrophic lateral sclerosis. *J. Biol. Chem.* **284**, 27746-27758, doi:10.1074/jbc.M109.043729 (2009).

46 Wu, C., Bowers, M. T. & Shea, J. E. On the origin of the stronger binding of PIB over thioflavin T to protofibrils of the Alzheimer amyloid-beta peptide: a molecular dynamics study. *Biophys J* **100**, 1316-1324, doi:10.1016/j.bpj.2011.01.058 (2011).

47 Haskard, C. A. & Li-Chan, E. C. Y. Hydrophobicity of Bovine Serum Albumin and Ovalbumin Determined Using Uncharged (PRODAN) and Anionic (ANS-) Fluorescent Probes. *J. Agric. Food Chem.* **46**, 2671-2677 (1998).

48 Greenspan, P., Mayer, E. P. & Fowler, S. D. Nile red: a selective fluorescent stain for intracellular lipid droplets. *J. Cell Biology* **100**, 965-973 (1985).

49 Robinson, G. W. *et al.* Picosecond studies of the fluorescence probe molecule 8-anilino-1-naphthalenesulfonic acid. *J. Am. Chem. Soc.* **100**, 7145-7150 (1978).

50 Rapaport, D. C. *The art of molecular dynamics simulation*. (Cambridge university press, 2004).

51 Bigelow, C. C. On the average hydrophobicity of proteins and the relation between it and protein structure. *J. Theor. Biol.* **16**, 187-211 (1967).

52 Bigelow, C. C. & Channon, M. *Handbook of Biochemistry and Molecular Biology*. 3 edn, Vol. 1 209–243 (CRC Press, 1976).

53 Kyte, J. & Doolittle, R. F. A Simple Method for Displaying the Hydropathic Character of a Protein. *J. Mol. Biol.* **157**, 105-132 (1982).

54 Fausnaugh, J. L., Kennedy, L. A. & Regnier, F. E. Comparison of hydrophobic-interaction and reversed-phase chromatography of proteins. *J.*

Chromatogr. A **317**, 141-155, doi:http://dx.doi.org/10.1016/S0021-9673(01)91654-1 (1984).

55 Lienqueo, M. E., Mahn, A. & Asenjo, J. A. Mathematical correlations for predicting protein retention times in hydrophobic interaction chromatography. *J. Chromatogr. A* **978**, 71-79, doi:http://dx.doi.org/10.1016/S0021-9673(02)01358-4 (2002).

56 Nakai, S., Li-Chan, E. & Arteaga, G. E. in *Methods of testing protein functionality* (ed G. M. Hall) Ch. 8, 226 - 255 (Blackie A & P, 1996).

Chapter 2: Probe design for detection and mapping the surface hydrophobicity of proteins

2.1.   Design of current fluorescent probes.

Currently, only a few probes exist for measuring the surface hydrophobicity of proteins. Existing probes that are available for detecting surface hydrophobicity are either in the ionic form or in the neutral form.[1] Due to the contribution of electrostatic interactions, cationic and anionic probes have different affinities for binding sites that affects the overall flourescence.[2] As an example, anionic probes have been shown to better interact with proteins;[1] however, these tend to show overestimation of protein hydrophobicity due to contribution from electrostatic interactions.[2] Neutral probes which are nonpolar are currently favored for measuring the surface hydrophobicity, but they come with a few limitations that will be discussed below.

Studies have shown that neutral probes exhibit poor water solubility along with the requirement of non-biocompatible solvents.[3,4] Even though, neutral probes show good sensitivity, poor solubility in aqueous media poses challenges in evaluating surface hydrophobicity. On the other hand, ionic probes often show inflated fluorescence signal due to electrostatic contribution[1,5] and some require a buried hydrophobic pocket to show measurable signal[6] (figure 2.1). These

properties seriously limits their use for surface hydrophobic measurements. Current existing ionic and neutral probes used for measuring protein hydrophobicity behave similarly in response to solvent polarity, both showing decreased fluorescence signal as polarity of solvent increases[2,4,5] despite their differences. These findings suggest a common mechanism for fluorescence enhancement for the two types of probes.
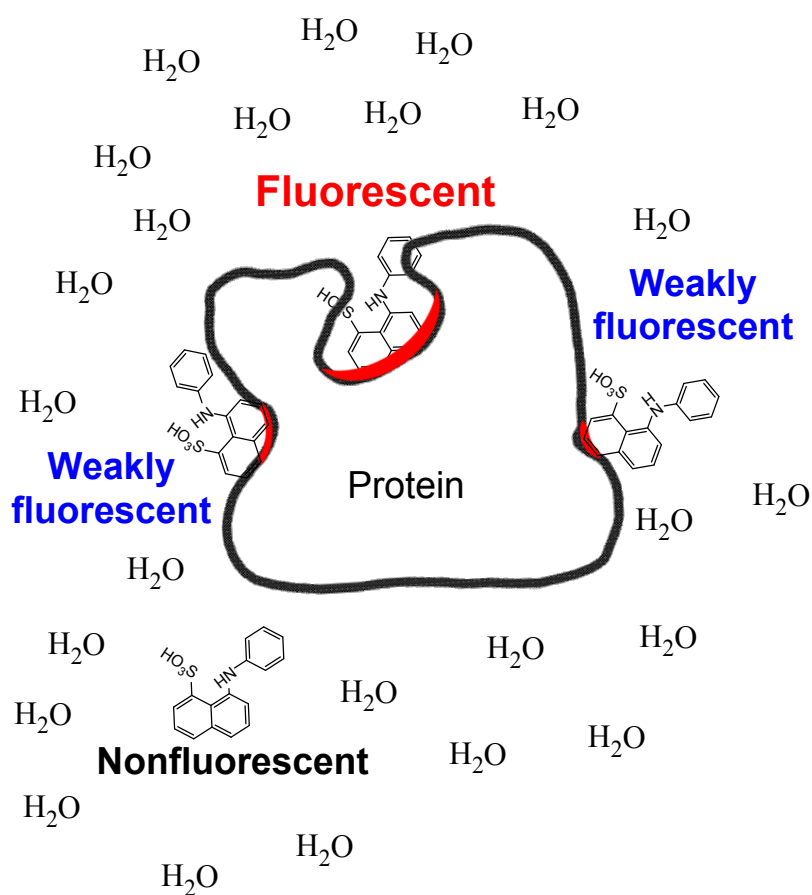

Figure 2.1. 8-anilino-1-naphthalenesulfonic acid (ANS) preferentially fluoresces when bound in a hydrophobic pocket. Adapted from Matulis et al 1999 with permission.[7] Only a small percentage of bound ANS, and specifically molecules in hydrophobic pockets contribute to observed fluorescence of ANS.

Currently, ANS is the most commonly used dye for measuring protein hydrophobicity. It is an anionic dye and its fluorescence contributions can be due to electrostatic as well as hydrophobic interactions leading to overestimation of the fluorescence signal.[2] In aqueous environment, the fluorescence signal of ANS is weak or gets quenched[6] limiting its use for surface hydrophobicity measurements. Now, a new class of fluorescent probes based on 4,4-difluoro-4-bora-3a,4a-diaza-s-indacene (BODIPY) are becoming increasingly popular. This is because they are highly fluorescent in nonpolar media but are also fluorescent in polar (aqueous) media. In addition, they have sharp and narrow emission peaks, possess reduced solvatochromic shifts,[27,28] and are highly tunable.[29-32] The goal is to use BODIPY based fluorescent probes that are able to differentiate between surface exposed hydrophobicity of proteins as opposed to hydrophobicity buried in pockets. Therefore, to design such probes, three major things need to be considered: the overall design of the probe (basic system on which the probe will be built: BODIPY, Naphthalene, etc), the method of detection/sensing (on-off vs off-on),[8] and the energy band gap (for efficient sensitivity).[9]

A typical fluorescent sensor generally is comprised of three parts: 1) the acceptor/fluorophore, 2) the spacer/linker, and 3) the sensor/receptor.[8] In our case, we have adapted these three parts to the solubilizer, the fluorescent

moiety, and the sensor (figure 2.2). Other arrangements of fluorophore and receptor include the integrated and the twisted conformations (figure 2.3).[8]
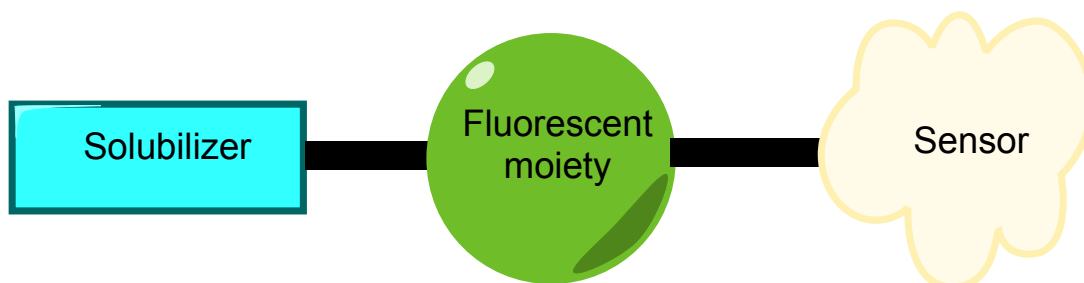

Figure 2.2. Overall concept of HPsensor design. The different parts work together to improve solubility and sensitivity of the probes.
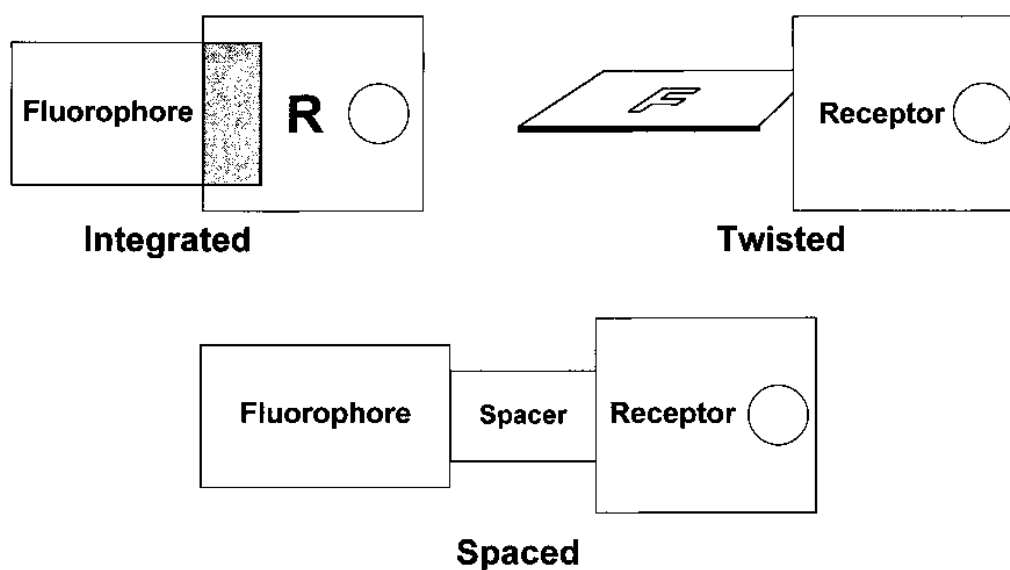

Figure 2.3. Sensor arrangements for fluorophore and receptor. Reproduced from De Silva et al 1997 with permission.[8] De Silva, A. P. et al. Signaling recognition events with fluorescent sensors and switches. Chemical Reviews 97, 1515-1566 (1997)

In the classical design, the fluorophore module functions as the site of both excitation and emission. The receptor/sensor module is responsible for complexing with the signal of interest and leads to the "on-off" or "off-on"

mechanism. Finally, the spacer module is primarily responsible for separating fluorophore and receptor so that they are close to each other but are still distinct structures.

2.2. **BODIPY based fluorescent probes.**

BODIPY based probes have been known for several great qualities: they are highly fluorescent in nonpolar media but are also fluorescent in polar (aqueous) media. While BODIPY dyes were first synthesized in the late 60's,[10] their use had been limited for biological applications due to poor solubility in aqueous media. These compounds and their derivatives show great potential for functionalization and use in countless scenarios.[11-22] This alone makes this class of dyes a favorite among synthetic chemists interested in spectroscopic studies of biological samples.
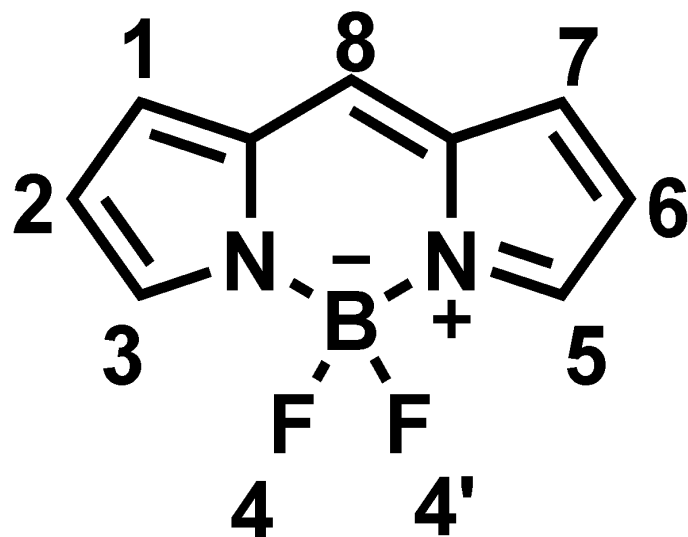
Fig. 2.4. The BODIPY core. Image of the BODIPY core showing the 8 available substitution points.

The BODIPY core (figure 2.4) is a neutral, nonpolar chromophore with eight possible positions for functionalization.[10] These substitution sites control the electronic properties of the BODIPY dyes[23-26] and can be used to improve its properties such as water solubility, quantum yield and sensing.[24-29] Therefore, tuning of the core with different functional groups that increase its sensitivity to solvent polarity would allow us to evaluate ideal substitutions for characterizing protein hydrophobicity.
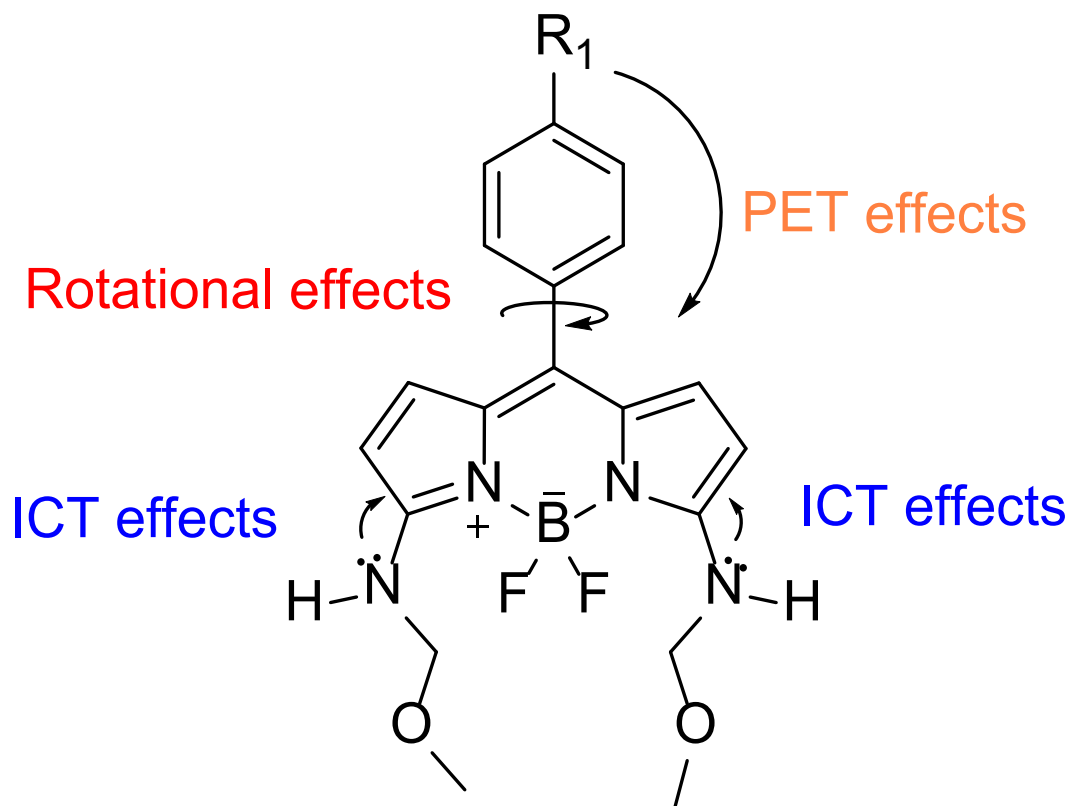
Figure 2.5. Possible quenching mechanisms for "turn-on" or "turn-off" sensing mechanism. Based on the structure, there are three possible mechanisms for fluorescence quenching, however, rotational quenching has the most significant impact on the fluorescence of these probes.

To increase water solubility we substituted 2-methoxyethylamine group at 3,5-position of the BODIPY core. For increasing hydrophobic sensing we focused our efforts on *aryl* substitutions at *meso* position on BODIPY dye.
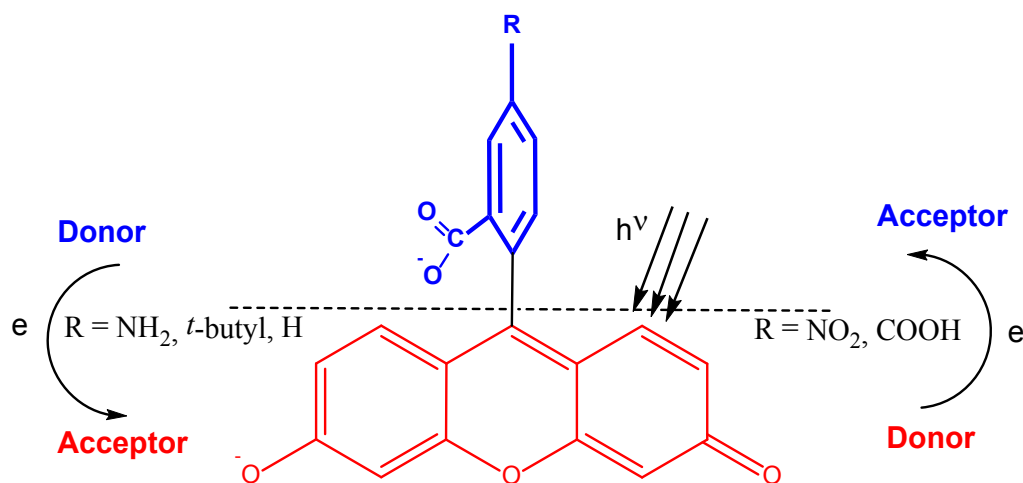
Figure 2.6. Impact of meso substituent on donor/acceptor role. Reproduced from Zhang 2010[30] with permission of The Royal Society of Chemistry (RSC) on behalf of the European Society for Photobiology, the European Photochemistry Association and the RSC.

Studies show that electron donating or electron withdrawing group substitutions impact fluorescence wavelength and the quantum yield of BODIPY dyes via the photo-induced electron transfer (PET) mechanism (figure 2.5).[30-32] The electron withdrawing group (EWG) or electron donating group (EDG) attached to the aryl counterparts are able to either activate or deactivate the aryl group respectively (figure 2.6).[33,34] As a result, selection of an EWG or EDG will ultimately alter the HOMO-LUMO energy gap and modulate the fluorescence of the hydrophobicity sensor.[9] Therefore, a rational design can be used in selecting and utilizing the correct electron donating group for maximum sensitivity (figure 2.7).
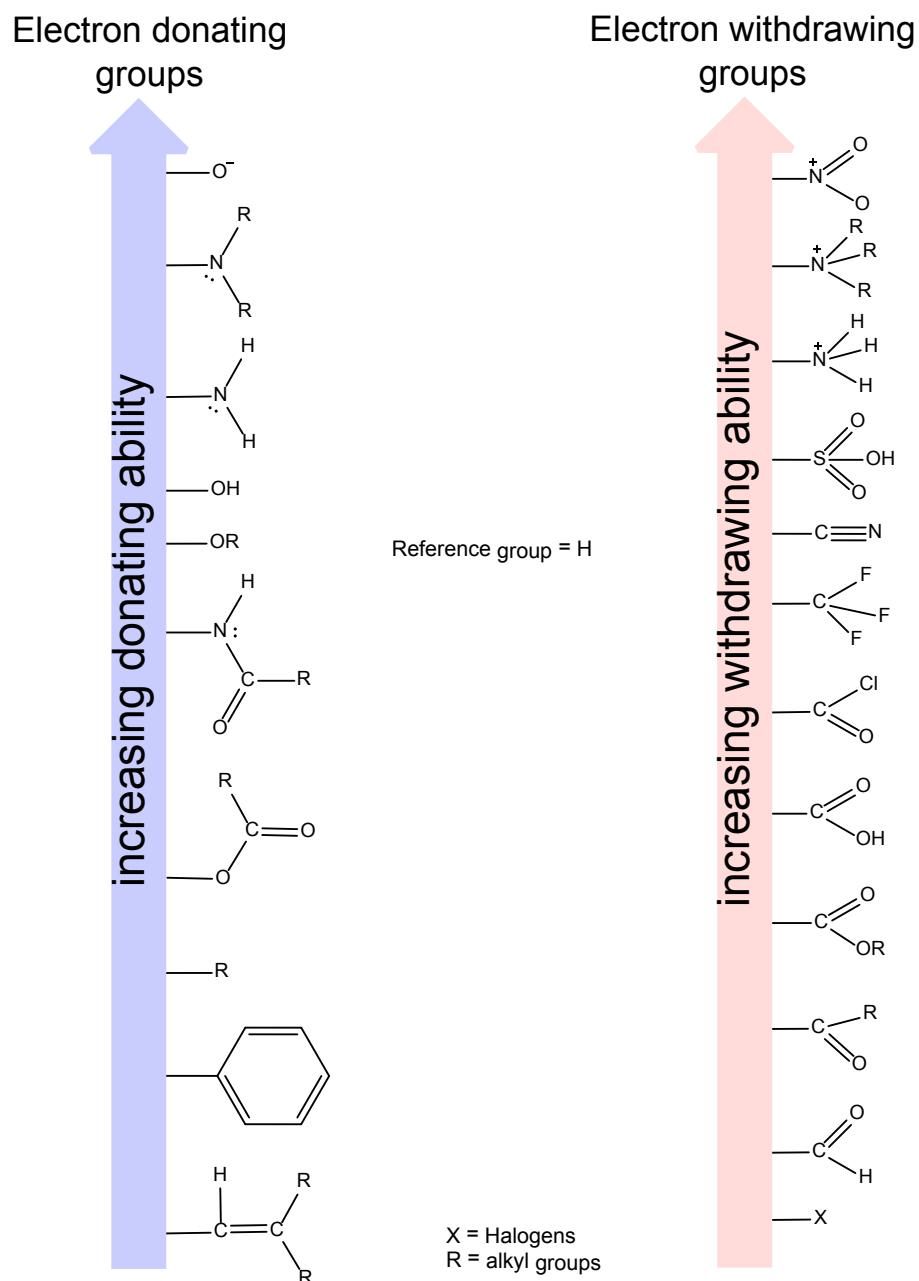
Figure 2.7. Electron withdrawing and donating ability of substituent groups in reference to hydrogen. Adapted from Carey 2000.[35]

As an example, in the case of HPsensors, modifications of BODIPY core by

adding 2-methoxyethylamine substitution at position 3,5 and *aryl* substitution at

meso position led to a red-shift in excitation and emission wavelength which is due to a slight decrease in energy gap for HPsensors (~0.22 eV) compared to **control** dye. This slight decrease in HOMO-LUMO energy gap led to an increased conjugation of π-system of chromophore improving the fluorescence quantum yield and hydrophobic sensing ability (See Chapter 4).
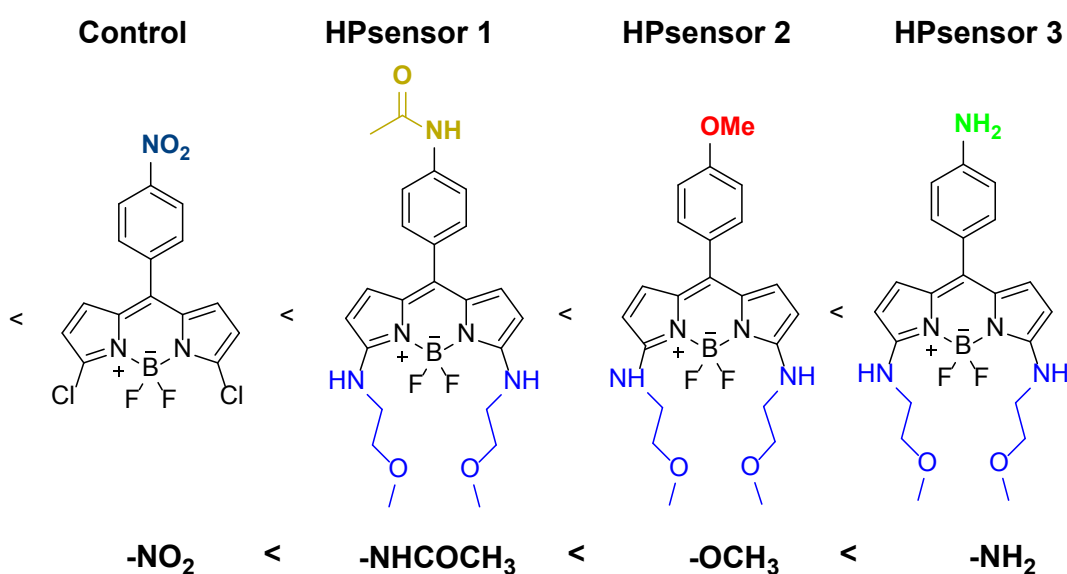

Figure 2.8. HPsensor modification in order of increasing electron donating ability.

The added bonus of the aryl substitution allows for modulation of both steric effects for quenching as well as the spacer for these sensors. In addition, by modulating the quenching mechanism, the sensitivity and mechanism of sensing of these probes can also be impacted. However, studies have shown that such substitutions alter the way in which these dyes interact with proteins as was noted in the case of the hydrophobic probe ANS.[36]

Based on the dye structures of HPsensors **1**, **2** and **3**, there are a few options for modulating low quantum yields in an aqueous environment; internal charge transfer (ICT), photo-induced electron transfer (PET) as well as the rotational effects of the aryl group (figure 2.8). Rotational effects are well known to affect quantum yield by reducing a coplanar arrangement of the donor and acceptor units which forms an extended LUMO,[37,38] and as such, this was the most effective means of controlling weak but measurable fluorescence in these probes. Of the previous substitutions made at the 8-position (meso),[12] the ones described here are the first to be used specifically for the purpose of reporting/sensing of the hydrophobicity of proteins.

2.3.   **Mapping the surface hydrophobicity.**

Currently, the majority of the probes available, respond to increases in hydrophobicity in the same linear fashion. As a result, their fluorescence in an aqueous environment is often weak or quenched and then increases as the polarity decreases. With a highly tunable dye such as the BODIPY core, it was possible to make probes that show high sensitivity and fluorescence in the polar environment. Probes could be designed to have weak but measurable fluorescence in aqueous media allowing a quantitative analysis of the change in fluorescence due to exposed surface hydrophobicity. In addition, it was also possible to build these probes using a pseudo "turn-on" mechanism whereby

interaction with surface hydrophobicity would significantly increase/enhance the fluorescence of these probes.
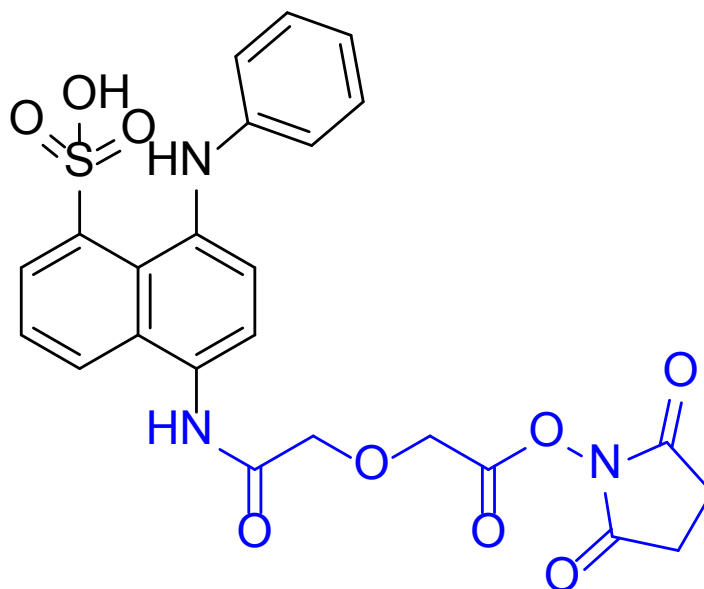

Figure 2.9. A functionalized ANS probe. The core hydrophobic sensor ANS is covalently modified by attaching a succinimide-functionalized ethynyl derivative (NHS ester) that can potentially interact with the amine groups found on lysine or arginine residues.

In an effort to make fluorescent dye that could be used for labeling of the hydrophobic surface of proteins through a tag covalently binding to hydrophobic site or very near it we used modified ANS (Figure 2.9). We used ANS as it is a small well characterized hydrophobic probe that is relatively small in size. In addition, it can be modified to attach a succinimide-functionalized ethynyl derivative that offers facile reaction with amine residues of proteins at physiological or basic pH. As the hydrophobic sensor group is small, it should

not sterically hinder the side NHS-ester to crosslink with a nearby amine group and bind covalently to stabilize the dye.

Another compelling reason for using 1,8-ANS as a test compound for such a modification was plethora of literature available on this compound for its application on protein and huge volumes of information available on the physicochemical properties of this compound. While ANS was used initially to attach a catalytic group (succinimide) that could covalently tag with the nearby amine group, in future other probes such as HPsensors can be modified for hydrophobic labeling and mapping of proteins.

Table 2.1. Theoretical conditions for nucleophilic attack of protein on coupler. Adapted from Hermanson 2008.[39]

Ionizable group	pK$_a$ range
α-carboxyl (C-terminus)	2.1 - 2.4
Aspartic acid γ-carboxyl	3.7 - 3.4
Glutamic acid γ-carboxyl	4.2 - 4.5
Histidine imidazol nitrogen	6.7 - 7.1
α-Amine (N-terminus)	7.6 - 8.0
Cysteine's sulfhydryl	8.8 - 9.1
ε-amine (Lysine)	9.3 - 9.5
Tyrosine phenolic hydroxyl	9.7 - 10.1
Arginine's guanidinyl	> 12

Although in this study we used an amine reactive group (succinimide) as a crosslinker, in future we can add a maleimide-group to tag available sulfhydryl

groups on proteins or an amine group to link through carboxylic groups. Such a choice will also be dictated by the intended pH at which we want to carry out these reactions.

This is because specificity of labeling is also impacted through the target (ionizable) group. Selection of the appropriate group can improve reaction specificity and efficiency. Currently, the theoretical pK_a values of the ionizable groups show a range in values for pk_a from 2.1 – 12+, however, the experimental data shows that ionization can also occur at pHs outside of that range.[39] This was attributed to the microenvironment around these amino acid side chains that favored ionization at values lower than the reported pk_a.[39] This finding allows for improved functionality of the selected ionizable group but also means that there is an overlap of ionization of other groups as well. Such groups could include the hydroxyl or sulfhydryl groups. In addition, due to the abundance of lysine residues,[40] lysine's extensive surface exposure and pk_a range,[39] this group was chosen as a suitable target of hydrophobic labelers such as the modified ANS probe.
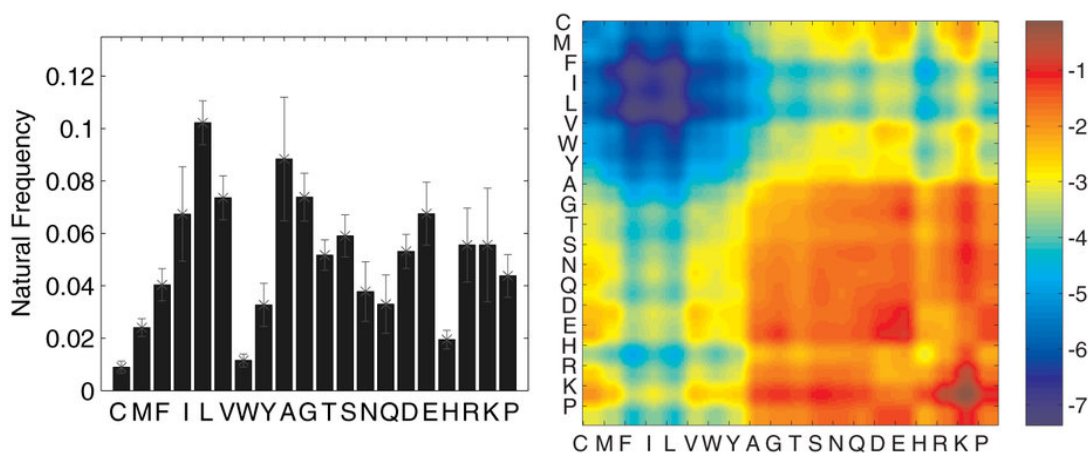
Figure 2.10. Relative abundance of amino acids. Reproduced from Hormoz 2013 with permission.[40]

Finally, when considering the type of couplers to be used for probe functionalization, several options are available. However, the most popular of these for use in amine labeling are found to be of three classes. These include the esters (such as succinimidyl esters (SE), sulfosuccini midyl esters (SSE), tetrafluorophenyl esters (TFP), and sulfodichlorophenol esters (SDP)), isothiocyanates (ITC), and sulfonyl chlorides (SC). However, the active esters such as succinimidyl esters are favored because of the formation of a stable carboxamide bond[41] and their ability to crosslink at pH close to physiological.[42] As might be expected, each group has optimal conditions for operation and can be used together with an appropriate target (ionizable) group to improve selectivity of the probe (Table 2.1).

Another advantage to the covalent linkage of the hydrophobic sensor to the protein structure is that it allows downstream analysis of the protein structure to

map the hydrophobic regions. While strong hydrophobic interactions are possible between probe and protein, these non-covalent interactions may not survive during sample preparation for mass spectrometry or X-ray crystallography experiments. Therefore, having a probe that can covalently bind to hydrophobic surface or very near it can provide very useful information about the size and location of the surface exposed hydrophobic regions of proteins by mass spectrometry, X-ray crystallography combined with molecular modeling.

2.4. References

1   Haskard, C. A. & Li-Chan, E. C. Y. Hydrophobicity of Bovine Serum Albumin and Ovalbumin Determined Using Uncharged (PRODAN) and Anionic (ANS-) Fluorescent Probes. *J. Agric. Food Chem.* **46**, 2671-2677 (1998).

2   Haskard, C. A. & Li-Chan, E. C. Y. Hydrophobicity of Bovine Serum Albumin and Ovalbumin Determined Using Uncharged (PRODAN) and Anionic (ANS-) Fluorescent Probes. *J. Agric. Food Chem.* **46**, 2671-2677 (1998).

3   Mozes, N. & Rouxhet, P. G. Methods for measuring hydrophobicity of microorganisms. *J. Microbiol. Meth.* **6** 99-112 (1987).

4   Nakai, S., Li-Chan, E. & Arteaga, G. E. in *Methods of testing protein functionality*   (ed G. M. Hall) Ch. 8, 226 - 255 (Blackie A & P, 1996).

5   Kato, A. & Nakai, S. Hydrophobicity determined by a fluorescence probe method and its correlation with surface properties of proteins. *Biochim. Biophys. Acta* **624**, 13-20 (1980).

6   Matulis, D. & Lovrien, R. 1-Anilino-8-Naphthalene Sulfonate Anion-Protein Binding Depends Primarily on Ion Pair Formation. *Biophys. J.* **74** 422–429 (1998).

7   Matulis, D., Baumann, C. G., Bloomfield, V. A. & Lovrien, R. E. 1-Anilino-8-naphthalene sulfonate as a protein conformational tightening

agent. *Biopolymers* **49**, 451-458, doi:10.1002/(SICI)1097-0282(199905)49:6<451::AID-BIP3>3.0.CO;2-6 (1999).

8   De Silva, A. P. *et al.* Signaling recognition events with fluorescent sensors and switches. *Chemical Reviews* **97**, 1515-1566 (1997).

9   Dorh, N. *et al.* BODIPY-Based Fluorescent Probes for Sensing Protein Surface-Hydrophobicity. *Sci Rep* **5**, 18337, doi:10.1038/srep18337 (2015).

10   Treibs, A. & Kreuzer, F.-H. Elektrophile Substitution an Pyrrolen mit Acylchloriden. *Justus Liebigs Annalen der Chemie* **721**, 105-115, doi:10.1002/jlac.19697210115 (1969).

11   Li, F. *et al.* Design, Synthesis, and Photodynamics of Light-Harvesting Arrays Comprised of a Porphyrin and One, Two, or Eight Boron-Dipyrrin Accessory Pigments. *J. Am. Chem. Soc.* **120**, 10001-10017 (1998).

12   Inokuma, Y., Yoon, Z. S., Kim, D. & Osuka, A. meso-Aryl-Substituted Subporphyrins: Synthesis, Structures, and Large Substituent Effects on Their Electronic Properties. *J. Am. Chem. Soc.* **129**, 4747-4761 (2007).

13   Sabatini, R. P. *et al.* Intersystem Crossing in Halogenated Bodipy Chromophores Used for Solar Hydrogen Production. *J. Phys. Chem. Lett.* **2**, 223-227, doi:Doi 10.1021/Jz101697y (2011).

14   Lazarides, T. *et al.* Sensitizing the Sensitizer: The Synthesis and Photophysical Study of Bodipy-Pt(II)(diimine)(dithiolate) Conjugates. *J. Am. Chem. Soc.* **133**, 350-364, doi:Doi 10.1021/Ja1070366 (2011).

15   Geng, H. *et al.* Photoelectrochemical properties and interfacial charge transfer kinetics of BODIPY-sensitized TiO_2 electrodes. *RSC Adv.* **3**, 2306, doi:10.1039/c2ra21656f (2013).

16   Heisig, F. *et al.* Synthesis of BODIPY Derivatives Substituted with Various Bioconjugatable Linker Groups: A Construction Kit for Fluorescent Labeling of Receptor Ligands. *J. Fluoresc.*, doi:10.1007/s10895-013-1289-4 (2013).

17   Chen, G. *et al.* Reactivity of functional groups on the protein surface: Development of epoxide probes for protein labeling. *J. Am. Chem. Soc.* **125**, 8130-8133, doi:Doi 10.1021/Ja034287m (2003).

18   Daphnomili, D. *et al.* A Synthetic Approach of New Trans-Substituted Hydroxylporphyrins. *Bioinorg. Chem. Appl.*, doi:10.1155/2010/307696 (2010).

19   Nepomnyashchii, A. B., Cho, S., Rossky, P. J. & Bard, A. J. Dependence of Electrochemical and Electrogenerated Chemiluminescence Properties on the Structure of BODIPY Dyes. Unusually Large Separation between Sequential Electron Transfers. *J. Am. Chem. Soc.* **132**, 17550-17559, doi:Doi 10.1021/Ja108108d (2010).

20   Krumova, K. & Cosa, G. Bodipy Dyes with Tunable Redox Potentials and Functional Groups for Further Tethering: Preparation,

Electrochemical, and Spectroscopic Characterization. *J. Am. Chem. Soc.* **132**, 17560-17569, doi:Doi 10.1021/Ja1075663 (2010).

21   Rosenthal, J. & Lippard, S. J. Direct Detection of Nitroxyl in Aqueous Solution Using a Tripodal Copper(II) BODIPY Complex. *J. Am. Chem. Soc.* **132**, 5536-+, doi:Doi 10.1021/Ja909148v (2010).

22   Karolin, J., Johansson, L. B. A., Strandberg, L. & Ny, T. Fluorescence and Absorption Spectroscopic Properties of Dipyrrometheneboron Difluoride (Bodipy) Derivatives in Liquids, Lipid-Membranes, and Proteins. *J. Am. Chem. Soc.* **116**, 7801-7806, doi:Doi 10.1021/Ja00096a042 (1994).

23   Zhu, S. *et al.* Highly water-soluble neutral near-infrared emissive BODIPY polymeric dyes. *J. Mater. Chem.* **22**, 2781-2790, doi:Doi 10.1039/C2jm14920f (2012).

24   Zhu, S. *et al.* Highly water-soluble BODIPY-based fluorescent probes for sensitive fluorescent sensing of zinc(ii). *J. Mater. Chem. B* **1**, 1722, doi:10.1039/c3tb00249g (2013).

25   Zhu, S. L. *et al.* Highly water-soluble neutral near-infrared emissive BODIPY polymeric dyes. *J. Mater. Chem.* **22**, 2781-2790, doi:Doi 10.1039/C2jm14920f (2012).

26   Vegesna, G. K. *et al.* Highly Water-Soluble BODIPY-Based Fluorescent Probe for Sensitive and Selective Detection of Nitric Oxide in Living

Cells. *ACS Appl. Mater. Interfaces* **5**, 4107-4112, doi:Doi
10.1021/Am303247s (2013).

27   Li, L., Han, J., Nguyen, B. & Burgess, K. Syntheses and spectral
properties of functionalized, water-soluble BODIPY derivatives. *J. Org.
Chem.* **73**, 1963-1970, doi:10.1021/jo702463f (2008).

28   Li, L., Nguyen, B. & Burgess, K. Functionalization of the 4,4-difluoro-4-
bora-3a,4a-diaza-s-indacene (BODIPY) core. *Bioorg. Med. Chem. Lett.*
18, 3112-3116, doi:10.1016/j.bmcl.2007.10.103 (2008).

29   Zhu, S. *et al.* Highly water-soluble, near-infrared emissive BODIPY
polymeric dye bearing RGD peptide residues for cancer imaging. *Anal.
Chim. Acta* **758**, 138-144, doi:10.1016/j.aca.2012.10.026 (2013).

30   Zhang, X.-F. The effect of phenyl substitution on the fluorescence
characteristics of fluorescein derivatives via intramolecular
photoinduced electron transfer. *Photochem. Photobiol. Sci.* **9**, 1261,
doi:10.1039/c0pp00184h (2010).

31   Li, L., Han, J., Nguyen, B. & Burgess, K. Syntheses and spectral
properties of functionalized, water-soluble BODIPY derivatives. *The
Journal of organic chemistry* **73**, 1963-1970, doi:10.1021/jo702463f
(2008).

32   O. Altan Bozdemir *et al.* Selective Manipulation of ICT and PET
Processes in Styryl-Bodipy Derivatives: Applications in Molecular Logic

and Fluorescence Sensing of Metal Ions. *J. Am. Chem. Soc.* **132**, 8029–8036 (2010).

33   Ding, L., Ding, Y. Q., Teng, Q. W. & Wang, K. The Effect of Substituents on the Fluorescent Properties of Para-Phenylenevinylene. *J. Chin. Chem. Soc.* **54**, 853-860 (2007).

34   Brune, S. N. & Bobbitt, D. R. Role of electron-donating/withdrawing character, pH, and stoichiometry on the chemiluminescent reaction of tris (2, 2'-bipyridyl) ruthenium (III) with amino acids. *Analytical Chemistry* **64**, 166-170 (1992).

35   Carey, F. A. in *Organic Chemistry, 4-th Ed*   (ed Kevin T. Kane) Ch. 12, 464 (Mc-Graw Hill Higher Education, 2000).

36   Gasymov, O. K. & Glasgow, B. J. ANS Fluorescence: Potential to Augment the Identification of the External Binding Sites of Proteins. *Biochim Biophys Acta.* **1774**, 403–411 (2007).

37   Loudet, A. & Burgess, K. BODIPY Dyes and Their Derivatives: Syntheses and Spectroscopic Properties. *Chem. Rev.* **107**, 4891-4932 (2007).

38   Ziessel, R. *et al.* Intramolecular energy transfer in pyrene-bodipy molecular dyads and triads. *Chem.-Eu. J.* **11**, 7366-7378, doi:10.1002/chem.200500373 (2005).

39   Hermanson, G. T. in *Bioconjugate Techniques (Second Edition)*   1-168 (Academic Press, 2008).

40   Hormoz, S. Amino acid composition of proteins reduces deleterious impact of mutations. *Sci Rep* **3**, 2919, doi:10.1038/srep02919 (2013).

41   Banks, P. R. & Paquette, D. M. Comparison of Three Common Amine Reactive Fluorescent Probes Used for Conjugation to Biomolecules by Capillary Zone Electrophoresis. *Bioconjugate Chemistry* **6**, 447-458, doi:10.1021/bc00034a015 (1995).

42   Hermanson, G. T. in *Bioconjugate Techniques (Second Edition)*   234-275 (Academic Press, 2008).

.

Chapter 3: Methods

Included in the following text is a concise description of some of the current technologies available for evaluating the surface hydrophobicity of proteins as well as the techniques employed in this dissertation. The major techniques will be briefly discussed, including some of the limitations of each technique.

3.1. Spectroscopic techniques for probe evaluation

3.1.1. UV-VIS spectroscopy

UV-VIS spectroscopy refers to the acquisition of the absorption spectra of a given molecule, protein or large macromolecule within the ultraviolet to visible region of the light spectrum.[1] This provides information based on the interaction between matter and electromagnetic radiation.[1] Individual spectra are composed of discrete lines which represent the transition of an electron from the ground state to an excited energy state in a given molecule.[1] The energy of a photon passing through a sample elevates the electron to this excited state, resulting in a reduction in the transmitted light detected (figure 3.1). The transmittance can then be converted to absorbance using the following relationship outlined in equation 1 below:

Equation 1.   A (absorbance) = 2 – log %T (transmittance)
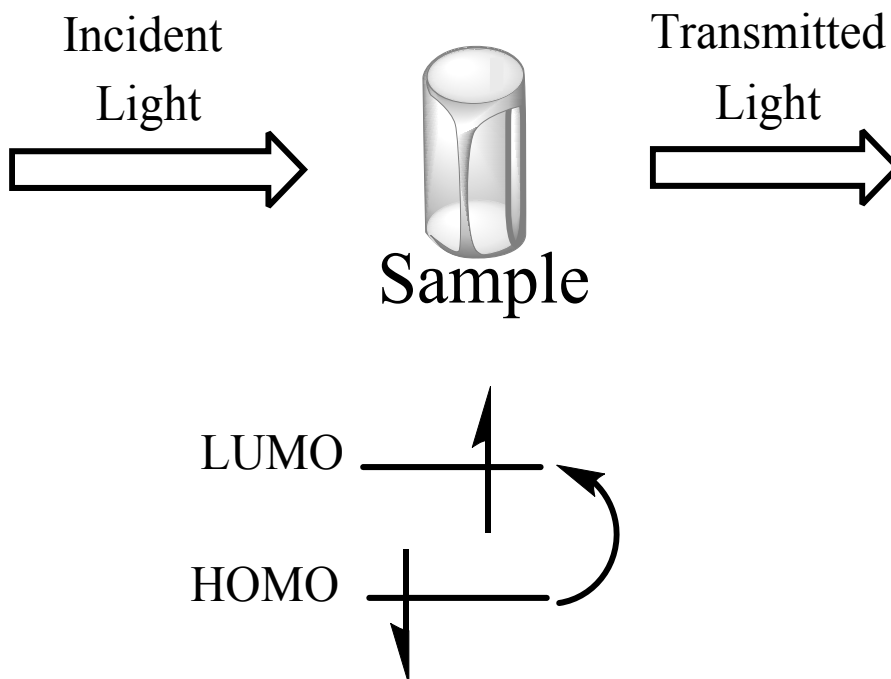
Figure 3.1. UV-VIS spectroscopy showing elevation of electron. As photon passes through a sample, an electron is excited to the LUMO reducing the amount of transmitted light.

Increasing the number of these excited states (vibrational and rotational) because of an increase in the complexity of the molecule results in line broadening.[1-3] A good example of this is the characteristic protein peaks that are normally seen in UV-VIS spectra. It is important to note that the absorption recorded in the UV-VIS region of organic molecules is due to two types of electrons: (1) unsaturated bonded electrons (double bond and higher arrangements) and (2) valence electrons.[3] As a result, it is possible to tease out intricate structural details about a molecule based on the absorption spectra.

Specifically, in the case of surface hydrophobicity and proteins, UV-VIS spectroscopy is capable of indirectly evaluating this based on aggregate formation. A common way to achieve this is by utilizing the absorption profile of dyes such as Thioflavin-T (ThT) and derivatives such as Pittsburgh compound B (PIB).[4] This indirect approach allows for measuring the loss of surface hydrophobicity as a result of the aggregate formation.

3.1.2.   Overview of Initial characterization of probes via UV VIS

The fluorescent probes were evaluated via UV VIS spectroscopy in solvents of decreasing polarity. Absorption of ultraviolet and visible radiation in organic molecules is due to valence electrons of low excitation energy of specific functional groups. The resultant absorption band can be used as an indicator of electronic transitions. Specifically, as the solvent polarity changes, stokes shifts are observed in the absorption spectra. For solvent testing, a water-ethanol solution mixture was used at 20% gradations to mimic the decrease in solvent polarity from 100% water to 100% ethanol. Dyes were incubated with each solvent for a period of 1 h before evaluation of the absorption spectra and corresponding dye response. Details of experiments are mentioned below.

3.1.3.   Initial characterization via UV VIS spectroscopy

Initial characterization were performed as per previous protocols and adapted as follows.[5] Probes were dissolved in ethanol or DMSO (dependent on solubility of each probe) at high concentration (1 -2 mM) to prepare primary stock solutions for subsequent experiments. Probes were then diluted to the micromolar range in test solvents (water/buffer, dimethylsulfoxide, dichloromethane). The absorption spectra was then acquired for each probe in the test solvent from 200 – 800 nm using quartz cuvettes.

3.1.4.   Sensitivity of probes to solvent polarity

Using primary stock solutions, the probes were diluted to micromolar range solutions in different concentrations of ethanol/water (MiliQ) mixtures. Samples were prepared as indicated below and as done previously,[5] after which the sample absorption spectra were then acquired from 200 – 800 nm using quartz cuvettes.

Table 3.1. Preparation considerations for ethanol water dilutions used in polarity sensitivity tests. Stock solutions at 100 ml of each condition solution were prepared.

Condition	% (v/v) water	% (v/v) Ethanol
0% Ethanol	100	0
20% Ethanol	80	20
40% Ethanol	60	40
60% Ethanol	40	60
80% Ethanol	20	80
100% Ethanol	0	100

3.2.   Fluorescence Spectroscopy

Fluorescence refers to the radiative decay mechanism whereby singlet electrons excited to the lowest unoccupied molecular orbital (LUMO) return to the ground state of the highest occupied molecular orbital (HOMO). This phenomenon is noted to occur on the nanosecond timescale and is

exponentially proportional to the absorbance of a given fluorophore (figure 3.2).[6]

It is important to include that after an electron has been excited, there are

several routes available through which the electron can return to the ground

state.

(a) Incident
Light

Fluorescence

Sample

(b) S_2

Internal conversion

LUMO S_1

Fluorescence

HOMO S_0
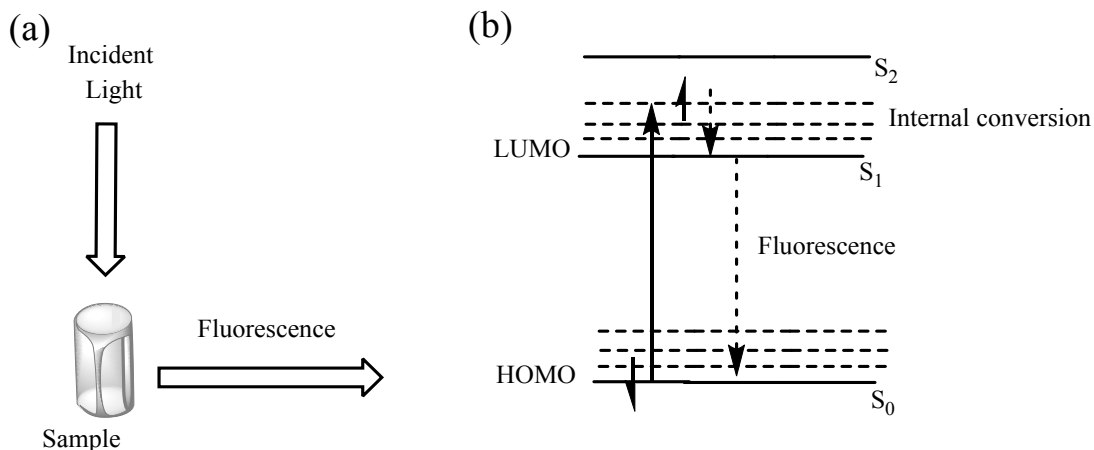
Figure 3.2. Fluorescence spectroscopy. (a) Incident light passes through a sample resulting in the promotion of an electron to the excited state. (b) After internal conversion, the singlet state electron returns to the ground state via radiative decay (fluorescence).

In the event that the excited electron maintains a triplet excited state, the

phenomenon of phosphorescence is then observed.[6] Phosphorescence is also

known to occur on a much longer timescale (usually $> 10^{-7}$ s).[6] As a result,

fluorescence requires excitation from a singlet state and subsequent relaxation

to a singlet state.[6]

In consideration of the fluorophore, there are several criteria that are considered

absolute in order for an organic molecule to exhibit good fluorescence. These

include aromaticity, extensive conjugation, and electron donating groups. Currently, it has been noted that electron withdrawing groups are deactivating in nature and reduce the fluorescence signal.[7,8] A good fluorescence signal is determined by the quantum yield of a specific fluorophore. The quantum yield of any fluorophore is an evaluation of the ratio of photons emitted to the photons absorbed by the fluorophore. The quantum yield can be calculated using equation 2: where st = standard; x = test dye; Grad – gradient of fitted slope; Q = quantum yield and η = refractive index of test solvent.

Equation 2.
$$Q_x = Q_{st}\left(\frac{Grad_x}{Grad_{st}}\right)\left(\frac{\eta_x^2}{\eta_{st}^2}\right)$$

Currently, fluorescence studies of proteins can be classified into two major categories, intrinsic fluorescence and extrinsic fluorescence. Intrinsic fluorescence is associated with fluorescence from aromatic amino acids such as tryptophan and tyrosine that are already available within the protein. These amino acids are able to absorb energy and fluoresce on returning the electron to the ground state. The term extrinsic fluorescence is usually reserved for noncovalent probes that are synthesized with the purpose of interacting with the specific areas of proteins or with specific targets in solution. This allows these probes to divulge information about protein structure, interactions, and a number of distinct properties.

3.2.1. Extrinsic fluorescent probes.

Current extrinsic fluorescent probes which show promise are limited by their sensitivity. Unfortunately, the overall structure of such probes are also known to dictate their functionality in biological systems. Extrinsic fluorescent probes provide an advantage over UV-VIS techniques in that they can directly assay the local environment of a protein. In addition, these molecules are among a wide range of aromatic molecules that can be tuned to fit the needs of the researcher. Extrinsic fluorescent probes commonly used in biophysical techniques include but are not limited to: 8-Anilinonaphthalene-1-sulfonic acid (ANS), 4,4-difluoro-4-bora-3a,4a-diaza-s-indacene (BODIPY) dyes, fluorescein, dansyl chloride, and their derivatives (Figure 3.3).
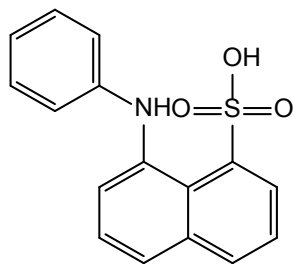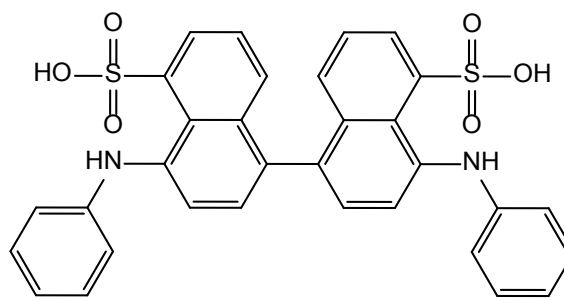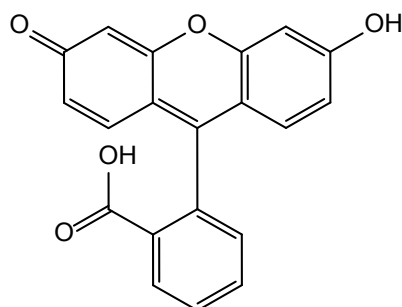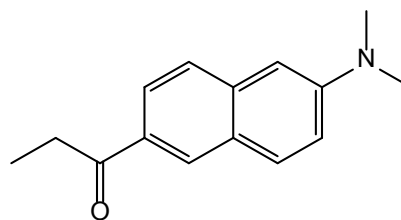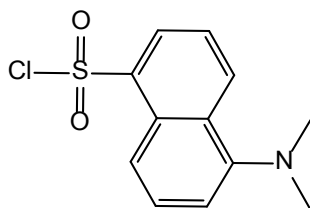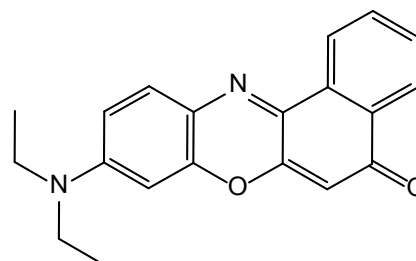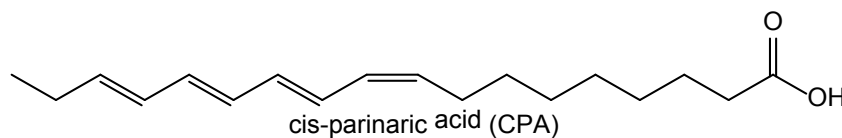
Figure 3.3. Fluorescent probes for surface hydrophobicity. Structures of common probes used in measuring surface hydrophobicity.

3.2.2. Fluorescence labeling

Fluorescence labeling refers to the process of covalently linking extrinsic dyes to the protein of interest. This technique is especially useful when it is necessary to track changes in a specific protein. Fluorescence labeling has also been successfully combined with other fluorescence techniques such as fluorescence resonance energy transfer (FRET) in order to evaluate protein-protein interactions. As it refers to surface hydrophobicity, the concept of fluorescence labeling for evaluating surface hydrophobicity has not yet been attempted. As such, we have proposed the use of a fluorescent probe which is sensitive to surface hydrophobicity of proteins as a hydrophobicity probe.

Protein labeling as a technique has been previously been used successfully to determine structural components of proteins,[9-11] however, this has not yet been done in the interest of just surface properties such as hydrophobicity. While there are many options available for covalent linkage,[12,13] we have opted to proceed via an N-hydroxysuccinimide (NHS) ester link. This linker is fairly simple to facilitate covalent attachment and the reaction conditions are relatively mild. The covalent attachment will be driven by the availability of a lysine or arginine residue within the vicinity of an exposed hydrophobic region.
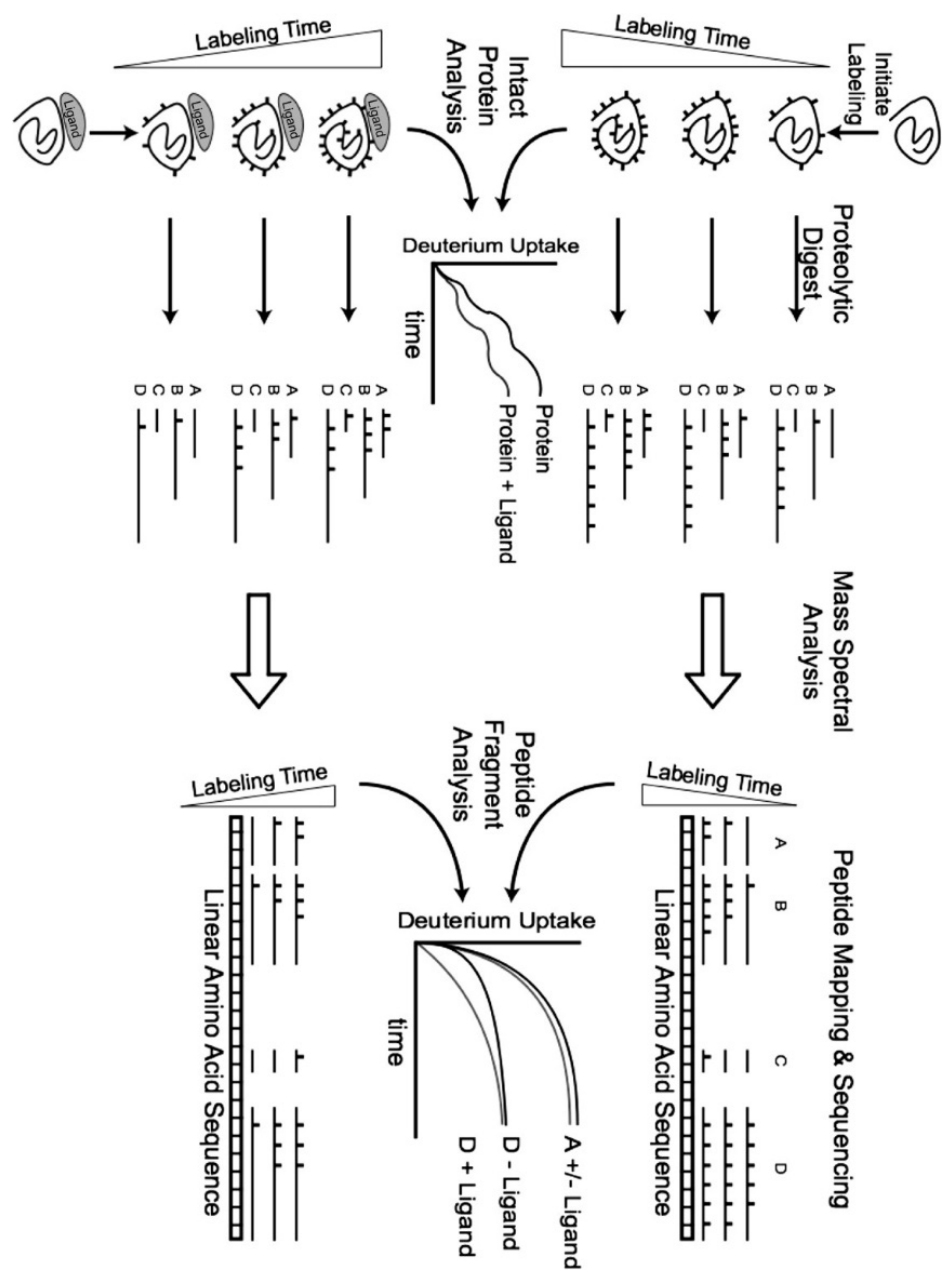
Figure 3.4. Flow-through of protein labeling and characterization. Taken from Fitzgerald and West, 2009 with permission.[12]

Coupled with tandem MS experiments (figure 3.4), these hydrophobic probes would allow the simultaneous identification of modified sites and determination

of the location and size of these hydrophobic regions. This data can then be visualized using computational methods allowing direct observation impacted areas.

3.2.3. Overview of Initial characterization of probes via Fluorescence spectroscopy

The fluorescent probes were also evaluated via fluorescence spectroscopy in solvents of different polarity as well as graded polarity solvents. Solvents used included ethanol, water and dichloromethane. Solutions of 0 – 100% ethanol/water were also used at 20% increments. Probes were incubated in solutions for a period of 1 h before measuring the fluorescence spectra at each condition.

3.2.4. Initial characterization via fluorescence spectroscopy

Using samples prepared for initial characterization via UV VIS spectroscopy, micromolar samples were placed in fluorescence cuvettes. Using the corresponding absorption maxima from the UV VIS spectra as excitation wavelengths, the emission spectra was acquired for each test solvent. Optimized excitation wavelengths were then selected based on the wavelength that produced the following paramters; the least impact from Rayleigh scattering, maximum fluorescence intensity, and minimal impact of input excitation on the emission spectra

3.2.5. Probe fluorescence sensitivity to solvent polarity

Using samples prepared from sensitivity to solvent polarity for UV VIS spectroscopy, the corresponding emission spectra was acquired for samples using the optimized emission spectra. The excitation/emission slit widths were kept at 2/2 nm ratio to maximize signal and reduce the level of noise in spectra. The emission range was selected to exclude the excitation signal and include the emission spectra up to 100 nm after the peak signal

3.2.6. Quantum yield measurements

All measurements were performed as previously done.[5] For quantum yield determination, the standard reference dye Sulforhodamine 101 was used which has a quantum yield of 0.95 in ethanol at 577 nm.[14] Next 5 - 7 dilutions of test probes and reference probes were prepared with an O.D. between 0 and 0.05 in each test solvent (CH_2Cl_2, H_2O, DMSO or Ethanol). The corresponding fluorescence spectrum for each sample was then acquired using the corresponding excitation wavelength. Note that the same excitation wavelength for sample and reference dye were used. The area under the peak for all of the collected emission spectra was then calculated using the integration option in OriginPro 9.1.

Using the integrated area in conjunction with the corresponding absorbance, graphs of integrated area vs. absorbance are then plotted. A linear fit was then

employed to determine the slope of the line (gradient) for the reference and the test probe. Then, using the following equation (equation 3), the quantum yield was then calculated for each probe.

Equation 3. $\quad Q_x = Q_{st}(\frac{Grad_x}{Grad_{st}})(\frac{\eta_x^2}{\eta_{st}^2})$

3.2.7. Surface Hydrophobicity determination

Surface hydrophobicity (S0) measurements were conducted established protocols.[15,16] Samples were prepared in the appropriate buffer or MiliQ water (adjusted to pH 8 using 0.1 M NaOH) and incubated at 8–10 concentrations of each test protein for 1 h at 25 °C. For each protein, the following conditions were held constant:

    a. Samples were prepared in triplicate for experiments

    b. Protein samples were prepared either in the prescence or absence of the fluorescent probe

Next, the fluorescence emission spectra for the fluorescent probe was then acquired. The net relative fluorescence intensity (RFI) was then calculated by subtracting the fluorescence of protein in buffer from that of protein + probe. The slope (linear regression fit) of net RFI vs protein concentration was plotted to determine the surface hydrophobicity of each protein.

3.2.8. Binding Affinity determination

Binding affinity measurements for fluorescent probes were conducted via fluorescence titration using the following established protocol.[15,17,18] Protein samples were prepared for 21–28 different concentrations of protein in the presence of the fluorescent probe. Protein samples at the same concentrations in the absence of fluorescent probe were also prepared. Note that protein samples both in the presence and absence of fluorescent probe were prepared in triplicate.

Using the same wavelength for average peak fluorescence for all samples, the fluorescence of probe in the presence of protein was corrected using protein without probe. The corrected peak fluorescence data was then used to plot the binding curve for each probe with the respective protein. The data was then analyzed by a non-linear regression method using the MichaelisMenten model function included in OriginPro 9.1.

3.3. *In Silico* modeling of a Protein Surface

In Silico modeling refers to the computational modeling of the structure of a given protein. As can be expected, the structure prediction and thus protein fold are important for determining and evaluating the function of a given protein. One useful application of molecular modeling is molecular docking. In docking

71

studies, a protein and ligand are evaluated for plausible interactions based on the thermodynamics of binding or their proposed interaction.

Essentially, molecular modeling is a multidisciplinary field that employs theoretical and computational techniques to furnish predictions of a protein surface or protein interactions (figure 3.5). This can be done using experimental data as a basis for the prediction tool or by using interactions between force fields attributed to each atom within a macromolecule (protein).[19] Typical force fields used in molecular modeling account for the overall energy of the system by generally describing bonding, angles, rotations, van der Waals interactions, non-bonding, and electrostatic energies. It is important to include that the force field accounts for the internal energy of the system which is a combination of the kinetic and potential energies of a system.[20]

.
Molecular modeling is frequently coupled with molecular dynamics, which provides the ability to link a protein's structure to a particular function of the protein. Time is included as a parameter to evaluate the structure and docking results generated by the algorithm. This is especially useful in helping to rank and evaluate the structures. In addition, the ability to compute vectors for every atom in the ligand and macromolecule allows for the possibility of surveying several conformations (folds) of the protein.
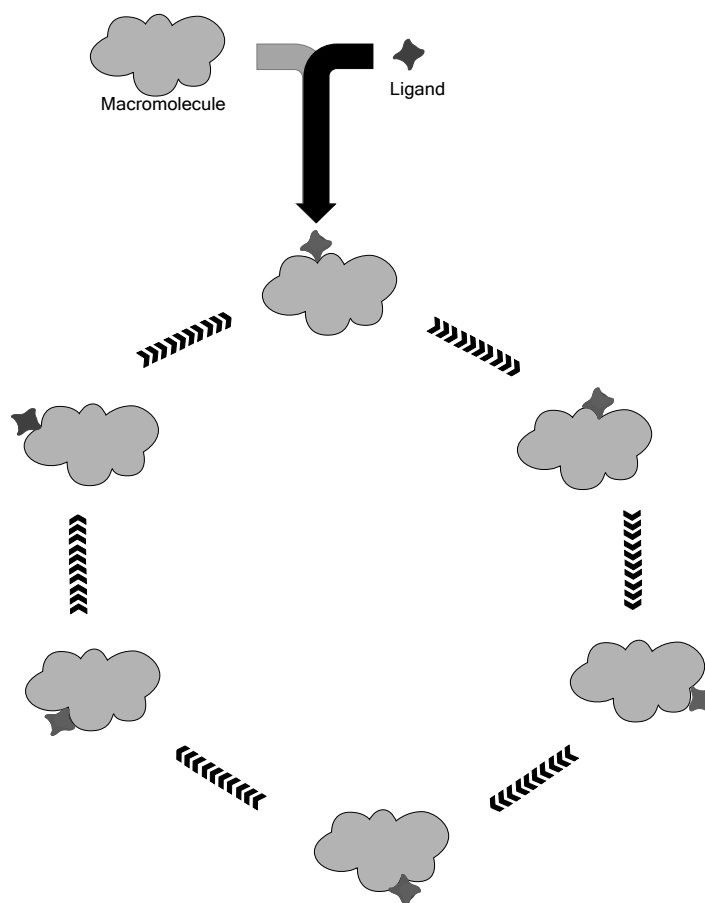
Figure 3.5. Simple flow-through of molecular docking simulation. Ligand and macromolecule are docked at several sites. Free energy for each site is measured and used as an indicator of the most plausible interaction sites.

Molecular modeling is especially important for theoretical evaluations of protein topography via homology modeling. This unique tool provides an opportunity to rely on experimental sequence data to help predict fold and function of unknown proteins. Coupled with this, it is also possible to evaluate surface electrostatics of proteins. The ability to model the surface electrostatics of a protein also allow the visualization of hydrophobic patches/regions on the protein of interest. With this information in hand, it then becomes possible to predict mechanisms by

73

which these various regions of the protein topography may direct interactions with other proteins or monomeric units of the same protein.

Unfortunately, this field is still growing and requires the corroboration of experimental data. In some cases, differences have been noted between theoretical predictions and experimental data; however, this data is still very useful for making initial predictions about protein structure.

3.4. **X-ray Crystallography**

X-ray crystallography is a technique used to ascertain the position of atoms in a snap-shot of the molecule's dynamic structure. Essentially, X-ray crystallography provides a three dimensional image of the molecular structure from a crystal.[21,22] It is currently the favored technique for structure determination of proteins, biological macromolecules and small molecules.[21,22] This snap-shot while very useful, imposes limitations on fully understanding dynamic or fluid systems. This is especially true for proteins that are known to maintain slightly fluid structures in aqueous media.

The crystal structure of the highly concentrated macromolecule is exposed to x-rays resulting in a diffraction pattern.[21] This diffraction pattern gives information about the packing symmetry and the individual units/repeating units in the

crystal being analyzed.[21] The diffraction pattern also relates to the electron density that then gives information about the identity of atoms. The use of the Bragg equation (equation 4) is then employed to relate the diffraction pattern to the position of each of the atoms in the diffraction pattern. In the Bragg equation, n = positive integer, λ = the wavelength of incident light, d = the interplanar distance and θ = the scattering angle.

Equation 4. $$n\lambda = 2d\sin\theta$$

X-ray crystal structures are very useful because the x-ray scattering gives information about the location and thus structure of a protein/molecule. This can often be done in the range of 1.5 – 3.0 Å. Therefore, one can visually determine the location of hydrophobic patches/regions that may be surface accessible. This kind of information goes a long way to improving molecular modeling and dynamics simulations in addition to allowing inferences to be made on function. Unfortunately, this technique is very time consuming and usually requires months before suitable crystallization conditions and high quality crystals can be grown. Another drawback to this technique is that the solved structure is a static representation of a dynamic structure.

3.5. NMR spectroscopy

Nuclear magnetic resonance (NMR) spectroscopy refers to the technique of measuring the electromagnetic radiation from nuclei in a magnetic field (figure 3.6). This is based on the principle that many atomic nuclei spin about an axis and generate their own magnetic field, or magnetic moment.[23] NMR yields precise information about the structure and dynamics of biomolecules in solution.[23] It has been successfully used for evaluating the structure and conformation of DNA, RNA, peptides, small proteins, oligosachharides and other natural products.[23,24] Like X-ray crystallography, this technique can provide information about the structure of a molecule/protein, however, it is able to provide a view of the structure in a more dynamic state. This advantage of NMR has made it a highly sought technique for structure elucidation.
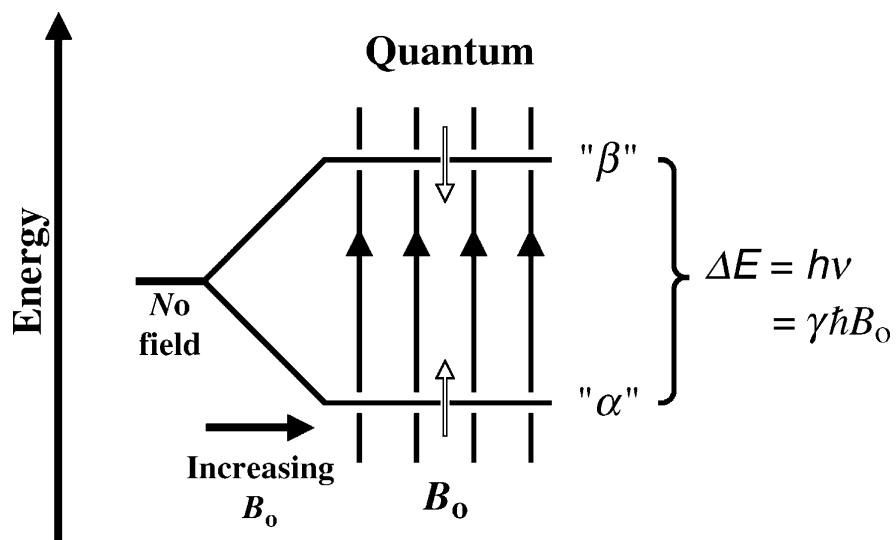
Figure 3.6. The quantum model. Taken from NMR spectroscopy explained with permission.[23]

Essentially, what is measured is the interaction of matter with radiowaves. It is important to note that nuclei must be NMR active in order to absorb radio frequency radiation when placed in a magnetic field. Common nuclei studied are ^{1}H, ^{2}H, ^{13}C, ^{15}N, ^{31}P, ^{19}F and ^{57}Fe.[23] The frequency of the radiowaves absorbed varies with the nucleus as well as for a given type of nucleus, and as such, slight variations are observed. It is also noted that the strength of the absorption is proportional to the number of nuclei.

Currently, protein structures to be studied need to be radiolabeled with radioactive atoms in order to allow these proteins to be studied. Then a combination of 2D and 3D NMR spectra provide information about the location of the atoms within the protein structure. This is done by making use of the through bond or through space interactions between nuclei to generate data about the relative location. This also takes into consideration the spin function (cross peaks) and coupling (diagonal peaks) that are also observed. 2D and 3D NMR have been very useful in evaluating structures of many macromolecules thus far. Unfortunately, the cost and safety measures associated with radioactive materials make NMR spectroscopy less feasible for many labs studying the structure of a given protein.

3.6. Polyacrylamide gel electrophoresis (PAGE) methods for evaluating Hydrophobic sensing of probes

In addition to spectroscopic techniques, PAGE techniques, specifically, native PAGE techniques were also employed. Native PAGE was used to separate proteins based on the mass to charge ratio of the individual proteins (macromolecules). In this case, it was used as a measure of the strength of the interaction between the fluorescent probes and the proteins in the native state.

Gels used were primarily 10 – 15% Tris-HCl gels prepared using a BIORAD gel cassette unit. Gel percentages were matched with the appropriate proteins so as to limit the gel running time for electrophoresis. On completion of each gel, UV light was then used to trigger the fluorescence of any probe still bound to the individual proteins. The level/amount of fluorescence was evaluated and correlated to the level of surface hydrophobicity.

Sodium dodecyl sulfate PAGE was used with labeled proteins to verify the covalent linkage of labeling probe to proteins as well as to evaluate the impact of linearization on the probe signal. SDS PAGE uses the unique property of the detergent SDS to linearize and provide a net negative charge to the protein. Proteins are then separated based on the molecular weight. All gels used for

PAGE were casted by hand and preparation was done according to the recipe outlined in the following table (Table 3.2). All buffers including sample buffers[25] were prepared from stock solutions of 10X buffers acquired from BioRad.

Table 3.2. SDS PAGE gel preparation protocol using BioRad gel cassettes.

Tris-HCl Polyacrylamide Gel Preparation sheet				
	Resolving Gel			**Stacking Gel**
Components	**10%**	**12%**	**15%**	**5%**
Water	3.755 ml	2.955 ml	1.755 ml	3.420 ml
30% Acrylamide solution	4.000 ml	4.800 ml	6.000 ml	0.850 ml
1.5 M Tris-HCl (pH 8.8)	4.000 ml	4.000 ml	4.000 ml	---
1.0 M Tris-HCl (pH 6.8)	---	---	---	0.625 ml
10% SDS	0.120 ml	0.120 ml	0.120 ml	0.050 ml
10% APS	0.120 ml	0.120 ml	0.120 ml	0.050 ml
TEMED	0.005 ml	0.005 ml	0.005 ml	0.005 ml
Total Volume:	*12 ml*	*12 ml*	*12 ml*	*5 ml*

3.6.1. Native Polyacrylamide Gel electrophoresis (PAGE)

Native PAGE was conducted in accordance with published protocols and adapted as indicated below.[26] Initially, proteins were incubated in the presence of increasing concentration (1X/3X/10X or 1X/5X/25X) of hydrophobic dyes for

1 h at room temperature. Proteins incubated with dye were then mixed (1:1) with native sample buffer. The entire sample was then loaded unto the appropriate concentration polyacrylamide gel (10 – 15%) before electrophoresis at 80 V. The following considerations were made depending on the protein being analyzed:

a. Larger proteins (>50 kDa) were typically run on smaller percentage gels (10%) to allow proper migration within the typical 3 hr run.

b. Smaller proteins (<50 kDa) were typically run on higher percentage gels (12 – 15%) to allow proper migration and resolution within the typical 3 hr run.

c. Some proteins were run longer depending on the effect of pI on the migration rate in the native PAGE. Isoelectric points close to pH 8.8 required roughly double the time for migration.

Then, UV images of gels were then acquired using the Bio Doc-It imaging system before staining with Coomassie blue. Gels were subject to exposure times from 0.04 s to 4.0 s. Comparison of different gels was done by using the same exposure time for each gel. Gels were then stained overnight in Coomassie Blue R-250 and subsequently destained.

3.6.2. SDS PAGE for fluorescent labeling verification

SDS PAGE was conducted in accordance with previous protocols with the following changes. Samples were prepared in Laemmli sample buffer (BioRad) with 5% beta-mercaptoethanol for disulfide reduction. Samples were then heated at 100 °C for 5 mins in a water bath before loading unto the corresponding gels. Gels were then run at 80 V for approximately 3 h at room temperature with reduced exposure to direct light. UV images of gels were then acquired using the Bio Doc-It imaging system before staining with Coomassie blue. Note that (1) gels were subject to exposure times from 0.04 s to 4.0 s and (2) comparison of different gels was done by using the same exposure time for each gel.

3.7. Hydrophobic labeling of proteins

The protein labeling was conducted by incubating protein with the fluorescent labeling probe at a molar ratio of 1:15 (protein:dye) in fresh 0.1M sodium bicarbonate buffer (pH 8.3). The reaction was then allowed to proceed for 2 hours at room temperature with gentle shaking on a nutator shaker with reduced exposure to direct light. The reaction was then quenched by adding 10% (v/v) of 1.5 M hydroxylamine (pH 8.5). Proteins were also incubated concurrently with control probes lacking the covalent linker following the same labeling protocol. Labeled protein, unlabeled protein, and protein incubated with control probe

were then analyzed using denaturing SDS PAGE by running the gel for approximately 2-3 hrs at 80 V. Gels were visualized first with UV and then stained with Coomassie R250 overnight before acquiring the image at 600 dpi using a scanner.

3.8. References

1   Chang, R. in *Basic Principles of Spectroscopy* (eds James L. Smith & Madelaine Eichberg) 1-30 (McGraw-Hill Inc, 1971).

2   Jerry Workman, J. in *Applied spectroscopy: A compact reference for practitioners* (eds Jr. Jerry Workman & Art W. Springsteen) 29 - 47 (Academic Press, 1998).

3   King, G. W. *Spectroscopy and Molecular Structure*. (Holt, Rinehart and Winston, Inc, 1965).

4   Wu, C., Bowers, M. T. & Shea, J. E. On the origin of the stronger binding of PIB over thioflavin T to protofibrils of the Alzheimer amyloid-beta peptide: a molecular dynamics study. *Biophys J* **100**, 1316-1324, doi:10.1016/j.bpj.2011.01.058 (2011).

5   Zhu, S. *et al.* Highly water-soluble neutral near-infrared emissive BODIPY polymeric dyes. *J. Mater. Chem.* **22**, 2781-2790, doi:Doi 10.1039/C2jm14920f (2012).

6   Lakowicz, J. R. *Principles of Fluorescence Spectroscopy*. Third edn, (Springer Science+Business Media LLC, 2006).

7   Skoog, D. A., Holler, F. J. & Crouch, S. R. *Principles of Instrumental Analysis*. 357 (Thomson Brooks/Cole, 2007).

8   Zhang, X.-F. The effect of phenyl substitution on the fluorescence characteristics of fluorescein derivatives via intramolecular

photoinduced electron transfer. *Photochem. Photobiol. Sci.* **9**, 1261, doi:10.1039/c0pp00184h (2010).

9 Zhou, Y. *Structural Analysis Of Proteins By Covalent Labeling And Mass Spectrometric Detection* Doctor Of Philosophy thesis, University of Massachusetts Amherst, (2014).

10 Zhou, Y. & Vachet, R. W. Covalent labeling with isotopically encoded reagents for faster structural analysis of proteins by mass spectrometry. *Anal Chem* **85**, 9664-9670, doi:10.1021/ac401978w (2013).

11 Keppler, A. *et al.* A general method for the covalent labeling of fusion proteins with small molecules in vivo. *Nat Biotechnol* **21**, 86-89, doi:10.1038/nbt765 (2003).

12 Fitzgerald, M. C. & West, G. M. Painting proteins with covalent labels: what's in the picture? *J Am Soc Mass Spectrom* **20**, 1193-1206, doi:10.1016/j.jasms.2009.02.006 (2009).

13 Wong, S. S. & Jameson, D. M. *Chemistry of Protein and Nucleic Acid Cross-Linking and Conjugation, Second Edition*. (CRC Press, 2011).

14 Velapoldi, R. A. & Tønnesen, H. H. Corrected Emission Spectra and Quantum Yields for a Series of Fluorescent Compounds in the Visible Spectral Region. *J. Fluoresc.* **Volume 14**, 465-472 (2004).

15 Haskard, C. A. & Li-Chan, E. C. Y. Hydrophobicity of Bovine Serum Albumin and Ovalbumin Determined Using Uncharged (PRODAN) and

Anionic (ANS-) Fluorescent Probes. *J. Agric. Food Chem.* **46**, 2671-2677 (1998).

16   Nakai, S., Li-Chan, E. & Arteaga, G. E. in *Methods of testing protein functionality*   (ed G. M. Hall) Ch. 8, 226 - 255 (Blackie A & P, 1996).

17   Haskard, C. A., Easton, C. J., May, B. L. & Lincoln, S. F. Cooperative Binding of 6-(p-Toluidinyl)naphthalene-2-sulfonate by β-Cyclodextrin Dimers. *J. Phys. Chem* **100**, 14457-14461 (1996).

18   Kato, A. & Nakai, S. Hydrophobicity determined by a fluorescence probe method and its correlation with surface properties of proteins. *Biochim. Biophys. Acta* **624**, 13-20 (1980).

19   Rapaport, D. C. *The art of molecular dynamics simulation*. (Cambridge university press, 2004).

20   Rapaport, D., Blumberg, R. L., McKay, S. R. & Christian, W. The Art of Molecular Dynamics Simulation. *Computers in Physics* **10**, 456-456 (1996).

21   Smyth, M. S. & Martin, J. H. J. X Ray crystallography. *J Clin Pathol:Mol Pathol* **53**, 8 - 14 (2000).

22   Rhodes, G. *Crystallography Made Crystal Clear: A Guide for Users of Macromolecular Models*. 3rd edn, (Academic Press, Elsevier, 2006).

23   Jacobsen, N. E. *NMR spectroscopy explained: simplified theory, applications and examples for organic chemistry and structural biology*. (John Wiley & Sons, 2007).

24   Ulrich, E. L. *et al.* BioMagResBank. *Nucleic Acids Res* **36**, D402-408, doi:10.1093/nar/gkm957 (2008).

25   Laemmli, U. K. Cleavage of Structural Proteins during the Assembly of the Head of Bacteriophage T4. *Nature* **227**, 680 - 685, doi:doi:10.1038/227680a0 (1970).

26   Arndt, C., Koristka, S., Bartsch, H. & Bachmann, M. *Protein Electrophoresis: Methods and Protocols*. Vol. 869 49 - 55 (Humana Press (Springer Science+Business Media, LLC), 2012).

Chapter 4: BODIPY-Based Fluorescent Probes for Sensing Protein Surface-Hydrophobicity

Nethaniah Dorh[a], Shilei Zhu[a,†], Kamal B. Dhungana[b], Ranjit Pati[b], Fen-Tair Luo[c], Haiying Liu[a], Ashutosh Tiwari[a]*.

[a]Department of Chemistry, Michigan Technological University, Houghton, MI 49931, USA

[b]Department of Physics, Michigan Technological University, Houghton, MI 49931, USA

[c]Institute of Chemistry, Academia Sinica, Taipei, Taiwan 11529, Republic of China

[†]Department of Chemistry & Biochemistry, University of Maryland, College Park, MD 20742, USA

4.1.　**Abstract**

Mapping surface hydrophobic interactions in proteins is key to understanding molecular recognition, biological functions, and is central to many protein misfolding diseases. Herein, we report synthesis and application of new BODIPY-based hydrophobic sensors (HPsensors) that are stable and highly fluorescent for pH values ranging from 7.0 to 9.0. Surface hydrophobic measurements of proteins (BSA, apomyoglobin, and myoglobin) by these HPsensors display much stronger signal compared to 8-anilino-1-naphthalene sulfonic acid (ANS), a commonly used hydrophobic probe; HPsensors show a 10- to 60-fold increase in signal strength for the BSA protein with affinity in the nanomolar range. This suggests that these HPsensors can be used as a sensitive indicator of protein surface hydrophobicity. A first principle approach was used to identify the molecular level mechanism for the substantial increase in the fluorescence signal strength. Our results show that conformational change and increased molecular rigidity of the dye due to its hydrophobic interaction with protein lead to fluorescence enhancement.

4.2. Introduction

Protein folding and stability in aqueous solution is governed by a delicate balance of hydrogen bonding, electrostatic interaction, and hydrophobic interactions; hydrophobic interactions provide the major structural stability to the proteins.[1-3] Surface hydrophobic interactions are fundamental to protein-ligand interaction, molecular recognition[4], and may influence intermolecular interactions and biological functions.[5,6] Furthermore, point mutations and (or) oxidative damage of proteins can result in increased surface hydrophobicity of proteins and have been linked to several age-related proteinopathies.[7-12] As a result, there has been a growing interest and need for developing probes and methods for sensing/mapping protein surface hydrophobicity[13-17] as this can help to design better drug molecules based on surface properties.[18-21]

Many extrinsic fluorophores have been designed and used to study protein dynamics including protein folding and misfolding processes that have led to a better understanding of several proteinopathies including neurodegenerative diseases. However, only a few fluorophores that can measure protein surface hydrophobicity have been reported thus far: this includes dyes such as 8-anilino-1-naphthalene sulfonic acid (ANS), 4,4′-dianilino-1,1'-binaphthyl-5,5'-disulfonic acid (Bis-ANS), 6-propionyl-2-(N,N-dimethylamino)naphthalene (PRODAN), tetraphenylethene derivative, and Nile Red.[5,15,16,22,23] For characterization of most of these dyes, bovine serum albumin (BSA) and human

serum albumin (HSA) have been used as test proteins. Of all these dyes, ANS is the most commonly used dye for measuring surface hydrophobicity. However, ANS dye is fraught with many issues such as: 1) it is an anionic dye and can contribute to fluorescence by both electrostatic as well as hydrophobic interactions leading to overestimation of fluorescence signal, and 2) it does not give measurable fluorescence signal when bound to solvent exposed hydrophobic surface of proteins due to quenching. [5,15,24-26] The other dye PRODAN, is a solvent-sensitive, neutral, fluorescent probe that has comparable fluorescence signal to ANS near physiological pH but has very poor solubility in water.[5,15] To address these problems, we have synthesized a series of 4,4-difluoro-4-bora-3a,4a-diaza-s-indacene (BODIPY) based hydrophobic sensors (HPsensors) for measuring protein hydrophobicity and tested these sensors on three proteins: BSA, myoglobin (Mb), and apomyoglobin (ApoMb). We chose BODIPY dyes for several reasons: they are highly fluorescent in non-polar media but are also fluorescent in polar (aqueous) media, have sharp and narrow emission peaks, and possess reduced solvatochromic shifts.[27,28] In addition, BODIPY dyes are highly tunable[29-32] making them excellent candidates for the purpose of selectively reporting the hydrophobicity of proteins.
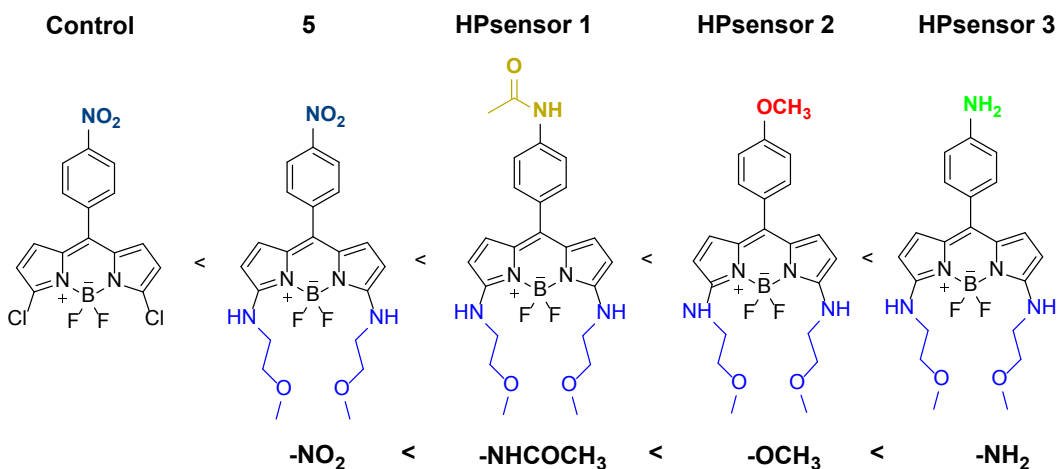
Figure 4.1. BODIPY dye structures in order of increasing electron donating ability. Schematic of dyes (control, dye 5, and HPsensors 1, 2, and 3) shown were synthesized according to detailed protocol outlined in the supplementary methods.

In this article we have focused our efforts on aryl substitution at 8-position (*meso*) on BODIPY dye for hydrophobic sensing of proteins. In figure 4.1, we show the structures of the synthesized HPsensors along with the control dye[27,33,34] arranged in order of increasing electron donating ability. We substituted 2-methoxyethylamine group at 3,5-positions of the BODIPY core that increases water solubility.

These HPsensors show weak but measurable fluorescence signal in water but are highly fluorescent in nonpolar environment (Figure 4.16). Furthermore, these HPsensors when tested with proteins (myoglobin (Mb), apomyoglobin (ApoMb), and BSA) show high fluorescence signal for hydrophobic proteins, BSA and ApoMb. Under same experimental conditions HPsensor **2** shows a 60-

fold increase in fluorescence signal strength for BSA compared to that observed for ANS with affinity in the nanomolar range, making this dye a very sensitive indicator of protein surface-hydrophobicity (S_0).

4.3. Results

Synthesis and characterization of fluorescent probes. The synthesis of dyes (Figs. 4.1 - 4.2; see Appendix A details on synthesis methods) was done by aryl substitutions at the *meso* position of the BODIPY core that increases dye sensitivity to solvent polarity and protein hydrophobicity; substitution of chloro groups with 2-methoxyethylamine groups at the 3,5-positions enhances water solubility (Fig. 4.16).

All dyes synthesized were fluorescent except for dye **5** (Fig. 4.16.). We calculated the quantum yield of each dye in three different solvents water, ethanol, and dichloromethane (Table 4.1; Figs. 4.3 - 4.14). Quantum yield data on the HPsensors showed the greatest yield in ethanol and dichloromethane with the yield in water being the lowest which was similar to that of the **control** dye. We then determined the extinction coefficient of HPsensors **1**, **2**, **3**, and **control** dye in ethanol.
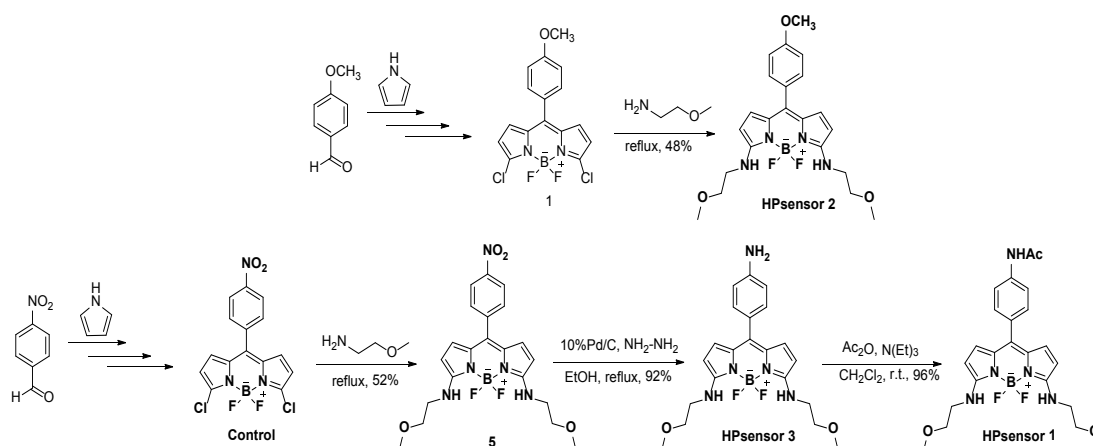
Figure 4.2. Synthetic route to HPsensors (1, 2, and 3), control dye, and dye 5.

Probe 1 and control were prepared by using 4-methoxybenzaldehyde and 4-nitrobenzaldehyde. Dye 5 and HPsensor 2 were prepared by replacing the chlorine groups at 3,5-positions of dyes 1 and control with a nucleophile, 2-methoxyethan-1-amine. HPsensor 3 was prepared by reducing a nitro group at meso-position of BODIPY dye 5 via catalytic hydrogenation using palladium-on carbon in the presence of hydrazine. HPsensor 1 was prepared by reacting an amino group at meso-position of HPsensor 3 with acetic anhydride at room temperature to form an amide bond.

Table 4.1. **Absorption and emission peak maxima of control dye, HPsensors 1, 2 and 3 with corresponding fluorescence quantum yield and the extinction coefficient in ethanol.**

Dye	Solvent	Absorption peak (nm)	Emission peak (nm)	Fluorescence Quantum Yield (%)	Extinction coefficient (ethanol)
Control	Ethanol	517	540	7.99	14880 $M^{-1}cm^{-1}$ (at 517 nm)
	Water	518	540	0.15	
	CH_2Cl_2	521	545	5.58	
HPsensor 1	Ethanol	565	585	23.99	50990 $M^{-1}cm^{-1}$ (at 565 nm)
	Water	564	584	6.77	
	CH_2Cl_2	569	587	19.92	
HPsensor 2	Ethanol	564	581	45.03	31930 $M^{-1}cm^{-1}$ (at 564 nm)
	Water	563	580	1.27	
	CH_2Cl_2	567	584	42.21	
HPsensor 3	Ethanol	562	577	36.17	53920 $M^{-1}cm^{-1}$ (at 562 nm)
	Water	561	579	0.25	
	CH_2Cl_2	566	582	35.39	

The measurements indicated an extinction coefficient of 14880 μM^{-1} cm^{-1} for

control dye. In contrast, for the HPsensors **1**, **2**, and **3** extinction coefficients

were 50990, 31930 and 53920 μM^{-1} cm^{-1}, respectively (Table 4.1).

Response of dyes to change in solvent polarity. The absorption and emission spectra of dyes were measured in solvents with different polarity (water, ethanol and dichloromethane). These measurements showed that all dyes were fluorescent with the exception of dye 5 that exhibited no fluorescence either in high or low polarity solvents. Of the dyes that were fluorescent (HPsensors 1, 2, and 3), the initial characterization showed a small red shift (2 to 5 nm) in absorbance and emission maxima with decreasing polarity (Figs. 4.3 – 4.14) which was similar to the control dye with the strong electron withdrawing substitution. To further investigate how polarity impacted the fluorescence spectra of each of these dyes, we measured the fluorescence in ethanol-water mixture with increasing concentration of ethanol (20% increments ranging from 0 to 100% ethanol) (Fig. 4.16). The results show that HPsensors 1, 2, and 3 responded similarly to the change in solvent conditions with maximum fluorescence in 60% ethanol. The exception was the control dye that showed a linear increase in fluorescence with increasing ethanol concentration (from 0% to 100% ethanol) (Fig. 4.16).
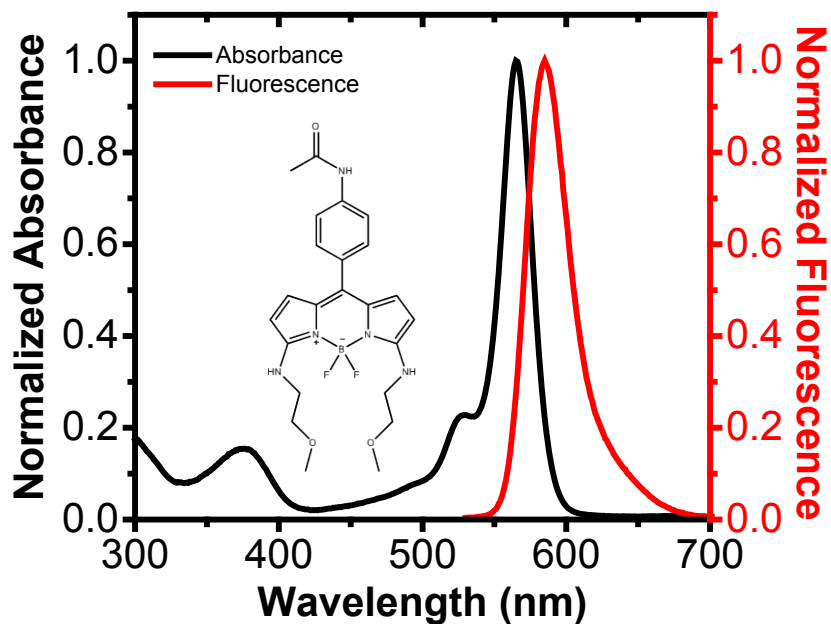
Figure 4.3. Normalized absorption and emission spectra for HPsensor 1 in ethanol. Ex λ = 520 nm.
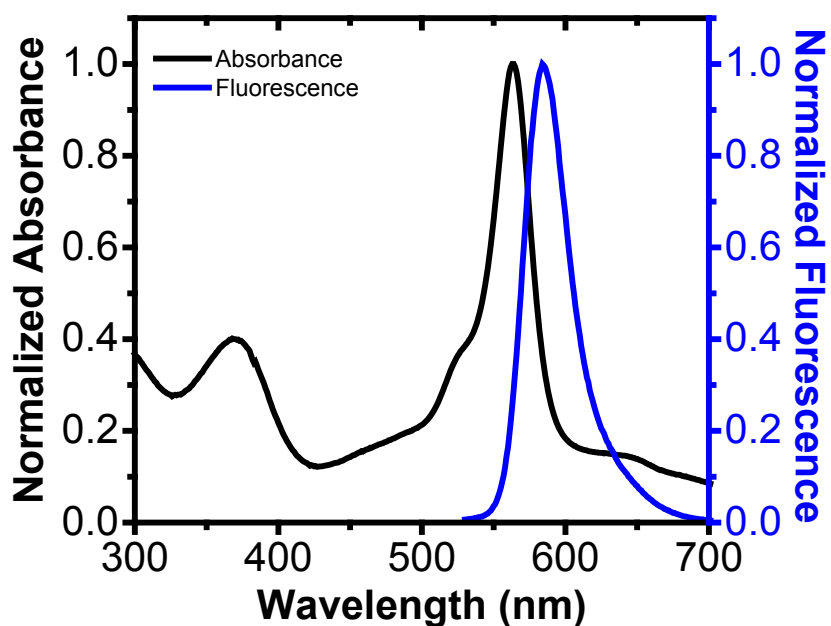
Figure 4.4. Normalized absorption and emission spectra for HPsensor 1 in H₂O. Ex λ = 520 nm
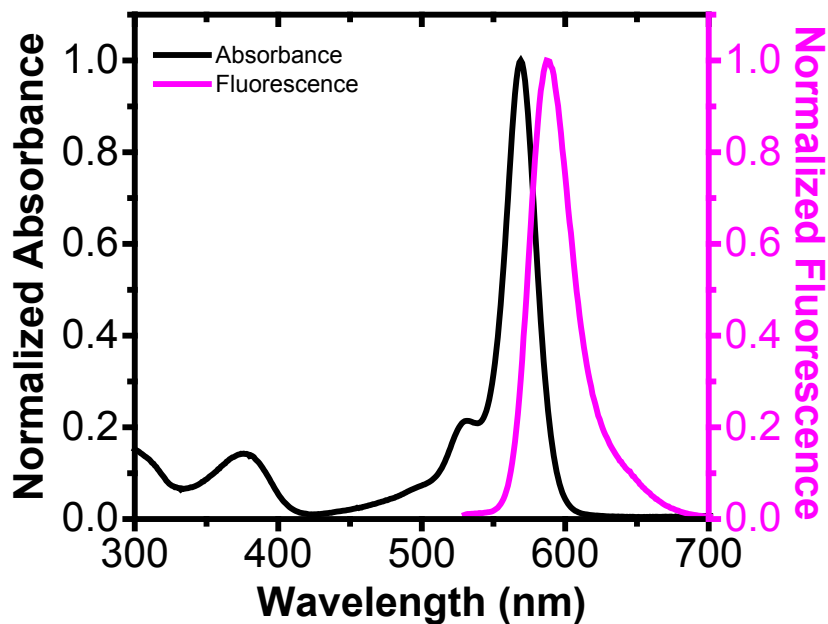
Figure 4.5. Normalized absorption and emission spectra for HPsensor 1 in CH₂Cl₂. Ex λ = 520 nm.
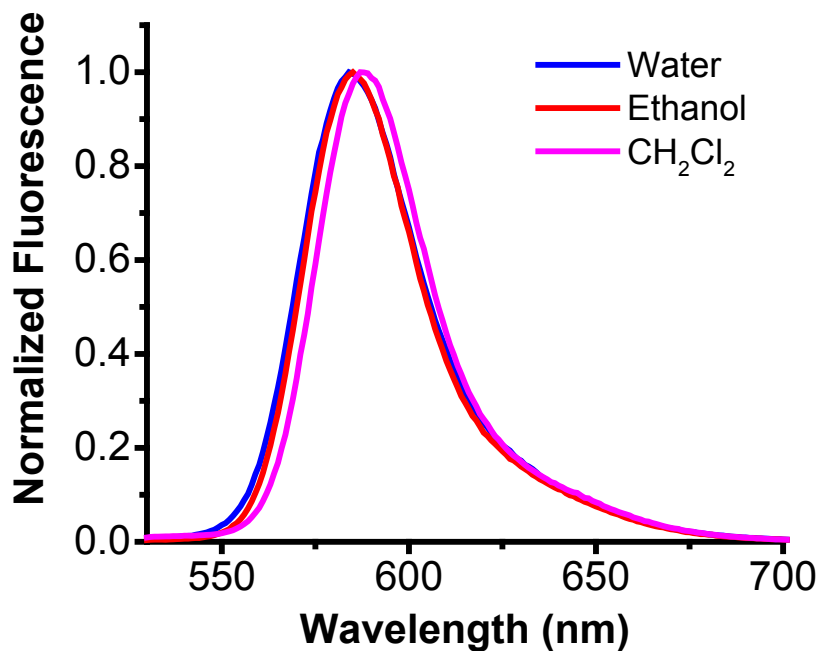
Figure 4.6. Normalized emission spectra for HPsensor 1 in ethanol, H₂O, and CH₂Cl₂. Ex λ = 520 nm.
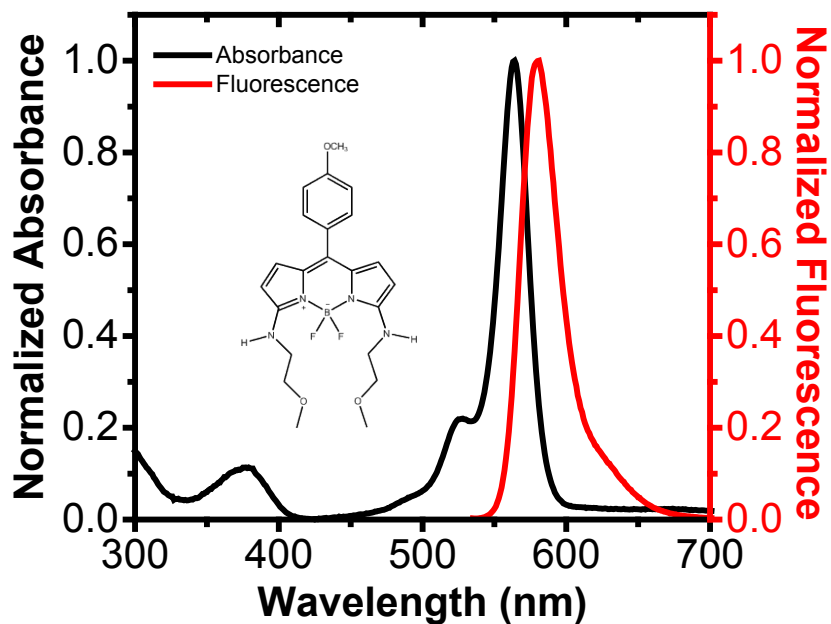
Figure 4.7. Normalized absorption and emission spectra for HPsensor 2 in ethanol. Ex λ = 528 nm.
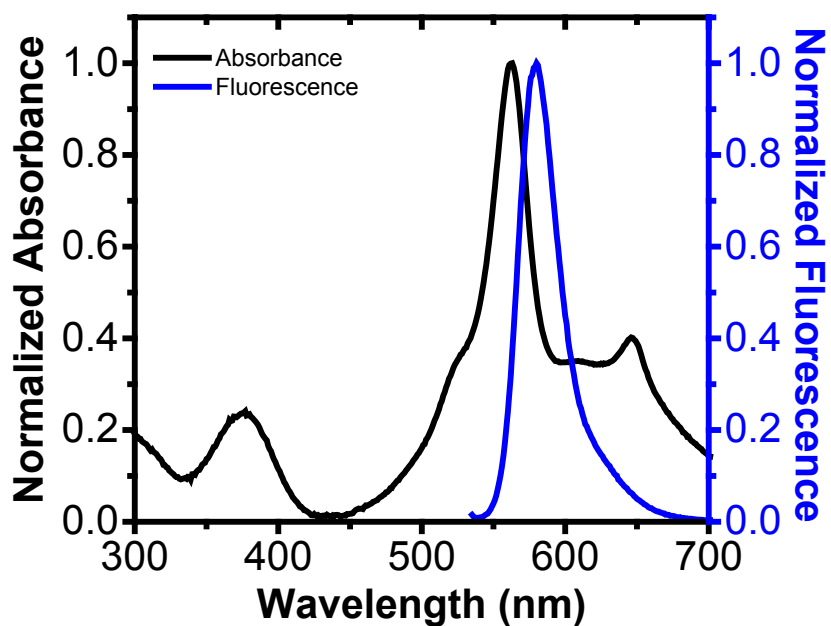
Figure 4.8. Normalized absorption and emission spectra for HPsensor 2 in H₂O. Ex λ = 528 nm.
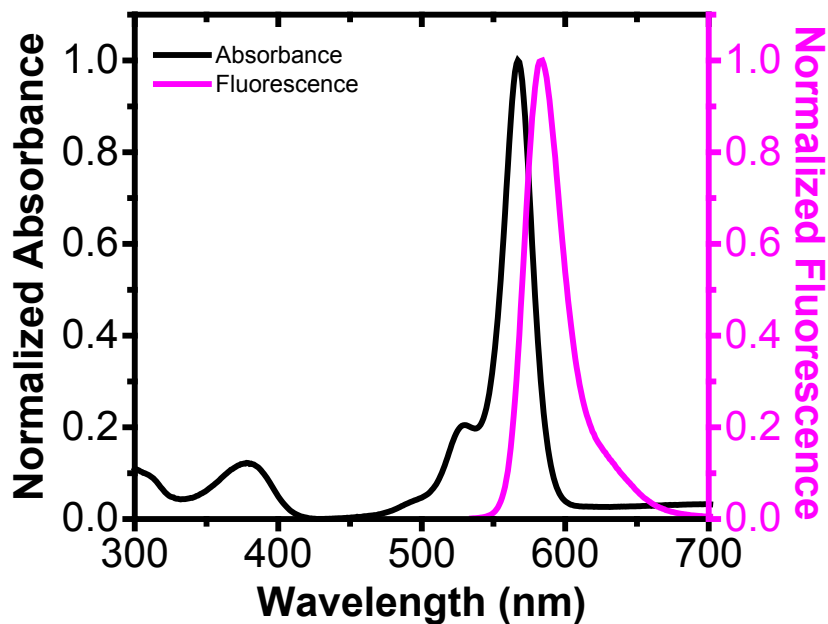
Figure 4.9. Normalized absorption and emission spectra for HPsensor 2 in CH₂Cl₂. Ex λ = 528 nm.
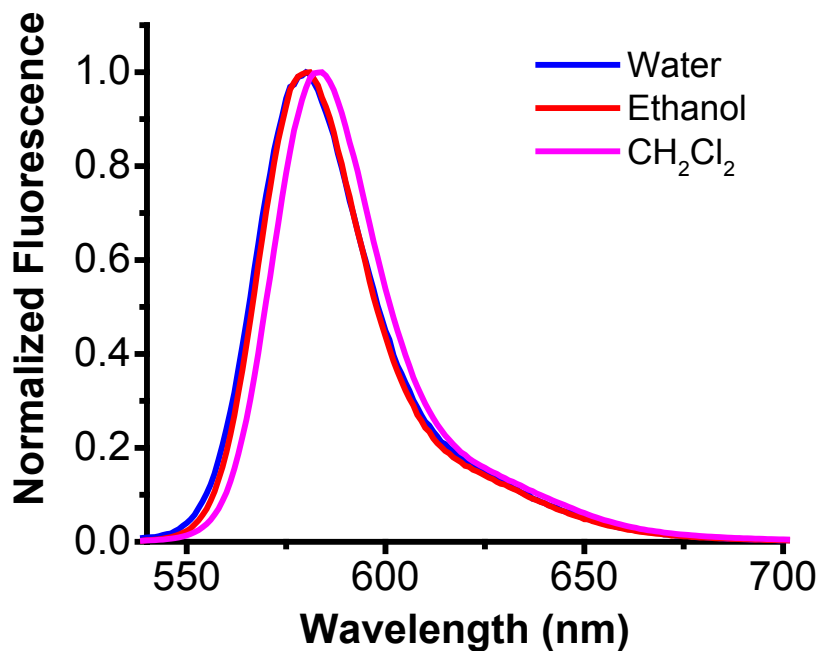
Figure 4.10. Normalized emission spectra for HPsensor 2 in ethanol, H₂O, and CH₂Cl₂. Ex λ = 528 nm.
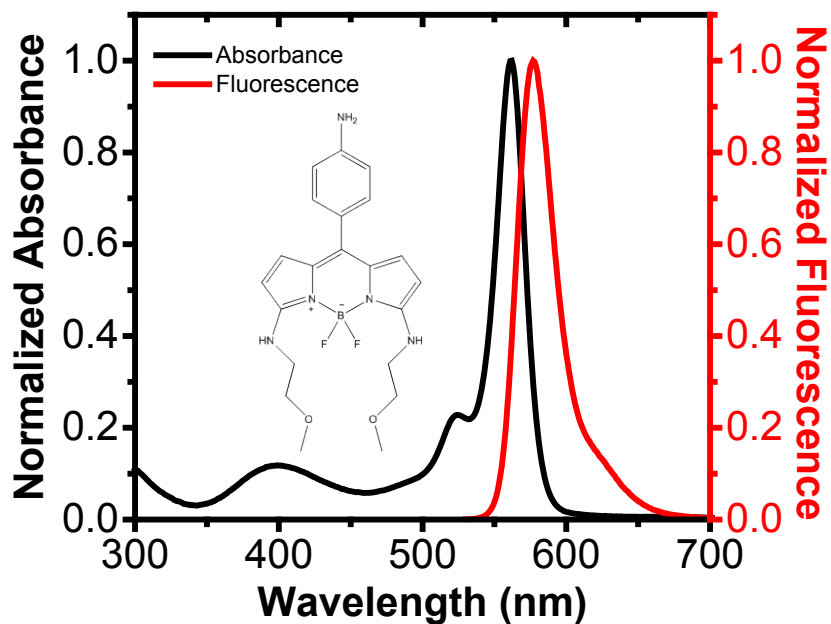
Figure 4.11. Normalized absorption and emission spectra for HPsensor 3 in ethanol. Ex λ = 520 nm.
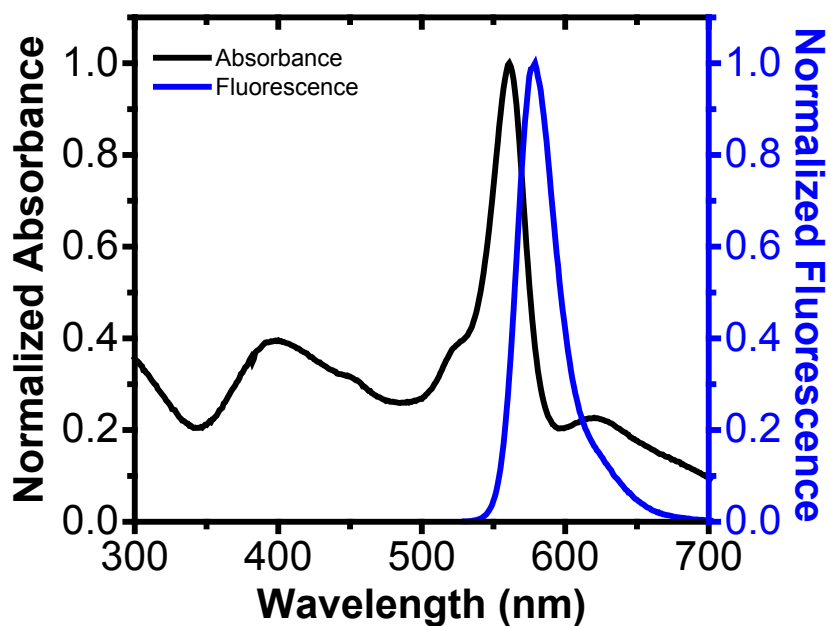
Figure 4.12. Normalized absorption and emission spectra for HPsensor 3 in H₂O. Ex λ = 520 nm.
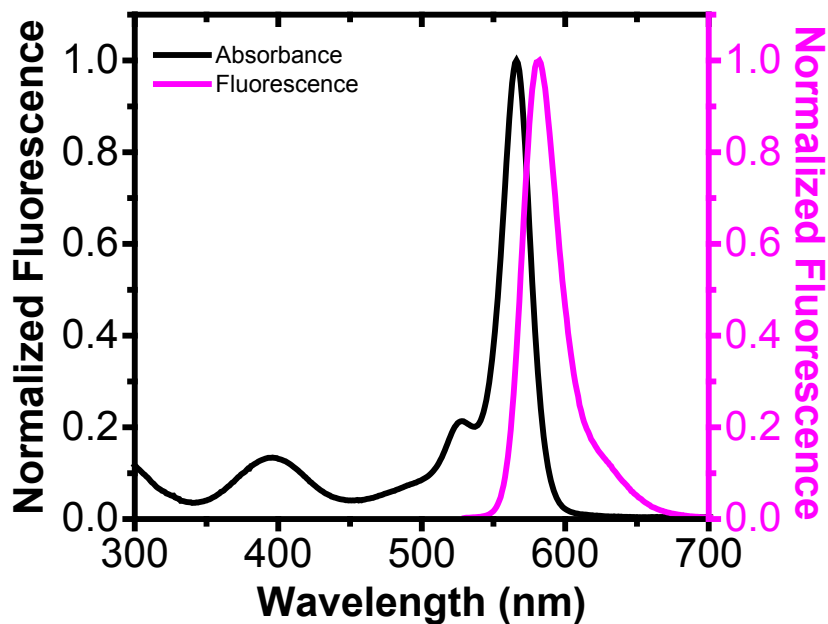
Figure 4.13. Normalized absorption and emission spectra for HPsensor 3 in CH₂Cl₂. Ex λ = 520 nm.
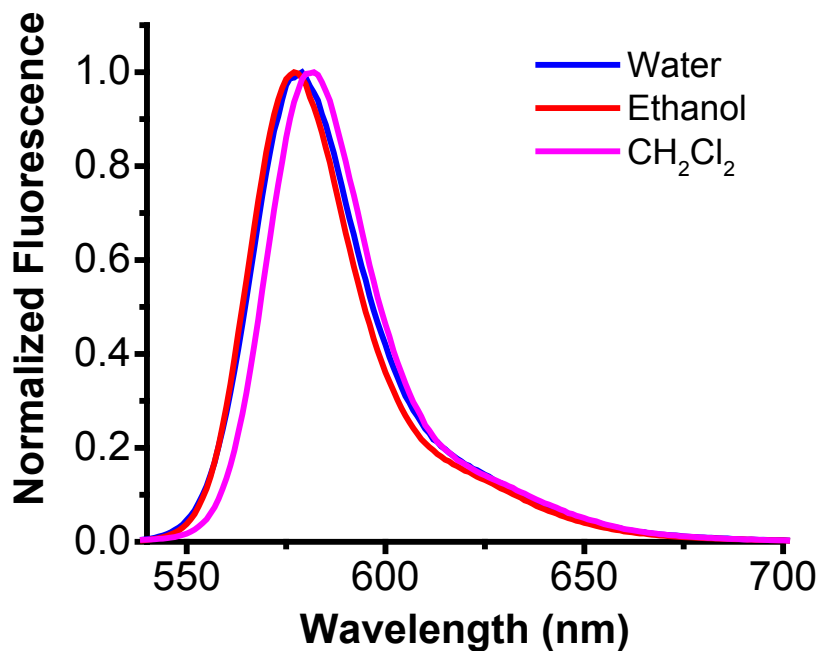
Figure 4.14. Normalized emission spectra for HPsensor 3 in ethanol, H₂O, and CH₂Cl₂. Ex λ = 520 nm.
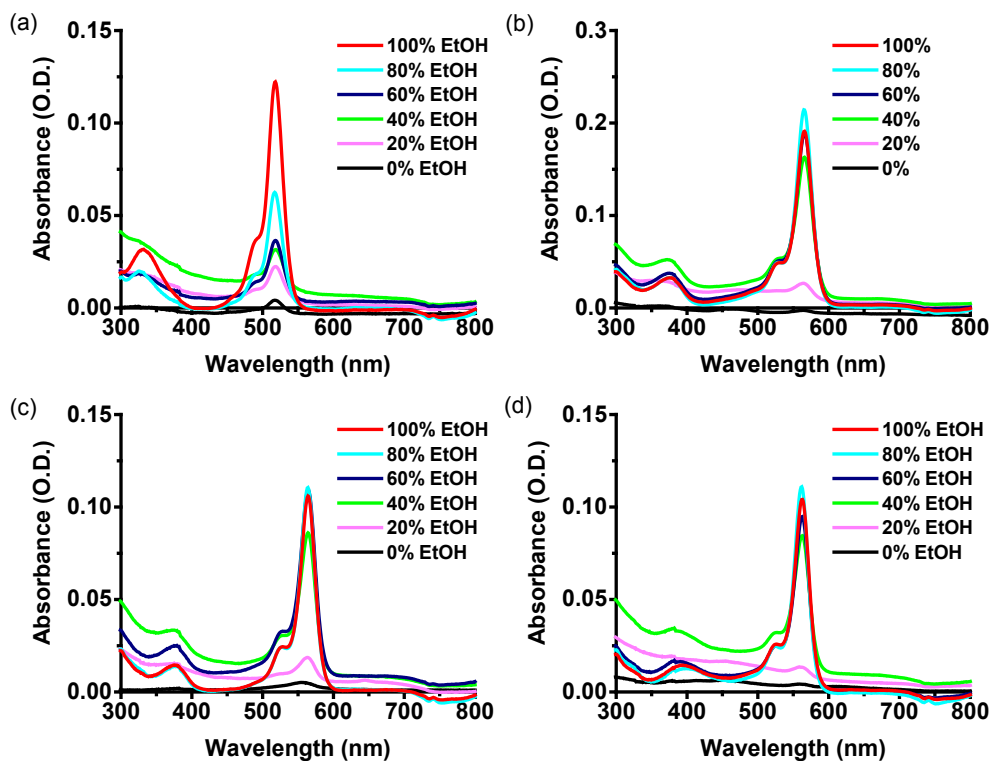
Figure 4.15. Absorption spectra of 2 µM of control dye (a) and HPsensors 1 (b), 2 (c), and 3 (d) in ethanol-water mixture. Absorption maxima for all probes was at 60 - 80% except for the control dye which showed a maximum absorbance at 100%.

Effect of pH on fluorescence of dyes. The dyes were tested for the effect of pH on fluorescence intensity using Carmody buffer series in pH range from 2 to 12 (Supplementary Figs. 6 and 7). The HPsensors (**1**, **2**, and **3**) are highly fluorescent for pH values ranging from 7.0 to 9.0 with maximum fluorescence observed in 60% ethanol (ethanol-water mixture) (Fig 4.16 - 4.17).
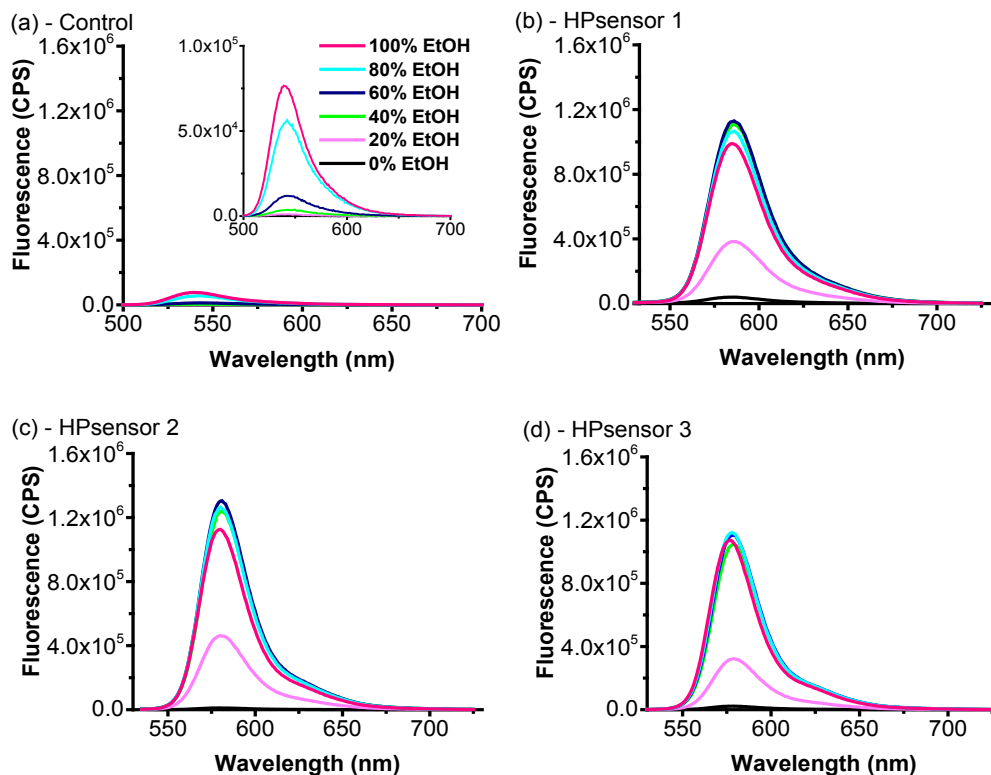
Figure 4.16. Fluorescence spectra of 2 µM of control dye (a) and HPsensors 1 (b), 2 (c), and 3 (d) in ethanol-water mixture. HPsensors 1, 2, and 3 show maximum fluorescence at 60% ethanol whereas the control dye shows increase in fluorescence proportional to decrease in polarity. The emission spectra were collected after excitation at 520 nm for HPsensors 1 and 3, at 528 nm for HPsensor 2, and at 475 nm for the control dye.

When the dyes were tested for the effect of pH on fluorescence intensity using Carmody buffer series in pH range from 2 to 12. The fluorescence spectra for 2 µM concentration of control and HPsensors were acquired at different pH values in triplicate and a mean peak intensity vs pH for each dye was plotted (Fig. 4.17). Mean peak fluorescence intensity for the control dye was at 540 nm, while for HPsensors **1**, **2** and **3** it was at 584, 579 and 578 nm, respectively.
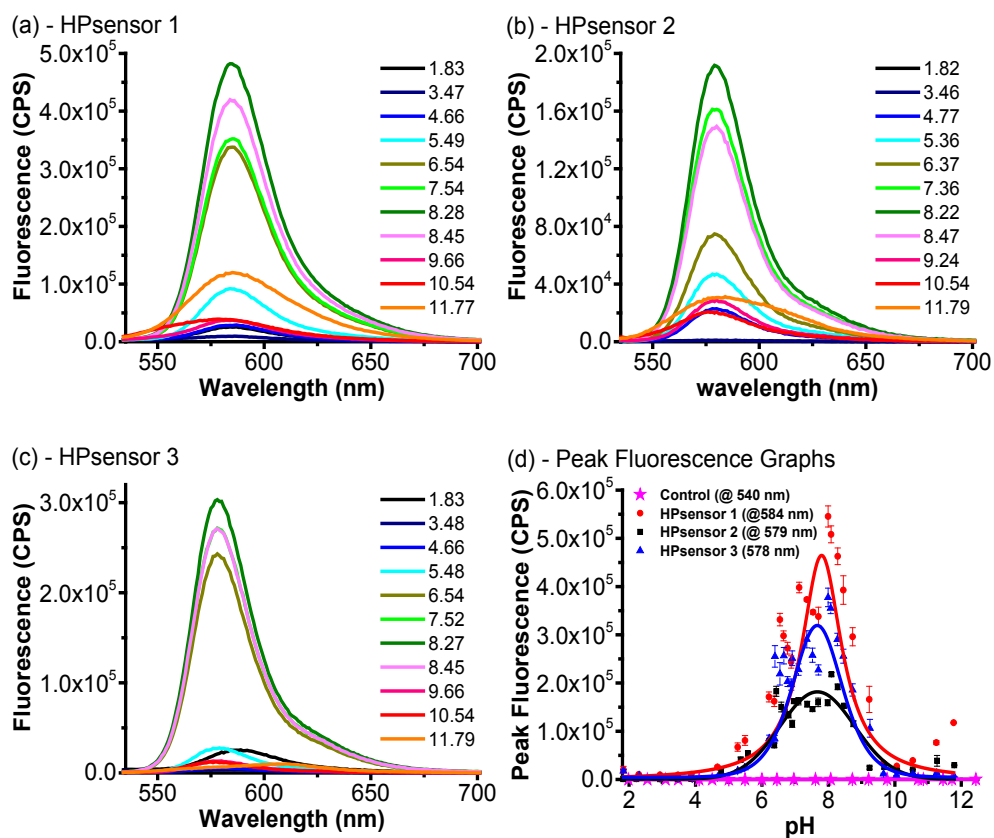
Figure 4.17. Fluorescence spectra of control and HPsensors 1, 2 and 3 show sensitivity to change in pH. Select plots of HPsensors **1, 2** and **3** with increasing pH (a – c). The mean peak intensity plotted at the indicated wavelength vs pH for all HPsensors and control dye (d). Dyes were incubated at 2 µM concentration at room temperature in Carmody buffer with pH ranging from ~ 2 to 12 before acquiring the emission spectra. The emission spectra were collected after excitation at 520 nm for HPsensors **1** and **3**, at 528 nm for HPsensor **2** and at 475 nm for the control dye.

While the HPsensors showed most sensitivity in the pH range from 6.5 to 9, the control dye did not show any pH sensitivity (Fig. 4.17). When tested for pH stability all HPsensors (**1**, **2** and **3**) showed an increase in fluorescence as the pH increased from 3 to 8; when the pH was decreased from 8 to 3, a comparable decrease in fluorescence was observed (Fig. 4.18).

104
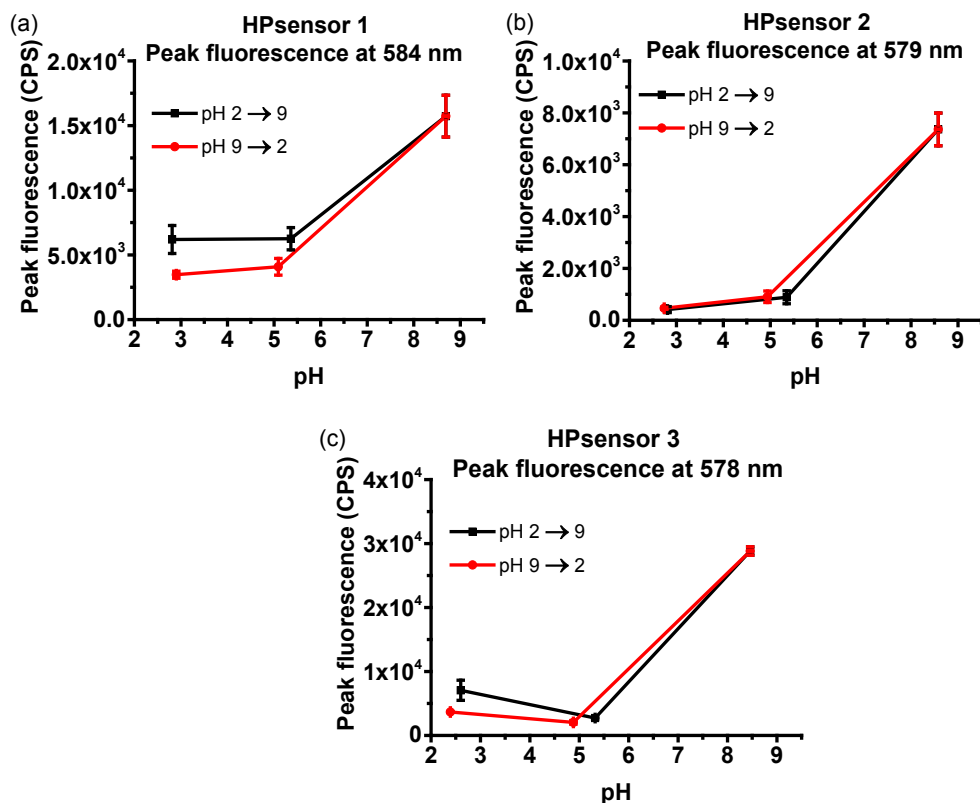
Figure 4.18. **Mean peak fluorescence of HPsensors with pH changes**. Mean peak fluorescence of each HPsensor (at 2 µM) is plotted with increasing pH (pH ~2.0 to pH ~ 9.0) followed by decrease in pH (pH ~ 9.0 to pH ~ 2.0). All experiments were done in triplicate. Error bars indicate ± SD. The excitation and emission wavelength for each dye used is: HPsensor **1**, Ex 520 nm, Em 584 nm; HPsensor **2**, Ex 528 nm, Em 579 nm; HPsensor **3**, Ex 520 nm, Em 578 nm.

Effect of ions on dye fluorescence. In addition, the dyes showed negligible response to ions (Na^+, Mg^{2+}, Fe^{2+}, Fe^{3+}, Ca^{2+}, Zn^{2+}) commonly found in buffer solutions or as impurities in solutions. Their fluorescence was not significantly enhanced or quenched in the presence of ions even up to physiologically relevant concentrations of 150 µM.[35,36]

105
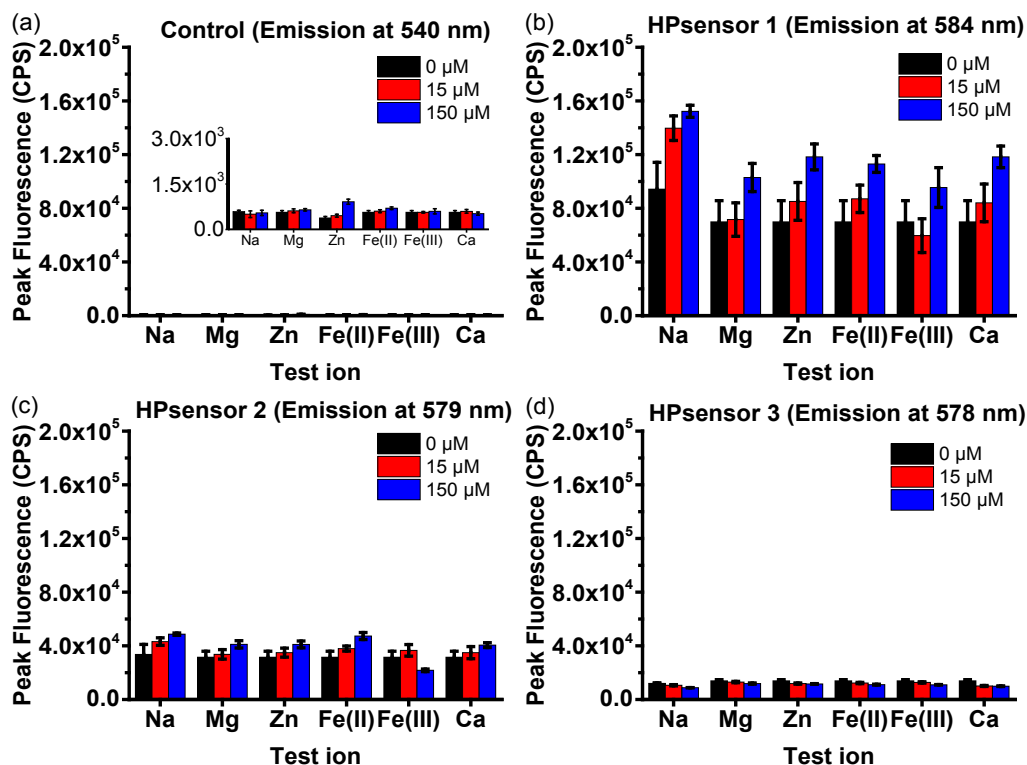
Figure 4.19. Mean peak fluorescence of control and HPsensors with test ions (Na⁺, Mg²⁺, Fe²⁺, Fe³⁺, Ca²⁺, Zn²⁺) in water. Mean peak fluorescence of each HPsensor (at 2 µM) is plotted in the presence of increasing concentration of ions (0 to 150 µM). All experiments were done in triplicate. Error bars indicate ± SD. The excitation and emission wavelength for each dye used is: Control dye, Ex 475 nm, Em 540 nm; HPsensor **1**, Ex 520 nm, Em 584 nm; HPsensor **2**, Ex 528 nm, Em 579 nm; HPsensor **3**, Ex 520 nm, Em 578 nm.
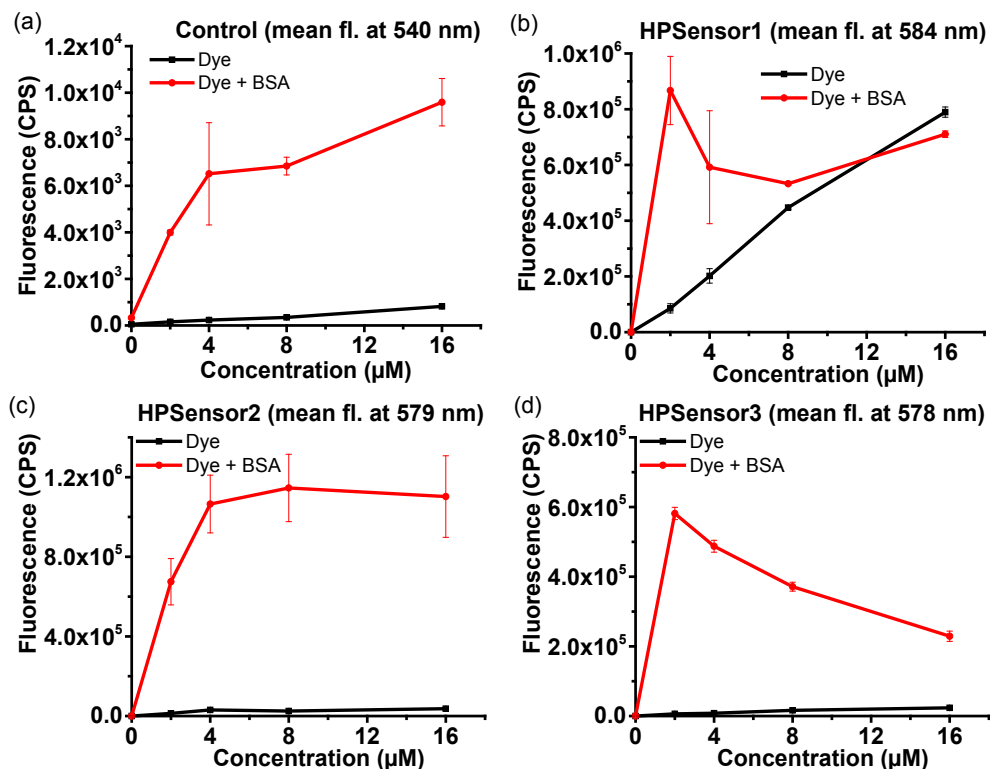
Figure 4.20. **Mean peak fluorescence of increasing concentration of control and HPsensors in presence and absence of BSA in water (pH adjusted to 8.0).** Mean peak fluorescence of each dye in the absence and presence of BSA (2 μM) is plotted with increasing concentration of control or HPsensor (0 – 16 μM). All experiments were done in triplicate. Error bars indicate ± SD. The excitation and emission wavelength for each dye used is: Control dye, Ex 475 nm, Em 540 nm; HPsensor **1**, Ex 520 nm, Em 584 nm; HPsensor **2**, Ex 528 nm, Em 579 nm; HPsensor **3**, Ex 520 nm, Em 578 nm.

Response of dyes to protein hydrophobicity. We first tested the dyes with

BSA to determine the appropriate concentration to be used for protein studies.

The dyes show a linear fluorescence response for 2 μM of BSA at low dye

concentration i.e. 1:1 or 1:2 protein:dye ratio (Fig. 4.20). Therefore, for

measuring the relative protein hydrophobicity, HPsensors were tested with BSA,

ApoMb, and Mb at 1:1 ratio of dye to protein (2 μM each) (Fig. 4.21 – 4.24).
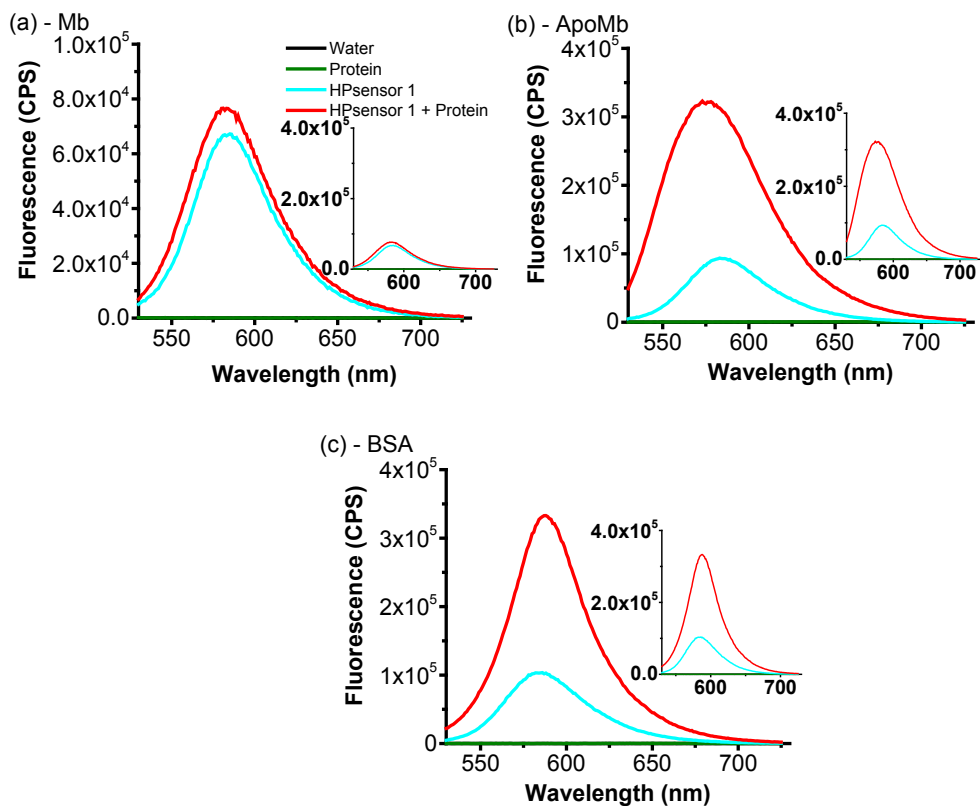
Figure 4.21. Fluorescence emission spectra for HPsensor 1 incubated with (a) myoglobin, (b) apomyoglobin, and (c) BSA. Insets are shown on the same scale for ease of comparison between relative protein signals. Dye was incubated with protein at 1:1 ratio (2 µM each) for 1 hour at 25 °C with appropriate controls before spectra were acquired. Excitation wavelength was 520 nm.
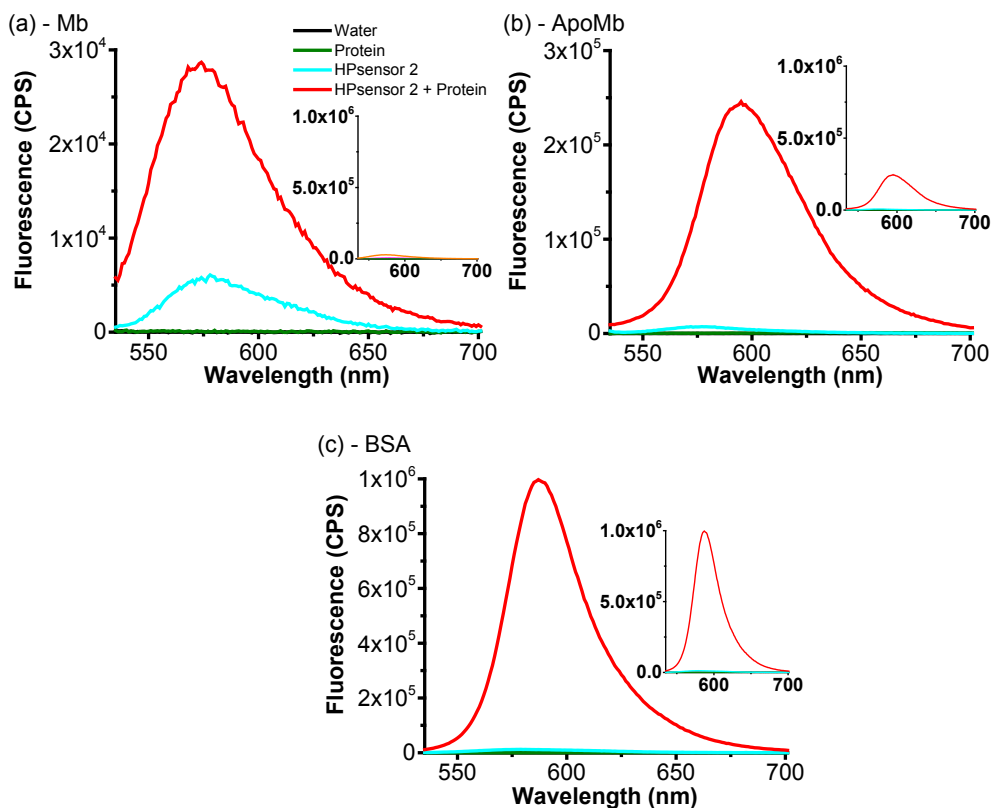
Figure 4.22. Fluorescence emission spectra for HPsensor 2 incubated with (a) myoglobin, (b) apomyoglobin, and (c) BSA. Insets are shown on the same scale for easy comparison of relative protein signals. Dye was incubated with protein at 1:1 ratio (2 µM each) for 1 h at 25 °C with appropriate controls before spectra were acquired. The emission spectra for HPsensor 2 were collected after excitation at 528 nm.
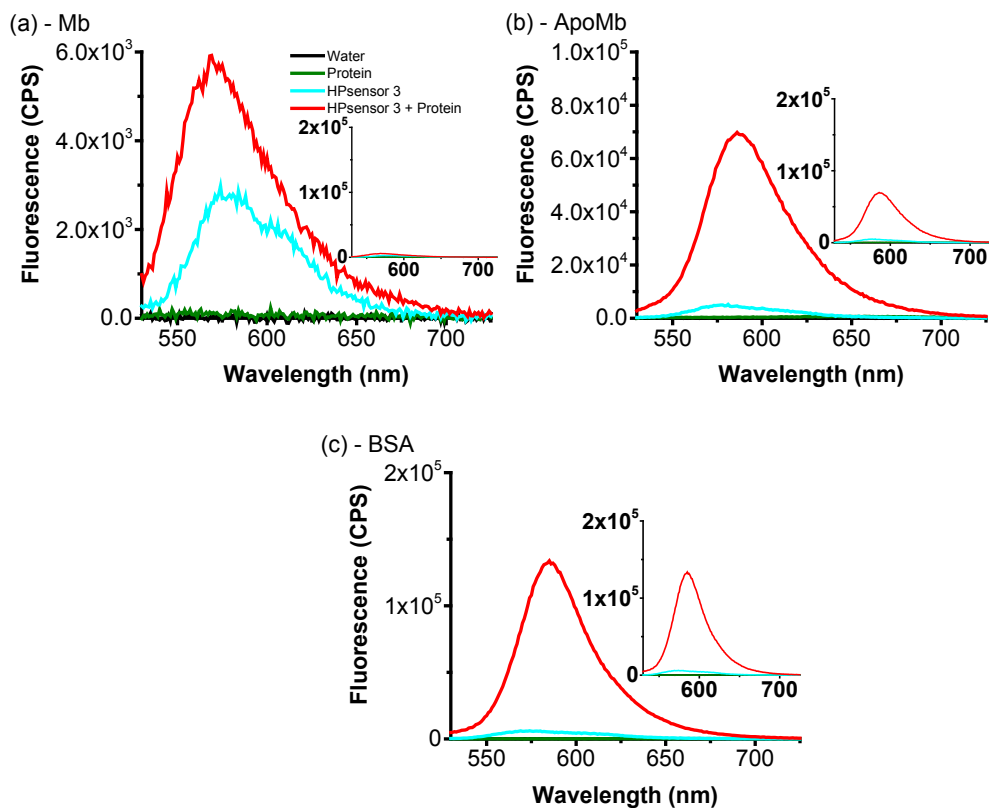
Figure 4.23. Fluorescence emission spectra for HPsensor 3 incubated with (a) myoglobin, (b) apomyoglobin, and (c) BSA. Insets are shown on the same scale for ease of comparison between relative protein signals. Dye was incubated with protein at 1:1 ratio (2 µM each) for 1 hour at 25 °C with appropriate controls before spectra were acquired. Excitation wavelength was 520 nm.
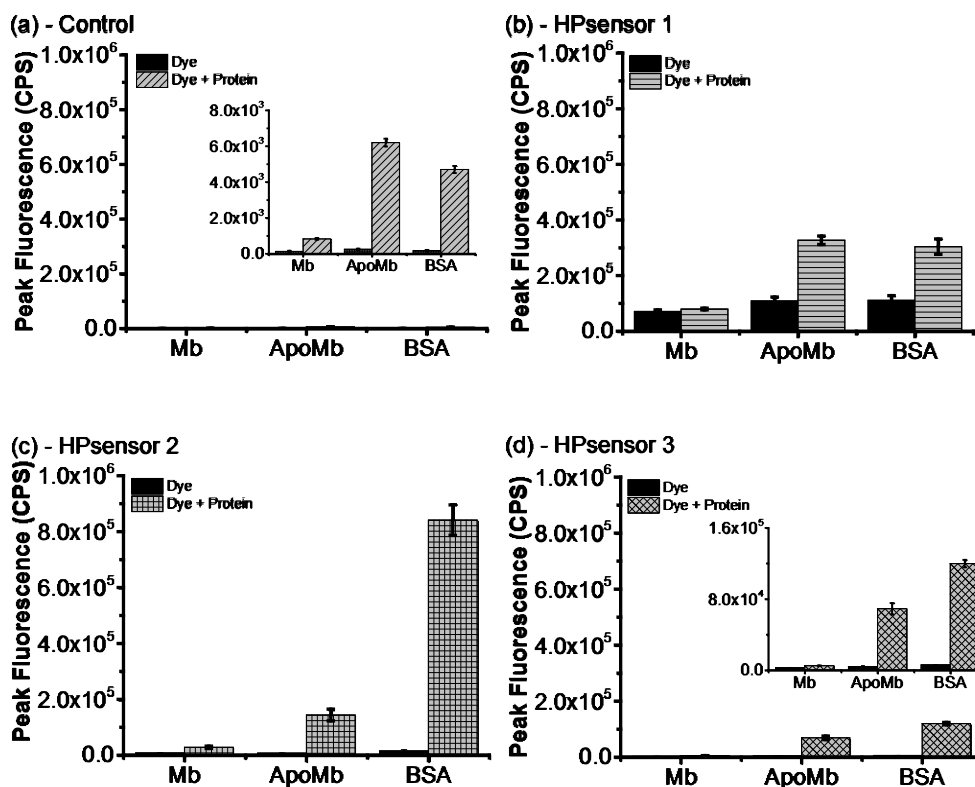
Figure 4.24. Mean peak fluorescence intensity of control (a), HPsensors 1 (b), 2(c), and 3(d) with Mb, ApoMb, and BSA proteins compared to free dye in water. All bar graphs are plotted on the same scale for ease of comparison. For control dye and HPsensor **3**, an inset bar graph with a smaller scale is also shown. All experiments were done in triplicate. Error bars indicate ± SD. Peak mean fluorescence used for plotting bar graphs are as follows: **control** dye at 540 nm, HPsensor **1** at 584 nm, HPsensor **2** at 579 nm, and HPsensor **3** at 578 nm.

In the presence of proteins, dyes exhibited a strong fluorescence signal for ApoMb and BSA but a weak signal for Mb (Fig. 4.21 – 4.24). All three HPsensors showed a progressive 3- to 11-fold increase in fluorescence signal for ApoMb and a 3- to 33-fold increase for BSA when compared to Mb for the respective dyes (Fig. 4.24); HPsensor **2** showed the greatest fluorescence increase for BSA. The signal for HPsensor **1** was nearly half of the signal

111

observed for HPsensors **2** (Fig. 4.24). In comparison, the **control** dye showed

very weak fluorescence signal for proteins (Fig. 4.24). When compared to ANS,

a well-known hydrophobic dye for proteins under similar conditions, HPsensor

2 gave 10- to 60-fold higher signal for the test proteins Mb, ApoMb, and BSA

(Fig. 4.25 – 4.26). Therefore, we measured the dissociation constant (K_d) for

HPsensor **2** for the three proteins and determined it to be 1.2 μM for Mb, 0.33

μM for ApoMb, and 0.034 μM for BSA (Fig. 4.27). In addition, we measured the

surface hydrophobicity (S_0) of proteins in presence of HPsensor **2** and

determined it to be 2934 for Mb, 65212 for ApoMb, and 658608 for BSA

(Supplementary Fig. 4.28).
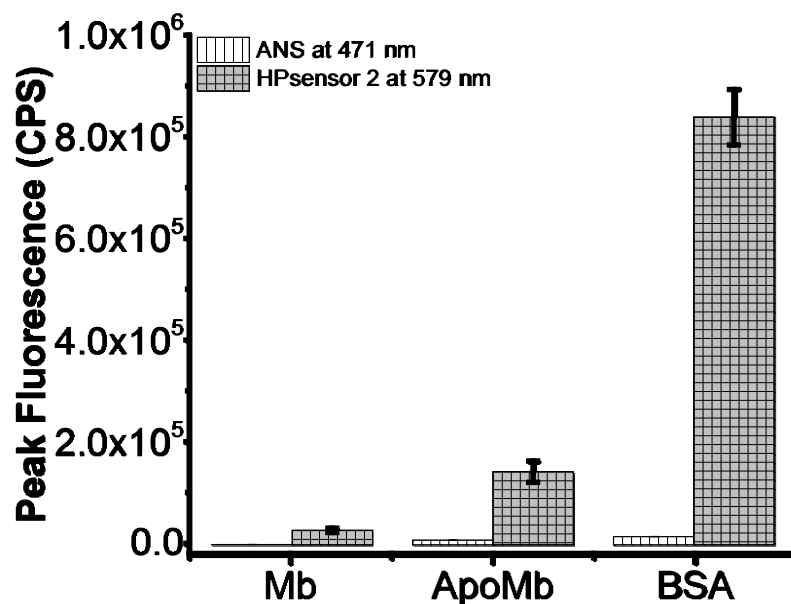
Figure 4.25. Mean peak fluorescence intensity of ANS and HPsensor 2 with Mb, ApoMb, and BSA proteins shown at the indicated wavelengths. All experiments were done in triplicate. Error bars indicate ± SD. Excitation wavelength used for ANS is 350 nm and for HPsensor **2** is 528 nm.
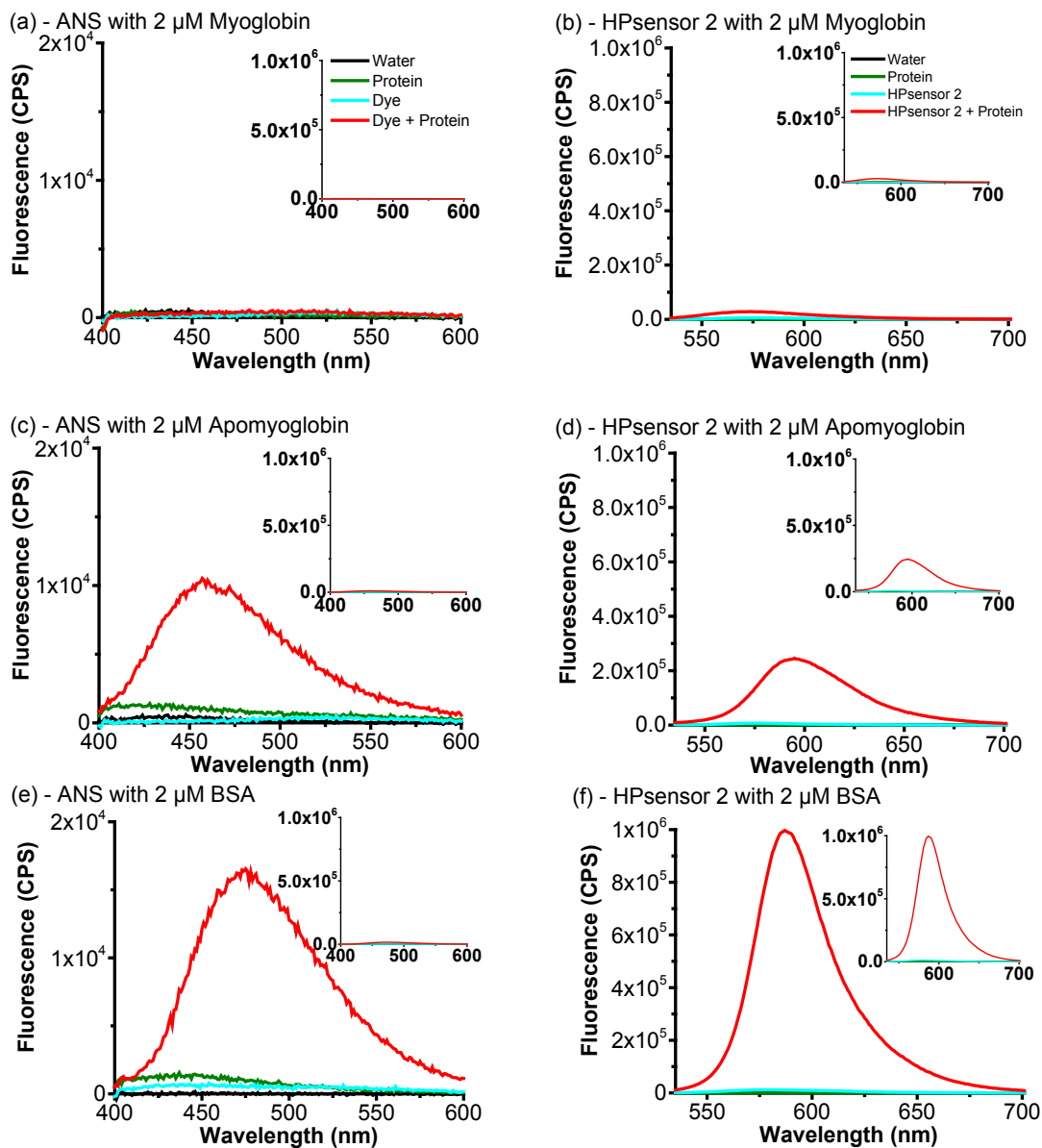
Figure 4.26. Fluorescence emission spectra for ANS and HPsensor 2 incubated with (a - b) myoglobin, (c - d) apomyoglobin, and (e - f) BSA, respectively. Insets are shown on the same scale for ease of comparison of relative protein + dye signal. Excitation wavelengths used are 350 nm for ANS and 528 nm for HPsensor **2**.

(a) Mb
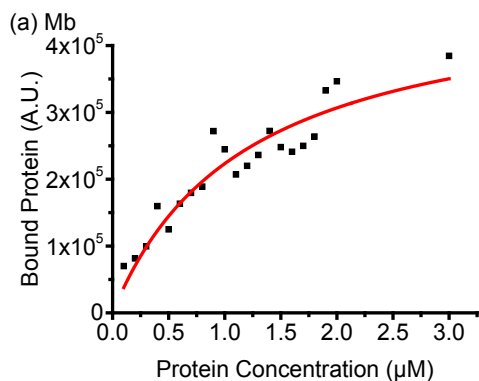
Model	MichaelisMenten	
Equation	$y = V_{max} * x / (K_m + x)$	
Reduced Chi-Sqr	9.13E+08	
Adj. R-Square	0.87047	
	Value	Standard Error
Bound Protein	Vmax	489495	58307.66
Bound Protein	Km	1.19197	0.30083

(b) ApoMb
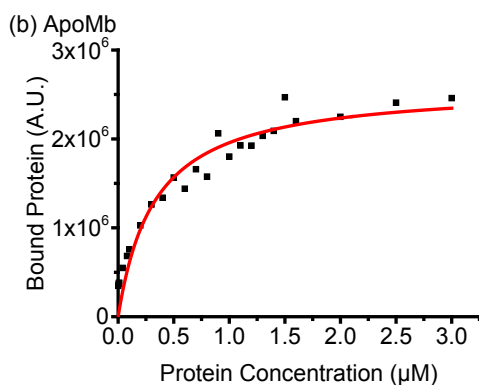
Model	MichaelisMenten	
Equation	$y = V_{max} * x / (K_m + x)$	
Reduced Chi-Sqr	3.93E+10	
Adj. R-Square	0.92582	
	Value	Standard Error
Bound Protein	Vmax	2.60E+06	137983.9
Bound Protein	Km	0.3305	0.06527

(c) BSA
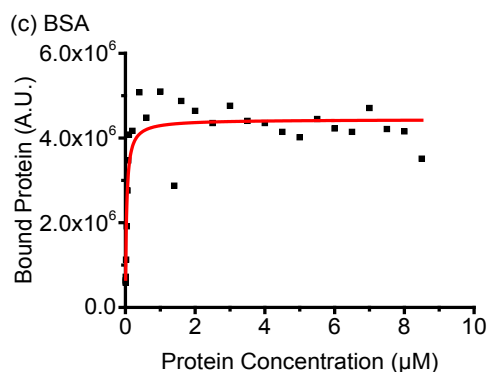
Model	MichaelisMenten	
Equation	$y = V_{max} * x / (K_m + x)$	
Reduced Chi-Sqr	2.76E+11	
Adj. R-Square	0.85572	
	Value	Standard Error
Bound Protein	Vmax	4.44E+06	126271
Bound Protein	Km	0.03395	0.00754

Figure 4.27. **Binding affinity of test proteins (Mb, ApoMb, BSA).** Plot of Bound protein vs protein concentration for Mb (a), ApoMb (b) and BSA (c) with 0.5 µM HPsensor **2**. Plots show non-linear regression using the MichaelisMenten model. Fitting parameters are indicated in tabular form next to each plot.

(a) - Mb
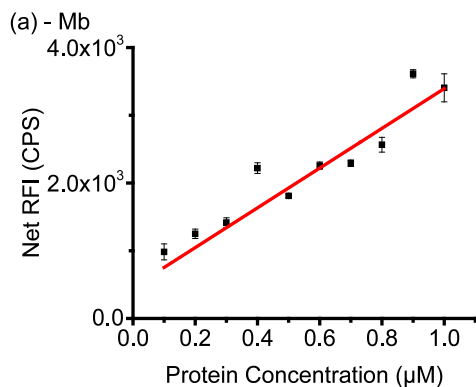
Equation	y = a + b*x	
Weight	Instrumental	
Residual Sum of Squares	32.61916	
Pearson's r	0.992156	
Adj. R-Square	0.981249	
		Value	Standard Error
Net RFI	Intercept	5708.557	230.1198
Net RFI	Slope	65212.15	3674.367

(b) - ApoMb
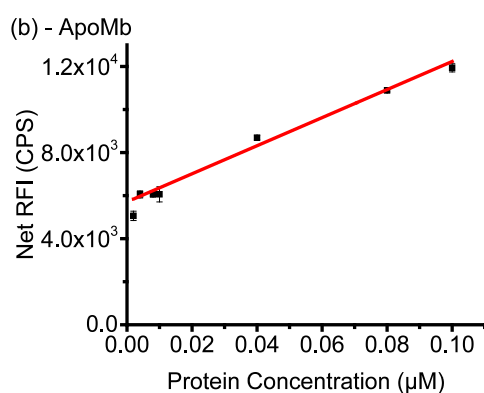
Equation	y = a + b*x	
Weight	Instrumental	
Residual Sum of Squares	190.9159	
Pearson's r	0.914497	
Adj. R-Square	0.815844	
		Value	Standard Error
Net RFI	Intercept	459.6181	258.7922
Net RFI	Slope	2934.333	458.9853

(c) - BSA
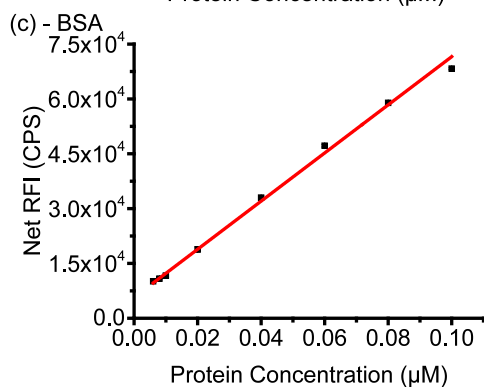
Equation	y = a + b*x	
Weight	Instrumental	
Residual Sum of Squares	249.0748	
Pearson's r	0.999324	
Adj. R-Square	0.998422	
		Value	Standard Error
Net RFI	Intercept	5701.874	505.8403
Net RFI	Slope	658608.5	9895.112

Figure 4.28. **Surface hydrophobicity of test proteins (Mb, ApoMb, BSA).** Plot of Net relative fluorescence intensity (RFI) vs protein concentration with 0.5 µM HPsensor **2**. Plots show linear regression for Mb (a), ApoMb (b) and BSA (c) at increasing concentration plotted with the Net RFI (at 579 nm). Fitting parameters are indicated in tabular form next to each plot.

115

To ascertain if change in surface polarity of proteins also affects HPsensor binding, we tested HPsensor **2** with two well studied proteins BSA and beta-lactoglobulin (β-lg) (Fig. 4.29). HPsensor **2** shows reduced fluorescence signal at low pH (Fig. 4.29). In comparison, heated proteins (both BSA and β-lg) showed even lower fluorescence signal than respective unheated proteins (Fig. 4.29). The only exception was pH 9 fluorescence signal for β-lg (Fig. 4.29).
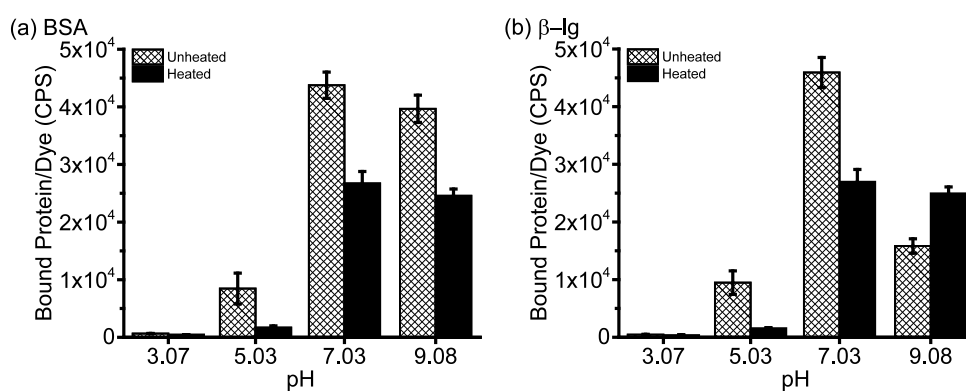
Figure 4.29. HPsensor 2 sensitivity to change in proteins surface polarity. 0.1 µM of proteins (a) BSA and (b) beta-lactoglobulin (β-lg) were incubated with 0.5 µM of HPsensor **2** at 25 °C in Carmody Buffer at pH 3, 5, 7 or 9. All experiments were done in triplicate and average peak fluorescence at 579 nm was used to calculate bound protein/dye. Error bars indicate ± SD. Excitation wavelength used for HPsensor **2** was 528 nm.
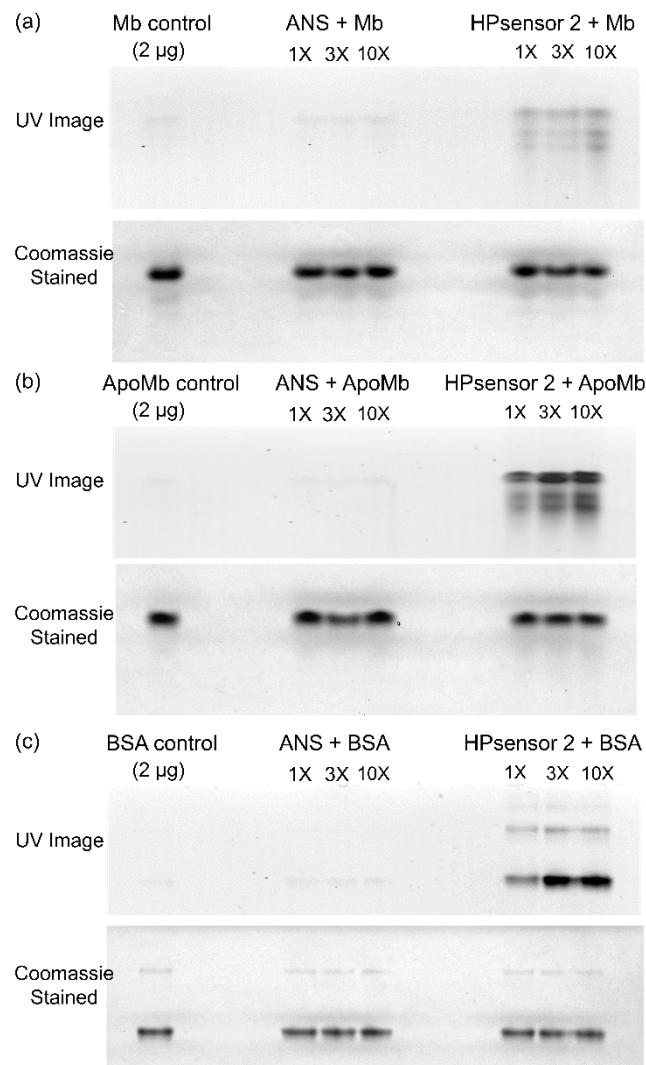
Figure 4.30. Native PAGE of 2 µg proteins with 1X, 3X, and 10X Dye (ANS or HPsensor 2). 2 µg of proteins Mb (a), ApoMb (b), and BSA (c) were incubated with 1X, 3X, and 10X concentration of dyes (ANS or HPsensor **2**) for 1 h at 25 °C. The BSA protein was run on a 10% gel for 3 h and Mb and ApoMb proteins were run on a 15% gel for 6 h at 80 V. Full length gels are included in supplementary figures 30 - 32. Brightness and contrast settings of gels were adjusted for aesthetic purposes.

Finally, we tested the three proteins Mb, ApoMb, and BSA with ANS and HPsensor **2** on a native PAGE. The UV gel image showed that HPsensor **2** exhibited a much stronger signal than ANS (Fig. 4.30) upon UV exposure for all

117

three proteins. It was interesting to see that HPsensor **2** showed decreased

signal with ApoMb and the least signal with Mb after exposure to UV light (Fig.

4.31) which is in line with the fluorescence data.
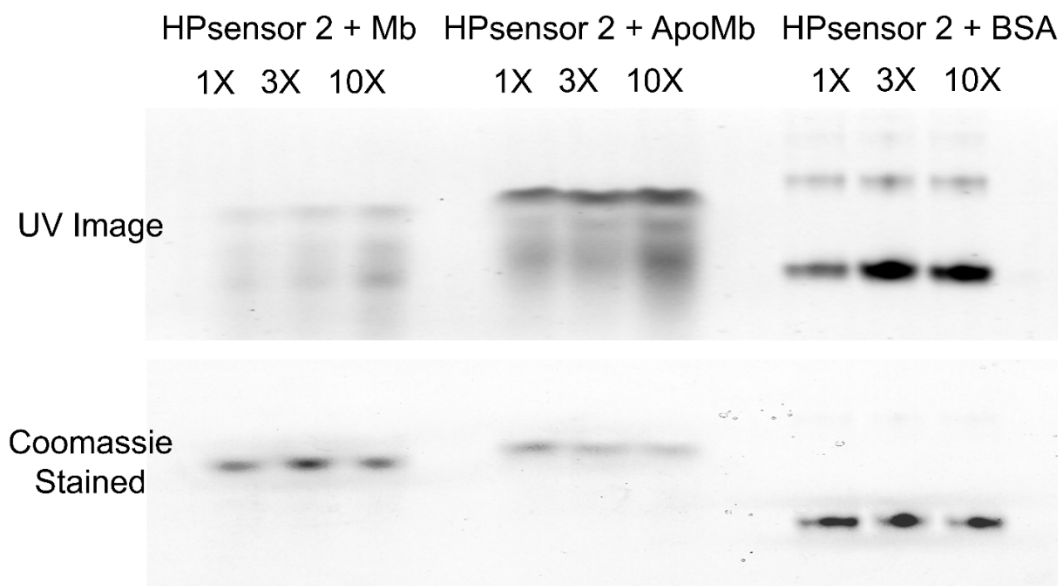
Figure 4.31. **Native PAGE of 2 µg of Proteins [Myoglobin (Mb), Apomyoglobin (ApoMb), BSA] with HPsensor 2**. 2 µg of each protein was incubated with HPsensor **2** at 1X, 3X, and 10X concentration for 1 h at room temperature. Proteins were then run on 10% Tris-HCl gel for 4 h at 80 V before exposure to UV light or Coomassie blue. Full length gel is included in supplementary figure 34. Brightness and contrast settings were adjusted for aesthetic purposes.

4.4.   Discussion

The novel BODIPY dyes with aryl substitutions (with NH_2, NHAc, or OCH_3

groups) at the *meso* position for sensing protein hydrophobicity and 2-

methoxyethylamine substitution at the 3,5-positions for increasing water

solubility were synthesized. The control dye (nitroaryl substitution at *meso*

118

position) has been reported in an earlier study and is known to have weak fluorescence[34,11c] primarily due to free rotation of the nitroaryl group resulting in high non-radiative decay rate unlike the methylaryl counterpart that gives quantum yields of 63%[33].

With previous literature suggesting that the *meso* aryl substitution has a profound effect on fluorescence characteristics irrespective of the lack of π-conjugation[37], we sought to investigate the role of the electron donating ability on fluorescence. The three donor groups (NH_2, NHAc, and OCH_3), substituted to aryl group at the *meso* position have been known to cause an enhancement in fluorescence[38] and thus served as an important starting point for our dyes. We used the 3,5-positions for 2-methoxyethylamine substitution to increase stability and solubility of control dye in polar environment by enhancing the hydrogen bonding ability. Interestingly, addition of the 2-methoxyethylamine groups to the control dye led to quenching of fluorescence as noted for dye **5** (Fig. 4.1). The fluorescence quenching may be due to photo-induced electron transfer with nitrophenyl group functioning as an electron acceptor. While decrease in fluorescence quantum yield was expected due to free rotation of aryl substituents at the *meso* position by non-radiative decay processes (k_{nr}),[28] a total loss of fluorescence (quenching) was unexpected. Quantum
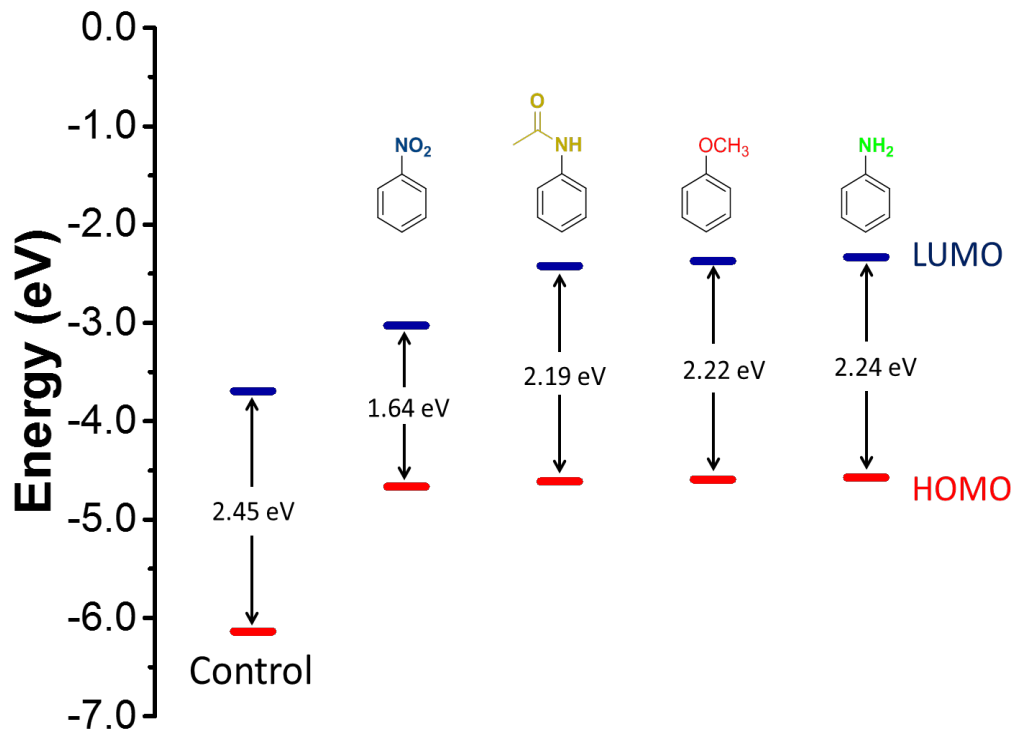
Figure 4.32. Schematic diagrams of frontier molecular orbitals of control dye, dye 5, and HPsensors (1, 2, and 3) showing their HOMO-LUMO energy gap (eV) in ethanol. The data was taken from Appendix A,Table 1.

mechanical calculations for HOMO and LUMO gap by first-principle density functional theory showed a significant decrease in HOMO-LUMO gap for dye 5 (1.639 eV) compared to control dye (2.445 eV) (Fig. 4.32 and Appendix A, Table 1). This decrease in HOMO-LUMO gap due to 2-methoxyethylamine substitution at 3,5-positions in combination with free rotation of nitroaryl substituent at *meso* position can account for quenching of fluorescence for the dye **5**.

However, the other substitutions (NH_2, NHAc, and OCH_3) showed a significant increase in fluorescence of the HPsensors upon binding to hydrophobic proteins (ApoMb and BSA) (Fig. 4.24 – 4.25). The HPsensors **1**, **2**, and **3** showed a red-shift in excitation (561—569 nm) and emission (577-587 nm) compared to the **control** dye (Ex 517 nm and Em 540 nm), with increase in fluorescence quantum yield (Φ_f) in different solvents (Table 1). This shift in excitation and emission maxima towards longer wavelength with decreasing solvent polarity could be due to slight decrease (~0.22 eV) in the energy gap for HPsensors (Fig. 4.32 and Appendix A, Table 1) compared to **control** dye leading to increased conjugation of π-system of the chromophore[39].

The amphiphilic nature of HPsensors is critical for surface hydrophobicity measurements in proteins as surface hydrophobic regions on proteins are exposed to solvent (aqueous) and require a balance of hydrophobic as well as hydrophilic interaction for achieving efficient binding of dye. The results show that increasing the electron donating ability of substituent aryl groups enhances the hydrophobic sensing of the HPsensors and help differentiate the degree of hydrophobicity in proteins. BSA had the highest level of surface hydrophobicity, followed by ApoMb and then Mb as measured by HPsensors (Fig. 4.24). This increase in fluorescence of HPsensors can be attributed to aryl substituents[40] (with NH_2, NHAc, or OCH_3 groups) restricting free rotation at the *meso* position. In addition, increased rigidity of dye due to binding of ring structure to proteins

121

hydrophobic surface and increased hydrogen bonding of 2-methoxyethylamine group with aqueous phase can reduce non-radiative deactivation resulting in fluorescence enhancement (Fig. 4.33)[41]. In addition, HPsensor **2** showed remarkable reporting ability of hydrophobicity with signal strength 10- to 60-fold higher compared to ANS when tested with Mb, ApoMb and BSA under identical conditions (Fig. 4.25 - 4.26). We evaluated the relative surface hydrophobicity of the three proteins (Mb, ApoMb, and BSA) using HPsensor **2** that showed BSA to be the most hydrophobic and Mb to be the least hydrophobic (Fig. 4.28). In addition, evaluation of the surface electrostatic and hydrophobic maps for proteins using computational modeling software SPDB[42] showed BSA to be the most hydrophobic (Appendix A, Fig. A3 – A6) compared to the other proteins tested.
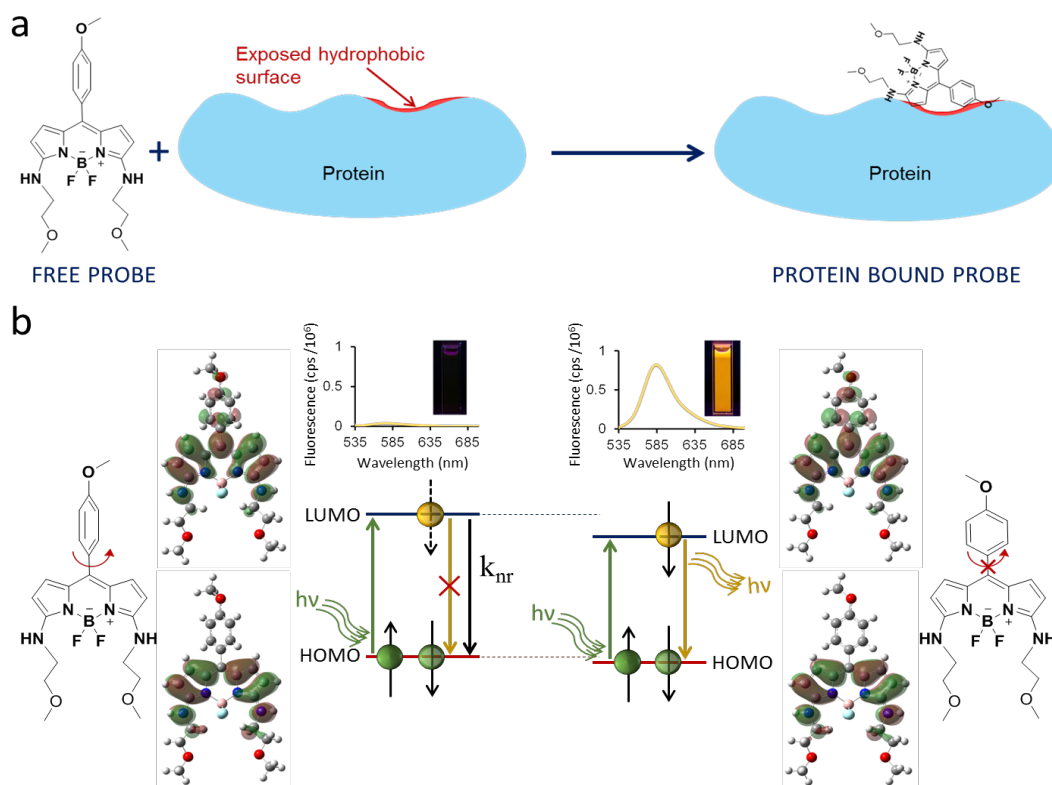
Figure 4.33. Plausible model for increase in fluorescence of HPsensors.
(a) Cartoon shows that free HPsensor **2** has very weak fluorescence in aqueous environment. However, upon binding to proteins HPsensor **2** shows marked enhancement in fluorescence due to binding of dye to proteins hydrophobic surface resulting in molecular twisting and increased rigidity due to steric hindrance; (b) Molecular mechanism shows that *meso* aryl substitution in ethanol can twist resulting in decrease in HOMO and LUMO gap; that combined with increased rigidity of dye inhibits free rotation of aryl substituents leading to decrease in non-radiative decay. This decrease in HOMO and LUMO gap combined with increased molecular rigidity leads to enhancement in fluorescence.

However, the difference in calculated hydrophobicity for Mb and ApoMb is negligible (Appendix A, Fig. A3 - A4), suggesting limitations of such calculations and delineation from the experimental evidence.[41-43] Independent studies show that ApoMb is partially unfolded and more flexible due to loss of heme group

resulting in loosening of helical structure when compared to Mb.[43,44] Therefore, this loosening of structure due to loss of metal ion can lead to increase in aberrant surface hydrophobicity of ApoMb in a manner similar to that seen for other metalloproteins.[12] To further evaluate the strength of the hydrophobic interaction between HPsensor **2** and proteins, we carried out native PAGE. Due to the large difference in isoelectronic point of BSA (pI ~ 4.5) and ApoMb/Mb (pI ~ 7.5 – 8.5), and their size, the amount of time required to sufficiently resolve proteins on the respective cross-linked percentage gels (10% for BSA and 15% for ApoMb and Mb) were adjusted accordingly. With BSA, ApoMb and Mb, the signal strength of HPsensor **2** was much greater than that of ANS under similar conditions as seen by UV imaging (Fig. 4.25). In addition, the signal intensity increased and was in line with the predicted level of exposed surface hydrophobicity of these proteins with BSA showing the highest hydrophobicity (Fig. 4.28).

We also evaluated the response of the most sensitive dye, HPsensor **2**, to change in surface polarity of BSA and β-lg upon heating and compared it to unheated proteins at different pHs (Fig. 4.29). Thermal denaturation of proteins at different pHs[15,45,46] have been shown to influence the extent of surface hydrophobic exposure of BSA and β-lg as measured by dyes such as PRODAN and ANS.[15] ANS being an anionic probe overestimates hydrophobicity at acidic pH due to electrostatic interactions whereas PRODAN being uncharged is not

influenced by changes in pH.[15] Our results show that HPsensor **2** was more responsive to change in surface hydrophobicity (Fig. 4.29). Furthermore, these surface hydrophobicity measurements of BSA and β-lg by HPsensor **2** are in line with the uncharged dye PRODAN. Considering all the properties of the dyes above, HPsensor **2** is an ideal dye for evaluating protein surface hydrophobicity (S_0) and can be used as a sensitive hydrophobic probe for proteins.

4.5.   **Conclusion**

We report novel HPsensors for mapping proteins surface hydrophobicity that show a 10- to 60-fold stronger signal compared to commonly used fluorophore ANS with affinity for proteins in the nanomolar range. The strong signal to noise ratio suggests that these dyes can be useful for applications even with a minute quantity of hydrophobic protein. Thus, this work provides a framework for synthesis of future amphiphilic dyes that can be used for specifically reporting protein surface hydrophobicity with higher sensitivity. We expect these dyes in combination with other techniques such as reverse phase-high performance liquid chromatography (RP-HPLC) have the potential for characterizing protein surface properties. This will help us better understand protein-ligand interactions, molecular recognition, and their biological functions.

125

4.6. Methods

Materials. Unless otherwise indicated, all reagents and solvents were obtained from commercial suppliers (Sigma and Fisher) and used without further purification. Protein samples of BSA and equine myoglobin were purchased from Sigma. ApoMb was prepared from equine myoglobin (Sigma) as per a modified protocol of Breslow (1965)[47] and Adams (1977)[48] outlined in Appendix A.

Instrumentation. ^{1}H NMR and ^{13}C NMR spectra were procured on a 400 MHz Varian Unity Inova spectrophotometer instrument. FTIR spectra were acquired using a Perkin Elmer Spectrum One FTIR. UV spectra were measured using the Perkin Elmer Lambda 35 UV/VIS spectrometer and the fluorescence spectra were measured using the Jobin Yvon Fluoromax-4 spectrofluorometer.

Spectroscopic studies. Fluorescence quantum yields of BODIPY dyes were measured in dichloromethane, ethanol and water and calculated using the previously reported method[30] outlined in the supporting methods. The sulforhodamine 101 dye (Φ_n = 95% using an excitation wavelength of 577 nm in ethanol)[49] was used as the fluorescence standard to measure fluorescence quantum yields of the new BODIPY dyes. The absorption spectra were measured from 300 nm to 800 nm in applicable solvents at 1 nm intervals. The emission spectra for fluorescent dyes were measured at 1 nm intervals using

excitation wavelengths of 520 nm for HPsensors **1** and **3** and 528 nm for HPsensor **2** with both excitation and emission band widths at 2 nm.

The absorption and emission spectra of 2 µM of each BODIPY dye were acquired in ethanol-water mixture with increasing concentration of ethanol (20% increments ranging from 0 to 100% ethanol) to check their fluorescence sensitivity to change in solvent polarity. These dyes were also investigated for their pH sensitivity using Carmody buffer series[50] from pH 2 to pH 12. Dyes were incubated at a concentration of 2 µM in increasing pH for 30 mins after which the emission spectra were acquired in triplicate. To check for dye stability with pH, fluorescence of 2 µM of dyes with change in pH from 3 to 8 and then back to pH 3 was measured using 5 M NaOH and 5 M HCl, respectively. Extinction coefficient was calculated for each dye in 100% ethanol using increasing dye concentrations from 5 µM to 30 µM.

In addition, the sensitivity of these dyes were investigated for ions (Na^+, Mg^{2+}, Zn^{2+}, Fe^{2+}, Fe^{3+}, Ca^{2+}) commonly found in aqueous solutions and buffers. The fluorescence emission spectra of dyes at 2 µM concentrations in distilled water (adjusted to pH 8 using 0.1 M NaOH) with increasing concentration of each test ion (0 to 150 µM) at room temperature was acquired in triplicate. For experiments with proteins, dye concentration dependence was investigated by measuring florescence of increasing concentration of dyes (0 to 100 µM range)

in the presence and absence of 2 μM BSA. All proteins were tested in water (adjusted to pH 8 using 0.1 M NaOH) because ApoMb is prone to aggregation in buffer salts. Fluorescence emission spectra of dyes with all three proteins (Mb, ApoMb, and BSA) were collected by incubating 2 μM dyes with 2 μM proteins (1:1 ratio) for 1 hour before acquiring the absorption and emission spectra. ANS dye was similarly tested at 2 μM concentration with Mb, ApoMb and BSA for comparison to these BODIPY based dyes (Supplementary Fig. 13). All protein and dye samples were freshly prepared and incubated at room temperature for 1 h before acquiring the fluorescence spectra. All spectra were plotted using OriginPro 9.1 and schemes were drawn using ChemBioDraw 14.

Surface Hydrophobicity and Binding Affinity. Surface hydrophobicity (S0) measurements and binding affinity of proteins (Mb, ApoMb and BSA) were determined using HPsensor **2** as per established protocol.[5,46] For the S0 measurements, 0.5 μM HPsensor **2** in distilled water (adjusted to pH 8 using 0.1 M NaOH) was incubated with 8 - 10 concentrations of each test protein (0.1 – 1 μM for Mb; 0.002 – 0.1 μM for ApoMb; and 0.006 – 0.1 μM for BSA) for 1 h at 25 °C before acquiring the emission spectra. The net relative fluorescence intensity (RFI) was then calculated by subtracting the fluorescence of protein in water from protein + HPsensor **2**. The slope (linear regression fit) of net RFI (at 579 nm) vs protein concentration gave the surface hydrophobicity of each protein (Supplementary Fig .17). To measure the binding affinity of HPsensor **2**

for the proteins, fluorescence titration curves were acquired using 21 – 28 different concentrations of protein in the presence of 0.5 µM HPsensor **2**. The range of protein concentrations used were: 0.1 – 3.0 µM for Mb, 0.002 – 3 µM for ApoMB, and 0.006 – 8.5 µM for BSA. The data was analyzed by a non-linear regression method using the MichaelisMenten model included in OriginPro 9.1. Finally, for evaluating the probe sensitivity to increasing polarity on protein's surface, an established protocol[15] was used with the following modification. The fluorescence of bound protein/dye was plotted against pH as opposed to the surface hydrophobicity. The proteins were prepared in 2 forms: either heated (80 °C for 30 mins) or unheated for analysis. To begin with, 0.1 µM of each protein (heated/unheated BSA or β-lg) tested was incubated with HPsensor **2** (0.5 µM) for ~30 mins in Carmody buffer series[50] at pH 3, 5, 7 or 9. Bound protein/dye fluorescence was determined by the difference of fluorescence for protein + HPsensor **2** to protein alone at 579 nm. All spectra were plotted using OriginPro 9.1.

Native PAGE of proteins. 2 µg each of BSA, ApoMb, and Mb proteins were incubated in the presence of increasing concentration (1X, 3X, and 10X) of dyes (ANS and HPsensor **2**) for 1 h at room temperature. In addition, 5 µg of BSA was also incubated with the two dyes (ANS and HPsensor **2**) at increasing concentration (1X, 5X. and 25X) for 1 h at room temperature. Proteins incubated with dye were then mixed (1:1) with native sample buffer before polyacrylamide

gel electrophoresis (PAGE) at 80 V. The proteins were run on different percentage gels for separation by electrophoresis on native PAGE. BSA protein was run on a 10% gel for 3 h and ApoMb and Mb were run on a 15% gel for 6 h. UV images of gels were acquired using the Bio Doc-It imaging system before staining with Coomassie blue.

Surface Electrostatic and Hydrophobic Molecular Modeling. In order to evaluate the differences between proteins surface properties used in this study, surface electrostatic maps were generated for Mb (PDB ID: 3RJ6), ApoMb (Modified from 3RJ6), beta lactoglobulin (PDB ID: 2Q2M) and BSA (PDB ID: 3V03) using the APBS software (http://www.poissonboltzmann.org/) at pH 8.[51,52,53] This was then displayed using the included web viewer Jmol_S. In addition, the Swiss-Prot software SPDB (http://spdbv.vital-it.ch/) was used to generate surface hydrophobic maps for each of these proteins.[42]

Computational methods. To identify the mechanism responsible for the selective enhancement of fluorescence behavior of the HPsensors, we have used a first-principles density functional theory (DFT)[54] that employs a range separated hybrid functional HSEH1PBE for the exchange and correlation[55] to carry out the electronic structure calculations. This functional has been used recently to study the electronic structure of various materials including organic molecules[56,57]. An all electron Gaussian basis set[55], 6-311g**, is used for the

calculations. To include the solvent effect due to water or ethanol, we have used

a polarizable continuum model (PCM) using Gaussian 09 suite program[55].

4.7. References

1   Dill, K. A. Dominant Forces in Protein Folding *Biochemistry* **29**, 7133-7154 (1990).

2   Malleshappa Gowder, S., Chatterjee, J., Chaudhuri, T. & Paul, K. Prediction and analysis of surface hydrophobic residues in tertiary structure of proteins. *Scientific World Journal* **2014**, 971258, doi:10.1155/2014/971258 (2014).

3   Nick Pace, C., Scholtz, J. M. & Grimsley, G. R. Forces stabilizing proteins. *FEBS Lett.* **588**, 2177-2184, doi:10.1016/j.febslet.2014.05.006 (2014).

4   Jamadagni, S. N., Godawat, R. & Garde, S. in *Annual Review of Chemical and Biomolecular Engineering, Vol 2* Vol. 2 *Annual Review of Chemical and Biomolecular Engineering* (ed J. M. Prausnitz) 147-171 (2011).

5   Haskard, C. A. & Li-Chan, E. C. Y. Hydrophobicity of Bovine Serum Albumin and Ovalbumin Determined Using Uncharged (PRODAN) and Anionic (ANS-) Fluorescent Probes. *J. Agric. Food Chem.* **46**, 2671-2677 (1998).

6   Young, L., Jernigan, R. L. & Covell, D. G. A role for surface hydrophobicity in protein-protein recognition. *Protein Sci.* **3**, 717-729 (1994).

7   Wang, B., Guo, C., Lou, Z. & Xu, B. Following the aggregation of human prion protein on Au(111) surface in real-time. *Chem. Commun. (Cambridge, U.K.)* **51**, 2088-2090, doi:10.1039/c4cc09209k (2015).

8   Xu, G., Stevens, S. M., Jr., Moore, B. D., McClung, S. & Borchelt, D. R. Cytosolic proteins lose solubility as amyloid deposits in a transgenic mouse model of Alzheimer-type amyloidosis. *Hum. Mol. Genet.* **22**, 2765-2774, doi:10.1093/hmg/ddt121 (2013).

9   Knowles, T. P. J., Vendruscolo, M. & Dobson, C. M. The amyloid state and its association with protein misfolding diseases. *Nat. Rev. Mol. Cell. Biol.* **15**, 384-396, doi:10.1038/nrm3810 (2014).

10   Ross, C. A. & Poirier, M. A. Protein aggregation and neurodegenerative disease. *Nat. Med.* **10**, S10-17, doi:10.1038/nm1066 (2004).

11   Tiwari, A., Xu, Z. & Hayward, L. J. Aberrantly Increased Hydrophobicity Shared by Mutants of Cu,Zn-Superoxide Dismutase in Familial Amyotrophic Lateral Sclerosis. *J. Biol. Chem.* **280**, 29771-29779, doi:10.1074/jbc.M504039200 (2005).

12   Tiwari, A. *et al.* Metal deficiency increases aberrant hydrophobicity of mutant superoxide dismutases that cause amyotrophic lateral sclerosis. *J. Biol. Chem.* **284**, 27746-27758, doi:10.1074/jbc.M109.043729 (2009).

13   Adams, M. M. & Anslyn, E. V. Differential Sensing Using Proteins: Exploiting the Cross-Reactivity of Serum Albumin To Pattern Individual

Terpenes and Terpenes in Perfume. *J. Am. Chem. Soc.* **131**, 17068–17069 (2009).

14 Lee, S. *et al.* Rational design of a structural framework with potential use to develop chemical reagents that target and modulate multiple facets of Alzheimer's disease. *J. Am. Chem. Soc.* **136**, 299-310, doi:10.1021/ja409801p (2014).

15 Alizadeh-Pasdar, N. & Li-Chan, E. C. Y. Comparison of Protein Surface Hydrophobicity Measured at Various pH Values Using Three Different Fluorescent Probes. *J. Agric. Food Chem.* **48**, 328-334 (2000).

16 Cardamone, M. & Puri, N. K. Spectrofluorimetric assessment of the surface hydrophobicity of proteins. *Biochem. J.* **282**, 589-593 (1992).

17 Scarsi, M., Majeux, N. & Caflisch, A. Hydrophobicity at the Surface of Proteins. *Proteins: Struct., Funct., Bioinf.* **37**, 565-575 (1999).

18 Balch, W. E., Fau, M. R., Fau, D. A. & Kelly, J. W. Adapting proteostasis for disease intervention. *Science* **319**, 916-919, doi:10.1126/science.1141448 (2008).

19 Giovambattista, N., Lopez, C. F., Rossky, P. J. & Debenedetti, P. G. Hydrophobicity of protein surfaces: Separating geometry from chemistry. *Proc. Natl. Acad. Sci. U.S.A.* **105**, 2274-2279, doi:10.1073/pnas.0708088105 (2008).

20 Raschke, T. M., Tsai, J. & Levitt, M. Quantification of the hydrophobic interaction by simulations of the aggregation of small hydrophobic

solutes in water. *Proc. Natl. Acad. Sci. U.S.A.* **98**, 5965-5969, doi:10.1073/pnas.111158498 (2001).

21   Saito, R. *et al.* Peptide-conjugated pterins as inhibitors of ricin toxin A. *J. Med. Chem.* **56**, 320-329, doi:10.1021/jm3016393 (2013).

22   Hawe, A., Sutter, M. & Jiskoot, W. Extrinsic fluorescent dyes as tools for protein characterization. *Pharm. Res.* **25**, 1487-1499, doi:10.1007/s11095-007-9516-9 (2008).

23   Peng, L. *et al.* A ratiometric fluorescent probe for hydrophobic proteins in aqueous solution based on aggregation-induced emission. *Analyst* **138**, 2068-2072, doi:10.1039/c3an36634k (2013).

24   Gasymov, O. K. & Glasgow, B. J. ANS Fluorescence: Potential to Augment the Identification of the External Binding Sites of Proteins. *Biochim. Biophys. Acta* **1774**, 403–411 (2007).

25   Togashi, D. M. & Ryder, A. G. A fluorescence analysis of ANS bound to bovine serum albumin: binding properties revisited by using energy transfer. *J. Fluoresc.* **18**, 519-526, doi:10.1007/s10895-007-0294-x (2008).

26   Matulis, D. & Lovrien, R. 1-Anilino-8-Naphthalene Sulfonate Anion-Protein Binding Depends Primarily on Ion Pair Formation. *Biophys. J.* **74** 422–429 (1998).

27   Li, L., Nguyen, B. & Burgess, K. Functionalization of the 4,4-difluoro-4-bora-3a,4a-diaza-s-indacene (BODIPY) core. *Bioorg. Med. Chem. Lett.* **18**, 3112-3116, doi:10.1016/j.bmcl.2007.10.103 (2008).

28   Loudet, A. & Burgess, K. BODIPY Dyes and Their Derivatives: Syntheses and Spectroscopic Properties. *Chem. Rev.* **107**, 4891-4932 (2007).

29   Zhang, Y. *et al.* Photoactivatable BODIPYs Designed To Monitor the Dynamics of Supramolecular Nanocarriers. *J. Am. Chem. Soc.* **137**, 4709-4719, doi:10.1021/ja5125308 (2015).

30   Zhu, S. *et al.* Highly water-soluble neutral near-infrared emissive BODIPY polymeric dyes. *J. Mater. Chem.* **22**, 2781-2790, doi:Doi 10.1039/C2jm14920f (2012).

31   Zhu, S. *et al.* Highly water-soluble, near-infrared emissive BODIPY polymeric dye bearing RGD peptide residues for cancer imaging. *Anal. Chim. Acta* **758**, 138-144, doi:10.1016/j.aca.2012.10.026 (2013).

32   Zhu, S. *et al.* Highly water-soluble BODIPY-based fluorescent probes for sensitive fluorescent sensing of zinc(ii). *J. Mater. Chem. B* **1**, 1722, doi:10.1039/c3tb00249g (2013).

33   Leen, V. *Synthesis and application of reactive BODIPY dyes* PhD thesis, Katholieke Universiteit Leuven, (2010).

34   Li, L., Han, J., Nguyen, B. & Burgess, K. Syntheses and spectral properties of functionalized, water-soluble BODIPY derivatives. *J. Org. Chem.* **73**, 1963-1970, doi:10.1021/jo702463f (2008).

35   Carpentieri, U., Myers, J., Thorpe, L., III, C. W. D. & Haggard, M. E. Copper, Zinc, and Iron in Normal and Leukemic Lymphocytes from Children. *Cancer Res.* **46**, 981 -984 (1986).

36   Page, M. J. & Cera, E. D. Role of Na$^+$ and K$^+$ in Enzyme Function. *Physiol. Rev.* **86** 1049–1092, doi:10.1152/physrev.00008.2006.-Metal (2006).

37   Zhang, X.-F. The effect of phenyl substitution on the fluorescence characteristics of fluorescein derivatives via intramolecular photoinduced electron transfer. *Photochem. Photobiol. Sci.* **9**, 1261, doi:10.1039/c0pp00184h (2010).

38   Skoog, D. A., Holler, F. J. & Crouch, S. R. *Principles of Instrumental Analysis*. 357 (Thomson Brooks/Cole, 2007).

39   Baruah, M., Qin, W., Basaric, N., Borggraeve, W. M. D. & Boens, N. BODIPY-Based Hydroxyaryl Derivatives as Fluorescent pH Probes. *J. Org. Chem.* **70**, 4152-4157 (2005).

40   Yamada, K., Toyota, T., Takakura, K., Ishimaru, M. & Sugawara, T. Preparation of BODIPY probes for multicolor fluorescence imaging studies of membrane dynamics. *New J. Chem.* **25**, 667-669, doi:Doi 10.1039/B100757m (2001).

41   Benniston, A. C. & Copley, G. Lighting the way ahead with boron dipyrromethene (BODIPY) dyes. *Phys Chem Chem Phys* **11**, 4124-4131, doi:10.1039/b901383k (2009).

42   Guex, N. & Peitsch, M. C. SWISS-MODEL and the Swiss-Pdb Viewer: An environment for comparative protein modeling. *ELECTROPHORESIS* **18**, 2714-2723, doi:10.1002/elps.1150181505 (1997).

43   Harrison, S. C. & Blout, E. R. Reversible conformational changes of myoglobin and apomyoglobin. *J. Biol. Chem.* **240**, 299-303 (1965).

44   Lee, D. W. & Cho, B. Y. Investigation of the Retention Behavior and Structural Change of Proteins in Reversed Phase and Hydrophobic Interaction Chromatography. *J. Liq. Chromatogr.* **17**, 2541-2558, doi:10.1080/10826079408013396 (1994).

45   Kato, A. & Nakai, S. Hydrophobicity determined by a fluorescence probe method and its correlation with surface properties of proteins. *Biochim. Biophys. Acta* **624**, 13-20 (1980).

46   Nakai, S., Li-Chan, E. & Arteaga, G. E. in *Methods of testing protein functionality*   (ed G. M. Hall) Ch. 8, 226 - 255 (Blackie A & P, 1996).

47   Breslow, E. Changes in Side Chain Reactivity Accompanying the Binding of Heme to Sperm Whale Apomyoglobin. *J. Biol. Chem.* **239**, 486-496 (1964).

48   Adams, P. A. The Kinetics of the Recombination Reaction between Apomyoglobin and Alkaline Haematin. *Biochem. J.* **163**, 153-158 (1977).

49   Velapoldi, R. A. & Tønnesen, H. H. Corrected Emission Spectra and Quantum Yields for a Series of Fluorescent Compounds in the Visible Spectral Region. *J. Fluoresc.* **Volume 14**, 465-472 (2004).

50   Carmody, W. R. An Easily Prepared Wide Range Buffer Series. *J. Chem. Educ.* **38**, 559-560 (1961).

51   Baker, N. A., Sept, D., Joseph, S., Holst, M. J. & McCammon, J. A. Electrostatics of nanosystems: application to microtubules and the ribosome. *Proc. Natl. Acad. Sci. USA* **98**, 10037 - 10041 (2001).

52   Dolinsky, T. J. *et al.* PDB2PQR: expanding and upgrading automated preparation of biomolecular structures for molecular simulations. *Nucleic acids research* **35**, W522-525, doi:10.1093/nar/gkm276 (2007).

53   Dolinsky, T. J., Nielsen, J. E., McCammon, J. A. & Baker, N. A. PDB2PQR: an automated pipeline for the setup of Poisson-Boltzmann electrostatics calculations. *Nucleic acids research* **32**, W665-667, doi:10.1093/nar/gkh381 (2004).

54   Parr, R. G. & Yang, W. *Density-functional theory of atoms and molecules*. Vol. 16 (Oxford University Press, 1994).

55   Frisch, M. J. *et al.*   (Gaussian, Inc., Wallingford, CT, USA, 2009).

56   Chevrier, V. L., Ong, S. P., Armiento, R., Chan, M. K. Y. & Ceder, G. Hybrid density functional calculations of redox potentials and formation energies of transition metal compounds. *Phys. Rev. B: Condens. Matter Mater. Phys.* **82**, 1-11, doi:10.1103/PhysRevB.82.075122 (2010).

57   Tamer, Ö. *et al.* Synthesis, structural and spectroscopic evaluations and nonlinear optical properties of 3,5-bis(4-methoxyphenyl)-4,5-dihydro-1H-pyrazole-1-carbothioic O-acid. *Spectrochim. Acta, Part A*, doi:10.1016/j.saa.2014.08.111 (2014).

4.8.   **Acknowledgment**

4.9.   **Author Contributions**

AT and ND conceived the project. HL and SZ designed and synthesized the hydrophobic dyes. ND characterized the dyes (fluorescence, quantum yield calculation, pH dependence, concentration dependence, surface hydrophobicity and affinity measurements, and generating surface electrostatic and hydrophobic maps of proteins) and carried out protein assays. RP and KBD carried out the HOMO-LUMO energy gap calculations. HRMS data were acquired by F-TL. AT, ND, HL, and RP analyzed the data. AT and ND wrote the manuscript. All the authors reviewed and contributed to the manuscript.

Chapter 5: Functionalized ANS probe for labeling hydrophobic surface of protein.

Nethaniah Dorh[a], Shilei Zhu[a†], Jagadeesh Janjanam[aφ], Haiying Liu[a], Ashutosh Tiwari[a*]

[a]Department of Chemistry, Michigan Technological University, 1400 Townsend Drive, Houghton, MI 49931, USA

[†]Department of Chemistry & Biochemistry, University of Maryland, College Park, MD 20742, USA

[φ]Department of Physiology, University of Tennessee, Health Science Center, Memphis, TN 38163, USA

Abstract

The major driving force in protein aggregation process are the intermolecular interactions in which hydrophobicity plays a dominant role. In case of neurodegenerative diseases, one classical question that arises is: "what is the toxic species?" This question has remained unanswered for a very long time due to the limitations of current techniques that fail to identify the toxic fold or its interacting surface hydrophobic region on the misfolded protein. The current studies on proteins links its aggregation propensity to surface hydrophobicity. Therefore, it is important to understand the role surface hydrophobicity plays in biological functions or the disease process. Currently, probes such as 1-Anilinonaphthalene-8-Sulfonic Acid (ANS) are used, but this probe preferentially binds to the hydrophobic pocket and is thus limited in its reporting ability. The anionic nature of ANS allows for increased solubility over other commercial probes and the potential to be used for surface hydrophobicity mapping. This study addressed the problem of surface hydrophobicity measurements at a quantitative level using hydrophobic labeling. To overcome the limitations discussed, we functionalized the well characterized hydrophobic probe, ANS, enabling it attach to available lysine/arginine residues on the protein surface. The caveat is that this covalent attachment is biased towards amine (lysine/arginine) residues on aqueous phase located near surface hydrophobic regions. The three test proteins used (BSA, Apomyoglobin, Myoglobin) all show

various degrees of labeling that correspond well to the expected level of surface exposed hydrophobicity (BSA > Apomyoglobin > Myoglobin). This is in line with surface hydrophobicity (S_0) measurements using this novel probe. This is also in line with steady state fluorescence experiments which showed a similar pattern. SDS PAGE experiments showed similar trend with labeled proteins displaying a strong signal for BSA and Apomyoglobin, but a weak signal for Myoglobin.

5.2. Introduction

In neurodegenerative diseases protein misfolding and aggregation play a central role wherein several non-native protein structures such as misfolded monomer, oligomers, and fibrils are observed.[1] All these diverse misfolded protein structures share one common property which is increase in surface hydrophobicity.[2] This aberrant hydrophobic exposure combined with disulfide-bond scrambling have been shown to influence the nature of aggregate formed.[3] This is a result of combination of insults (cellular stress, oxidative stress, metal ion loss, etc) to the protein structure or instability introduced through point mutation.[4] However, mapping of the surface hydrophobicity due to lack of suitable probes is a challenge.

Currently in the field of protein chemistry, hydrophobicity of proteins is described by two terms '*average hydrophobicity*' and '*surface hydrophobicity*'. The '*average hydrophobicity*' of a protein is calculated by the percentage of hydrophobic amino acids present in the protein sequence and information on proteins structural fold is not taken into consideration.[5,6] Specifically, a score is calculated based on the number of hydrophobic amino acids present within the sequence. However, this measure is useful in predicting HPLC retention and protein interaction in hydrophobic interaction chromatography.[7] While this is

144

useful, it fails to account how structural change (that can be due to misfolding of protein or natural fold) can impact the proteins hydrophobicity.

The '*surface hydrophobicity*' is directly dependent on proteins structure and measures exposure of hydrophobic amino-acid residues to solvent environment of proteins due to a natural fold or as a consequence of misfolding. This is hard to measure accurately due to lack of proper tools and limitations of existing techniques. Some of these limitations include poor solubility of probes in aqueous media,[8,9] and high fluorescence signal for probe such ANS when it binds to proteins buried hydrophobic pockets but very poor or no signal when it binds to hydrophobic surface that is solvent exposed.[10] In addition, techniques such as X-ray crystallography and NMR spectroscopy prove of limited use as large amounts of protein are required. Furthermore, misfolded proteins may be very difficult to crystallize. Currently, '*surface hydrophobicity*' and its impact on aggregation mechanisms are still poorly understood. Therefore, any improvement in quantitative measurement and ability to identify exposed hydrophobic surface will lead to a better understanding of aggregation mechanisms. In addition, it will provide structural insights that will help with rational drug design approach for exploring novel therapeutic avenues. Therefore to address this gap, we propose to map the hydrophobic surface using fluorescent probes that can covalently bind to the protein.

Hydrophobic labeling is the biased labeling of proteins using an extrinsic fluorescent tag. The exact location and driving force for covalent localization is directed by nearby regions of hydrophobicity on the protein surface. Labeling the protein allows a quantitative analysis of protein topography including the exposed hydrophobic surface but can be biased depending upon the probe used. To date, a few extrinsic fluorescent probes are available for protein folding and aggregation studies, including ANS,[10-12] Bis-ANS,[11,13,14] ThT.[15,16] However, these report total hydrophobicity and cannot be used for surface hydrophobicity in their current forms.

A modification that restricts localization of a probe such as ANS to the surface of the protein would allow its use in measuring surface hydrophobicity of proteins that tend to misfold, aggregate, and form fibrils.[17] This kind of modification can be achieved through coupling systems such as the ε-amino group of lysine, the α-amino group of the N-terminus, or the thiol group of cysteine that have all been used previously.[18]

ANS has been used for a long time as a preferred hydrophobic probe for proteins due to its small size and high fluorescence when it binds to hydrophobic pocket, giving it distinct advantage over other fluorescent probes.[19,20] Upon binding to buried hydrophobic cavities, the fluorescence intensity of ANS is significantly increased and is accompanied by a stokes shift to shorter

wavelength.[20,21] Probes such as ANS are noted to work through either solvent relaxation, intramolecular charge transfer or even twisted intramolecular charge transfer mechanisms.[18] ANS fluorescence is also impacted by the charged sulfonate group through electrostatic interactions with charged protein side chains.[20,22] In addition, its use is limited for surface hydrophobicity measurements as it shows very low to no fluorescence in aqueous media. Due to the relatively small size of ANS, it has been shown that ANS dimerization is important at acidic pH and as a result, electrostatic interactions play a significant role.[23] However, at physiological conditions near pH 7, ANS has been shown to be monomeric.[23] This feature can be further exploited as this dye is coupled to proteins. Along with this, research conducted almost two decades ago also showed that ANS was able to qualitatively differentiate several proteins based on levels of hydrophobicity.[24]

Therefore, we chose ANS dye for functionalization due to its small size, its well characterized properties for measuring protein hydrophobicity, and its ability to be modified with a succinimide-functionalized ethynyl derivative for covalent linking to amine groups on proteins near surface hydrophobic regions. The structure of this new dye shown in figure 1 differs from ANS only in the addition of a succinimide-functionalized ethynyl derivative (NHS linker) at position 5 of ANS. The succinimide group offers facile reaction with amine residue of proteins in buffer solution at pH 7.4.

147
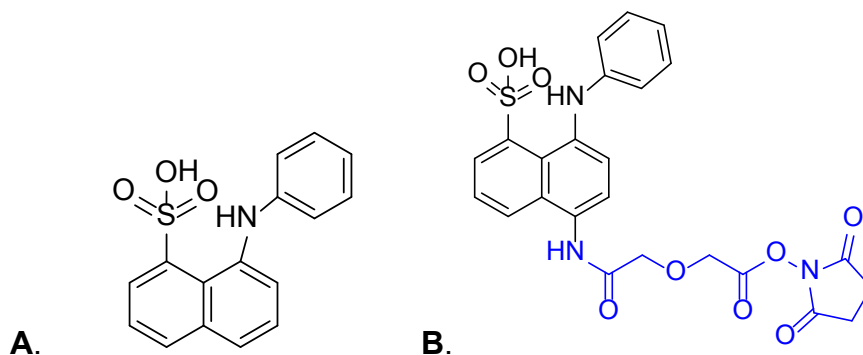
Figure 5.1. Structure of the commercially available ANS (A) and the functionalized ANS (B). The succinimide-functionalized ethynyl derivative (NHS linker) is shown in blue and is linked to ANS at position 5.

The introduction of an NHS linker allows a non-cleavable covalent bond targeted at amine groups such as lysine or arginine that are common but not overly abundant in most proteins.[25] This design limits the number of dye molecules that can bind to proteins surface hydrophobic regions at two levels: 1) requires a hydrophobic patch on proteins surface to interact, and 2) needs to have a lysine/arginine amino acid residue within few Å of the hydrophobic patch to covalently interact. In addition, the increase in size of ANS due to the linker also provides steric hindrance for interaction with the hydrophobic pocket of proteins. This unique combination of ANS characteristics[24] [26] [18] [10] [27] with NHS crosslinking ability can provide information on surface hydrophobicity as well as prospect to determine its precise location which could not be addressed previously[24].

To aid in the proof of concept of application of these ANS modified dyes for surface hydrophobic mapping we used three well characterized test proteins for the study. We chose 1) bovine serum albumin which has been studied extensively,[28 - 33] 2) apomyoglobin and 3) myoglobin which is the holo-protein counterpart of apomyglobin . BSA has 60 lysine and 26 arginine residues in comparison apomyoglobin and myoglobin contain 19 lysine and 2 arginine residues. In addition, apomyoglobin and myoglobin differ only in the lack of the metal ion (Fe) in apomyoglobin making the apo-protein more hydrophobic.[34] Exploiting the above properties, biased labeling of each test protein was achieved showing a difference in the level of ANS fluorescence for each protein.

5.3. Methods and Materials

5.3.1. Instrumentation and Materials

Unless otherwise indicated, all reagents and solvents were obtained from commercial suppliers such as Sigma-Aldrich, Fisher and Bio-Rad or affiliated major suppliers and used without further purification. Absorbance measurements were taken using the Perkin Elmer Lambda 35 UV/VIS spectrometer. Fluorescence spectra measurements were recorded on a Jobin Yvon Fluoromax-4 spectrofluorometer. ^{1}H NMR and ^{13}C NMR spectra were

taken on a 400 MHz Varian Unity Inova spectrophotometer instrument.

Apomyoglobin was prepared according to previously reported protocol.[34]

5.3.2. Dye synthesis

The ANS-modified probe was prepared according to the following scheme.

Details of synthesis are included in Appendix B.
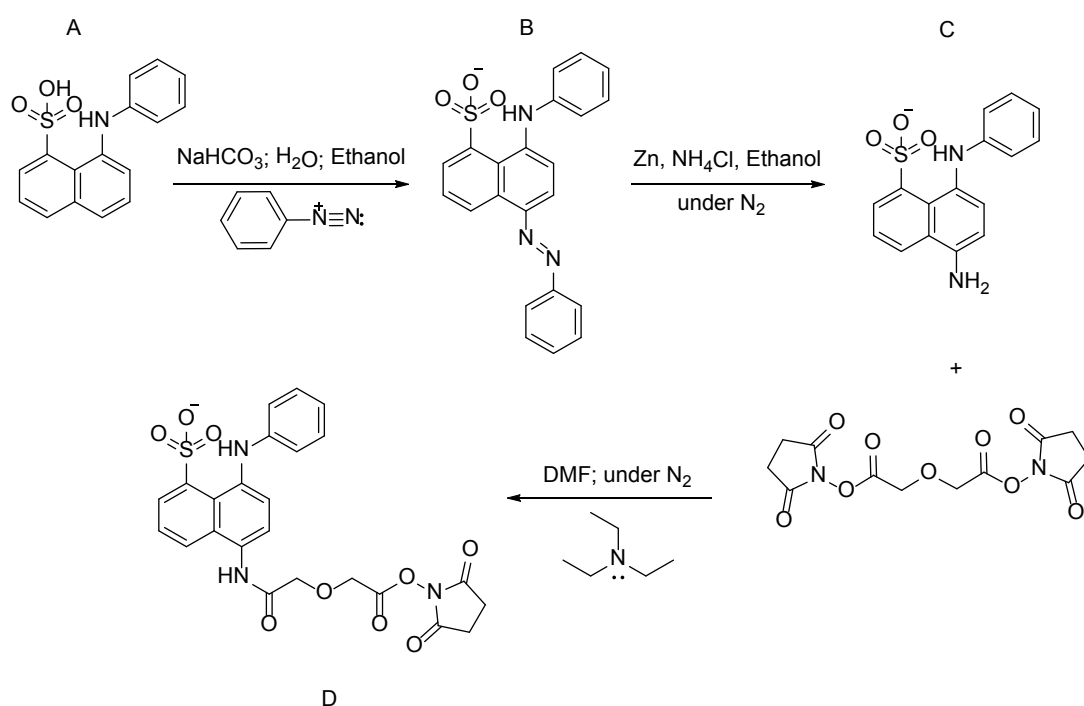
Figure 5.2. Synthetic scheme for ANS-modified probe. Commercially available ANS was modified to include a succinimide-functionalized ethynyl derivative (NHS ester).

5.3.3. Spectroscopy experiments

5.3.3.1. Dye in various solvents

The dye was prepared at a concentration of approximately 5 µM in 0.1 M sodium bicarbonate buffer (pH 8.3), DMSO and 100% ethanol. The absorption was then measured from 250 – 500 nm followed by the fluorescence measurements using an excitation λ= 385 nm, excitation slit width of 2 nm with an emission slit width of 2 nm. An average of three scans was collected at 1 nm intervals over the range of 390 – 750 nm.

5.3.3.2. Dye in ethanol-water dilutions

The dye was prepared at a 5 µM concentration in various ethanol/water dilutions (0%, 20%, 40%, 60%, 80% and 100%). The absorption was then measured from 250 – 800 nm followed by the measurement of fluorescence using an excitation λ= 385 nm, excitation slit width of 2 nm with an emission slit width of 2 nm. An average of three scans was collected at 1 nm intervals over the range of 390 – 750 nm.

5.3.3.3. Surface Hydrophobicity of Proteins

Surface hydrophobicity (S_0) measurements for proteins (Mb, ApoMb, and BSA) were determined using 5 µM ANS in 0.1 M Sodium Bicarbonate buffer (pH 8.3) as per established protocol.[6,34] Proteins were prepared at 8 – 10 concentrations that showed a linear dye response to increasing protein concentration (BSA: 0.5

– 5 µM; Apomyoglobin: 2 -10 µM) and incubated for 1 h at 25 °C before acquiring the emission spectra. Measurements with Mb showed little to no significant response compared to noise and could not be acquired. The net relative fluorescence intensity (RFI) was then calculated by subtracting the fluorescence of protein in water from protein + ANS. The slope (linear regression fit) of net RFI (at 500 nm – BSA; 504 nm – ApoMb) vs protein concentration gave the surface hydrophobicity of each protein.

5.3.3.4. Dye with Proteins

The dye was prepared at a 5 µM concentration with 5 µM protein (BSA, Lysozyme, Apomyoglobin or Myoglobin) in 0.1 M sodium bicarbonate buffer (pH 8.3). The dye was then incubated with protein for 1 hours at 25 °C. The fluorescence was then measured using an excitation λ= 385 nm, excitation slit width of 2 nm with an emission slit width of 2 nm. An average of three scans was collected at 1 nm intervals over the range of 390 – 750 nm.

5.3.3.5. Surface Electrostatic and Hydrophobic Molecular Modeling

In order to evaluate the difference between proteins surface properties used in this study, surface electrostatic maps were generated for Mb (PDB ID: 3RJ6), ApoMb (Modified from 3RJ6), and BSA (PDB ID: 3V03) using the APBS software (http://www.poissonboltzmann.org/) at pH 8.3. This was then displayed using the included web viewer Jmol_S.

5.3.3.6.   Labeling of protein

The protein labeling was conducted using a molar ratio for protein:dye of 1:15 in fresh 0.1M sodium bicarbonate buffer (pH 8.3). The reaction was then allowed to proceed for 2 hours at room temperature. The reaction was then quenched using 10% of 1.5 M hydroxylamine (pH 8.5). Proteins were also incubated concurrently with ANS following the same labeling protocol. Labeled and unlabeled protein along with protein incubated with ANS were then analyzed using denaturing SDS PAGE by running the gel for approximately 2.5 - 3 hrs at 80 V after reduction with 2-mercaptoethanol and exposure to 100 °C for 5 minutes. Gels were visualized first with UV and then stained with Coomassie blue R250 overnight before acquiring the image at 600 dpi.

5.4.   **Results**

The synthesis of the modified ANS dye was conducted as described in the methods section of appendix B. The new dye was then characterized using several techniques including NMR, mass spectrometry, UV VIS and fluorescence spectroscopic techniques and finally, SDS PAGE.

The modified ANS dye was first characterized by ^{1}H NMR and ^{13}C NMR (Appendix Figure B2 - 9). Peak locations and relative intensities are described in the methods and shown in the supplementary data. Due to the high reactivity

of the NHS linker attached to the ANS moiety, ESI-MS data showed a mass of approximately 411 Da for the final product described in Appendix B.

A comparison of the spectroscopic properties of the modified ANS and the commercial ANS dye revealed a few differences in absorption and emission spectra (Appendix Figure B1; Figure 5.3 – 5.5). The absorption and corresponding emission spectra of the ANS modified dye was noted to be red shifted compared to that of ANS in the various solvents (Figure 5.4). Absorption spectra was red shifted by an average of 10 nm while the emission spectra was red shifted by an average of 20 nm (figure 5.4; Appendix figure B1). In contrast, both dyes were shown to respond similarly to solvents of differing polarity or dielectric constant (figure 5.3 – 5.4) except in the overall magnitude of the fluorescence intensity.
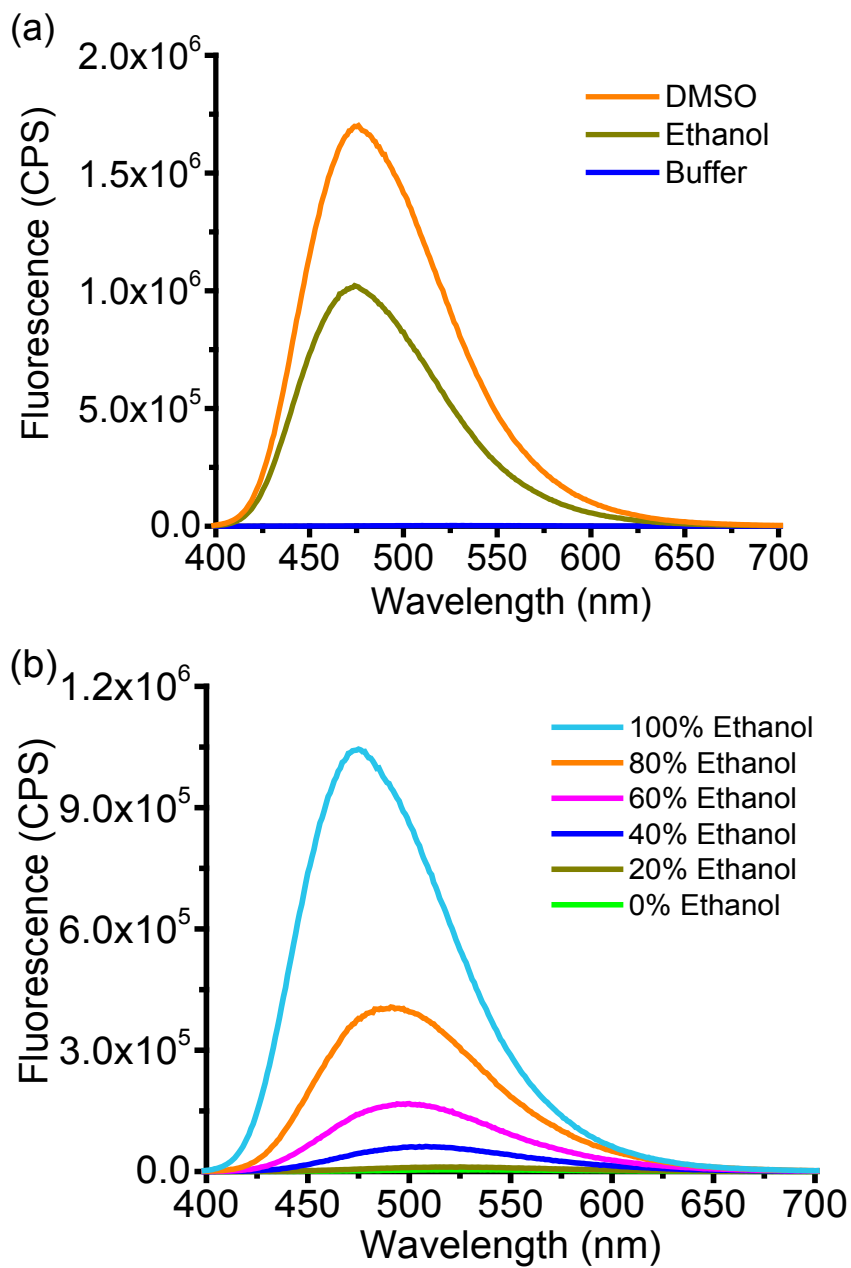
Figure 5.3. ANS response to solvent polarity. Emission spectra of ANS in (a) varying polarity solvents (DMSO, 100% Ethanol and 0.1 M Sodium Bicarbonate Buffer (pH 8.3)) as well as in (b) ethanol-water dilutions.
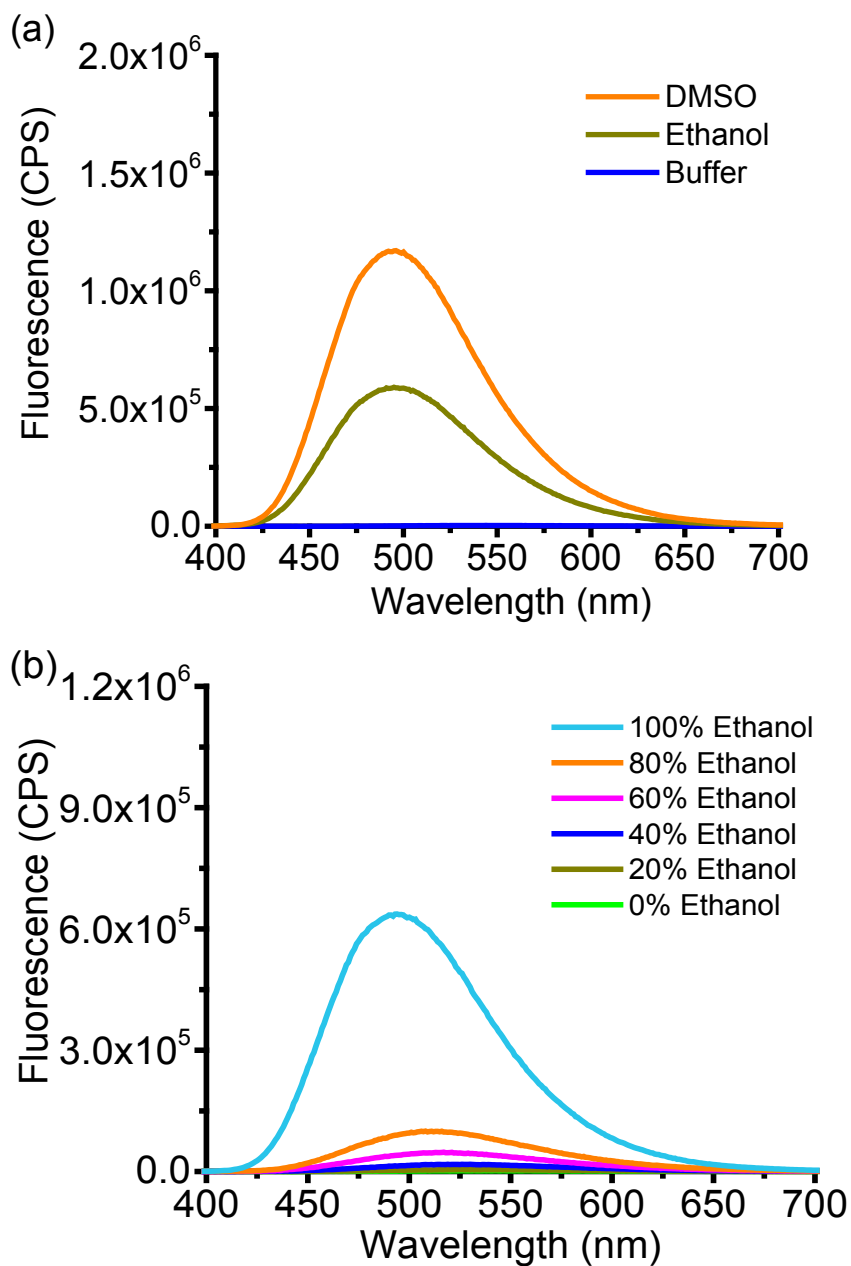
Figure 5.4. ANS modified dye response to solvent polarity. Emission spectra of ANS in (a) varying polarity solvents (DMSO, 100% Ethanol and 0.1 M Sodium Bicarbonate Buffer (pH 8.3)) as well as in (b) ethanol-water dilutions.
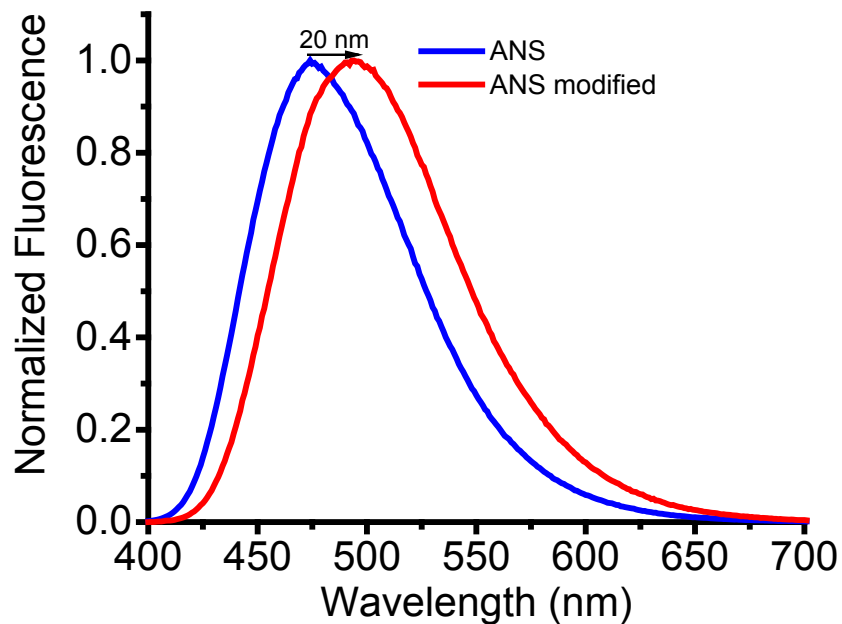
Figure 5.5. Stokes shift of modified ANS dye. Emission spectra of ANS and ANS-NHS in 100% ethanol showing 20 nm red shift in emission maxima, from 474 nm to 494 nm.

Further analysis of the ANS modified probe with protein samples also revealed a similar response to that of ANS with the order of surface hydrophobicity indicated as BSA>Apomyoglobin>Myoglobin (figure 5.7 – 5.8). This was further supported by surface hydrophobicity measurements of the proteins using the ANS modified probe. The S_0 values for proteins were as follows: Mb (not determined); Apomyoglobin (912); and BSA (26563). Again, as observed previously, the ANS modified dye showed lower levels of fluorescence compared to ANS samples.

(a)

Equation	y = a + b*x		
Weight	Instrumental		
Residual Sum of Squares	22.2314 4		
Pearson's r	0.99926		
Adj. R-Square	0.99831		
		Value	Standard Err
NET RFI	Intercept	35483.266	1203.35137
	Slope	26563.109	385.99426

(b)

Equation	y = a + b*x		
Weight	Instrumental		
Residual Sum of Squares	74.77184		
Pearson's r	0.99266		
Adj. R-Square	0.98328		
		Value	Standard Error
NET RFI	Intercept	4564.2021	413.78496
	Slope	911.61241	41.98089

158

Figure 5.6. Surface hydrophobicity (S₀) of proteins with the modified ANS probe. (a) BSA; (b) Apomyoglobin; (c) Myoglobin. Surface hydrophobicity measurements for BSA showed a value of 26563 in comparison to apomyoglobin which showed a value of 912. No value could be determine for myoglobin due to the negative exponential decay relationship observed.

(a)

(b)
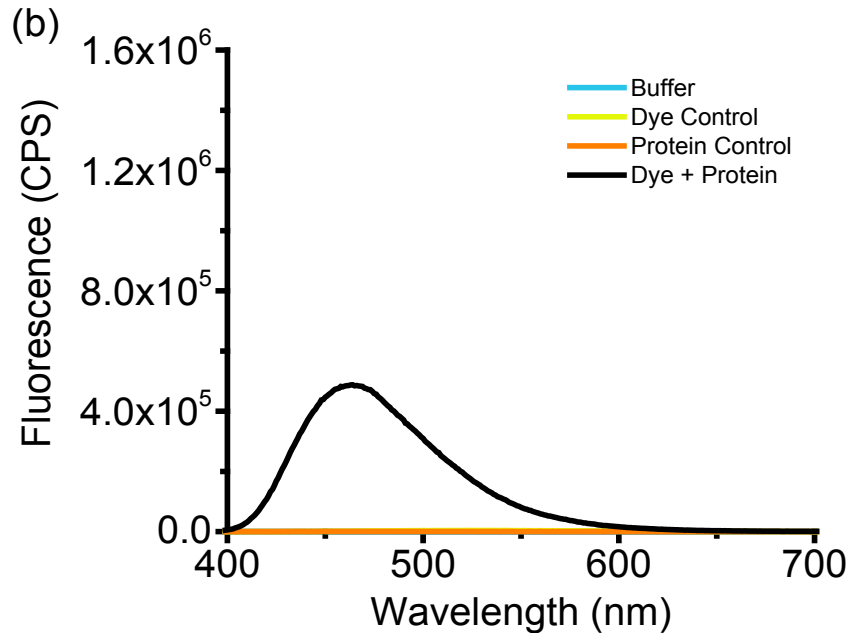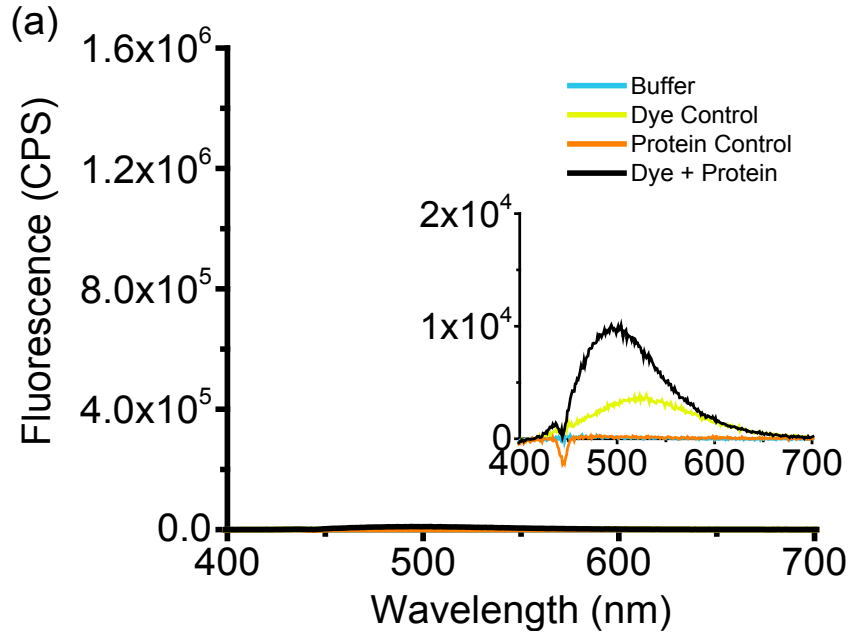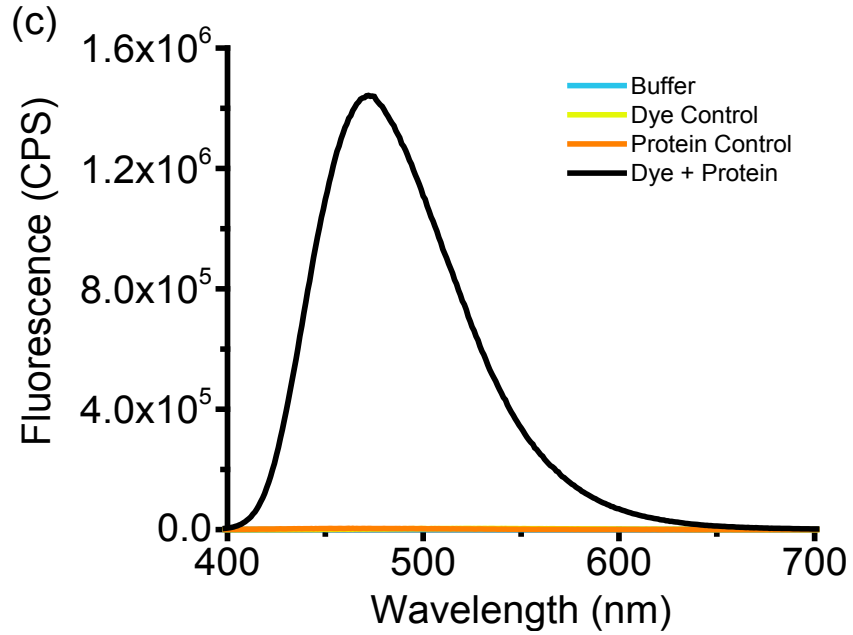
Figure 5.7. Surface hydrophobicity of proteins (Myoglogbin, Apomyoglobin, Lysozyme and BSA) using ANS. ANS (5 µM) incubated with 5 µM proteins (Myoglobin, Apomyoglobin, Lysozyme and BSA) at r.t. for 1 h. (a) Myoglobin; (b) Apomyoglobin; (c) BSA. Where shown, insets show spectra on smaller scale for easy comparison.

161
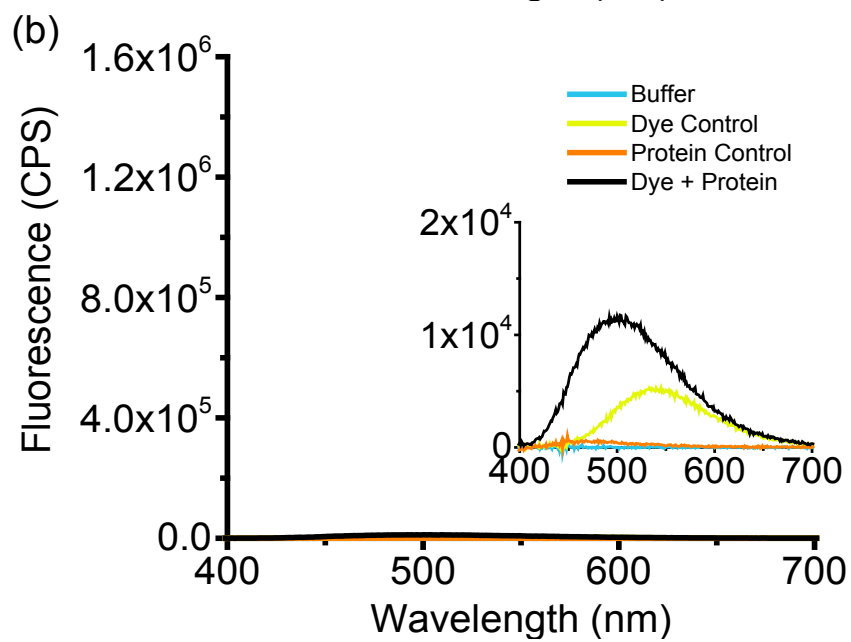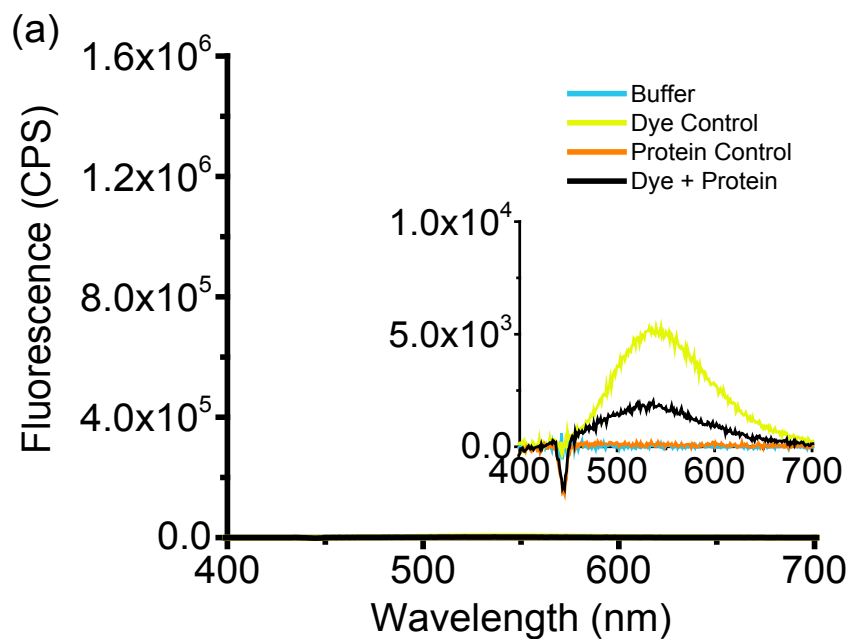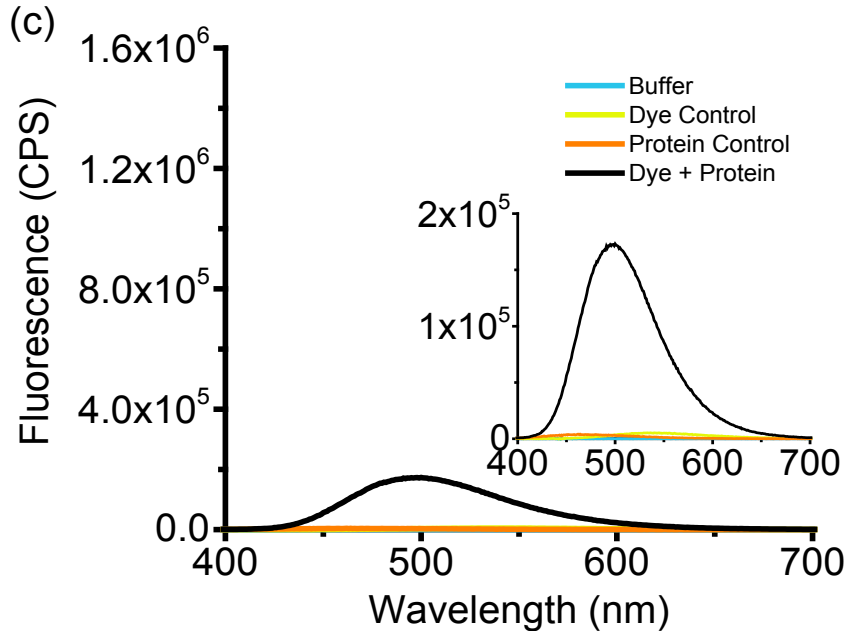
Figure 5.8. Surface hydrophobicity of proteins (Myoglogbin, Apomyoglobin, Lysozyme and BSA) using ANS modified dye. ANS modified dye (5 µM) incubated with 5 µM proteins (Myoglobin, Apomyoglobin, Lysozyme and BSA) at r.t. for 1 h shown on the same scale as that of ANS samples (Fig. 2). (a) Myoglobin; (b) Apomyoglobin; (c) BSA. Where shown, insets show spectra on smaller scale for easy comparison.

After labeling of protein with the ANS modified dye, the samples were analyzed via SDS PAGE. Gel images showed a strong signal for labeled BSA and apomyoglobin but there was no signal detected for myoglobin (figure 5.9 – 5.11). In addition, comparison of labeled protein to unlabeled control or proteins with ANS via UV illumination (figure 5.9 – 5.10) showed much greater signal for BSA and Apomyoglobin. In contrast, the labeled myoglobin (figure 5.11) showed no difference for labeled protein compared to the controls. In addition, the Coomassie stained version of each gel showed comparable levels of proteins in each lane (figure 5.9 – 5.11).

163

BSA
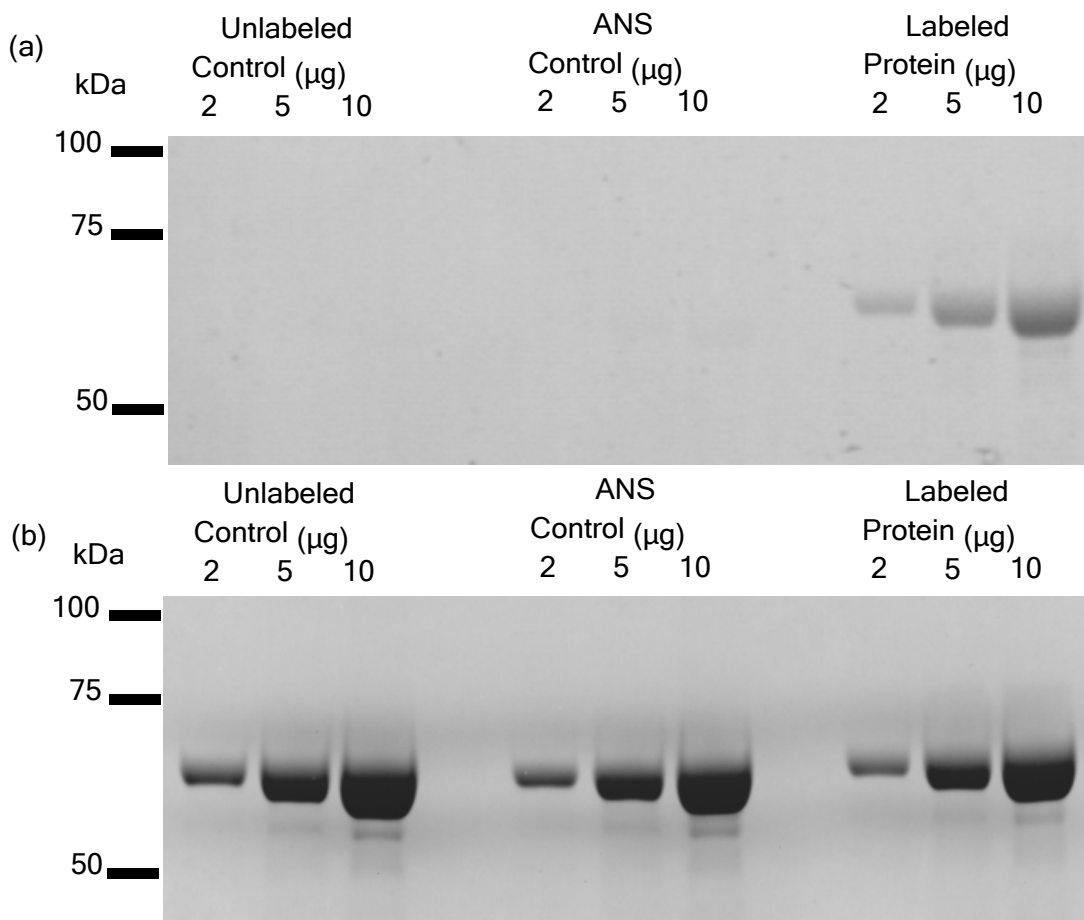
Figure 5.9. SDS-PAGE gel images of BSA after labeling with ANS probe.
Images of 10% TRIS-GLY gel of BSA shown of gel illuminated with UV light (a)
or stained with Coomassie blue (b). Lanes indicate position of protein markers,
unlabeled protein, protein incubated with ANS and labeled protein. All proteins
were run in triplicate of 2, 5 and 10 µg respectively.

Apomyoglobin

(a)

	Unlabeled Control (µg)			ANS Control (µg)			Labeled Protein (µg)		
kDa	2	5	10	2	5	10	2	5	10

(b)

	Unlabeled Control (µg)			ANS Control (µg)			Labeled Protein (µg)		
kDa	2	5	10	2	5	10	2	5	10
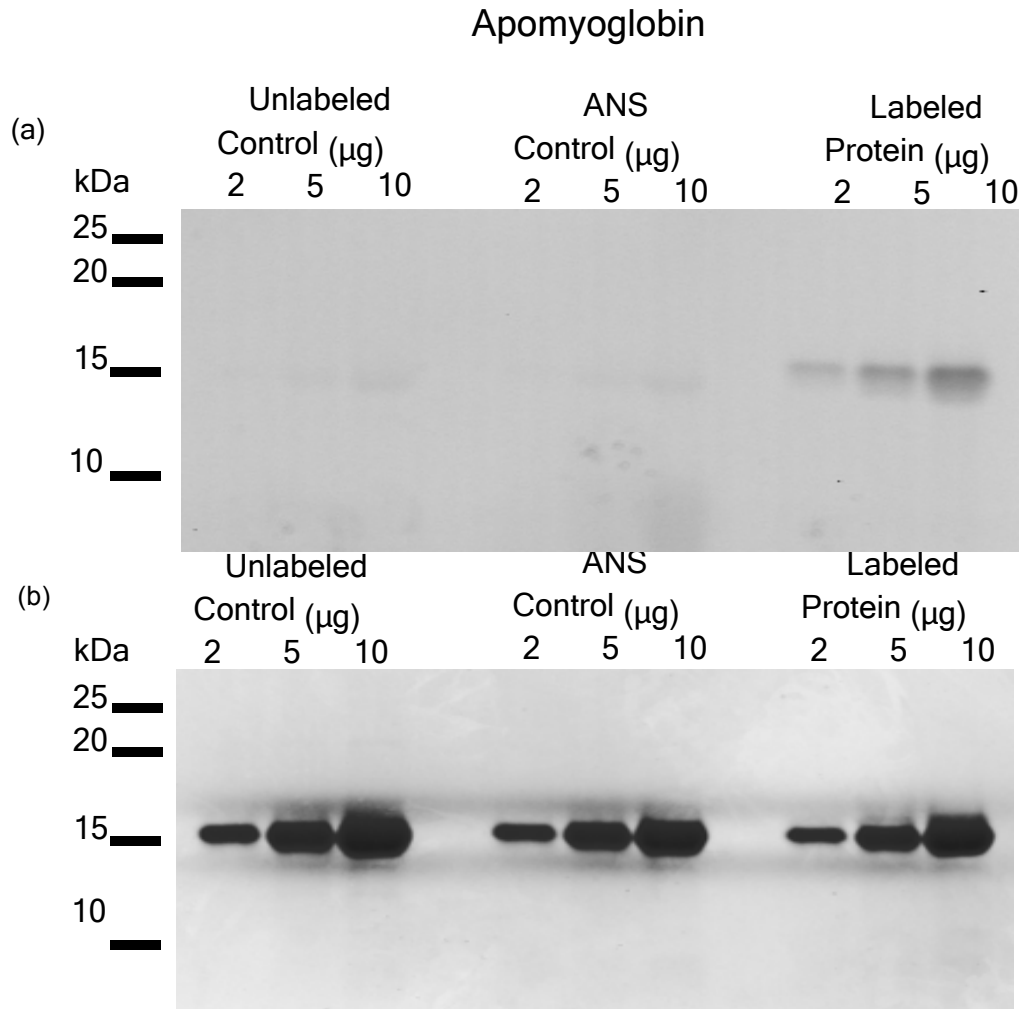
Figure 5.10. **SDS-PAGE gel images of apomyoglobin after labeling with ANS probe**. 15% TRIS-GLY gel illuminated with UV light (a) or stained with Coomassie blue (b). Lanes indicate position of protein markers, unlabeled protein, protein incubated with ANS and labeled protein. All proteins were run in triplicate of 2, 5 and 10 µg respectively.

Myoglobin
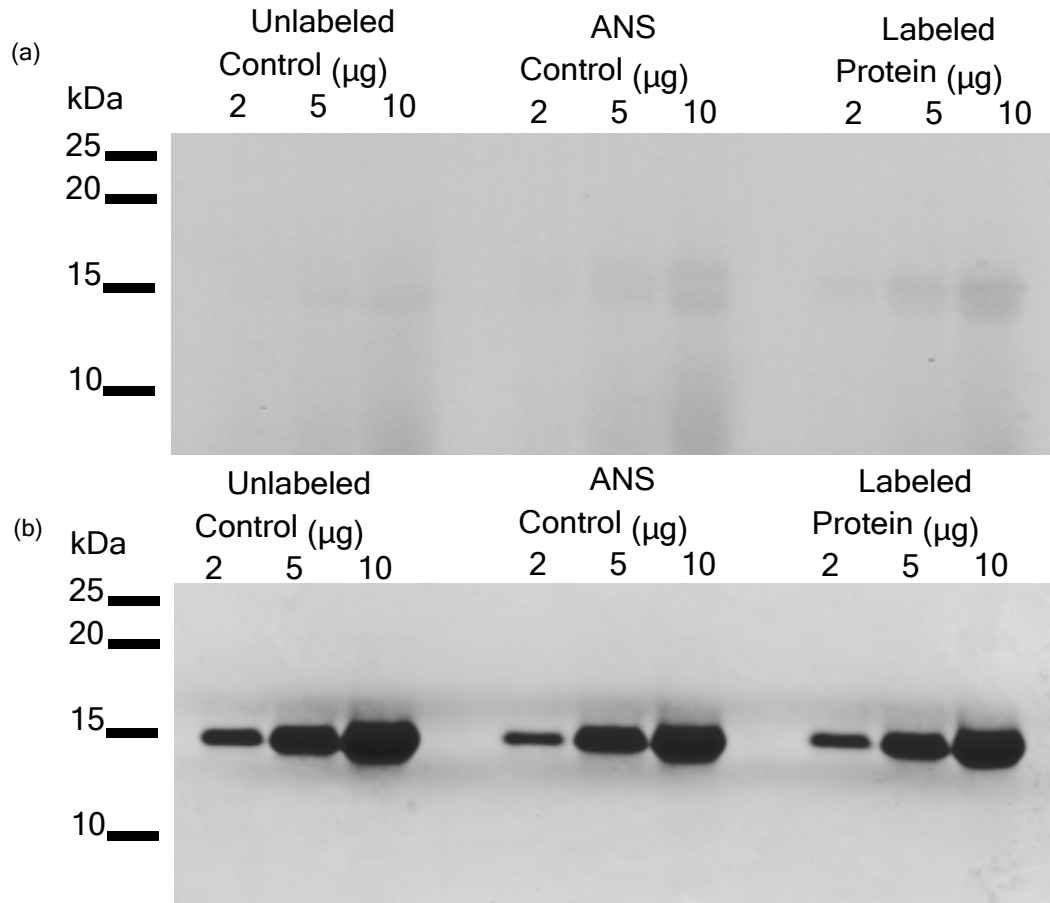
Figure 5.11. **SDS-PAGE gel images of myoglobin after labeling with ANS probe**. 15% TRIS-GLY gel illuminated with UV light (a) or stained with Coomassie blue (b). Lanes indicate position of protein markers, unlabeled protein, protein incubated with ANS and labeled protein. All proteins were run in triplicate of 2, 5 and 10 µg respectively.

5.5. **Discussion**

This study shows application of a novel modified version of ANS with a linker tail for mapping protein surface hydrophobicity. The modified ANS dye used in this experiment showed physicochemical properties comparable to commercial ANS with a reduction in overall intensity but no change in the overall emission spectra. However, a reduction in quantum yield was observed (Figure 5.3 – 5.4) between free ANS and the modified version (Figure 5.12 – 5.13).

Modified ANS is restricted to surface hydrophobic regions resulting in weak fluorescence whereas free ANS is able to bind in the hydrophobic pocket resulting in the higher fluorescence levels observed. On the surface of proteins, lysine groups are the most abundant amines and a source of nucleophiles.[25] In a typical globular protein, the amount of lysine residues can be 6 – 9%.[35] In contrast, arginine has an abundance of 3 – 5%.[35] Of the proteins used in this study, BSA contained the most lysine and arginine residues with 60 and 26 residues respectively. Apomyoglobin and Myoglobin contained 19 lysine and 2 arginine residues respectively. However, not every lysine or arginine residue is near a region of surface hydrophobicity (Figure
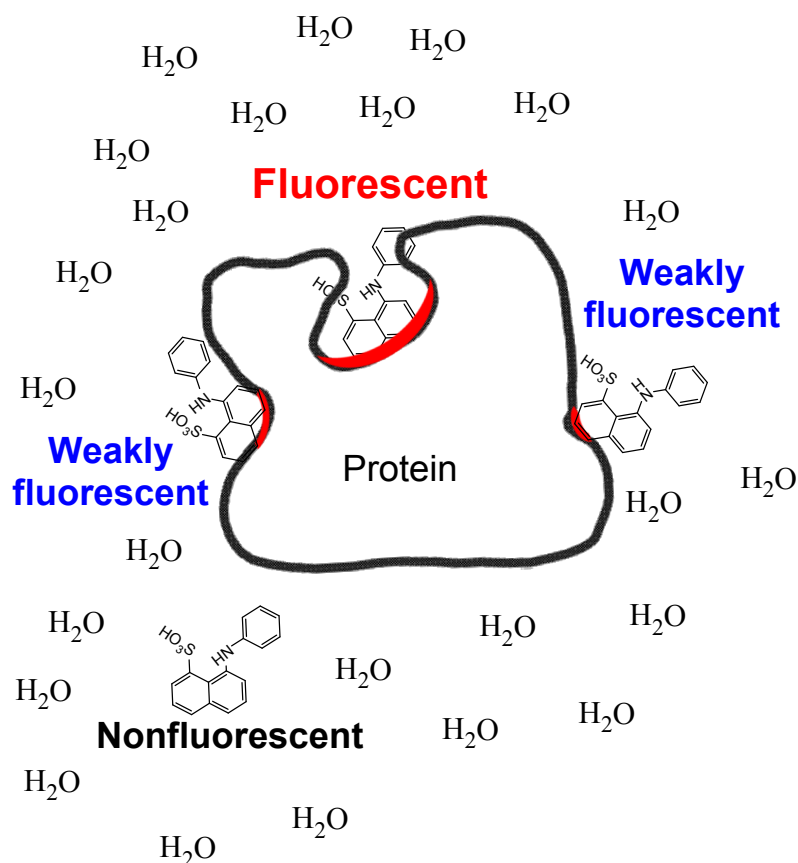
Figure 5.12. ANS is fluorescent when bound to hydrophobic pocket. ANS molecules bound to the hydrophobic pocket are most fluorescent and weakly fluorescent when bound to exposed hydrophobic surface of proteins.

This difference in quantum yield was attributed to the difference in mechanism 5.14). This allows the labeling process to be biased towards amine groups that are near surface exposed hydrophobicity. As a result, we have designed an NHS modification to a well characterized fluorescent probe ANS[10-12,19,20,22,26,36] which has been successfully used in mapping the surface hydrophobicity of proteins. This type of technology can improve our understanding of and help characterize toxic species that cause protein aggregation.

168
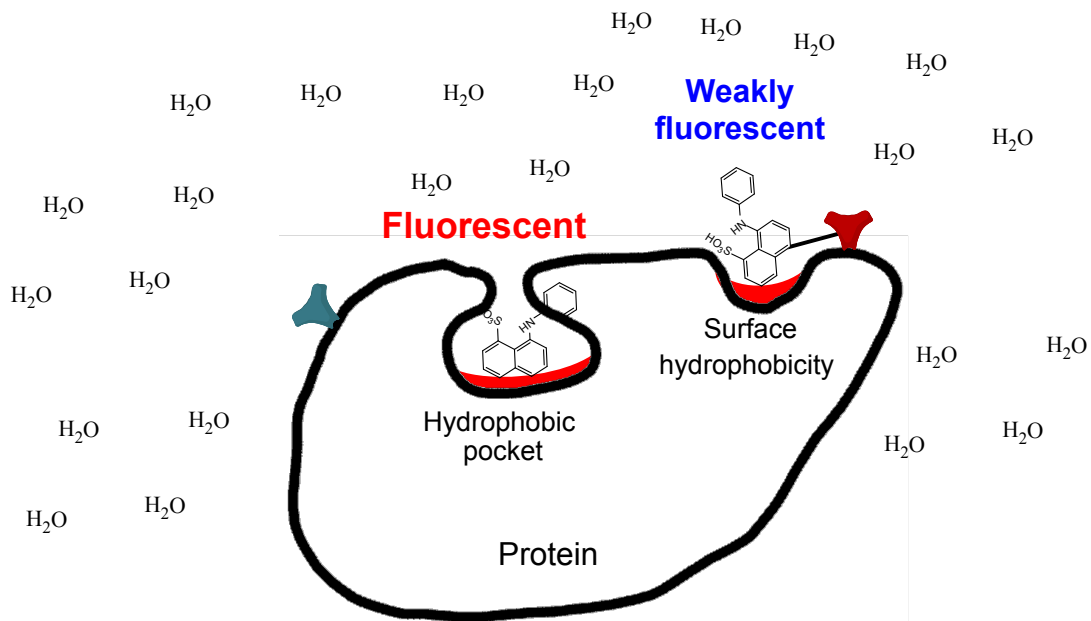
Figure 5.13. ANS binds to hydrophobic pocket while modified ANS detects surface hydrophobicity. Free ANS is able to fit into and bind to the hydrophobic pockets of proteins. Modified ANS is restricted to only surface hydrophobicity of proteins due to covalent attachment to an amine group near region of surface hydrophobicity.

The modification of ANS with the NHS ester increases the steric hindrance of the probe in addition to increasing the size of the protein by approximately 415 Da. The NHS modification also increases sensitivity of this probe to surface hydrophobicity as seen with myoglobin. In the presence of ANS, the fluorescence signal is significant compared to just the probe alone (Figure 5.7). However, in the presence of the modified-ANS probe, the signal is significantly reduced. Also, a comparison of myoglobin and apomyoglobin shows that the modified ANS probe is sensitive to the increase in surface hydrophobicity due to the loss of the metal ion stabilizing the holo-protein (Figure 5.7 – 5.8).
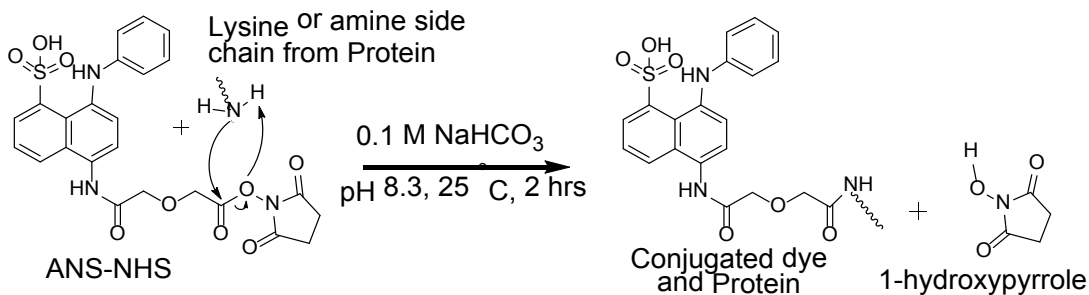
Figure 5.14. Mechanism of covalent linkage of ANS-modified probe to lysine or amine side chain group of protein.[37] In the two step process, the lone pair of electrons from a lysine or amine side chain of the protein first attack the carbocation closest to the pyrrole group and then cause the release of 1-hydroxypyrrole. The ANS-modified probe is then covalently bound to the protein

A 20 nm stokes shift was observed for the modified-ANS probe in ethanol compared to ANS. One possible explanation for this shift may be due to the addition of the NHS ester. The addition of the NHS ester at position 5 may result in the nitrogen lone pair of electrons stabilizing the polarized carbonyl on the ester chain as opposed to activating the naphthalene ring.

Analysis of the surface hydrophobicity of protein using the modified probe were in line with previous publications [34,36] showing increase in surface hydrophobicity as BSA > Apomyoglobin > Myoglobin.[34] The negative exponential slope of the modified-ANS probe with myoglobin was unexpected but may be explained by the quenching of solvent exposed ANS[8,12,22,38] as well as the lack of surface exposed hydrophobicity. As a result, a covalent linkage of this modified probe to myoglobin would result in very little fluorescence. In addition, an increase in the concentration of protein results in greater

fluorescence signal from intrinsic fluorescence than from the modified-ANS probe. Therefore, correcting for this intrinsic fluorescence with very weak fluorescence from the probe results in a reduction of fluorescence compared to free probe.

Labeling efficiency and success were analyzed through gel electrophoresis. Labeling conditions were such that maintaining the pH just above 8 allowed the ε-amino group to be deprotonated.[39] Deprotonation was key for labeling success as this initial step allowed for nucleophilic attack toward the NHS ester while minimizing unwanted attacks from hydroxyl ions.[39]

Comparison of the labeled proteins using SDS PAGE revealed that the interaction between the modified ANS probe and with proteins was not a hydrophobic interaction (Figure 5.8 – 5.10). In comparison to ANS samples incubated with protein, the UV signal was stronger with the modified probes. In addition, because solvent exposed ANS has weak fluorescence, the presence of a signal was an indicator of a hydrophobic interaction as well (Figure 5.8 – 5.10). The denaturing conditions under which SDS PAGE were conducted were strong enough to abolish hydrophobic interactions of ANS with protein, but had no impact on the covalently bound ANS (Figure 5.8 – 5.10).
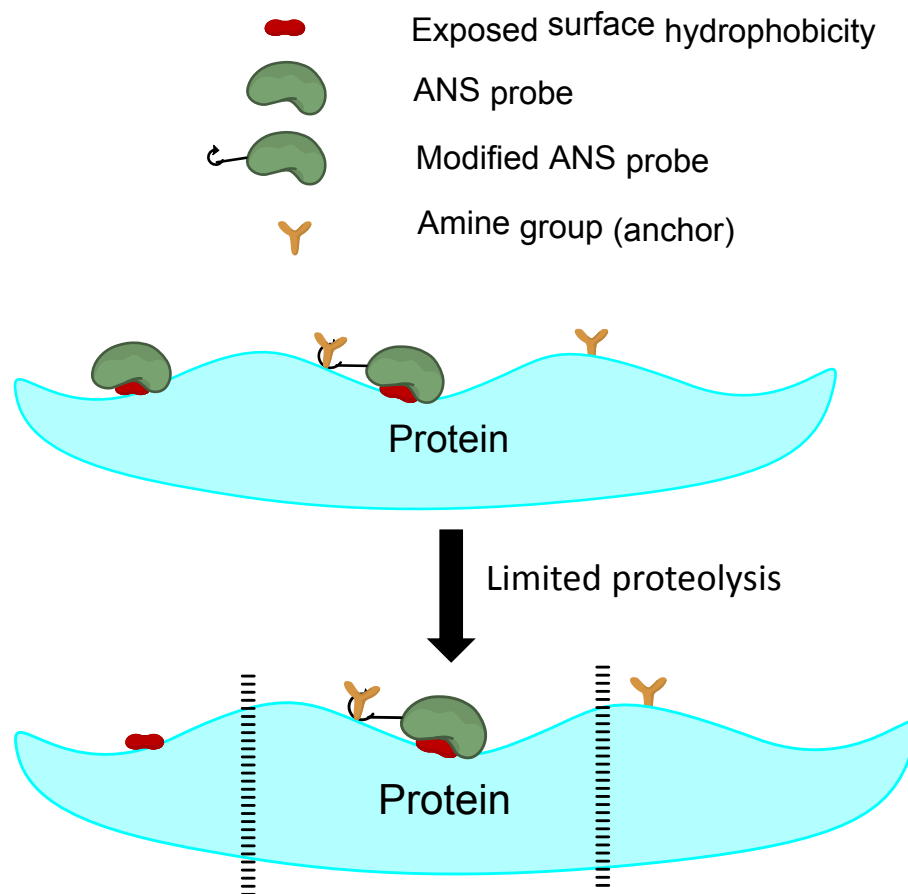
Figure 5.15. Hydrophobic Mapping of proteins. ANS probes that are covalently bound to the protein are retain post proteolysis and can be used to identify hydrophobic regions via ESI-Mass spectrometry.

The mechanism of covalent labeling of proteins with the modified ANS probe was calculated as a 415 Da change in mass (Figure 5.14). This mass change further allows identification of modified region by electrospray ionization mass spectrometry techniques after limited proteolysis (Figure 5.15) to identify the location of modified residue. An understanding of the location of each attached probe would allow for a map of the hydrophobic surface to be developed. The ability to map the protein hydrophobic surface will then allow for visualization of

hydrophobic surface using crystallographic database that can be used for *in-silico* screening of small molecules for rational drug design.

5.6. **Conclusion**

This paper shows how a conventional hydrophobic probe such as ANS can be potentially modified for mapping surface hydrophobic regions on proteins. The modified ANS probe was able to distinguish between the different levels of surface hydrophobicity for BSA, apomyoglobin and myoglobin as shown by SDS-PAGE. This also opens up possibility of modifying other hydrophobic probes such as HPsensors and adding this covalent linking properties that will provide a strong fluorescence signal as well help in identification of surface hydrophobic regions on proteins at very low concentrations. Combining this tool with mass spectrometry will allows us to the map the hydrophobic surface of proteins. Eventually, employing this tool to oligomeric species that are known to be toxic would provide details about its structures that can be targeted for rational drug design to combat neurodegenerative diseases.

5.7. References

1   Campioni, S. *et al.* A causative link between the structure of aberrant protein oligomers and their toxicity. *Nat Chem Biol* **6**, 140-147, doi:10.1038/nchembio.283 (2010).

2   Munch, C. & Bertolotti, A. Exposure of hydrophobic surfaces initiates aggregation of diverse ALS-causing superoxide dismutase-1 mutants. *J Mol Biol* **399**, 512-525, doi:10.1016/j.jmb.2010.04.019 (2010).

3   Yang, M., Dutta, C. & Tiwari, A. Disulfide-bond scrambling promotes amorphous aggregates in lysozyme and bovine serum albumin. *J Phys Chem B* **119**, 3969-3981, doi:10.1021/acs.jpcb.5b00144 (2015).

4   Tiwari, A., Xu, Z. & Hayward, L. J. Aberrantly Increased Hydrophobicity Shared by Mutants of Cu,Zn-Superoxide Dismutase in Familial Amyotrophic Lateral Sclerosis. *J. Biol. Chem.* **280**, 29771-29779, doi:10.1074/jbc.M504039200 (2005).

5   Bigelow, C. C. On the average hydrophobicity of proteins and the relation between it and protein structure. *J. Theor. Biol.* **16**, 187-211 (1967).

6   Nakai, S., Li-Chan, E. & Arteaga, G. E. in *Methods of testing protein functionality* (ed G. M. Hall) Ch. 8, 226 - 255 (Blackie A & P, 1996).

7   Kato, A. & Nakai, S. Hydrophobicity determined by a fluorescence probe method and its correlation with surface properties of proteins. *Biochim. Biophys. Acta* **624**, 13-20 (1980).

8   Alizadeh-Pasdar, N. & Li-Chan, E. C. Y. Comparison of Protein Surface Hydrophobicity Measured at Various pH Values Using Three Different Fluorescent Probes. *J. Agric. Food Chem.* **48**, 328-334 (2000).

9   Haskard, C. A. & Li-Chan, E. C. Y. Hydrophobicity of Bovine Serum Albumin and Ovalbumin Determined Using Uncharged (PRODAN) and Anionic (ANS-) Fluorescent Probes. *J. Agric. Food Chem.* **46**, 2671-2677 (1998).

10   Matulis, D., Baumann, C. G., Bloomfield, V. A. & Lovrien, R. E. 1-Anilino-8-Naphthalene Sulfonate as a protein Conformational Tightening Agent. *Biopolymers* **49**, 451-458 (1999).

11   Hawe, A., Sutter, M. & Jiskoot, W. Extrinsic fluorescent dyes as tools for protein characterization. *Pharm. Res.* **25**, 1487-1499, doi:10.1007/s11095-007-9516-9 (2008).

12   Matulis, D. & Lovrien, R. 1-Anilino-8-Naphthalene Sulfonate Anion-Protein Binding Depends Primarily on Ion Pair Formation. *Biophys. J.* **74** 422–429 (1998).

13   Takashi, R., Tonomura, Y. & Morales, M. F. 4,4'-Bis(1-anilinonaphthalene 8-sulfonate) (bis-ANS): A new probe of the active site of myosin. *Proc. Nati. Acad. Sci.* **74**, 2334-2338 (1977).

14   Bothra, A., Bhattacharyya, A., Mukhopadhyay, C., Bhattacharyya, K. & Roy, S. A fluorescence spectroscopic and molecular dynamics study of

bis-ANS/protein interaction. *Journal of biomolecular structure & dynamics* **15**, 959-966, doi:10.1080/07391102.1998.10508216 (1998).

15   Hudson, S. A., Ecroyd, H., Kee, T. W. & Carver, J. A. The thioflavin T fluorescence assay for amyloid fibril detection can be biased by the presence of exogenous compounds. *FEBS Journal* **276**, 5960-5972, doi:10.1111/j.1742-4658.2009.07307.x (2009).

16   Khurana, R. *et al.* Mechanism of thioflavin T binding to amyloid fibrils. *J Struct Biol* **151**, 229-238, doi:10.1016/j.jsb.2005.06.006 (2005).

17   Mozes, E. *et al.* A novel application of the fluorescent dye bis-ANS for labeling neurons in acute brain slices. *Brain research bulletin* **86**, 217-221, doi:10.1016/j.brainresbull.2011.07.004 (2011).

18   Hawe, A., Sutter, M. & Jiskoot, W. Extrinsic fluorescent dyes as tools for protein characterization. *Pharm Res* **25**, 1487-1499, doi:10.1007/s11095-007-9516-9 (2008).

19   Gasymov, O. K. & Glasgow, B. J. ANS Fluorescence: Potential to Augment the Identification of the External Binding Sites of Proteins. *Biochim. Biophys. Acta* **1774**, 403–411 (2007).

20   Togashi, D. M. & Ryder, A. G. A fluorescence analysis of ANS bound to bovine serum albumin: binding properties revisited by using energy transfer. *J. Fluoresc.* **18**, 519-526, doi:10.1007/s10895-007-0294-x (2008).

21   Stryer, L. The interaction of a naphthalene dye with apomyoglobin and apohemoglobin. A fluorescent probe of non-polar binding sites. *J Mol Biol* **13**, 482-495 (1965).

22   Haskard, C. A. & Li-Chan, E. C. Y. Hydrophobicity of Bovine Serum Albumin and Ovalbumin Determined Using Uncharged (PRODAN) and Anionic (ANS-) Fluorescent Probes. *J. Agric. Food Chem.* **46**, 2671-2677 (1998).

23   Andujar-Sanchez, M., Jara-Perez, V., Cobos, E. S. & Camara-Artigas, A. A thermodynamic characterization of the interaction of 8-anilino-1-naphthalenesulfonic acid with native globular proteins: the effect of the ligand dimerization in the analysis of the binding isotherms. *Journal of molecular recognition : JMR* **24**, 548-556, doi:10.1002/jmr.1065 (2011).

24   Cardamone, M. & Puri, N. K. Spectrofluorimetric assessment of the surface hydrophobicity of proteins. *The Biochemical journal* **282 (Pt 2)**, 589-593 (1992).

25   Hormoz, S. Amino acid composition of proteins reduces deleterious impact of mutations. *Sci Rep* **3**, 2919, doi:10.1038/srep02919 (2013).

26   Slavik, J. Anilinonaphthalene Sulfonate As A Probe Of Membrane Composition And Function. *Blochemica et Biophysica Acta* **694**, 1-25 (1982).

27   Matulis, D. & Lovrien, R. 1-Anilino-8-Naphthalene Sulfonate Anion-Protein Binding Depends Primarily on Ion Pair Formation. *Biophysical Journal* **74** 422–429 (1998).

28   Alexander, P., Hamilton, L. D. & Stacey, K. A. Irradiation of proteins in the solid state. I. Aggregation and disorganization of secondary structure in bovine serum albumin. *Radiation research* **12**, 510-525 (1960).

29   Baker, G. A. *et al.* Effects of fluorescent probe structure on the dynamics at cysteine-34 within bovine serum albumin: evidence for probe-dependent modulation of the cybotactic region. *Biopolymers* **59**, 502-511, doi:10.1002/1097-0282(200112)59:7<502::AID-BIP1055>3.0.CO;2-I (2001).

30   Bloomfield, V. The structure of bovine serum albumin at low pH. *Biochemistry* **5**, 684-689 (1966).

31   Cheng, X. X., Lui, Y., Zhou, B., Xiao, X. H. & Liu, Y. Probing the binding sites and the effect of berbamine on the structure of bovine serum albumin. *Spectrochimica acta. Part A, Molecular and biomolecular spectroscopy* **72**, 922-928, doi:10.1016/j.saa.2008.12.003 (2009).

32   Jin, Y. J., Li, W. L. & Wang, Q. R. Tb(III) as a fluorescent probe for the structure of bovine serum albumin. *Biochemical and biophysical research communications* **177**, 474-479 (1991).

33   Huang, B. X., Kim, H. Y. & Dass, C. Probing three-dimensional structure of bovine serum albumin by chemical cross-linking and mass

spectrometry. *J Am Soc Mass Spectrom* **15**, 1237-1247, doi:10.1016/j.jasms.2004.05.004 (2004).

34   Dorh, N. *et al.* BODIPY-Based Fluorescent Probes for Sensing Protein Surface-Hydrophobicity. *Sci Rep* **5**, 18337, doi:10.1038/srep18337 (2015).

35   Cummings, A. J. & Flynn, F. V. Amino-acid composition of serum proteins in health and disease. *Journal of clinical pathology* **8**, 153-159 (1955).

36   Cardamone, M. & Puri, N. K. Spectrofluorimetric assessment of the surface hydrophobicity of proteins. *Biochem. J.* **282**, 589-593 (1992).

37   Hermanson, G. T. in *Bioconjugate Techniques (Second Edition)*   234-275 (Academic Press, 2008).

38   Matulis, D., Baumann, C. G., Bloomfield, V. A. & Lovrien, R. E. 1-Anilino-8-naphthalene sulfonate as a protein conformational tightening agent. *Biopolymers* **49**, 451-458, doi:10.1002/(SICI)1097-0282(199905)49:6<451::AID-BIP3>3.0.CO;2-6 (1999).

39   Modesti, M. in *Single Molecule Analysis: Methods and Protocols*   (eds G. Erwin J. Peterman & L. Gijs J. Wuite) 101-120 (Humana Press, 2011).

Chapter 6: Future work

The work described here was done primarily with a focus of applying the new tools in the field of neurodegeneration. The use of the HPsensors with proteins such as superoxide dismutase 1 (SOD1) would provide valuable structural information on the toxic species as well as provide enough details for mechanism formulation. Beyond this, there is still much room for improvement of the HPsensors by modulating the substituent groups at the meso position.

Sensor

Fluorescent moiety
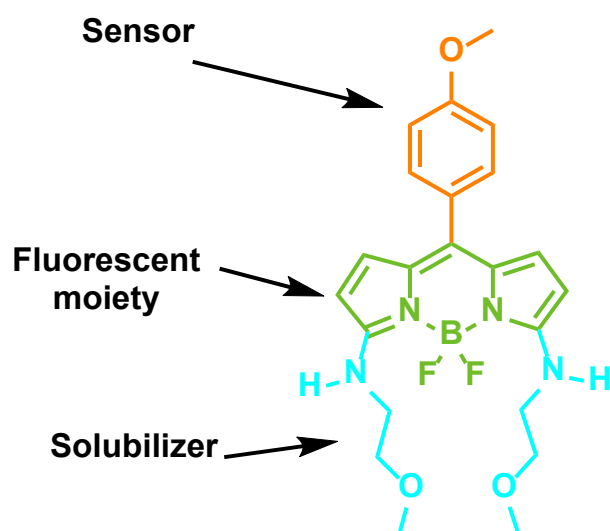
Solubilizer

Figure 6.1. HPsensor design. The different parts work together to improve solubility and sensitivity of the probes.

These groups found in the sensor portion of the probe impact sensitivity of the probes to surface hydrophobicity and thus could be further improved. Currently, we have used some moderate to strong activating groups on the aryl groups. Use of slightly weaker activating groups may provide the ideal band gap for

increased sensitivity. In addition, the use of amine-free solubilizers may also significantly reduce the sensitivity to pH of these sensors. The ideal probe would be pH insensitive, water soluble, yet extremely responsive to surface hydrophobicity.

To map the hydrophobic surface on proteins, covalently modified proteins will be digested and analyzed using mass spectrometry (Figure 6.2). Analysis of protein fragments would then allow for identification of the regions of surface exposed hydrophobicity. Including also *in-silico* techniques such as homology modeling, it would be possible to determine 3D structures of each protein and the dimensions of the hydrophobic regions. The 3D model of the proteins can then be combined with docking studies to screen small molecule libraries. These small molecules will be tailored to the exposed hydrophobic surface using a rational drug design approach. As a result, novel therapeutic avenues can then be explored.
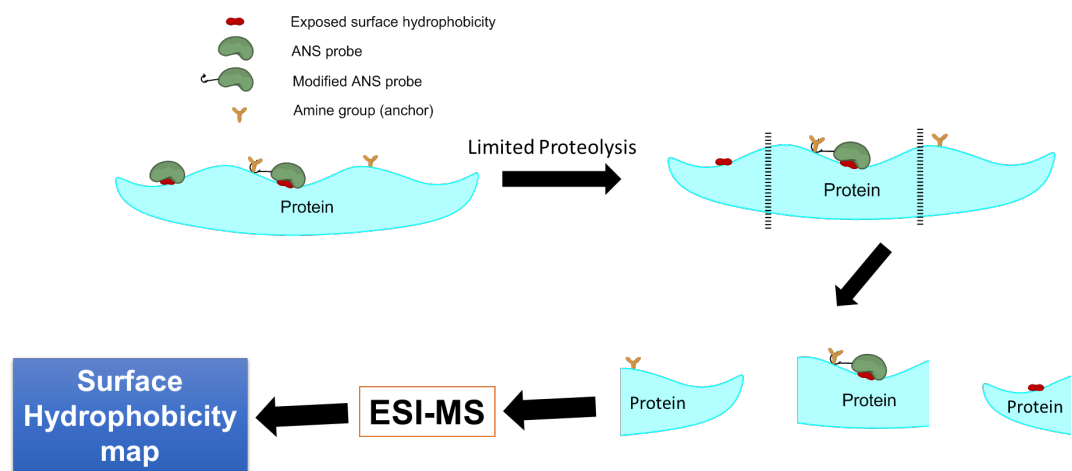
Figure 6.2. Hydrophobic mapping of protein surface hydrophobicity. Limited proteolysis of labeled proteins will allow ESI-MS analysis and the formulation of a surface hydrophobicity map for the protein.

Improvements to the process of hydrophobic labeling can also be accomplished by using more sensitive probes than the test probe ANS. HPsensors have shown greater sensitivity than ANS in detecting surface hydrophobicity and would allow for fluorescence visualization as well as improved sensitivity in hydrophobic mapping.

A combinatory approach of hydrophobic sensing and hydrophobic mapping would provide the necessary quantitative details for rational drug designs and would impact the way that toxic aggregation-prone species are characterized and visualized.

Summary

This work describes the design and application of fluorescent probes for characterizing the surface hydrophobicity of proteins. The disparity between average hydrophobicity and surface hydrophobicity has been a concern in the field of protein chemistry for some time. While importance of protein surface hydrophobicity in health and disease is well recognized, the lack of tools that are highly sensitive and can quantitatively measure the surface hydrophobicity of proteins has seriously hampered progress in this area. In addition, a more recent question in the field of proteinopathies have focused on the need to identify the toxic protein species in these diseases including neurodegenerative diseases.

While, the major driving force for these observed aggregates (oligomer, amorphous or fibrillary aggregates) is surface hydrophobic interactions, probes that can quantitatively and precisely measure this property are lacking. To address this major need in the protein field, we used two pronged approach: 1) Develop tools for sensing surface hydrophobicity of proteins with high sensitivity, and 2) develop tools to accurately map the hydrophobic surface of proteins. Finally, the future goal is to combine these two properties in a new generation of sensors that can detect surface hydrophobicity with high sensitivity and also map that area accurately.

The work reported in Chapter 4 focuses on developing sensors that can detect surface hydrophobicity of proteins with high sensitivity. These hydrophobicity sensors (HPsensors **1**, **2**, and **3**) were capable of detecting surface hydrophobicity with high sensitivity. Improvements in sensitivity were noted to be up to 60-fold when compared to a commonly used commercial probe ANS. Method development of these probes allowed us to outline several parameters that were essential to sensitivity and function of these probes. Parameters such as the HOMO-LUMO gap, the nature of the substituent groups and the type of solubilizer were all very important considerations and will serve as a good foundation for building and improving future generation of probes.

The work reported in Chapter 5 addresses the mapping of surface hydrophobic regions on protein with high accuracy. For this work we started with ANS as it has been successfully used for sensing protein hydrophobicity. Despite its several limitations (discussed in great detail in chapter 5) it was a very suitable candidate for further modification as its physicochemical properties are very well known. The ANS dye was modified to add an NHS-ester that can covalently tag to an amine residue in the vicinity of hydrophobic region. Although, the conventional ANS probe is known to bind to hydrophobic pockets on protein, the modification will add a tail that will prevent binding to tight pockets due to steric hindrance. This new modified ANS dye was successfully used to label

three proteins with varying degree of hydrophobicity (BSA, myoglobin, apomyoglobin) and verify the covalent binding by luminescence on electrophoretic gels. This new tool, coupled with high resolution mass spectrometry techniques can be utilized to map the hydrophobic surface of any protein at a quantitative level.

In future the goal will be to combine the high fluorescence sensing of the proteins surface hydrophobicity with a catalytic side chain that can covalently tag to nearby amine, carboxylic, or free sulfhydryl group. The linker chains of varying length will be used. This will help us precisely target surface regions of proteins to identify the surface folds which in turn can be modeled to screen for small molecules that can act as drug. This has potential for application not only in the neurodegenerative disease field but any area of protein chemistry where surface hydrophobic interactions are key to their function.

Appendix A: Supplementary Information for Chapter 4

BODIPY-Based Fluorescent Probes for Sensing Protein Surface-Hydrophobicity

Nethaniah Dorh[a], Shilei Zhu[a,†], Kamal B. Dhungana[b], Ranjit Pati[b], Fen-Tair Luo[c], Haiying Liu[a], Ashutosh Tiwari[a]*.

[a]Department of Chemistry, Michigan Technological University, Houghton, MI 49931, USA

[b]Department of Physics, Michigan Technological University, Houghton, MI 49931, USA

[c]Institute of Chemistry, Academia Sinica, Taipei, Taiwan 11529, Republic of China

[†]Department of Chemistry & Biochemistry, University of Maryland, College Park, MD 20742, USA

*Corresponding Author: tiwari@mtu.edu

Methods:

Apomyoglobin preparation:

Myoglobin was dissolved in water at (1 to 3 % w/v) and then incubated 4 °C. To the solution, 1 M HCl was added until pH 2.0 was achieved. Then an equal volume of -20 °C 2-butanone was added followed by thorough mixing. After phase separation at 4 °C the top layer of ketone supernatant containing heme was then removed and discarded. This was repeated two more times until the remaining solution was pale yellow to whitish. The solution was then dialyzed against buffer for a total of nine washes using the Spectra/Por 7 dialysis tubing, 6-8K MWCO. Protein concentration was determined using absorbance at 280 nm (ε_{280} equine apomyoglobin: 15,700 M^{-1}cm^{-1}).[1]

Buffer solutions used to dialyze apomyoglobin solution in order of progression:

- Deionized MQ water (pH 2.5, adjusted with 1M HCl; 1 mM EDTA) at 4°C for 1 h and then repeat for 2 h.

- 20 mM glycine HCl buffer (pH 2.5) with 2 mM EDTA at 4°C for 4 h.

- 20 mM glycine HCl buffer (pH 2.5) with 2 mM EDTA at 4°C for 8 h.

- 20 mM glycine HCl buffer (pH 2.5; with chelex) at 4°C for 1 h initially and then for 6 h for two runs.

- 20 mM citrate buffer at pH 5.5 with chelex at 4°C.

- Deionized MilliQ water overnight.

Dye Synthesis

Instrumentation and materials. ^{1}H NMR and ^{13}C NMR spectra were taken on a 400 MHz Varian Unity Inova spectrophotometer instrument. ^{1}H and ^{13}C NMR spectra were recorded in CDCl$_3$, chemical shifts (δ) are given in ppm relative to solvent peaks (^{1}H: δ 7.26; ^{13}C: δ 77.3) as internal standard. Unless otherwise indicated, all reagents and solvents were obtained from commercial suppliers (Aldrich, Sigma, Fluka, Acros Organics, Fisher Scientific, and Lancaster) and used without further purification.

Compound 1 was prepared according to a reported procedure (J. Org. Chem., 2008, 73 (5), 1963–1970). ^{1}H NMR (400 MHz, CDCl$_3$): δ 7.43 (d, *J* = 8.8 Hz, 2H), 7.02 (d, *J* = 8.8 Hz, 2H), 6.86 (d, *J* = 5.2 Hz, 2H), 6.41 (d, *J* = 5.2 Hz, 2H), 3.89 (s, 3H). ^{13}C NMR (100 MHz, CDCl$_3$): δ 162.5, 144.1, 133.8, 132.6, 131.8, 124.8, 118.8, 114.5, 114.4, 55.8.
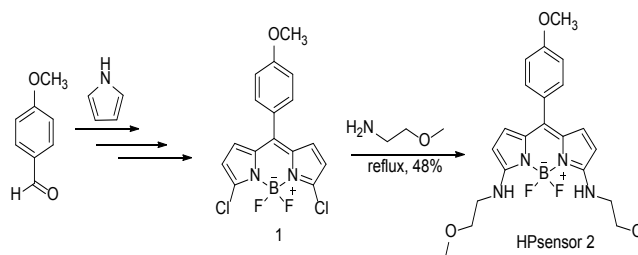
HPsensor 2: The mixture of compound 1 (40 mg, 0.11 mmol) in 2-methoxyethylamine (10 mL) was refluxed overnight under nitrogen atmosphere, and concentrated under reduced pressure. The residues were purified by column chromatography using hexanes/CH_2Cl_2/EtOAc (3:2:1, v/v) to yield 2 as oil (23 mg, 48%). ^1H NMR (400 MHz, $CDCl_3$): δ 7.36 (d, J = 8.4 Hz, 2H), 6.92 (d, J = 8.4 Hz, 2H), 6.54 (d, J = 4.4 Hz, 2H), 5.72 (d, J = 4.4 Hz, 2H), 3.84 (s, 3H), 3.57 (t, J = 5.6 Hz, 4H), 3.42 (t, J = 5.6 Hz, 4H), 3.39 (s, 6H). . ^{13}C NMR (100 MHz, $CDCl_3$): δ 160.2, 156.7, 131.8, 131.6, 129.3, 128.6, 127.6, 113.6, 101.2, 71.4, 59.2, 55.5, 44.5. IR (cm^{-1}): 3417, 3132, 2923, 2300, 1732, 1593, 1542, 1504, 1472, 1423, 1390, 1368, 1337, 1304, 1290, 1275, 1247, 1194, 1175, 1155, 1094, 1055, 1011, 969, 918, 886, 836, 781, 764, 750, 726, 702, 680. HRMS (ESI) calcd for $C_{22}H_{27}BF_2N_4O_3Na$ [M+Na]$^+$ 467.2042; found 467.2039.
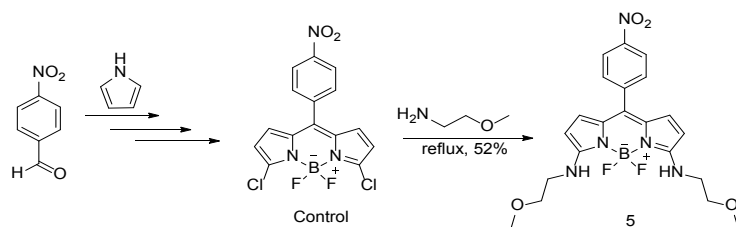
Control was prepared according to a reported procedure (*J. Org. Chem.*, **2008**, *73* (5), 1963–1970).

Compound 5 was prepared from control in 52% yields according to the method for HPsensor **2**. ^1H NMR (400 MHz, $CDCl_3$): δ 8.25 (d, J = 8.4 Hz, 2H), 7.59 (d,

J = 8.4 Hz, 2H), 6.42 (d, *J* = 4.8 Hz, 2H), 5.77 (d, *J* = 4.8 Hz, 2H), 3.58 (t, *J* =

5.6 Hz, 4H), 3.44 (t, *J* =5.6 Hz, 4H), 3.39 (s, 6H). ^{13}C NMR (100 MHz, CDCl3):

δ 157.1, 148.2, 142.1, 131.4, 128.7, 128.1, 127.9, 123.5, 102.3, 71.3, 59.3, 44.5.

IR (cm^{-1}): 3410, 3316, 3106, 2919, 1590, 1546, 1475, 1427, 1344, 1098, 1013,

971, 848, 788, 764, 735, 707, 674. HRMS (ESI) calcd for $C_{21}H_{24}BF_2N_5O_4Na$

[M+Na]$^+$ 482.1787; found 482.1789.
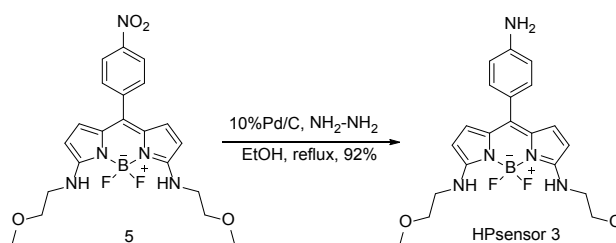
HPsensor 3 was prepared according to a reported procedure (*J. Org. Chem.*,

2008, *73* (5), 1963–1970). ^{1}H NMR (400 MHz, CDCl$_3$): δ 7.20 (d, *J* = 8.4 Hz,

2H), 6.65 (d, *J* = 8.4 Hz, 2H), 6.58 (d, *J* = 4.4 Hz, 2H), 5.70 (d, *J* = 4.4 Hz, 2H),

3.56 (t, *J* = 5.6 Hz, 4H), 3.42-3.35 (m, 10H). ^{13}C NMR (100 MHz, CDCl$_3$): δ

156.5, 147.4, 132.3, 131.8, 129.1, 128.6, 125.1, 114.6, 100.9, 71.4, 59.2, 44.4.

IR (cm^{-1}): 3413,3229, 3129, 2924, 1729, 1589, 1539, 1422, 1337, 1263, 1156,

1093, 1052, 1010, 965, 884, 835, 781, 764, 728, 679. HRMS (ESI) calcd for

$C_{21}H_{26}BF_2N_5O_2Na$ [M+Na]$^+$ 430.2226; found 430.2227.
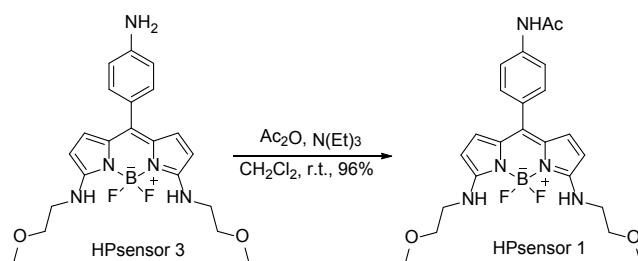
HPsensor 1: The solution of HPsensor 3 (20 mg, 0.047 mmol), acetic anhydride (0.2 mL), triethylamine (0.5 mL) and 4-DMAP(cat.) in CH_2Cl_2 (10 mL) was stirred under ice bath for 2 h, diluted by EtOAc, washed by H_2O, aqueous NH_4Cl, saturated aqueous $NaHCO_3$ and brine respectively, and dried (anhydrous Na_2SO_4), concentrated by rotated evaporation and purified by column chromatography using hexanes/CH_2Cl_2/EtOAc (3:2:1, v/v) to yield HPsensor 1 as oil (21 mg, 96%). ^1H NMR (400 MHz, $CDCl_3$): δ 7.64 (br, 1H), 7.50 (d, J = 8.4 hz, 2H), 7.32 (d, J = 8.4 Hz, 2H), 6.48 (d, J = 4.4 Hz, 2H), 5.70 (d-br, J =4.8 Hz, 4H), 3.56 (t, J = 5.2 Hz, 4H), 3.37-3.30 (m, 10H), 2.16 (s, 3H). ^{13}C NMR (100 MHz, $CDCl_3$): δ 168.9, 156.7, 138.7, 131.2, 131.0, 129.0, 128.6, 119.4, 101.4, 71.3, 59.2, 44.4, 29.5, 24.7. IR (cm^{-1}): 3421, 3308, 3180, 3111, 2925, 2893, 1731, 1665, 1594, 1545, 1474, 1425, 1339, 1260, 1086, 1055, 1009, 894, 846, 781, 762, 696. HRMS (ESI) calcd for $C_{23}H_{28}BF_2N_5O_3Na$ [M+Na]$^+$ 494.2151; found 494.2148.

Quantum yields of dyes in various solvents:

Quantum yield measurements were conducted in accordance with previously published protocol from Zhu et al 2012.[2] Quantum yields of dyes were

calculated from absorption and emission measurements of dyes in dichloromethane, ethanol and water corrected for quantum yield of the dye standard at test wavelengths. Quantum yields of dyes were calculated using the following equation where st = standard; x = test dye; Grad – gradient of fitted slope; Q = quantum yield and η = refractive index of test solvent.

$$Q_x = Q_{st}\left(\frac{Grad_x}{Grad_{st}}\right)\left(\frac{\eta_x^2}{\eta_{st}^2}\right) \qquad \text{(equation 1)}$$
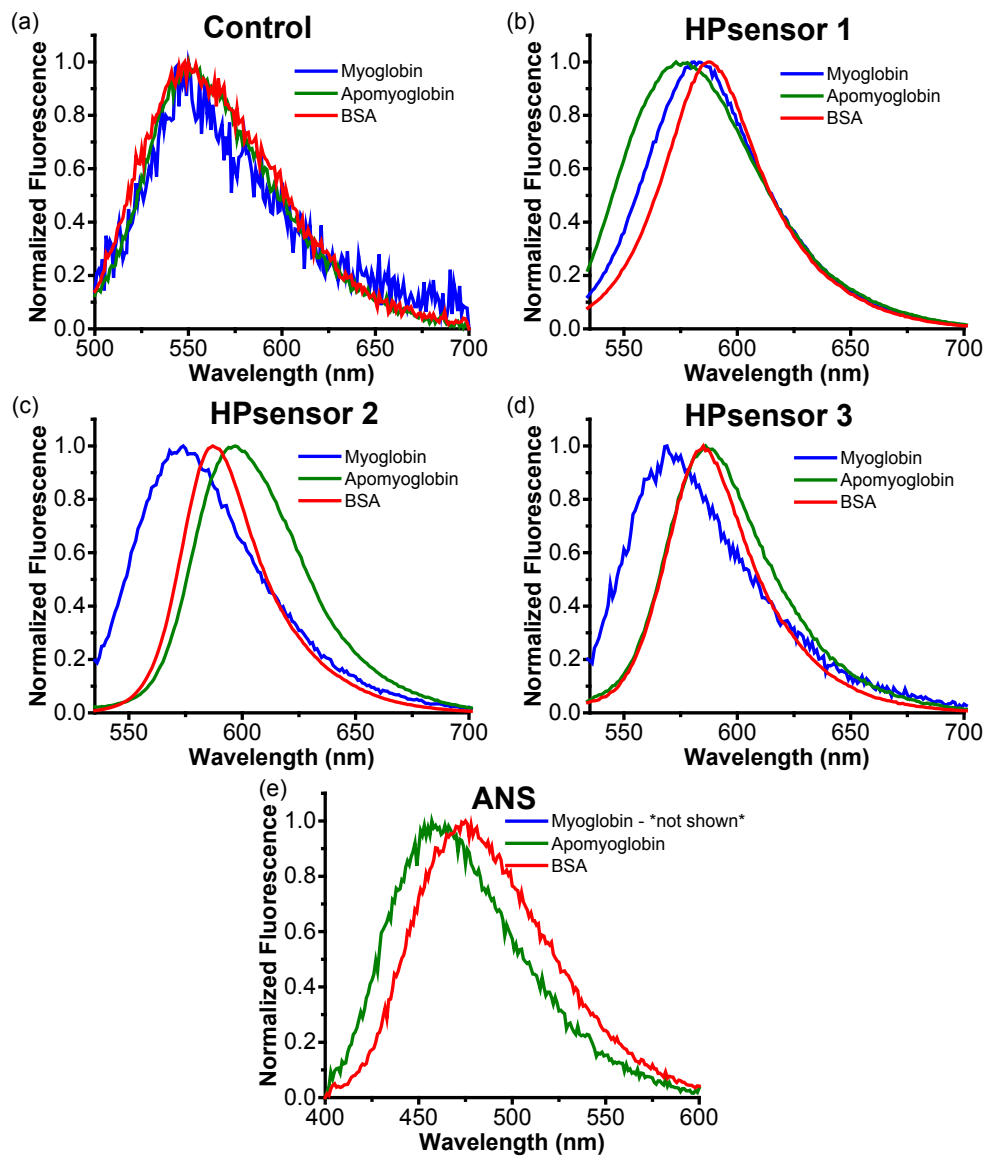
Figure A1. Normalized emission spectra for control and HPsensors incubated with myoglobin (blue), apomyoglobin (green), and BSA (red). (a) Control dye, (b) HPsensor 1 dye, (c) HPsensor 2, (d) HPsensor 3 and (e) ANS were all incubated with protein at 1:1 ratio (2 µM) for 1 hour at 25 °C with appropriate controls before emission spectra were acquired. For ANS with Mb, no significant fluorescence signal was measured, and as a result, the normalized plot was not included.
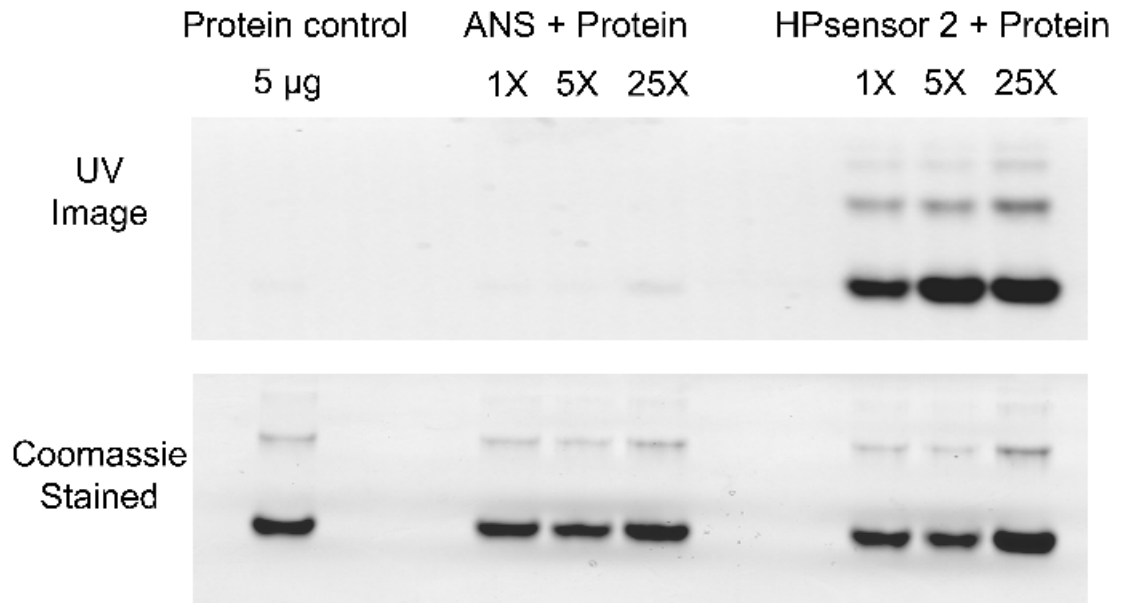
Figure A2. Native PAGE of BSA (5 µg) with ANS and HPsensor **2**. 5 µg of BSA was incubated with dyes (ANS or HPsensor **2**) at 1X, 5X, and 25X concentration for 1 h at room temperature. BSA was then run on 10% Tris-HCl gel for 3 h at 80 V before exposure to UV light or Coomassie blue. Full length gel is included in supplementary figure 33. Brightness and contrast settings were adjusted for aesthetic purposes.

(a)

+ 5 KT/e   -5 KT/e

(b)

■ (yellow) Hydrophobic patches

■ (blue) Molecular surface of protein
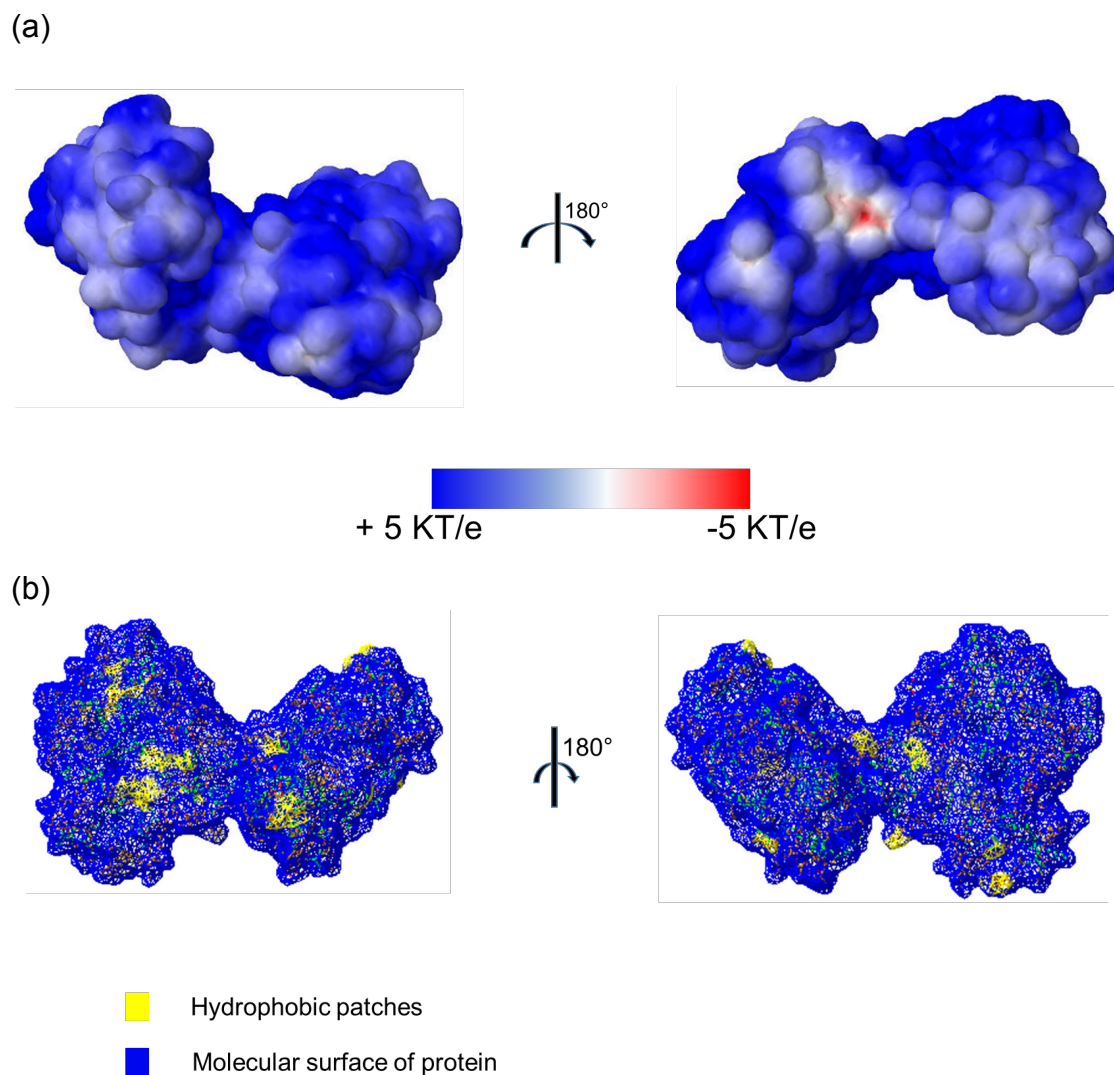
Figure A3. **Electrostatic and Hydrophobic patch maps of Myoglobin (Mb: PDB ID 3RJ6).** Maps show (a) the electrostatic surface potentials of Mb visualized as isocontours at +5.0 kT/e (blue) and -5.0 kT/e (red) using APBS and (b) predicted hydrophobic patches (yellow) visualized against the molecular surface (blue) using SPDB software.

(a)

+ 5 KT/e   -5 KT/e

■ Hydrophobic patches

■ Molecular surface of protein

(b)
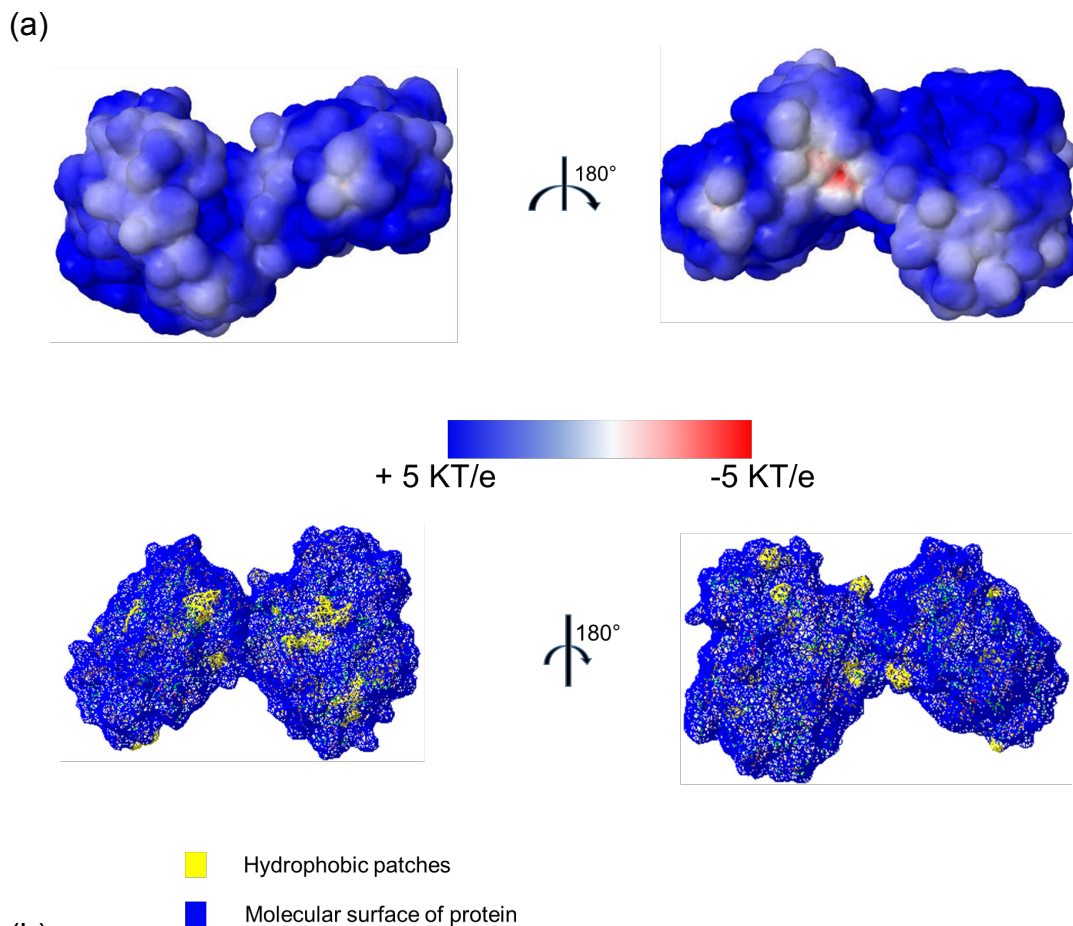
Figure A4. **Electrostatic and Hydrophobic patch maps of Apomyoglobin (ApoMb: modified from PDB ID 3RJ6).** Maps show (a) the electrostatic surface potentials of ApoMb visualized as isocontours at +5.0 kT/e (blue) and -5.0 kT/e (red) using APBS and (b) predicted hydrophobic patches (yellow) visualized against the molecular surface (blue) using SPDB software.

(a)

(b)
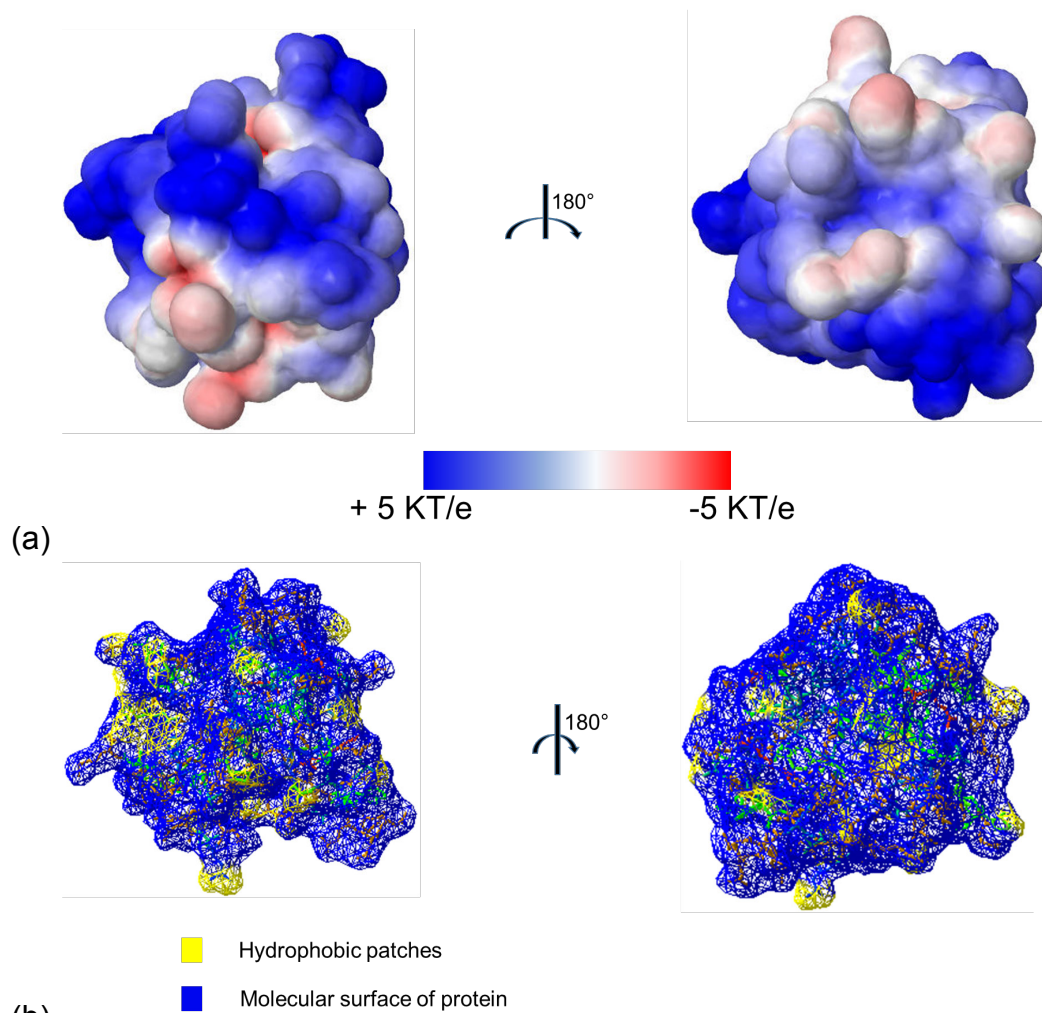
Figure A5. **Electrostatic and Hydrophobic patch maps of beta lactoglobulin (β-lg: PDB ID 2Q2M).** Maps show (a) the electrostatic surface potentials of β-lg visualized as isocontours at +5.0 kT/e (blue) and -5.0 kT/e (red) using APBS and (b) predicted hydrophobic patches (yellow) visualized against the molecular surface (blue) using SPDB software.

(a)

◻ Hydrophobic patches

◻ Molecular surface of protein

(b)
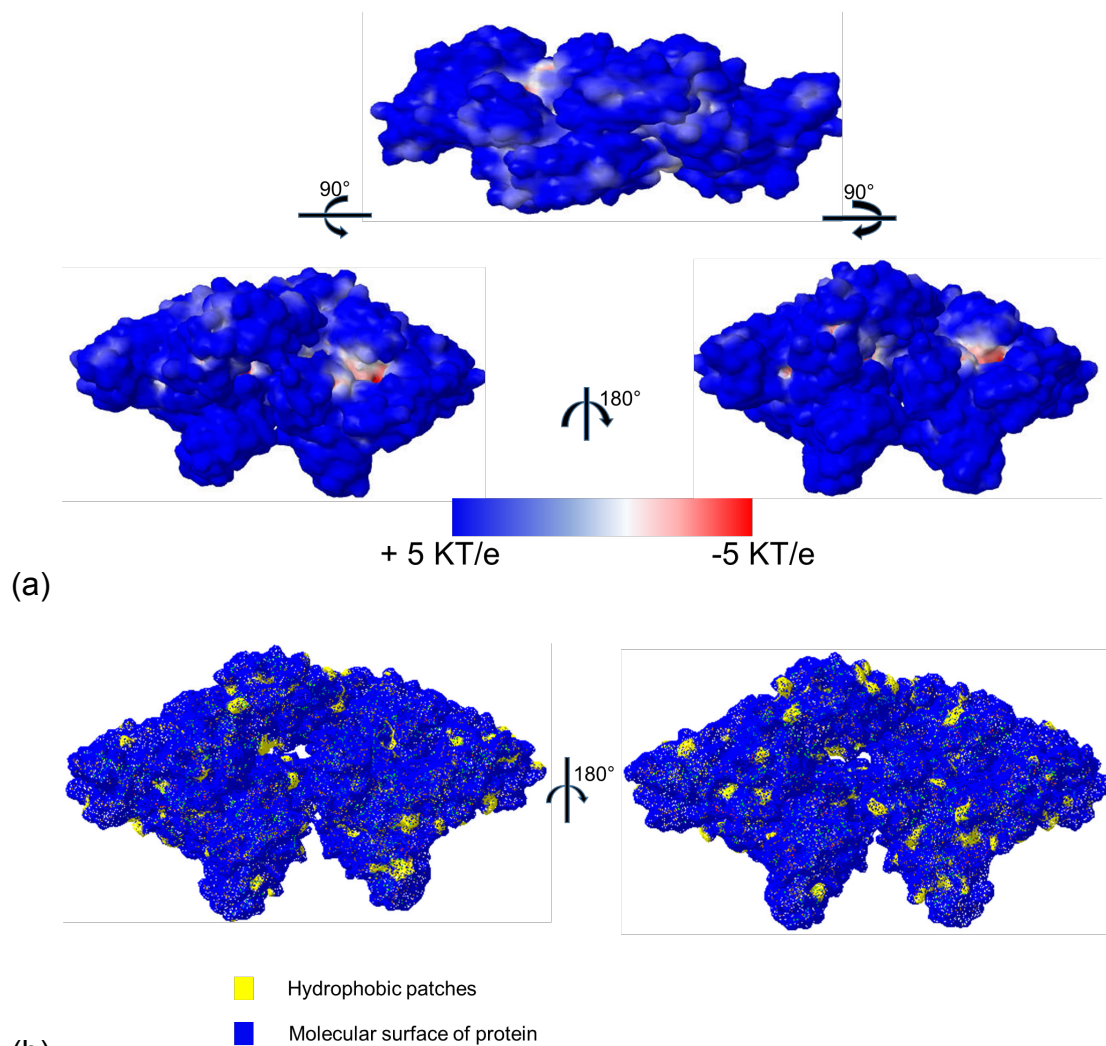
Figure A6. **Electrostatic and Hydrophobic patch maps of bovine serum albumin (BSA: PDB ID 3V03).** Maps show (a) the electrostatic surface potentials of BSA visualized as isocontours at +5.0 kT/e (blue) and -5.0 kT/e (red) using APBS and (b) predicted hydrophobic patches (yellow) visualized against the molecular surface (blue) using SPDB software.
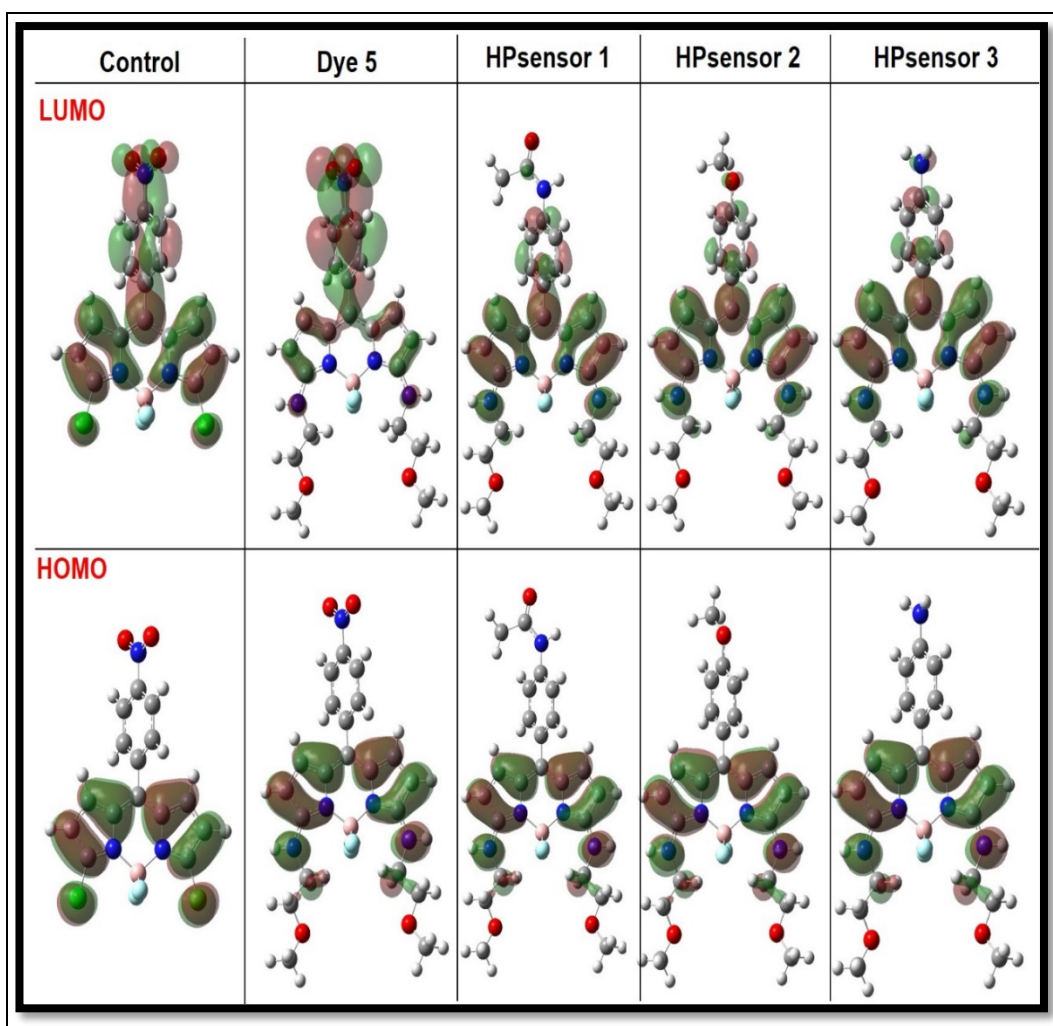
Figure A7. Calculated frontier molecular orbitals for dyes in ethanol. (Top panel) LUMO energy distribution for control, dye 5, and HPsensors 1, 2, and 3. (Bottom panel) HOMO energy distribution for control, dye 5 and HPsensors 1, 2, and 3.
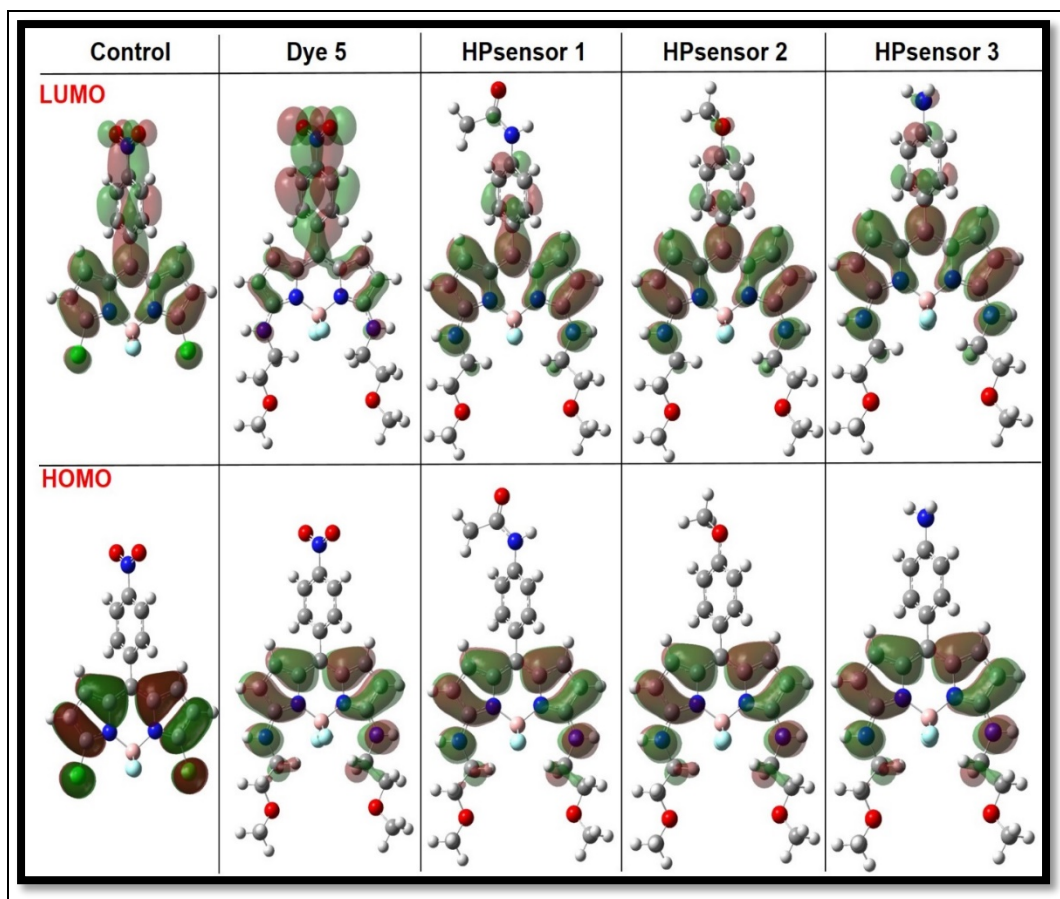
Figure A8. Calculated frontier molecular orbitals for dyes in water. (Top panel) LUMO energy distribution for control, dye 5, and HPsensors 1, 2, and 3. (Bottom panel) HOMO energy distribution for control, dye 5 and HPsensors 1, 2, and 3.

Table 1. HOMO-LUMO energy gap calculation and associated wavelength of dyes (control, dye **5**, HPsensors **1**, **2**, and **3**) in vacuum, ethanol and water with range separated functional (HSEH1PBE) and 6-311g** basis set.

Vacuum					
Molecule	energy	H0 (a.u.)	L0 (a.u.)	Gap (eV)	Wavelength (nm)
Control	-2035.022	-0.23003	-0.14207	2.393532336	518.76
Dye **5**	-1612.674	-0.16895	-0.1044	1.75650878	706.06
HPsensor **1**	-1616.161	-0.16294	-0.08283	2.179921276	569
HPsensor **2**	-1522.741	-0.1572	-0.07547	2.224004068	557.48
HPsensor **3**	-1463.623	-0.15493	-0.07279	2.235160824	554.74
Ethanol					
Molecule	energy	H0 (a.u.)	L0 (a.u.)	Gap (eV)	Wavelength (nm)
Control	-2035.038	-0.22556	-0.1357	2.445234376	507.09
Dye **5**	-1612.696	-0.17143	-0.1112	1.638954668	756.92
HPsensor **1**	-1616.187	-0.16947	-0.08897	2.1905338	566.14
HPsensor **2**	-1522.762	-0.16877	-0.08705	2.223731952	557.56
HPsensor **3**	-1463.646	-0.16801	-0.08563	2.241691608	553.25
Water					
Molecule	energy	H0 (a.u.)	L0 (a.u.)	Gap (eV)	Wavelength (nm)
Control	-2035.039	-0.22707	-0.13734	2.441696868	508.13
Dye **5**	-1612.698	-0.17184	-0.11255	1.613375764	770.9
HPsensor **1**	-1616.189	-0.17022	-0.09014	2.179104928	569
HPsensor **2**	-1522.764	-0.16979	-0.08846	2.213119428	560.25
HPsensor **3**	-1463.648	-0.16932	-0.08731	2.231623316	555.98

Table 2. HOMO-LUMO energy gap calculation and associated wavelength of dyes (control, dye **5**, HPsensors **1**, **2**, and **3**) in ethanol and with range separated functional (HSEH1PBE) and 6-311g** basis and internal rotation of up to 58°.

Degree	energy	H0 (a.u.)	L0 (a.u.)	Gap (eV)	Wavelength (nm)
Rotation of HPsensor 2 in ethanol					
5	-1522.686	-0.1709	-0.09822	1.977739088	626.91
15	-1522.716	-0.17039	-0.09635	2.014746864	615.61
25	-1522.741	-0.1697	-0.09334	2.077877776	596.71
35	-1522.755	-0.16915	-0.09043	2.142097152	578.82
45	-1522.761	-0.16885	-0.08835	2.1905338	566.14
58	-1522.762	-0.16877	-0.08705	2.223731952	557.56
Rotation of HPsensor 3 in ethanol					
5	-1463.574	-0.16971	-0.09547	2.020189184	613.78
15	-1463.603	-0.16926	-0.09365	2.057469076	602.74
25	-1463.627	-0.16864	-0.0908	2.118150944	585.38
35	-1463.64	-0.16819	-0.08816	2.177744348	569.34
45	-1463.645	-0.16799	-0.08643	2.219378096	558.74
56	-1463.646	-0.16801	-0.08563	2.241691608	553.25
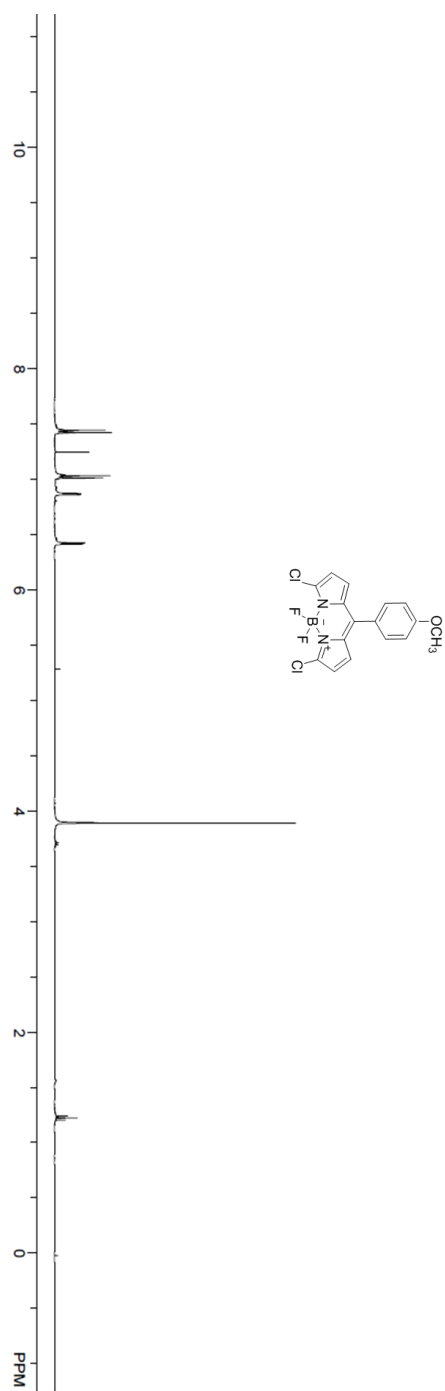
Figure A9. ^{1}H NMR spectrum of control dye in CDCl$_3$ solution.
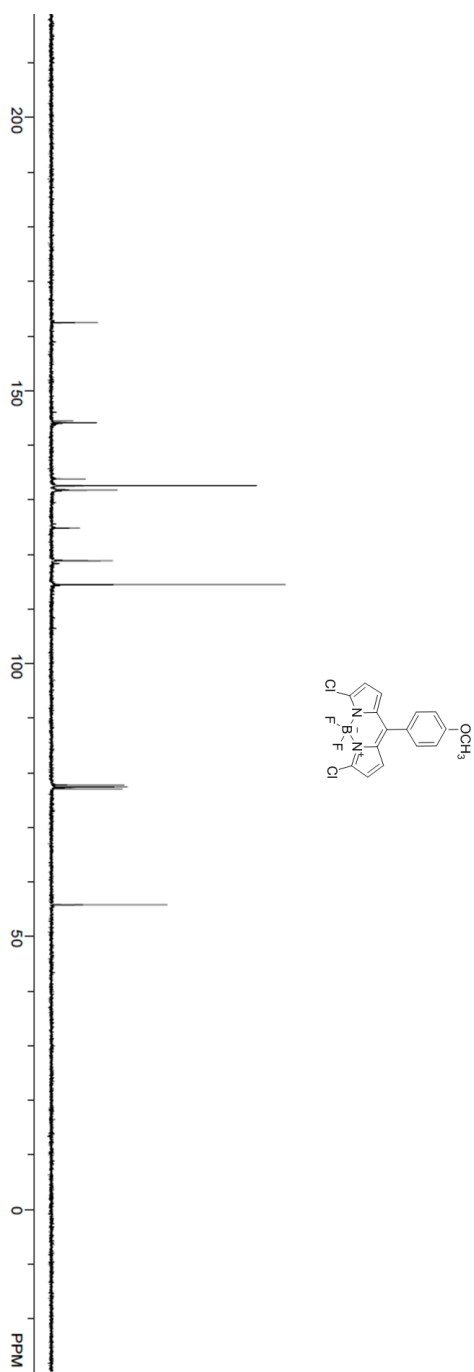
Figure A10 ^{13}C NMR spectrum of control dye in CDCl$_3$ solution.
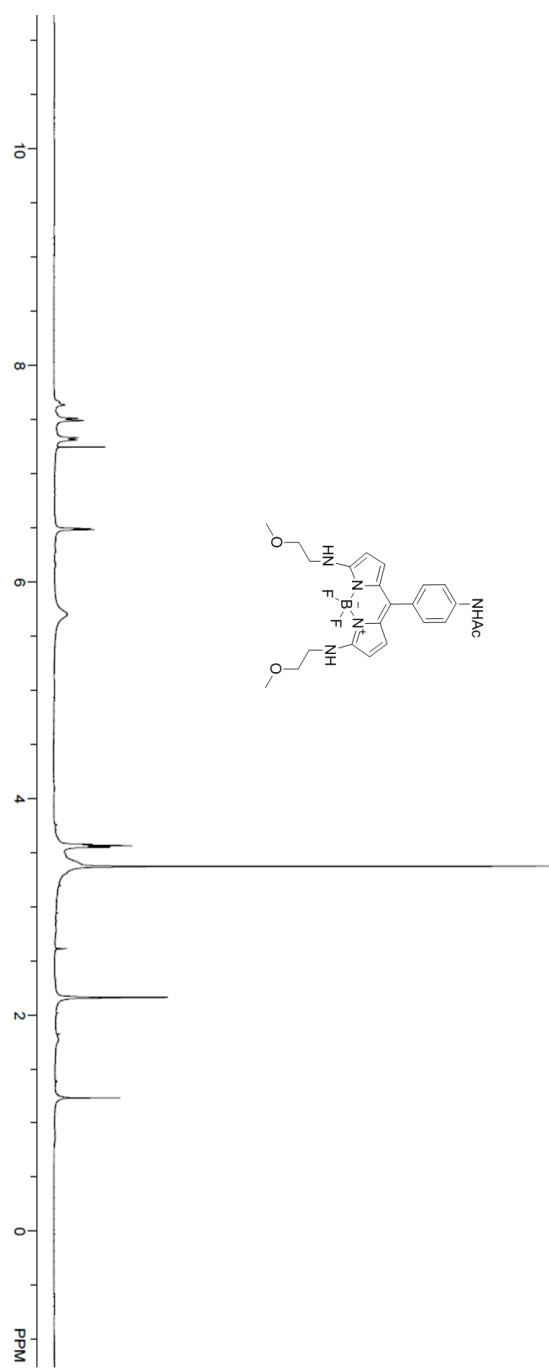
Figure A11. ^{1}H NMR spectrum of HPsensor **1** in CDCl$_3$ solution.
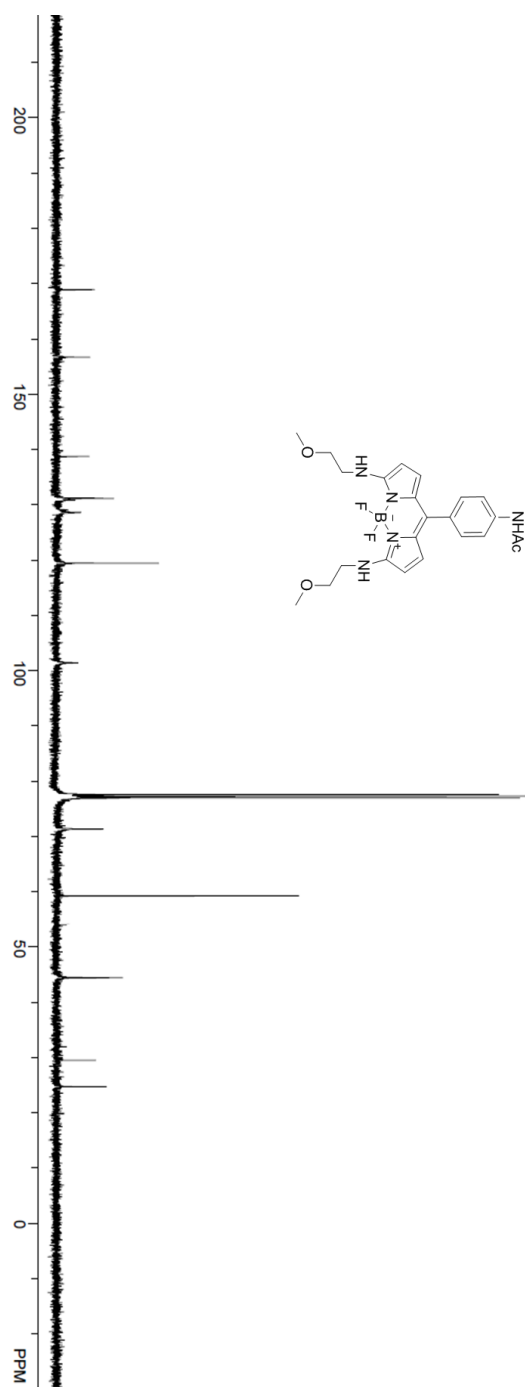
Figure A12. ^{13}C NMR spectrum of HPsensor **1** in CDCl$_3$ solution.
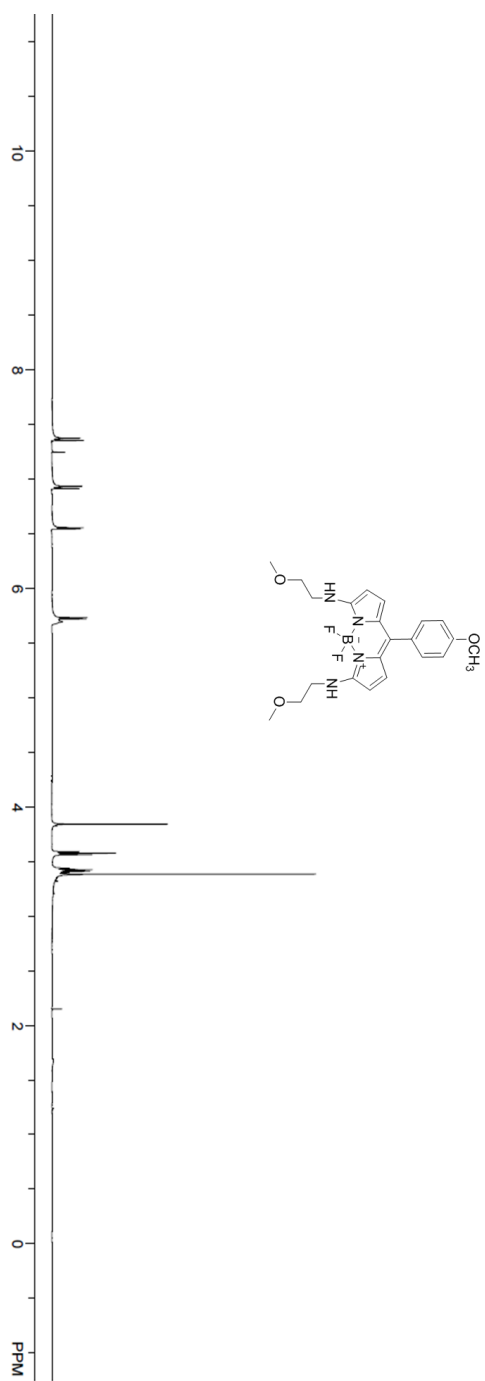
Figure A13. ^{1}H NMR spectrum of HPsensor **2** in CDCl$_3$ solution.
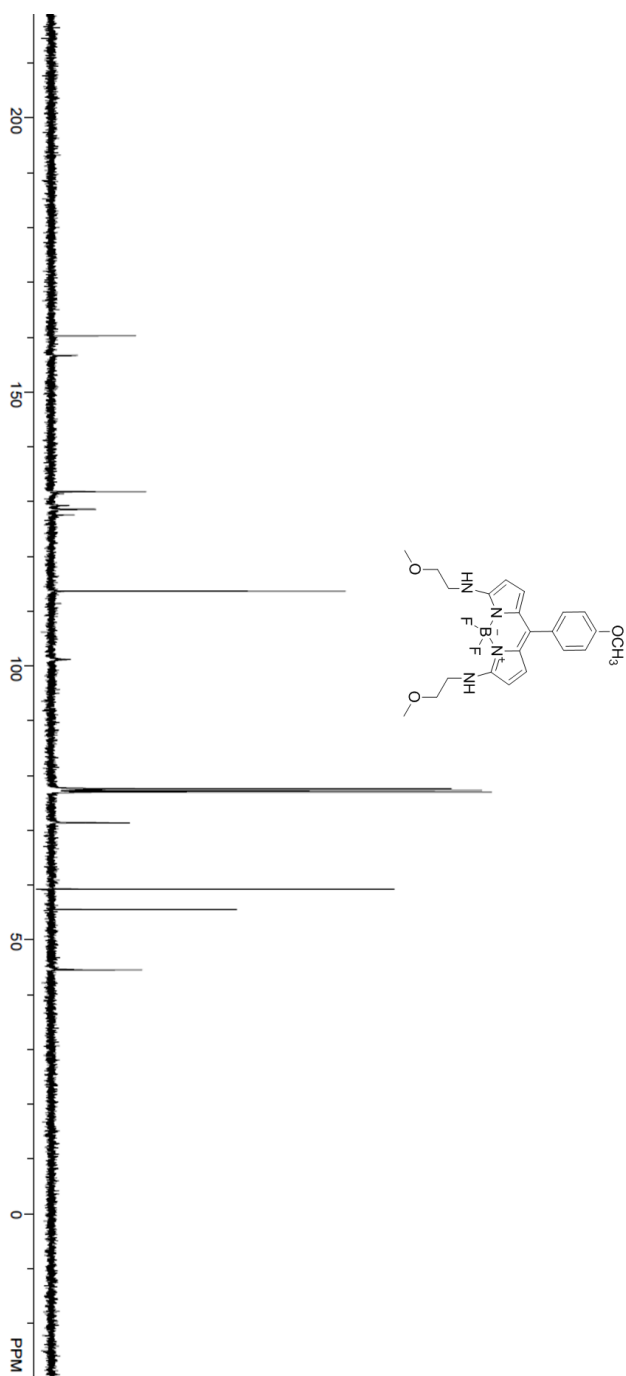
Figure A14. ^{13}C NMR spectrum of HPsensor **2** in CDCl$_3$ solution.
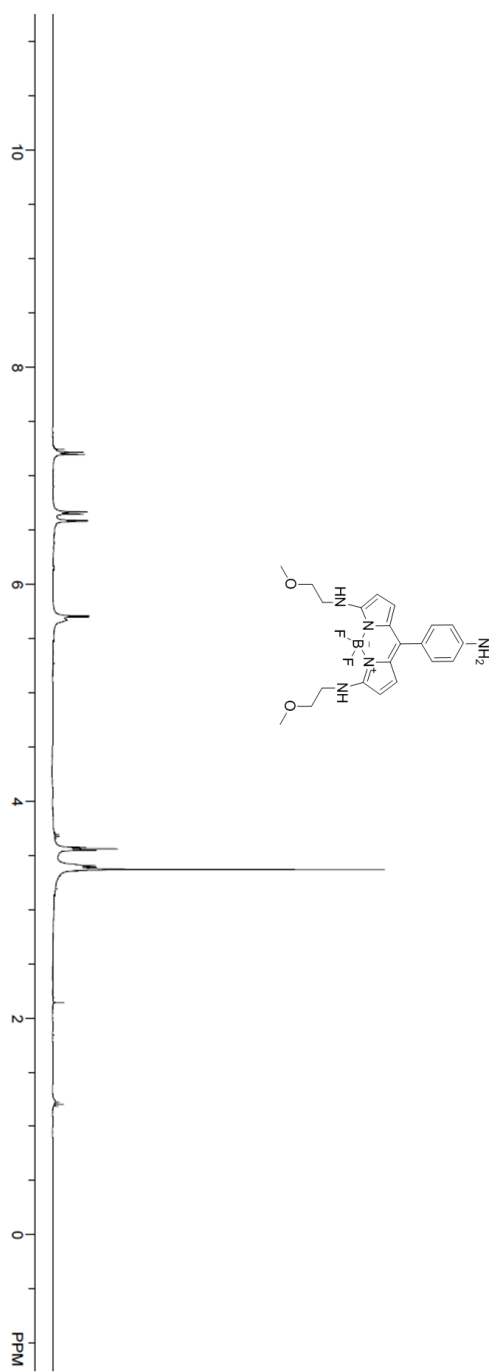
Figure A15. ^{1}H NMR spectrum of HPsensor **3** in CDCl$_3$ solution.
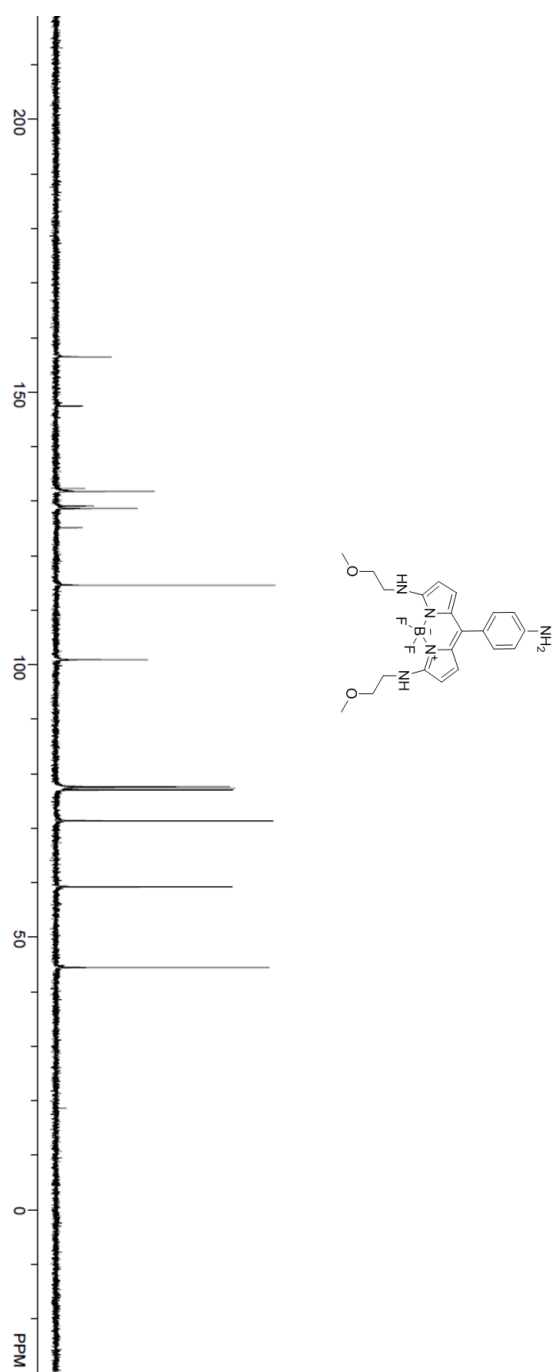
Figure A16. ^{13}C NMR spectrum of HPsensor **3** in CDCl$_3$ solution.
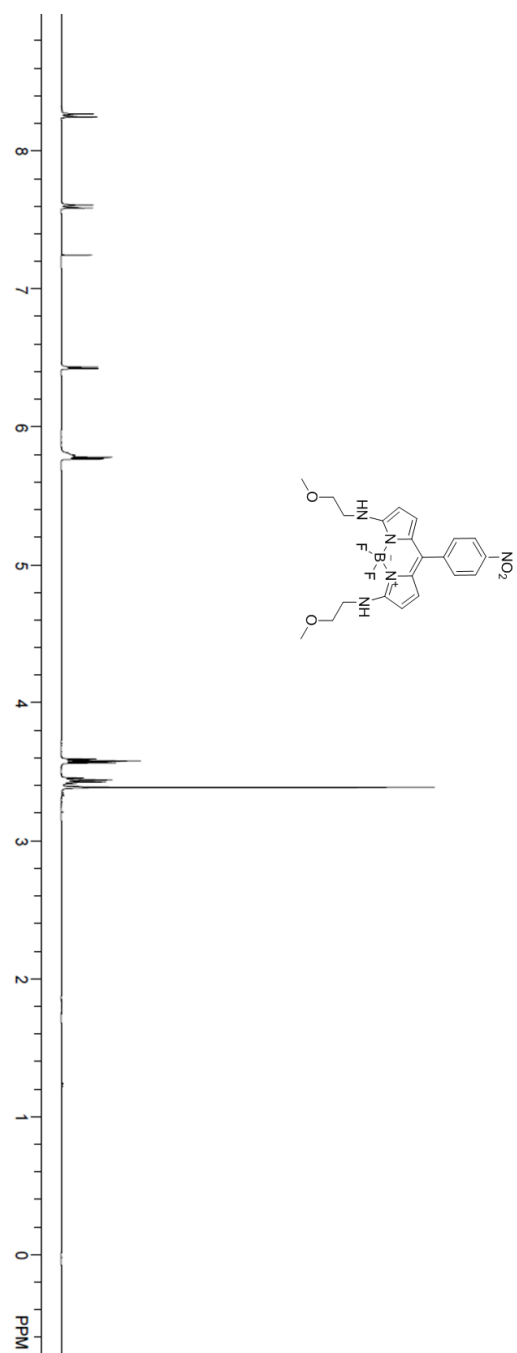
Figure A17. ^{1}H NMR spectrum of dye **5** in CDCl$_3$ solution.
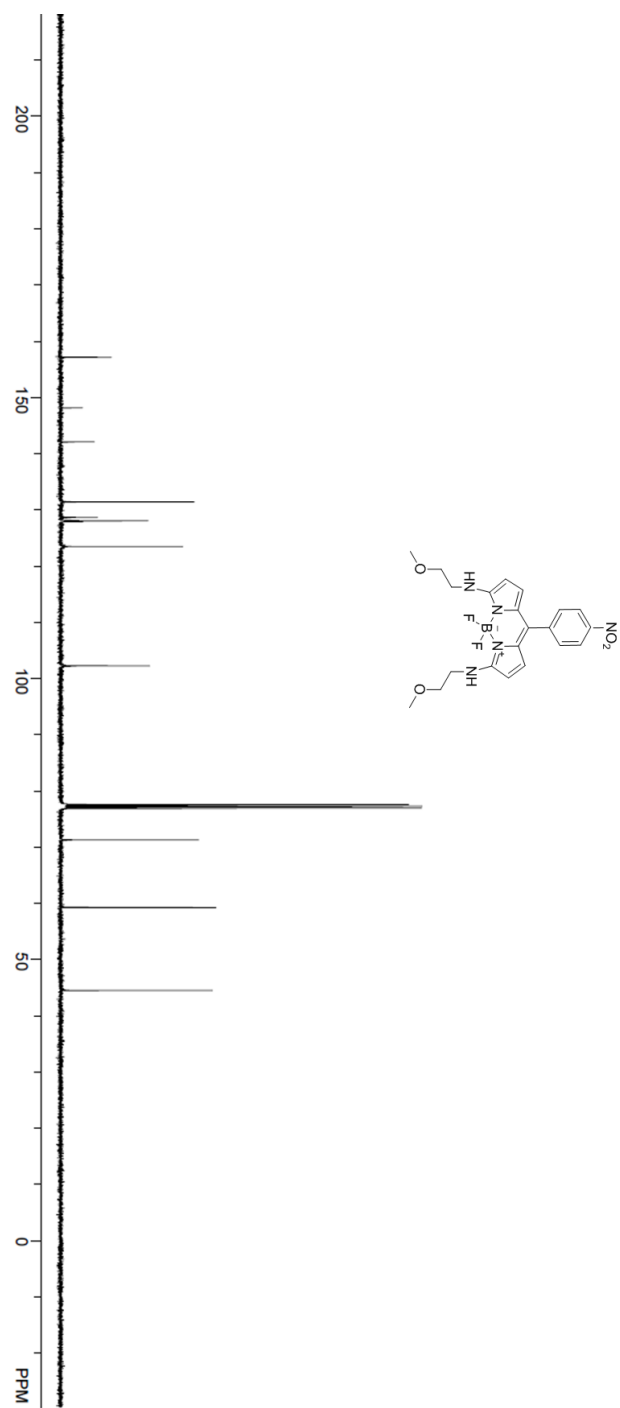
Figure A18. ^{13}C NMR spectrum of dye **5** in CDCl$_3$ solution.
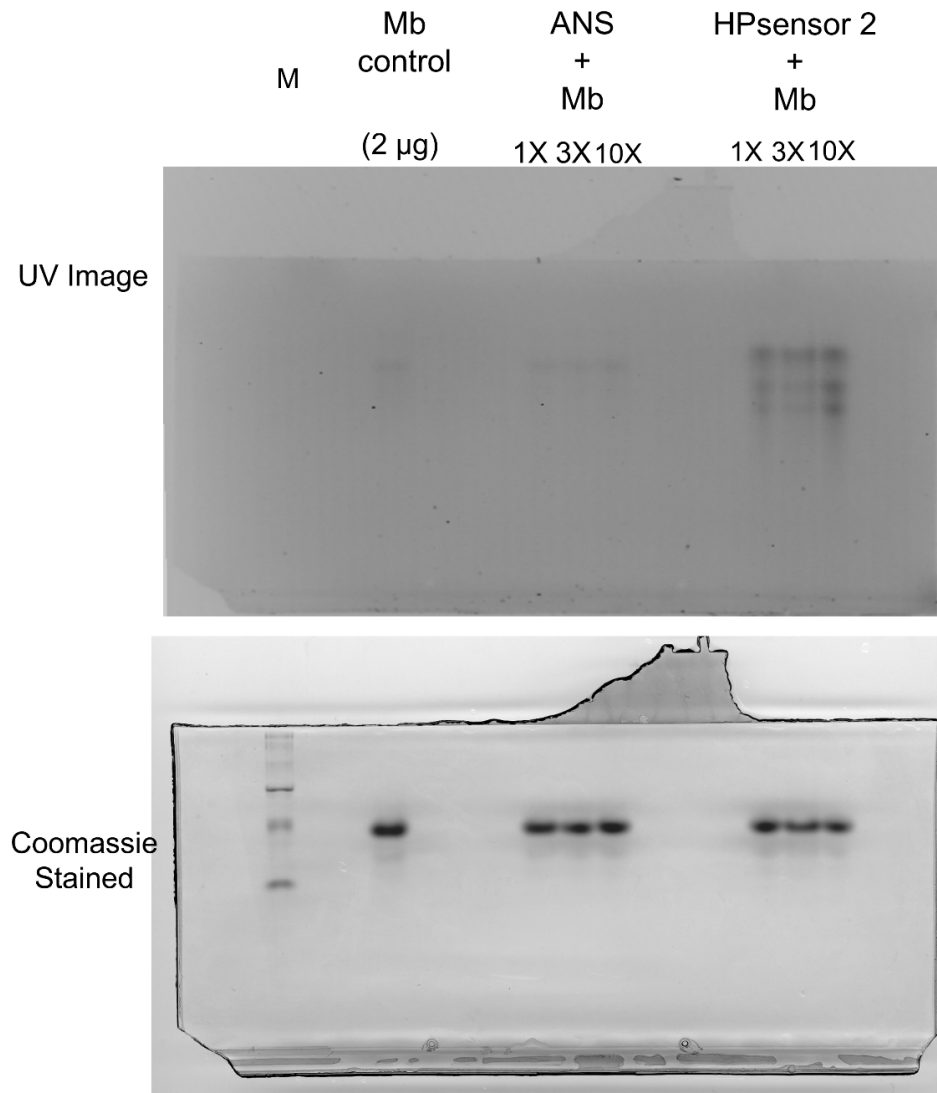
Figure A19. Full length gel of Native PAGE of 2 μg Mb with 1X, 3X, and 10X Dye (ANS or HPsensor 2). Full gel image of 2 μg of Mb incubated with 1X, 3X, and 10X concentration of dyes (ANS or HPsensor 2) for 1 h at 25 °C. The Mb and protein was run on a 15% gel for 6 h at 80 V. M – indicates molecular weight marker.
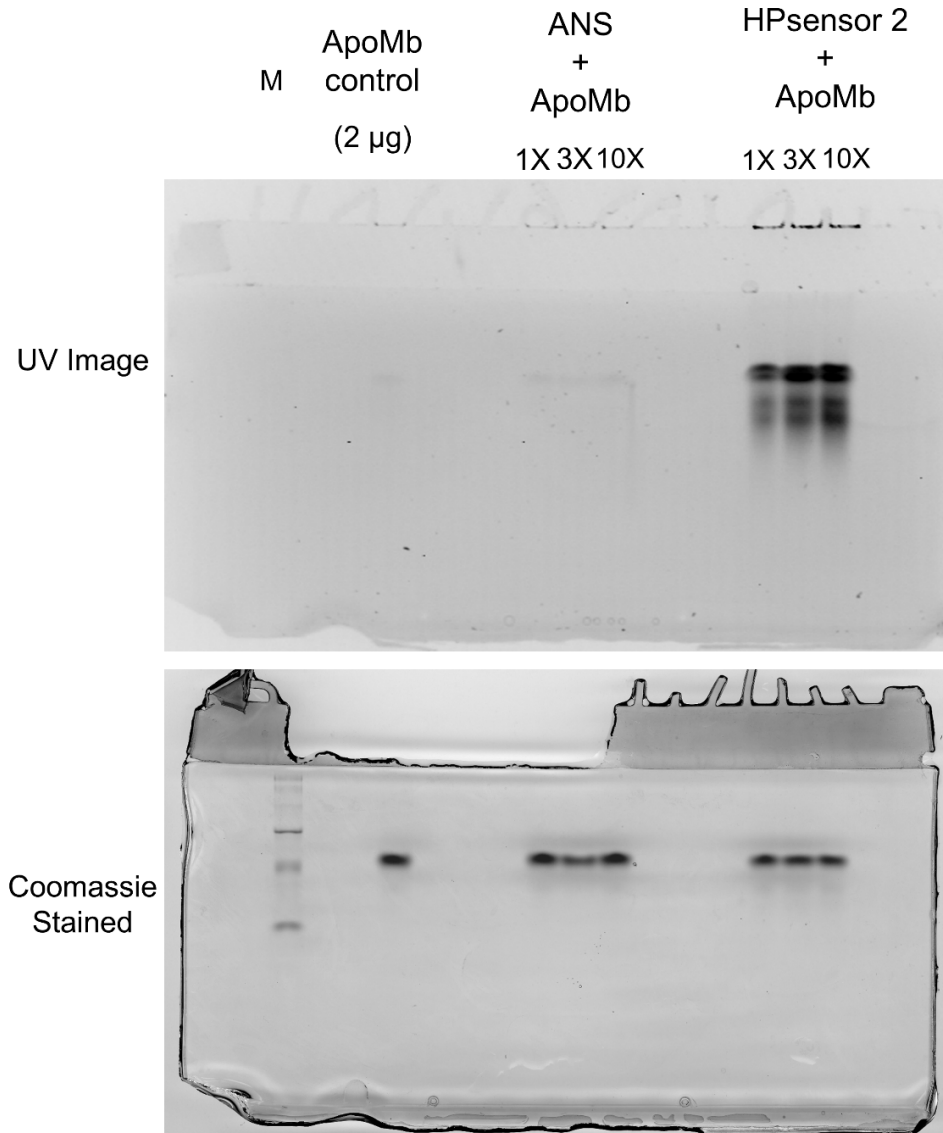
Figure A20. Full length gel of Native PAGE of 2 μg ApoMb with 1X, 3X, and 10X Dye (ANS or HPsensor 2). Full gel image of 2 μg of ApoMb incubated with 1X, 3X, and 10X concentration of dyes (ANS or HPsensor 2) for 1 h at 25 °C. The ApoMb protein was run on a 15% gel for 6 h at 80 V. M – indicates molecular weight marker.
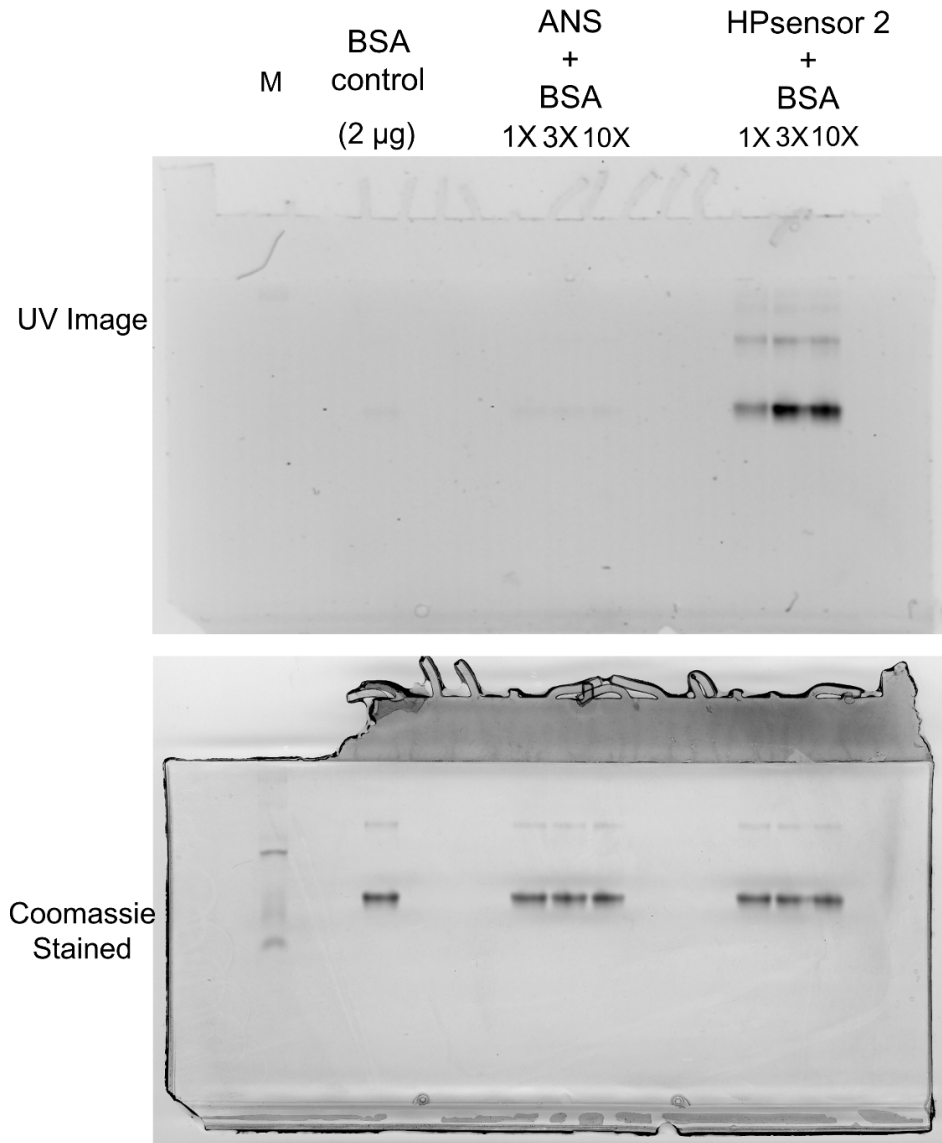
Figure A21. Full length gel of Native PAGE of 2 µg BSA with 1X, 3X, and 10X Dye (ANS or HPsensor 2). Full gel image of 2 µg of ApoMb incubated with 1X, 3X, and 10X concentration of dyes (ANS or HPsensor 2) for 1 h at 25 °C. The BSA protein was run on a 10% gel for 3 h at 80 V. M – indicates molecular weight marker.
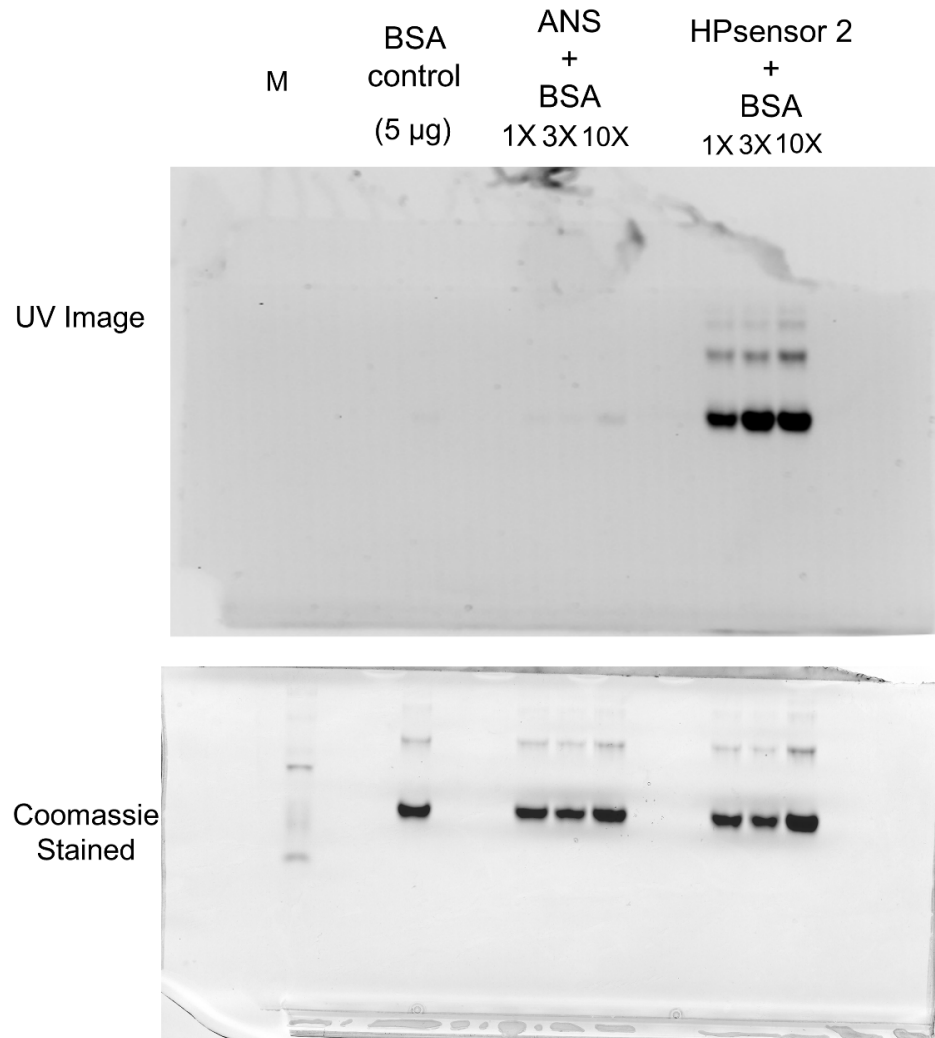
Figure A22. **Full length gel of Native PAGE of BSA (5 µg) with ANS and HPsensor 2.** Full length gel of 5 µg of BSA incubated with dyes (ANS or HPsensor **2**) at 1X, 5X, and 25X concentration for 1 h at room temperature. BSA was then run on 10% Tris-HCl gel for 3 h at 80 V before exposure to UV light or Coomassie blue. M – indicates molecular weight marker.
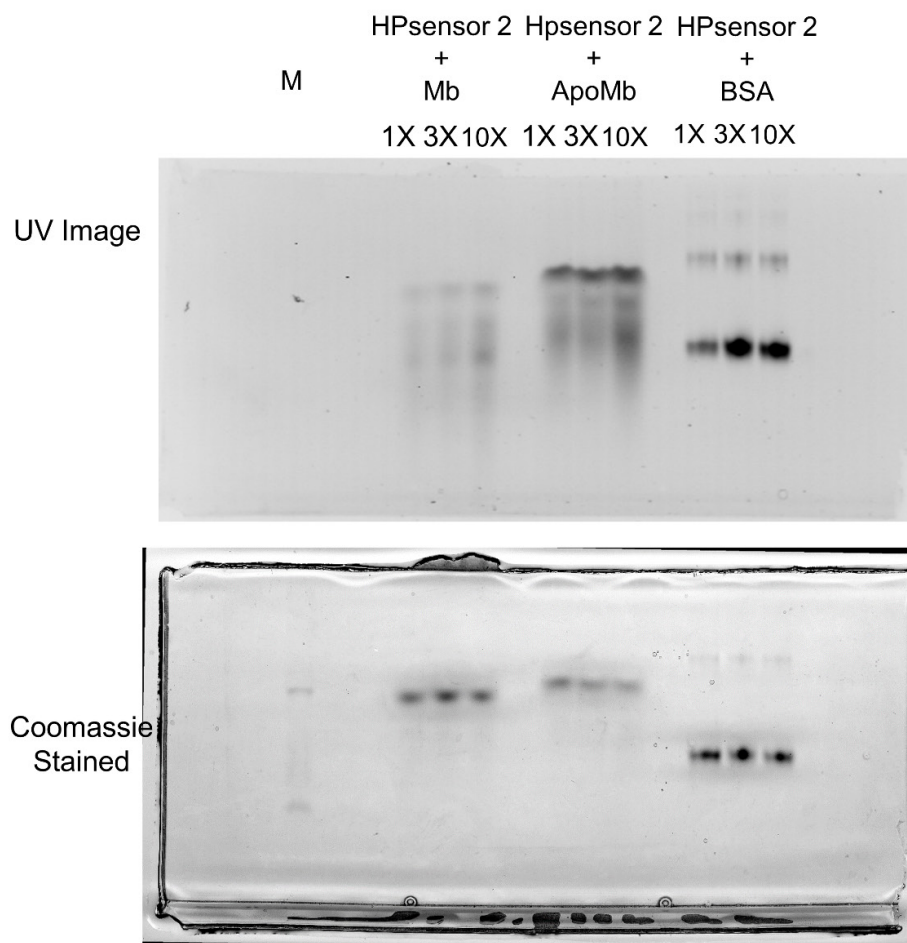
Figure A23. **Full length gel of Native PAGE of 2 μg of Proteins [Myoglobin (Mb), Apomyoglobin (ApoMb), BSA] with HPsensor 2.** Full length gel of 2 μg of each protein incubated with HPsensor **2** at 1X, 3X, and 10X concentration for 1 h at room temperature. Proteins were then run on 10% Tris-HCl gel for 4 h at 80 V before exposure to UV light or Coomassie blue. M – indicates molecular weight marker.

References for Appendix A

1   Fink, A. L., Oberg, K. A. & Seshadri, S. Discrete intermediates versus

molten globule models for protein folding: characterization of partially

folded intermediates of apomyoglobin. *Fold. Des.* **3**, 19-25,

doi:10.1016/s1359-0278(98)00005-4 (1998).

2   Zhu, S. *et al.* Highly water-soluble neutral near-infrared emissive

BODIPY polymeric dyes. *J. Mater. Chem.* **22**, 2781-2790, doi:Doi

10.1039/C2jm14920f (2012).

Appendix B: Supporting information for Chapter 5

Functionalized ANS probe for mapping protein surface hydrophobicity.

Nethaniah Dorh[a], Shilei Zhu[a†], Jagadeesh Janjanam[aφ], Haiying Liu[a], Ashutosh Tiwari[a*]

[a]Department of Chemistry, Michigan Technological University, 1400 Townsend Drive, Houghton, MI 49931, US

[†]Department of Chemistry & Biochemistry, University of Maryland, College Park, MD 20742, USA

[φ]Department of Physiology, University of Tennessee, Health Science Center, Memphis, TN 38163, USA

Synthesis of modified-ANS probe

Compound 1. ANS was purchased from Sigma Aldrich and used without further purification.

1   **2**
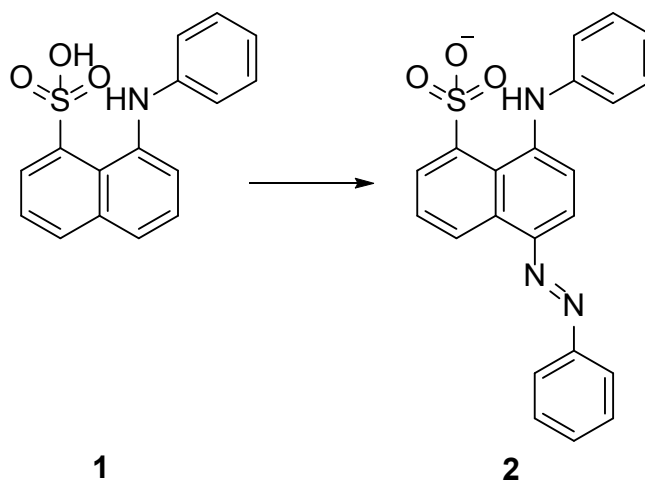
Compound 2. To a suspension of the aromatic amine (2.18 mL, 24.0 mmol) in water (20 mL) was added concentrated hydrochloric acid (6 mL) until the mixture was homogeneous. The solution was cooled and kept at 0-5 °C in an ice bath and diazotized by addition of a solution of sodium nitrite (1.68 g, 24.4 mmol) in cooled water (10 mL), followed by stirring for 30 min at 0 - 5 °C. To a solution of compound 1 (6.0 g, 20 mmol) and $NaHCO_3$ (25 g) in ethanol (200 mL) and water (50 mL) was slowly added a solution of the diazonium salt at 0 - 5 °C. The resulting mixture was stirred for 5 h and then evaporated under vacuum to dryness. The residues were purified by column chromatography, eluting with a mixture of dichloromethane, acetone and ethanol (6:3:0.3) to obtain compound 2 as red foamy solid (5.8 g, 72%). ^{1}H NMR (400 MHz, acetone-d6): δ 11.02 (br,

1H), 9.22 (d, J = 8.8 Hz, 1H), 8.50 (d, J = 7.6 Hz, 1H), 7.94 (d, J = 8.8 Hz, 3H),

7.56-7.44 (m, 5H), 7.31-7.29 (m, 4H), 6.98 (m, 1H). ^{13}C NMR (100 MHz,

acetone-d6): δ 153.9, 146.1, 143.0, 140.1, 136.3, 129.8, 129.4, 127.5, 126.1,

125.5, 122.6, 122.3, 120.9, 113.7, 111.5. HRMS (ESI) calcd for $C_{22}H_{16}N_3O_3S^-$

[M]$^-$, 402.0918; found, 402.0911.
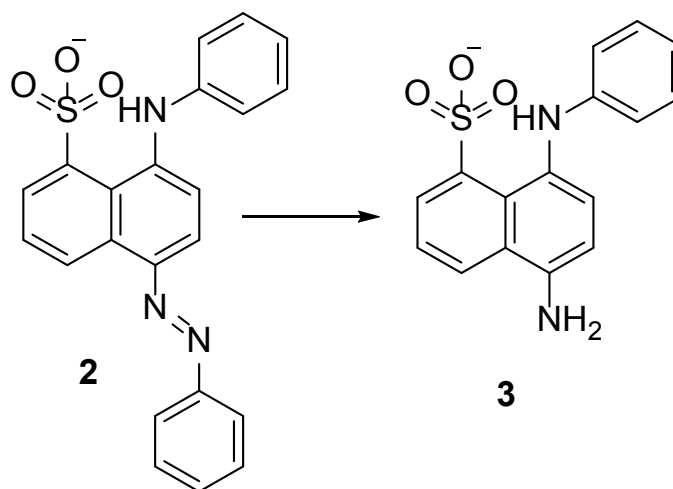
Compound 3. A mixture of compound 2 (403 mg, 1.0 mmol), zinc powder (640

mg) and ammonium chloride (1.06 g) in the ethanol (16 mL) with 3 drops water

was strongly stirred at 60 °C for 2 hrs under a nitrogen atmosphere and for

another 5 hrs at room temperature. After the completion of the reaction

(monitored by TLC), the reaction mixture was filtered through a Celite pad and

washed with ethanol. After the filtrate was dried in a rotary evaporator, the

residue was dissolved in acetone, filtered through a Celite pad again and

washed with acetone. After the filtrate was concentrated in a rotary evaporator,

the mixture was purified by TLC plate suing dichloromethane, acetone and

ethanol (6:3:0.7) to obtain compound 3 as yellow powder solid (52 mg, 17%). ^{1}H

NMR (400 MHz, acetone-d$_6$): δ 8.40 (dd, J = 7.6, 1.6 Hz, 1H), 7.86 (dd, J = 8.4,

1.6 Hz, 1H), 7.50 (d, J = 8.0 Hz, 1H), 7.29 (dd, J = 8.4, 7.6 Hz, 1H), 7.14-7.05

(m, 4H), 6.77 (dd, J = 8.4, 2.4 Hz, 1H), 6.68 (t, J = 7.2 Hz, 1H). ^{13}C NMR (100

MHz, acetone-d$_6$): δ 146.2, 141.7, 140.8, 135.7, 129.5, 129.0, 128.1, 127.3,

124.1, 123.9, 118.5, 115.9. HRMS (ESI) calcd for $C_{16}H_{13}N_2O_3S^-$ [M]-, 313.0652;

found, 313.0639.
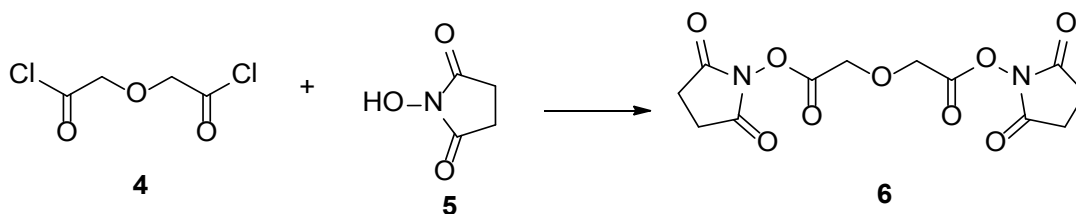
Compound 6. To a solution of compound 5 (2.2 g, 14.6 mmol) and 4-DMAP (2.5

g, 20 mmol) in dichloride methane (30 mL) was added compound 4 (1mL, 7.4

mmol) at 0 °C. After stirring for 5 h, the mixture was transferred into a separatory

funnel and washed by ice water three times. The organic layer was separated

out, dried with anhydrous Na_2SO_4 and filtered. After the filtrate was

concentrated in a rotary evaporator, the crude product 6 was formed as white

solid. The crude product 6 can be used in the next step without further. ^{1}H NMR

(400 MHz, DMSO-d6): δ 4.75 (s, 4H), 2.80 (s, 4H). ^{13}C NMR (100 MHz, DMSO-

d$_6$): δ 170.6, 166.3, 66.4, 26.1.
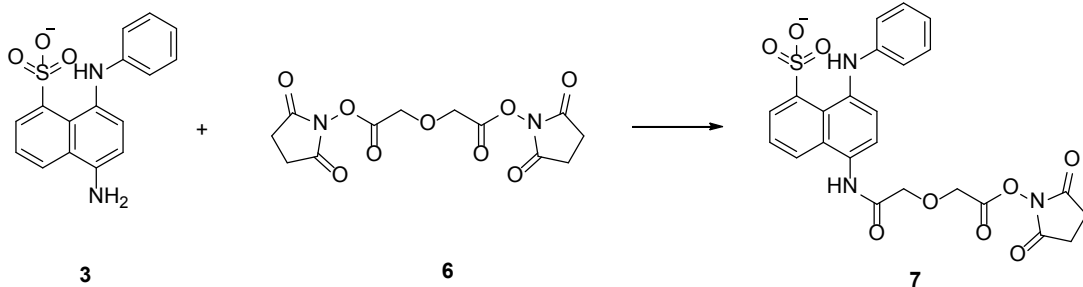
Compound 7. The solution of compound 3 (58 mg, 0.185 mmol), compound 6 (606 mg, 1.85 mmol), triethylamine (5 drops) in dry DMF (20 mL) was stirred at room temperature under nitrogen atmosphere. After stirring for 36 h, the mixture was concentrated in a rotary evaporator and purified by TLC plate using dichloromethane, acetone and ethanol (6:3:0.5) to obtain compound 7 (29 mg, 30%). ^{1}H NMR (400 MHz, acetone-d_6): δ 10.71 (s, 1H), 8.40 (dd, J = 7.6, 1.2 Hz, 1H), 7.72 (dd, J = 8.4, 1.2 Hz, 1H), 7.56 (d, J = 7.6 Hz, 1H), 7.38 (t, J = 8.4 Hz, 1H), 7.28 (d, J = 8.4 Hz, 1H), 7.24-7.23 (m, 4H), 6.87-6.84 (m, 1H), 4.66 (d, J = 16.0 Hz, 4H), 2.97-2.92 (m, 4H). ^{13}C NMR (100 MHz, acetone-d_6): δ 170.2, 144.7, 143.4, 142.0, 133.8, 129.2, 127.6, 127.4, 125.4, 125.3, 123.2, 122.1, 120.4, 118.3, 113.5, 68.1, 46.4. ESI MS (m/z): 411.1 (M-$C_4H_5NO_3$)-.

ANS

ANS modified
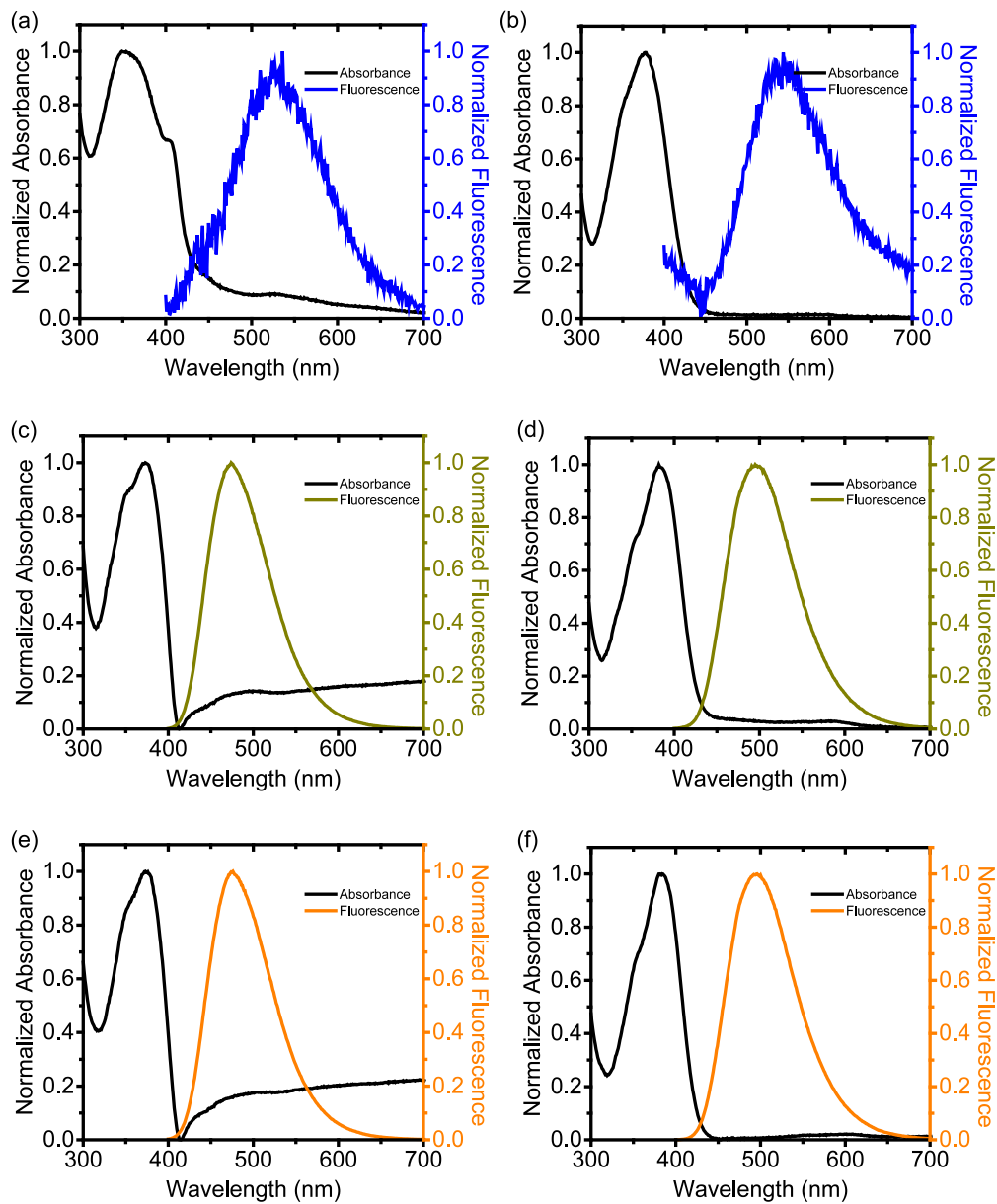
Figure B1. Normalized absorption and emission spectra of ANS and ANS modified dye in 0.1 M NaHCO$_3$ (a – b), ethanol (c-d) and DMSO (e-f).
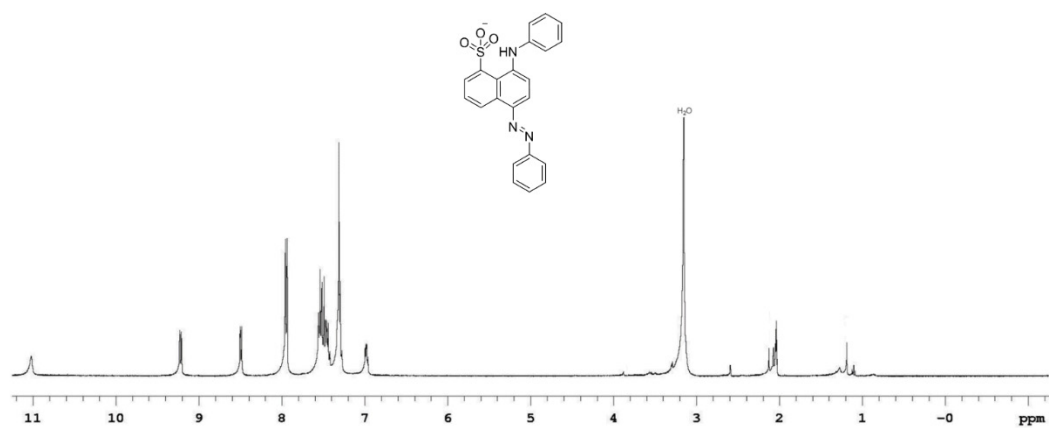
Figure B2 ^{1}H NMR in acetone-d$_6$
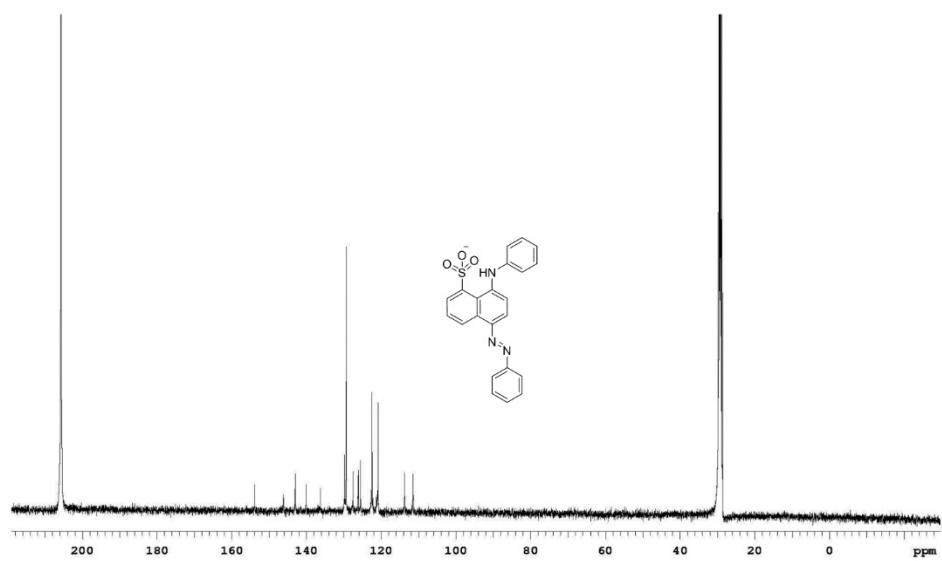
Figure B3. ^{13}C NMR in acetone-d$_6$

Figure B4. ^{1}H NMR in acetone-d$_6$

Figure B5. ^{13}C NMR in acetone-d$_6$

226
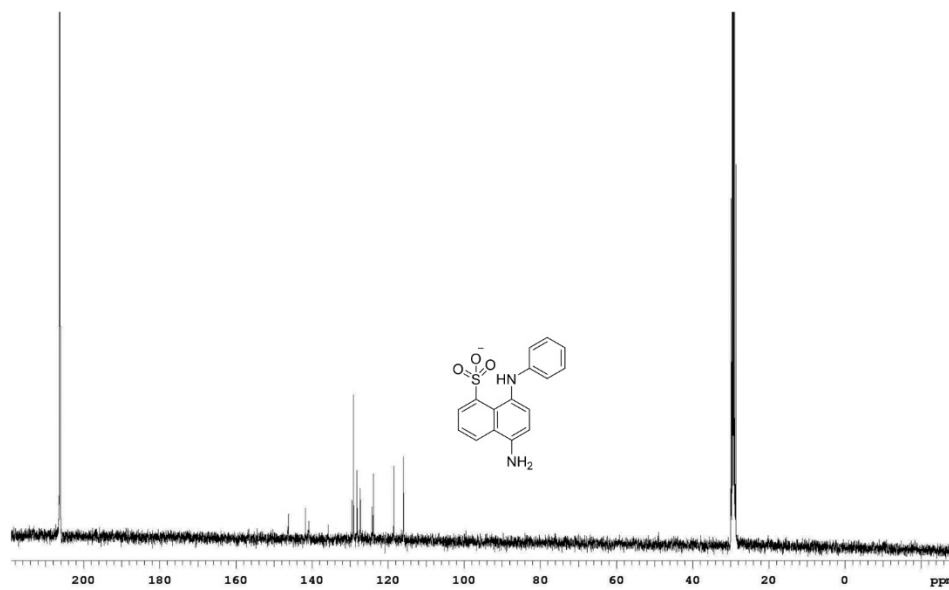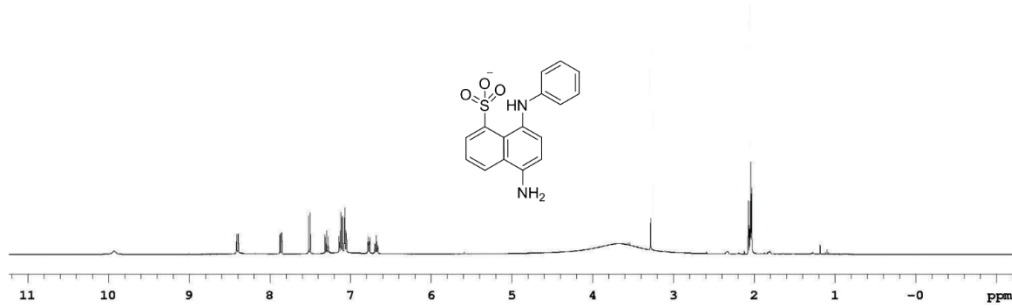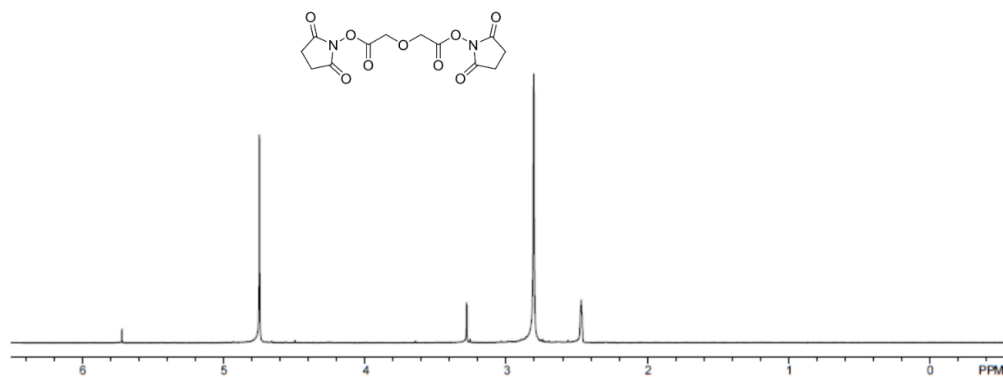
Figure B6. ^{1}H NMR in DMSO-d$_6$
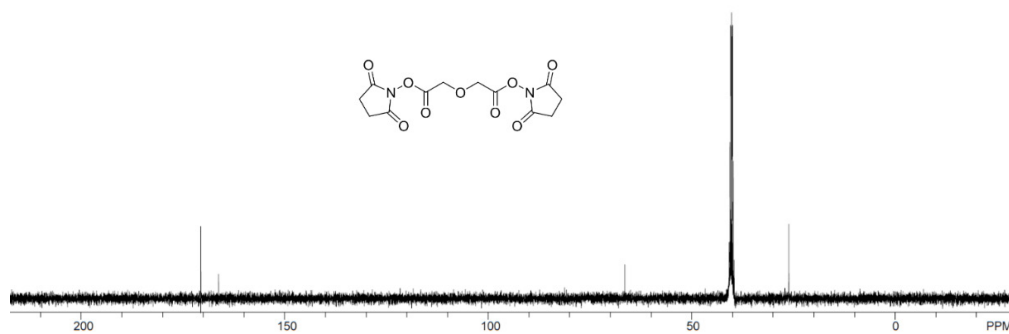
Figure B7. ^{13}C NMR in Acetone-d$_6$

227
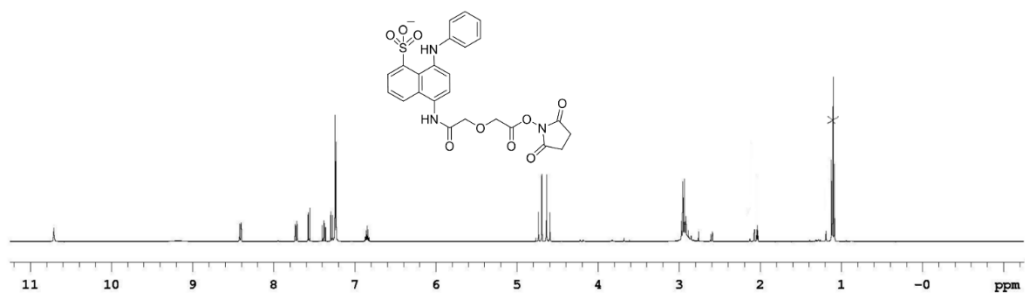
Figure B8. ^{1}H NMR in acetone-d$_6$
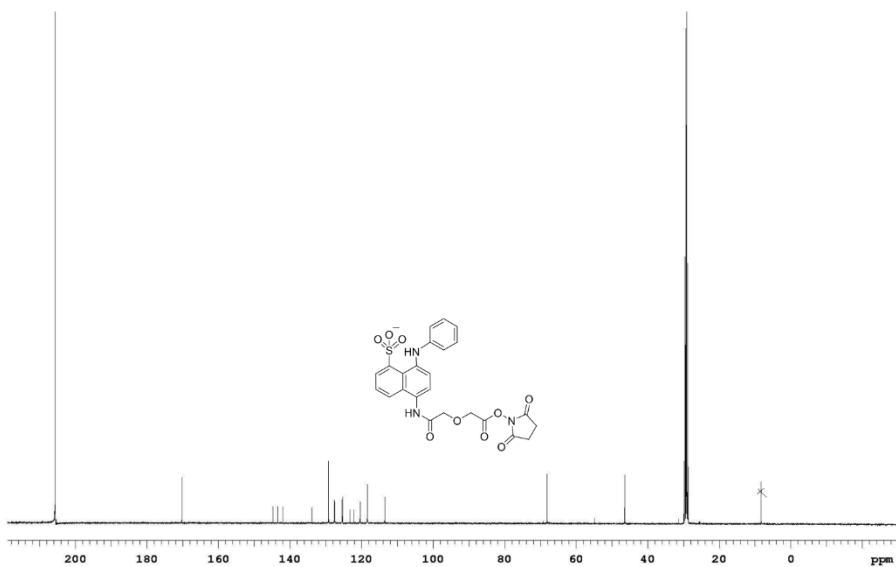
Figure B9. ^{13}C NMR in acetone-d$_6$

(a)

+ 5 KT/e   -5 KT/e

(b)

+ 5 KT/e   -5 KT/e

(c)

+ 5 KT/e   -5 KT/e
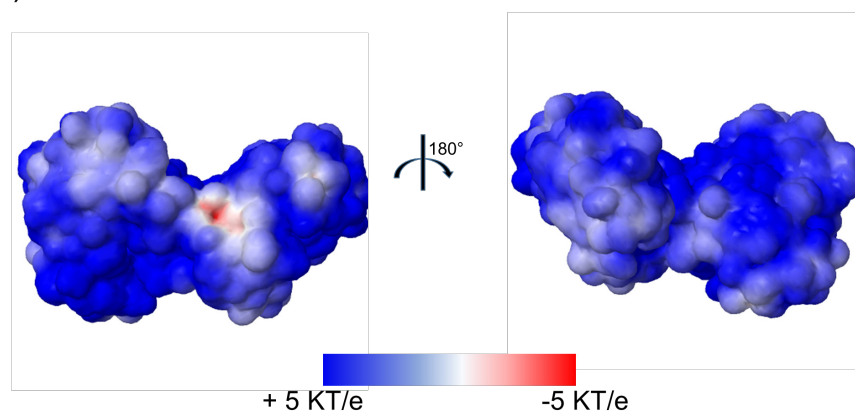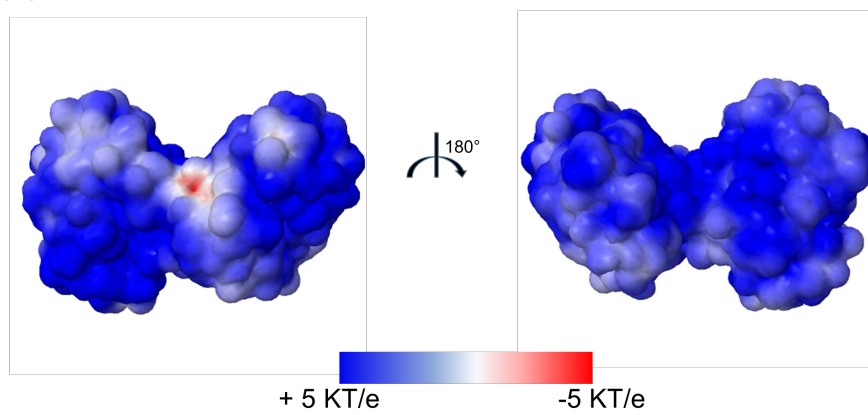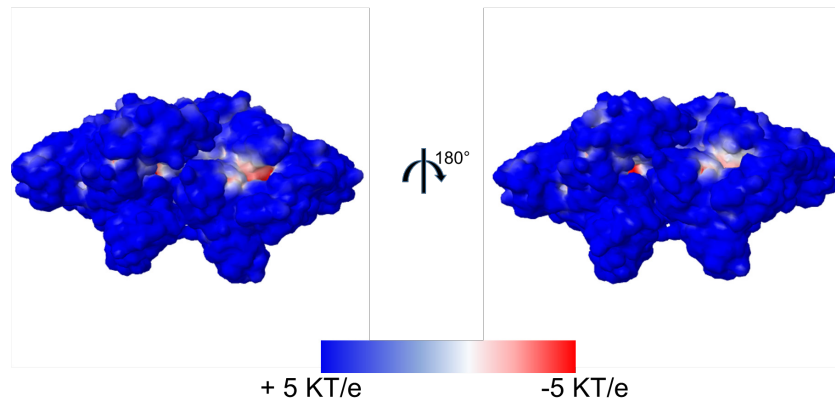
Figure B10. Electrostatics maps of proteins (Myoglobin, Apomyoglobin, Lysozyme and BSA) at pH 8.3 using the blue-white-red scheme. (a) Myoglobin; (b) Apomyoglobin; (d) BSA.

Appendix C: Copyright Permissions

Permission for Figure 1.1

Permission for Figure 1.2

Permission for Figure 1.3

This is a License Agreement between Nethaniah Dorh ("You") and Nature Publishing Group ("Nature Publishing Group") provided by Copyright Clearance Center ("CCC"). The license consists of your order details, the terms and conditions provided by Nature Publishing Group, and the payment terms and conditions.

All payments must be made in full to CCC. For payment instructions, please see information listed at the bottom of this form.

License Number	3817400580835
License date	Feb 27, 2016
Licensed content publisher	Nature Publishing Group
Licensed content publication	Nature
Licensed content title	The structure and function of G-protein-coupled receptors
Licensed content author	Daniel M. Rosenbaum, Soren G. F. Rasmussen and Brian K. Kobilka
Licensed content date	May 20, 2009
Volume number	459
Issue number	7245
Type of Use	reuse in a dissertation / thesis
Requestor type	academic/educational
Format	print and electronic
Portion	figures/tables/illustrations
Number of figures/tables/illustrations	1
High-res required	no
Figures	Figure 1
Author of this NPG article	no
Your reference number	None
Title of your thesis / dissertation	On the design and characterization of fluorescent probes for sensing and mapping of the surface hydrophobicity of proteins
Expected completion date	Apr 2016
Estimated size (number of pages)	200
Total	0.00 USD
Terms and Conditions	

Terms and Conditions for Permissions

Nature Publishing Group hereby grants you a non-exclusive license to reproduce this material for this purpose, and for no other use,subject to the conditions below:

233

1. NPG warrants that it has, to the best of its knowledge, the rights to license reuse of this material. However, you should ensure that the material you are requesting is original to Nature Publishing Group and does not carry the copyright of another entity (as credited in the published version). If the credit line on any part of the material you have requested indicates that it was reprinted or adapted by NPG with permission from another source, then you should also seek permission from that source to reuse the material.

2. Permission granted free of charge for material in print is also usually granted for any electronic version of that work, provided that the material is incidental to the work as a whole and that the electronic version is essentially equivalent to, or substitutes for, the print version.Where print permission has been granted for a fee, separate permission must be obtained for any additional, electronic re-use (unless, as in the case of a full paper, this has already been accounted for during your initial request in the calculation of a print run).NB: In all cases, web-based use of full-text articles must be authorized separately through the 'Use on a Web Site' option when requesting permission.

3. Permission granted for a first edition does not apply to second and subsequent editions and for editions in other languages (except for signatories to the STM Permissions Guidelines, or where the first edition permission was granted for free).

4. Nature Publishing Group's permission must be acknowledged next to the figure, table or abstract in print. In electronic form, this acknowledgement must be visible at the same time as the figure/table/abstract, and must be hyperlinked to the journal's homepage.

5. The credit line should read:
Reprinted by permission from Macmillan Publishers Ltd: [JOURNAL NAME] (reference citation), copyright (year of publication)
For AOP papers, the credit line should read:
Reprinted by permission from Macmillan Publishers Ltd: [JOURNAL NAME], advance online publication, day month year (doi: 10.1038/sj.[JOURNAL ACRONYM].XXXXX)

Note: For republication from the *British Journal of Cancer,* the following credit lines apply.
Reprinted by permission from Macmillan Publishers Ltd on behalf of Cancer Research UK: [JOURNAL NAME] (reference citation), copyright (year of publication)For AOP papers, the credit line should read:
Reprinted by permission from Macmillan Publishers Ltd on behalf of Cancer Research UK: [JOURNAL NAME], advance online publication, day month year (doi: 10.1038/sj.[JOURNAL ACRONYM].XXXXX)

6. Adaptations of single figures do not require NPG approval. However, the adaptation should be credited as follows:

Adapted by permission from Macmillan Publishers Ltd: [JOURNAL NAME] (reference citation), copyright (year of publication)

Note: For adaptation from the *British Journal of Cancer,* the following credit line applies.
Adapted by permission from Macmillan Publishers Ltd on behalf of Cancer Research UK: [JOURNAL NAME] (reference citation), copyright (year of publication)

7. Translations of 401 words up to a whole article require NPG approval. Please visit http://www.macmillanmedicalcommunications.com for more information.Translations of up to a 400 words do not require NPG approval. The translation should be credited as follows:

Translated by permission from Macmillan Publishers Ltd: [JOURNAL NAME] (reference citation), copyright (year of publication).

Note: For translation from the *British Journal of Cancer,* the following credit line

<u>applies.</u>
Translated by permission from Macmillan Publishers Ltd on behalf of Cancer Research UK:
[JOURNAL NAME] (reference citation), copyright (year of publication)

We are certain that all parties will benefit from this agreement and wish you the best in the use of this material. Thank you.
Special Terms:
v1.1

Questions? <u>customercare@copyright.com</u> or +1-855-239-3415 (toll free in the US) or +1-978-646-2777.

Permission for figure 1.4

License Number	3831681318000
License date	Mar 17, 2016
Licensed content publisher	Nature Publishing Group
Licensed content publication	Nature Reviews Molecular Cell Biology
Licensed content title	TGF[beta]-SMAD signal transduction: molecular specificity and functional flexibility
Licensed content author	Bernhard Schmierer and Caroline S. Hill
Licensed content date	Dec 1, 2007
Volume number	8
Issue number	12
Type of Use	reuse in a dissertation / thesis
Requestor type	academic/educational
Format	print and electronic
Portion	figures/tables/illustrations
Number of figures/tables/illustrations	1
High-res required	no
Figures	Figure 2
Author of this NPG article	no
Your reference number	None
Title of your thesis / dissertation	On the design and characterization of fluorescent probes for sensing and mapping of the surface hydrophobicity of proteins
Expected completion date	Apr 2016
Estimated size (number of pages)	200
Total	0.00 USD
Terms and Conditions	

Terms and Conditions for Permissions
Nature Publishing Group hereby grants you a non-exclusive license to reproduce this material for this purpose, and for no other use,subject to the conditions below:

1. NPG warrants that it has, to the best of its knowledge, the rights to license reuse of this material. However, you should ensure that the material you are requesting is original to Nature Publishing Group and does not carry the copyright of another entity (as credited in the published version). If the credit line on any part of the material you have requested indicates that it was reprinted or adapted by NPG with permission from another source, then you should also seek permission from that source to reuse the material.

2. Permission granted free of charge for material in print is also usually granted for any electronic version of that work, provided that the material is incidental to the work as a whole and that the electronic version is essentially equivalent to, or substitutes for, the print version.Where print permission has been granted for a fee, separate permission must be obtained for any additional, electronic re-use (unless, as in the case of a full paper, this has already been accounted for during your initial request in the calculation of a print run).NB: In all cases, web-based use of full-text articles must be authorized separately through the 'Use on a Web Site' option when requesting permission.

3. Permission granted for a first edition does not apply to second and subsequent editions and for editions in other languages (except for signatories to the STM Permissions Guidelines, or where the first edition permission was granted for free).

4. Nature Publishing Group's permission must be acknowledged next to the figure, table or abstract in print. In electronic form, this acknowledgement must be visible at the same time as the figure/table/abstract, and must be hyperlinked to the journal's homepage.

5. The credit line should read:
Reprinted by permission from Macmillan Publishers Ltd: [JOURNAL NAME] (reference citation), copyright (year of publication)
For AOP papers, the credit line should read:
Reprinted by permission from Macmillan Publishers Ltd: [JOURNAL NAME], advance online publication, day month year (doi: 10.1038/sj.[JOURNAL ACRONYM].XXXXX)

Note: For republication from the _British Journal of Cancer,_ the following credit lines apply.
Reprinted by permission from Macmillan Publishers Ltd on behalf of Cancer Research UK: [JOURNAL NAME] (reference citation), copyright (year of publication)For AOP papers, the credit line should read:
Reprinted by permission from Macmillan Publishers Ltd on behalf of Cancer Research UK: [JOURNAL NAME], advance online publication, day month year (doi: 10.1038/sj.[JOURNAL ACRONYM].XXXXX)

6. Adaptations of single figures do not require NPG approval. However, the adaptation should be credited as follows:

Adapted by permission from Macmillan Publishers Ltd: [JOURNAL NAME] (reference citation), copyright (year of publication)

Note: For adaptation from the _British Journal of Cancer,_ the following credit line applies.
Adapted by permission from Macmillan Publishers Ltd on behalf of Cancer Research UK: [JOURNAL NAME] (reference citation), copyright (year of publication)

7. Translations of 401 words up to a whole article require NPG approval. Please visit http://www.macmillanmedicalcommunications.com for more information.Translations of up to a 400 words do not require NPG approval. The translation should be credited as follows:

Translated by permission from Macmillan Publishers Ltd: [JOURNAL NAME] (reference citation), copyright (year of publication).

Note: For translation from the _British Journal of Cancer,_ the following credit line

We are certain that all parties will benefit from this agreement and wish you the best in the use of this material. Thank you.

Special Terms:

v1.1

Questions? customercare@copyright.com or +1-855-239-3415 (toll free in the US) or +1-978-646-2777.

238

Permission for Figure 1.5

239

1. NPG warrants that it has, to the best of its knowledge, the rights to license reuse of this material. However, you should ensure that the material you are requesting is original to Nature Publishing Group and does not carry the copyright of another entity (as credited in the published version). If the credit line on any part of the material you have requested indicates that it was reprinted or adapted by NPG with permission from another source, then you should also seek permission from that source to reuse the material.

2. Permission granted free of charge for material in print is also usually granted for any electronic version of that work, provided that the material is incidental to the work as a whole and that the electronic version is essentially equivalent to, or substitutes for, the print version.Where print permission has been granted for a fee, separate permission must be obtained for any additional, electronic re-use (unless, as in the case of a full paper, this has already been accounted for during your initial request in the calculation of a print run).NB: In all cases, web-based use of full-text articles must be authorized separately through the 'Use on a Web Site' option when requesting permission.

3. Permission granted for a first edition does not apply to second and subsequent editions and for editions in other languages (except for signatories to the STM Permissions Guidelines, or where the first edition permission was granted for free).

4. Nature Publishing Group's permission must be acknowledged next to the figure, table or abstract in print. In electronic form, this acknowledgement must be visible at the same time as the figure/table/abstract, and must be hyperlinked to the journal's homepage.

5. The credit line should read:
Reprinted by permission from Macmillan Publishers Ltd: [JOURNAL NAME] (reference citation), copyright (year of publication)
For AOP papers, the credit line should read:
Reprinted by permission from Macmillan Publishers Ltd: [JOURNAL NAME], advance online publication, day month year (doi: 10.1038/sj.[JOURNAL ACRONYM].XXXXX)

Note: For republication from the _British Journal of Cancer,_ the following credit lines apply.
Reprinted by permission from Macmillan Publishers Ltd on behalf of Cancer Research UK: [JOURNAL NAME] (reference citation), copyright (year of publication)For AOP papers, the credit line should read:
Reprinted by permission from Macmillan Publishers Ltd on behalf of Cancer Research UK: [JOURNAL NAME], advance online publication, day month year (doi: 10.1038/sj.[JOURNAL ACRONYM].XXXXX)

6. Adaptations of single figures do not require NPG approval. However, the adaptation should be credited as follows:

Adapted by permission from Macmillan Publishers Ltd: [JOURNAL NAME] (reference citation), copyright (year of publication)

Note: For adaptation from the _British Journal of Cancer,_ the following credit line applies.
Adapted by permission from Macmillan Publishers Ltd on behalf of Cancer Research UK: [JOURNAL NAME] (reference citation), copyright (year of publication)

7. Translations of 401 words up to a whole article require NPG approval. Please visit http://www.macmillanmedicalcommunications.com for more information.Translations of up to a 400 words do not require NPG approval. The translation should be credited as follows:

Translated by permission from Macmillan Publishers Ltd: [JOURNAL NAME] (reference citation), copyright (year of publication).

Note: For translation from the _British Journal of Cancer,_ the following credit line

applies.

We are certain that all parties will benefit from this agreement and wish you the best in the use of this material. Thank you.
Special Terms:
v1.1

Permission for Figure 1.7

To whom it may concern,

It is the policy of the American Society for Biochemistry and Molecular Biology to allow reuse of any material published in its journals (the Journal of Biological Chemistry, Molecular & Cellular Proteomics and the Journal of Lipid Research) in a thesis or dissertation at no cost and with no explicit permission needed. Please see our copyright permissions page on the journal site for more information.

Best wishes,

Sarah Crespi

American Society for Biochemistry and Molecular Biology
11200 Rockville Pike, Rockville, MD
Suite 302
240-283-6616
JBC | MCP | JLR

242

Permission for figure 2.1 and 5.12

TERMS AND CONDITIONS

This copyrighted material is owned by or exclusively licensed to John Wiley & Sons, Inc. or one of its group companies (each a"Wiley Company") or handled on behalf of a society with which a Wiley Company has exclusive publishing rights in relation to a particular work (collectively "WILEY"). By clicking "accept" in connection with completing this licensing transaction, you agree that the following terms and conditions apply to this transaction (along with the billing and payment terms and conditions established by the Copyright Clearance Center Inc., ("CCC's Billing and Payment terms and conditions"), at the time that you opened your RightsLink account (these are available at any time at http://myaccount.copyright.com).

Terms and Conditions

- The materials you have requested permission to reproduce or reuse (the "Wiley Materials") are protected by copyright.

- You are hereby granted a personal, non-exclusive, non-sub licensable (on a stand-alone basis), non-transferable, worldwide, limited license to reproduce the Wiley Materials for the purpose specified in the licensing process. This license, **and any CONTENT (PDF or image file) purchased as part of your order,** is for a one-time use only and limited to any maximum distribution number specified in the license. The first instance of republication or reuse granted by this license must be completed within two years of the date of the grant of this license (although copies prepared before the end date may be distributed thereafter). The Wiley Materials shall not be used in any other manner or for any other purpose, beyond what is granted in the license. Permission is granted subject to an appropriate acknowledgement given to the author, title of the material/book/journal and the publisher. You shall also duplicate the copyright notice that appears in the Wiley publication in your use of the Wiley Material. Permission is also granted on the understanding that nowhere in the text is a previously published source acknowledged for all or part of this Wiley Material. Any third party content is expressly excluded from this permission.

- With respect to the Wiley Materials, all rights are reserved. Except as expressly granted by the terms of the license, no part of the Wiley Materials may be copied, modified, adapted (except for minor reformatting required by the new Publication), translated, reproduced, transferred or distributed, in any form or by any means, and no derivative works may be made based on the Wiley Materials without the prior permission of the respective copyright owner.**For STM Signatory Publishers clearing permission under the terms of the STM Permissions Guidelines only, the terms of the license are extended to include subsequent editions and for editions in other languages, provided such editions are for the work as a whole in situ and does not involve the separate exploitation of the permitted figures or extracts,** You may not alter, remove or suppress in any manner any copyright, trademark or other notices displayed by the Wiley Materials. You may not license, rent, sell, loan, lease, pledge, offer as security, transfer or assign the Wiley Materials on a stand-alone basis, or any of the rights granted to you hereunder to any other person.

244

- The failure of either party to enforce any term or condition of this Agreement shall not constitute a waiver of either party's right to enforce each and every term and condition of this Agreement. No breach under this agreement shall be deemed waived or excused by either party unless such waiver or consent is in writing signed by the party granting such waiver or consent. The waiver by or consent of a party to a breach of any provision of this Agreement shall not operate or be construed as a waiver of or consent to any other or subsequent breach by such other party.

- This Agreement may not be assigned (including by operation of law or otherwise) by you without WILEY's prior written consent.

- Any fee required for this permission shall be non-refundable after thirty (30) days from receipt by the CCC.

- These terms and conditions together with CCC's Billing and Payment terms and conditions (which are incorporated herein) form the entire agreement between you and WILEY concerning this licensing transaction and (in the absence of fraud) supersedes all prior agreements and representations of the parties, oral or written. This Agreement may not be amended except in writing signed by both parties. This Agreement shall be binding upon and inure to the benefit of the parties' successors, legal representatives, and authorized assigns.

- In the event of any conflict between your obligations established by these terms and conditions and those established by CCC's Billing and Payment terms and conditions, these terms and conditions shall prevail.

- WILEY expressly reserves all rights not specifically granted in the combination of (i) the license details provided by you and accepted in the course of this licensing transaction, (ii) these terms and conditions and (iii) CCC's Billing and Payment terms and conditions.

- This Agreement will be void if the Type of Use, Format, Circulation, or Requestor Type was misrepresented during the licensing process.

- This Agreement shall be governed by and construed in accordance with the laws of the State of New York, USA, without regards to such state's conflict of law rules. Any legal action, suit or proceeding arising out of or relating to these Terms and Conditions or the breach thereof shall be instituted in a court of competent jurisdiction in New York County in the State of New York in the United States of America and each party hereby consents and submits to the personal jurisdiction of such court, waives any objection to venue in such court and consents to service of process by registered or certified mail, return receipt requested, at the last known address of such party.

WILEY OPEN ACCESS TERMS AND CONDITIONS
Wiley Publishes Open Access Articles in fully Open Access Journals and in Subscription journals offering Online Open. Although most of the fully Open Access journals publish open access articles under the terms of the Creative Commons Attribution (CC BY) License only, the subscription journals and a few of the Open Access Journals offer a choice of

- The Wiley Materials and all of the intellectual property rights therein shall at all times remain the exclusive property of John Wiley & Sons Inc, the Wiley Companies, or their respective licensors, and your interest therein is only that of having possession of and the right to reproduce the Wiley Materials pursuant to Section 2 herein during the continuance of this Agreement. You agree that you own no right, title or interest in or to the Wiley Materials or any of the intellectual property rights therein. You shall have no rights hereunder other than the license as provided for above in Section 2. No right, license or interest to any trademark, trade name, service mark or other branding ("Marks") of WILEY or its licensors is granted hereunder, and you agree that you shall not assert any such right, license or interest with respect thereto

- NEITHER WILEY NOR ITS LICENSORS MAKES ANY WARRANTY OR REPRESENTATION OF ANY KIND TO YOU OR ANY THIRD PARTY, EXPRESS, IMPLIED OR STATUTORY, WITH RESPECT TO THE MATERIALS OR THE ACCURACY OF ANY INFORMATION CONTAINED IN THE MATERIALS, INCLUDING, WITHOUT LIMITATION, ANY IMPLIED WARRANTY OF MERCHANTABILITY, ACCURACY, SATISFACTORY QUALITY, FITNESS FOR A PARTICULAR PURPOSE, USABILITY, INTEGRATION OR NON-INFRINGEMENT AND ALL SUCH WARRANTIES ARE HEREBY EXCLUDED BY WILEY AND ITS LICENSORS AND WAIVED BY YOU.

- WILEY shall have the right to terminate this Agreement immediately upon breach of this Agreement by you.

- You shall indemnify, defend and hold harmless WILEY, its Licensors and their respective directors, officers, agents and employees, from and against any actual or threatened claims, demands, causes of action or proceedings arising from any breach of this Agreement by you.

- IN NO EVENT SHALL WILEY OR ITS LICENSORS BE LIABLE TO YOU OR ANY OTHER PARTY OR ANY OTHER PERSON OR ENTITY FOR ANY SPECIAL, CONSEQUENTIAL, INCIDENTAL, INDIRECT, EXEMPLARY OR PUNITIVE DAMAGES, HOWEVER CAUSED, ARISING OUT OF OR IN CONNECTION WITH THE DOWNLOADING, PROVISIONING, VIEWING OR USE OF THE MATERIALS REGARDLESS OF THE FORM OF ACTION, WHETHER FOR BREACH OF CONTRACT, BREACH OF WARRANTY, TORT, NEGLIGENCE, INFRINGEMENT OR OTHERWISE (INCLUDING, WITHOUT LIMITATION, DAMAGES BASED ON LOSS OF PROFITS, DATA, FILES, USE, BUSINESS OPPORTUNITY OR CLAIMS OF THIRD PARTIES), AND WHETHER OR NOT THE PARTY HAS BEEN ADVISED OF THE POSSIBILITY OF SUCH DAMAGES. THIS LIMITATION SHALL APPLY NOTWITHSTANDING ANY FAILURE OF ESSENTIAL PURPOSE OF ANY LIMITED REMEDY PROVIDED HEREIN.

- Should any provision of this Agreement be held by a court of competent jurisdiction to be illegal, invalid, or unenforceable, that provision shall be deemed amended to achieve as nearly as possible the same economic effect as the original provision, and the legality, validity and enforceability of the remaining provisions of this Agreement shall not be affected or impaired thereby.

Creative Commons Licenses. The license type is clearly identified on the article.

The Creative Commons Attribution License

The Creative Commons Attribution License (CC-BY) allows users to copy, distribute and transmit an article, adapt the article and make commercial use of the article. The CC-BY license permits commercial and non-

Creative Commons Attribution Non-Commercial License

The Creative Commons Attribution Non-Commercial (CC-BY-NC)License permits use, distribution and reproduction in any medium, provided the original work is properly cited and is not used for commercial purposes.(see below)

Creative Commons Attribution-Non-Commercial-NoDerivs License

The Creative Commons Attribution Non-Commercial-NoDerivs License (CC-BY-NC-ND) permits use, distribution and reproduction in any medium, provided the original work is properly cited, is not used for commercial purposes and no modifications or adaptations are made. (see below)

Use by commercial "for-profit" organizations

Use of Wiley Open Access articles for commercial, promotional, or marketing purposes requires further explicit permission from Wiley and will be subject to a fee.

Further details can be found on Wiley Online Library

http://olabout.wiley.com/WileyCDA/Section/id-410895.html

Other Terms and Conditions:

v1.10 Last updated September 2015

Questions? customercare@copyright.com or +1-855-239-3415 (toll free in the US) or +1-978-646-2777.

247

Permission for Figure 2.3

Permission for Figure 2.6

249

Terms and Conditions

This License Agreement is between {Requestor Name} ("You") and The Royal Society of Chemistry ("RSC") provided by the Copyright Clearance Center ("CCC"). The license consists of your order details, the terms and conditions provided by the Royal Society of Chemistry, and the payment terms and conditions.

RSC / TERMS AND CONDITIONS

INTRODUCTION

The publisher for this copyrighted material is The Royal Society of Chemistry. By clicking "accept" in connection with completing this licensing transaction, you agree that the following terms and conditions apply to this transaction (along with the Billing and Payment terms and conditions established by CCC, at the time that you opened your RightsLink account and that are available at any time at .

LICENSE GRANTED

The RSC hereby grants you a non-exclusive license to use the aforementioned material anywhere in the world subject to the terms and conditions indicated herein. Reproduction of the material is confined to the purpose and/or media for which permission is hereby given.

RESERVATION OF RIGHTS

The RSC reserves all rights not specifically granted in the combination of (i) the license details provided by your and accepted in the course of this licensing transaction; (ii) these terms and conditions; and (iii) CCC's Billing and Payment terms and conditions.

REVOCATION

The RSC reserves the right to revoke this license for any reason, including, but not limited to, advertising and promotional uses of RSC content, third party usage, and incorrect source figure attribution.

THIRD-PARTY MATERIAL DISCLAIMER

If part of the material to be used (for example, a figure) has appeared in the RSC publication with credit to another source, permission must also be sought from that source. If the other source is another RSC publication these details should be included in your RightsLink request. If the other source is a third party, permission must be obtained from the third party. The RSC disclaims any responsibility for the reproduction you make of items owned by a third party.

PAYMENT OF FEE

If the permission fee for the requested material is waived in this instance, please be advised that any future requests for the reproduction of RSC materials may attract a fee.

ACKNOWLEDGEMENT

The reproduction of the licensed material must be accompanied by the following acknowledgement:

Reproduced ("Adapted" or "in part") from {Reference Citation} (or Ref XX) with permission of The Royal Society of Chemistry.

If the licensed material is being reproduced from New Journal of Chemistry (NJC), Photochemical & Photobiological Sciences (PPS) or Physical Chemistry Chemical Physics (PCCP) you must include one of the following acknowledgements:

For figures originally published in NJC:

Reproduced ("Adapted" or "in part") from {Reference Citation} (or Ref XX) with

250

permission of The Royal Society of Chemistry (RSC) on behalf of the European Society for Photobiology, the European Photochemistry Association and the RSC.

For figures originally published in PPS:

Reproduced ("Adapted" or "in part") from {Reference Citation} (or Ref XX) with permission of The Royal Society of Chemistry (RSC) on behalf of the Centre National de la Recherche Scientifique (CNRS) and the RSC.

For figures originally published in PCCP:

Reproduced ("Adapted" or "in part") from {Reference Citation} (or Ref XX) with permission of the PCCP Owner Societies.

HYPERTEXT LINKS

With any material which is being reproduced in electronic form, you must include a hypertext link to the original RSC article on the RSC's website. The recommended form for the hyperlink is http://dx.doi.org/10.1039/DOI suffix, for example in the link http://dx.doi.org/10.1039/b110420a the DOI suffix is 'b110420a'. To find the relevant DOI suffix for the RSC article in question, go to the Journals section of the website and locate the article in the list of papers for the volume and issue of your specific journal. You will find the DOI suffix quoted there.

LICENSE CONTINGENT ON PAYMENT

While you may exercise the rights licensed immediately upon issuance of the license at the end of the licensing process for the transaction, provided that you have disclosed complete and accurate details of your proposed use, no license is finally effective unless and until full payment is received from you (by CCC) as provided in CCC's Billing and Payment terms and conditions. If full payment is not received on a timely basis, then any license preliminarily granted shall be deemed automatically revoked and shall be void as if never granted. Further, in the event that you breach any of these terms and conditions or any of CCC's Billing and Payment terms and conditions, the license is automatically revoked and shall be void as if never granted. Use of materials as described in a revoked license, as well as any use of the materials beyond the scope of an unrevoked license, may constitute copyright infringement and the RSC reserves the right to take any and all action to protect its copyright in the materials.

WARRANTIES

The RSC makes no representations or warranties with respect to the licensed material.

INDEMNITY

You hereby indemnify and agree to hold harmless the RSC and the CCC, and their respective officers, directors, trustees, employees and agents, from and against any and all claims arising out of your use of the licensed material other than as specifically authorized pursuant to this licence.

NO TRANSFER OF LICENSE

This license is personal to you or your publisher and may not be sublicensed, assigned, or transferred by you to any other person without the RSC's written permission.

NO AMENDMENT EXCEPT IN WRITING

This license may not be amended except in a writing signed by both parties (or, in the case of "Other Conditions, v1.2", by CCC on the RSC's behalf).

OBJECTION TO CONTRARY TERMS

You hereby acknowledge and agree that these terms and conditions, together with CCC's Billing and Payment terms and conditions (which are incorporated herein), comprise the entire agreement between you and the RSC (and CCC) concerning this licensing transaction, to the exclusion of all other terms and conditions, written or verbal, express or implied (including any terms contained in any purchase order, acknowledgment, check endorsement or other writing prepared by you). In the event of any conflict between your obligations

251

established by these terms and conditions and those established by CCC's Billing and Payment terms and conditions, these terms and conditions shall control.
JURISDICTION
This license transaction shall be governed by and construed in accordance with the laws of the District of Columbia. You hereby agree to submit to the jurisdiction of the courts located in the District of Columbia for purposes of resolving any disputes that may arise in connection with this licensing transaction.
LIMITED LICENSE
The following terms and conditions apply to specific license types:
Translation
This permission is granted for non-exclusive world English rights only unless your license was granted for translation rights. If you licensed translation rights you may only translate this content into the languages you requested. A professional translator must perform all translations and reproduce the content word for word preserving the integrity of the article.
Intranet
If the licensed material is being posted on an Intranet, the Intranet is to be password-protected and made available only to bona fide students or employees only. All content posted to the Intranet must maintain the copyright information line on the bottom of each image. You must also fully reference the material and include a hypertext link as specified above.
Copies of Whole Articles
All copies of whole articles must maintain, if available, the copyright information line on the bottom of each page.
Other Conditions
v1.2
Gratis licenses (referencing $0 in the Total field) are free. Please retain this printable license for your reference. No payment is required.
If you would like to pay for this license now, please remit this license along with yourpayment made payable to "COPYRIGHT CLEARANCE CENTER" otherwise you will be invoiced within 48 hours of the license date. Payment should be in the form of a check or money order referencing your account number and this invoice number {Invoice Number}. Once you receive your invoice for this order, you may pay your invoice by credit card. Please follow instructions provided at that time.
Make Payment To:
Copyright Clearance Center
Dept 001
P.O. Box 843006
Boston, MA 02284-3006
For suggestions or comments regarding this order, contact Rightslink Customer Support: customercare@copyright.com or +1-855-239-3415 (toll free in the US) or +1-978-646-2777.

Questions? customercare@copyright.com or +1-855-239-3415 (toll free in the US) or +1-978-646-2777.

Permission for Figure 2.10

Permission for Figure 3.4

License Number	3812580701662
License date	Feb 19, 2016
Licensed content publisher	Springer
Licensed content publication	Journal of The American Society for Mass Spectrometry
Licensed content title	Painting proteins with covalent labels: What's in the picture?
Licensed content author	Michael C. Fitzgerald
Licensed content date	Jan 1, 2009
Volume number	20
Issue number	6
Type of Use	Thesis/Dissertation
Portion	Figures/tables/illustrations
Number of figures/tables/illustrations	1
Author of this Springer article	No
Order reference number	None
Original figure numbers	figure 2
Title of your thesis / dissertation	On the design and characterization of fluorescent probes for sensing and mapping of the surface hydrophobicity of proteins
Expected completion date	Apr 2016
Estimated size(pages)	200

granted according to STM Permissions Guidelines: http://www.stm-assoc.org/permissions-guidelines/

For any electronic use not mentioned in the Guidelines, please contact Springer at permissions.springer@spi-global.com. If you request to reuse more content than stipulated in the STM Permissions Guidelines, you will be charged a permission fee for the excess content.

Permission is valid upon payment of the fee as indicated in the licensing process. If permission is granted free of charge on this occasion, that does not prejudice any rights we might have to charge for reproduction of our copyrighted material in the future.

-If your request is for reuse in a Thesis, permission is granted free of charge under the following conditions:

This license is valid for one-time use only for the purpose of defending your thesis and with a maximum of 100 extra copies in paper. If the thesis is going to be published, permission needs to be reobtained.

- includes use in an electronic form, provided it is an author-created version of the thesis on his/her own website and his/her university's repository, including UMI (according to the definition on the Sherpa website: http://www.sherpa.ac.uk/romeo/);

- is subject to courtesy information to the co-author or corresponding author.

Geographic Rights: Scope

Licenses may be exercised anywhere in the world.

Altering/Modifying Material: Not Permitted

Figures, tables, and illustrations may be altered minimally to serve your work. You may not alter or modify text in any manner. Abbreviations, additions, deletions and/or any other alterations shall be made only with prior written authorization of the author(s).

Reservation of Rights

Springer reserves all rights not specifically granted in the combination of (i) the license details provided by you and accepted in the course of this licensing transaction and (ii) these terms and conditions and (iii) CCC's Billing and Payment terms and conditions.

License Contingent on Payment

While you may exercise the rights licensed immediately upon issuance of the license at the end of the licensing process for the transaction, provided that you have disclosed complete and accurate details of your proposed use, no license is finally effective unless and until full payment is received from you (either by Springer or by CCC) as provided in CCC's Billing and Payment terms and conditions. If full payment is not received by the date due, then any license preliminarily granted shall be deemed automatically revoked and shall be void as if never granted. Further, in the event that you breach any of these terms and conditions or any of CCC's Billing and Payment terms and conditions, the license is automatically revoked and shall be void as if never granted. Use of materials as described in a revoked license, as well

Total   0.00 USD

Terms and Conditions

Introduction

The publisher for this copyrighted material is Springer. By clicking "accept" in connection with completing this licensing transaction, you agree that the following terms and conditions apply to this transaction (along with the Billing and Payment terms and conditions established by Copyright Clearance Center, Inc. ("CCC"), at the time that you opened your Rightslink account and that are available at any time at http://myaccount.copyright.com).

Limited License

With reference to your request to reuse material on which Springer controls the copyright, permission is granted for the use indicated in your enquiry under the following conditions:

- Licenses are for one-time use only with a maximum distribution equal to the number stated in your request.

- Springer material represents original material which does not carry references to other sources. If the material in question appears with a credit to another source, this permission is not valid and authorization has to be obtained from the original copyright holder.

- This permission

• is non-exclusive

• is only valid if no personal rights, trademarks, or competitive products are infringed.

• explicitly excludes the right for derivatives.

- Springer does not supply original artwork or content.

- According to the format which you have selected, the following conditions apply accordingly:

• **Print and Electronic:** This License include use in electronic form provided it is password protected, on intranet, or CD-Rom/DVD or E-book/E-journal. It may not be republished in electronic open access.

• **Print:** This License excludes use in electronic form.

• **Electronic:** This License only pertains to use in electronic form provided it is password protected, on intranet, or CD-Rom/DVD or E-book/E-journal. It may not be republished in electronic open access.

For any electronic use not mentioned, please contact Springer at permissions.springer@spi-global.com.

- Although Springer controls the copyright to the material and is entitled to negotiate on rights, this license is only valid subject to courtesy information to the author (address is given in the article/chapter).

- If you are an STM Signatory or your work will be published by an STM Signatory and you are requesting to reuse figures/tables/illustrations or single text extracts, permission is

256

accordance with German law.
V 12AUG2015

Permission for Figure 3.6

	1047 2nd Street
	HANCOCK, MI 49930 United States Attn: Nethaniah Dorh
Billing Type	Invoice
Billing Address	Nethaniah Dorh 1047 2nd Street
	HANCOCK, MI 49930 United States Attn: Nethaniah Dorh
Total	0.00 USD
Terms and Conditions	

in New York County in the State of New York in the United States of America and each party hereby consents and submits to the personal jurisdiction of such court, waives any objection to venue in such court and consents to service of process by registered or certified mail, return receipt requested, at the last known address of such party.

WILEY OPEN ACCESS TERMS AND CONDITIONS
Wiley Publishes Open Access Articles in fully Open Access Journals and in Subscription journals offering Online Open. Although most of the fully Open Access journals publish open access articles under the terms of the Creative Commons Attribution (CC BY) License only, the subscription journals and a few of the Open Access Journals offer a choice of Creative Commons Licenses. The license type is clearly identified on the article.
The Creative Commons Attribution License
The Creative Commons Attribution License (CC-BY) allows users to copy, distribute and transmit an article, adapt the article and make commercial use of the article. The CC-BY license permits commercial and non-
Creative Commons Attribution Non-Commercial License
The Creative Commons Attribution Non-Commercial (CC-BY-NC)License permits use, distribution and reproduction in any medium, provided the original work is properly cited and is not used for commercial purposes.(see below)

Creative Commons Attribution-Non-Commercial-NoDerivs License
The Creative Commons Attribution Non-Commercial-NoDerivs License (CC-BY-NC-ND) permits use, distribution and reproduction in any medium, provided the original work is properly cited, is not used for commercial purposes and no modifications or adaptations are made. (see below)
Use by commercial "for-profit" organizations
Use of Wiley Open Access articles for commercial, promotional, or marketing purposes requires further explicit permission from Wiley and will be subject to a fee.
Further details can be found on Wiley Online Library
http://olabout.wiley.com/WileyCDA/Section/id-410895.html

Other Terms and Conditions:

- The failure of either party to enforce any term or condition of this Agreement shall not constitute a waiver of either party's right to enforce each and every term and condition of this Agreement. No breach under this agreement shall be deemed waived or excused by either party unless such waiver or consent is in writing signed by the party granting such waiver or consent. The waiver by or consent of a party to a breach of any provision of this Agreement shall not operate or be construed as a waiver of or consent to any other or subsequent breach by such other party.

- This Agreement may not be assigned (including by operation of law or otherwise) by you without WILEY's prior written consent.

- Any fee required for this permission shall be non-refundable after thirty (30) days from receipt by the CCC.

- These terms and conditions together with CCC's Billing and Payment terms and conditions (which are incorporated herein) form the entire agreement between you and WILEY concerning this licensing transaction and (in the absence of fraud) supersedes all prior agreements and representations of the parties, oral or written. This Agreement may not be amended except in writing signed by both parties. This Agreement shall be binding upon and inure to the benefit of the parties' successors, legal representatives, and authorized assigns.

- In the event of any conflict between your obligations established by these terms and conditions and those established by CCC's Billing and Payment terms and conditions, these terms and conditions shall prevail.

- WILEY expressly reserves all rights not specifically granted in the combination of (i) the license details provided by you and accepted in the course of this licensing transaction, (ii) these terms and conditions and (iii) CCC's Billing and Payment terms and conditions.

- This Agreement will be void if the Type of Use, Format, Circulation, or Requestor Type was misrepresented during the licensing process.

- This Agreement shall be governed by and construed in accordance with the laws of the State of New York, USA, without regards to such state's conflict of law rules. Any legal action, suit or proceeding arising out of or relating to these Terms and Conditions or the breach thereof shall be instituted in a court of competent jurisdiction

260

EXPRESS, IMPLIED OR STATUTORY, WITH RESPECT TO THE MATERIALS OR THE ACCURACY OF ANY INFORMATION CONTAINED IN THE MATERIALS, INCLUDING, WITHOUT LIMITATION, ANY IMPLIED WARRANTY OF MERCHANTABILITY, ACCURACY, SATISFACTORY QUALITY, FITNESS FOR A PARTICULAR PURPOSE, USABILITY, INTEGRATION OR NON-INFRINGEMENT AND ALL SUCH WARRANTIES ARE HEREBY EXCLUDED BY WILEY AND ITS LICENSORS AND WAIVED BY YOU.

- WILEY shall have the right to terminate this Agreement immediately upon breach of this Agreement by you.

- You shall indemnify, defend and hold harmless WILEY, its Licensors and their respective directors, officers, agents and employees, from and against any actual or threatened claims, demands, causes of action or proceedings arising from any breach of this Agreement by you.

- IN NO EVENT SHALL WILEY OR ITS LICENSORS BE LIABLE TO YOU OR ANY OTHER PARTY OR ANY OTHER PERSON OR ENTITY FOR ANY SPECIAL, CONSEQUENTIAL, INCIDENTAL, INDIRECT, EXEMPLARY OR PUNITIVE DAMAGES, HOWEVER CAUSED, ARISING OUT OF OR IN CONNECTION WITH THE DOWNLOADING, PROVISIONING, VIEWING OR USE OF THE MATERIALS REGARDLESS OF THE FORM OF ACTION, WHETHER FOR BREACH OF CONTRACT, BREACH OF WARRANTY, TORT, NEGLIGENCE, INFRINGEMENT OR OTHERWISE (INCLUDING, WITHOUT LIMITATION, DAMAGES BASED ON LOSS OF PROFITS, DATA, FILES, USE, BUSINESS OPPORTUNITY OR CLAIMS OF THIRD PARTIES), AND WHETHER OR NOT THE PARTY HAS BEEN ADVISED OF THE POSSIBILITY OF SUCH DAMAGES. THIS LIMITATION SHALL APPLY NOTWITHSTANDING ANY FAILURE OF ESSENTIAL PURPOSE OF ANY LIMITED REMEDY PROVIDED HEREIN.

- Should any provision of this Agreement be held by a court of competent jurisdiction to be illegal, invalid, or unenforceable, that provision shall be deemed amended to achieve as nearly as possible the same economic effect as the original provision, and the legality, validity and enforceability of the remaining provisions of this Agreement shall not be affected or impaired thereby.

261

within two years of the date of the grant of this license (although copies prepared before the end date may be distributed thereafter). The Wiley Materials shall not be used in any other manner or for any other purpose, beyond what is granted in the license. Permission is granted subject to an appropriate acknowledgement given to the author, title of the material/book/journal and the publisher. You shall also duplicate the copyright notice that appears in the Wiley publication in your use of the Wiley Material. Permission is also granted on the understanding that nowhere in the text is a previously published source acknowledged for all or part of this Wiley Material. Any third party content is expressly excluded from this permission.

- With respect to the Wiley Materials, all rights are reserved. Except as expressly granted by the terms of the license, no part of the Wiley Materials may be copied, modified, adapted (except for minor reformatting required by the new Publication), translated, reproduced, transferred or distributed, in any form or by any means, and no derivative works may be made based on the Wiley Materials without the prior permission of the respective copyright owner.**For STM Signatory Publishers clearing permission under the terms of the STM Permissions Guidelines only, the terms of the license are extended to include subsequent editions and for editions in other languages, provided such editions are for the work as a whole in situ and does not involve the separate exploitation of the permitted figures or extracts,** You may not alter, remove or suppress in any manner any copyright, trademark or other notices displayed by the Wiley Materials. You may not license, rent, sell, loan, lease, pledge, offer as security, transfer or assign the Wiley Materials on a stand-alone basis, or any of the rights granted to you hereunder to any other person.

- The Wiley Materials and all of the intellectual property rights therein shall at all times remain the exclusive property of John Wiley & Sons Inc, the Wiley Companies, or their respective licensors, and your interest therein is only that of having possession of and the right to reproduce the Wiley Materials pursuant to Section 2 herein during the continuance of this Agreement. You agree that you own no right, title or interest in or to the Wiley Materials or any of the intellectual property rights therein. You shall have no rights hereunder other than the license as provided for above in Section 2. No right, license or interest to any trademark, trade name, service mark or other branding ("Marks") of WILEY or its licensors is granted hereunder, and you agree that you shall not assert any such right, license or interest with respect thereto

- NEITHER WILEY NOR ITS LICENSORS MAKES ANY WARRANTY OR REPRESENTATION OF ANY KIND TO YOU OR ANY THIRD PARTY,

262

v1.10 Last updated September 2015

Permission for Chapter 4

Copyright Clearance Center

RightsLink®

Home | Account Info | Help | Live Chat

nature publishing group

Title:	BODIPY-Based Fluorescent Probes for Sensing Protein Surface-Hydrophobicity
Author:	Nethaniah Dorh, Shilei Zhu, Kamal B. Dhungana, Ranjit Pati, Fen-Tair Luo et al.
Publication:	Scientific Reports
Publisher:	Nature Publishing Group
Date:	Dec 18, 2015

Copyright © 2015, Rights Managed by Nature Publishing Group

Logged in as:
Nethaniah Dorh
Account #:
3001001475

LOGOUT

Creative Commons

CLOSE WINDOW

Are you the author of this NPG article?

For commercial reprints of this content, please select the Order Commercial Reprints link located beside the Rights and Permissions link on the Nature Publishing Group Web site.

RightsLink®

Home | Account Info | Help | Live Chat

npg
nature publishing group

Title: BODIPY-Based Fluorescent Probes for Sensing Protein Surface-Hydrophobicity

Author: Nethaniah Dorh, Shilei Zhu, Kamal B. Dhungana, Ranjit Pati, Fen-Tair Luo et al.

Publication: Scientific Reports

Publisher: Nature Publishing Group

Date: Dec 18, 2015

Copyright © 2015, Rights Managed by Nature Publishing Group

Logged in as:
Nethaniah Dorh
Account #:
3001001475

LOGOUT

Author Use

Authors of NPG articles do not require permission to use content from their article in most cases as stated in the author's guidelines.

Authors wishing to use their article for commercial purposes must request permission in the normal way.

For further questions, please contact NPG's permissions department: permissions@nature.com

BACK | CLOSE WINDOW